Cell migration under confinement : how can a cell squeeze through narrow gaps ?

Hawa-Racine Thiam

UNIVERSITÉ PARIS DESCARTES - PARIS 5

Spécialité : BIOPHYSICS
Ecole doctorale Frontières du Vivant

THÈSE DE DOCTORAT

Présentée par

Hawa-Racine THIAM

Cell migration under confinement: How can a cell squeeze through narrow gaps?

Thèse dirigée par **Matthieu PIEL**

Soutenue le 29 septembre 2014 devant le jury composé de:

Rapporteurs:	Dr. Edgar GOMES	-	University of Lisbon
	Dr. Jan LAMMERDING	-	Cornell University
Examinateurs:	Dr. Ana-Maria LENNON-DUMÉNIL	-	Insitut Curie
	Pr. Benoit LADOUX	-	Institut Jacques Monod
	Dr. Guillaume CHARRAS	-	University College of London
Directeur de thèse:	Dr. Matthieu PIEL	-	Institut Curie

Compartiment et dynamique cellulaire, Institut Curie/CNRS UMR144,

26 rue d'Ulm 75248 Paris Cedex 05

Acknowledgments

I would like to thank my thesis committee which accepted to judge this work, particularly Edgar Gomes and Jan Lammerding who reviewed this long thesis manuscript. I also thank Benoit ladoux with whom I first met during my Master 1, when I was struggling in finding a lab for an internship. Benoit is following me since then and it was great to have him around during this last 4 years in my thesis advisory committee. Many thanks to Edgar Gomes whose kindness and availability made discussions about the nucleus and the LINC complex so much nicer!!!!

Now, I would like to greatly acknowledge Matthieu who, knowing my personality, was the best PhD supervisor I could dream of. Thank you for hosting me in your lab for a PhD despite the issues I had during my Master 2 internship. Thank you for giving me so much freedom in managing my time as well as my experiments. Thank you for all the time you spent listening to me talking about experiments. It might seem obvious but it was great to be talking to someone who could listen to and find my thoughts interesting (at least I hope they were interesting :)). Thank you for having, almost :), never crashed with me when I was too stubborn to follow all your advises. Not following all your advises definitely made me lose a lot of time but allowed me to develop my own way of thinking. Thank you for supporting me each time I as was so desperate with my experiments. It was great to discuss with you as after most of the discussions I was thinking " Well, the project is not going so badly...". And most of all, thank you for showing and teaching me your way of doing science and being a scientist. It was impressive to see the rate at which you generate nice and original ideas!!! Being around you make believe that everything is possible as long as you let your imagination free to fly!!! Thank you for giving me the opportunity of being part of such an interdisciplinary lab. It was great to be able to interact with people coming from such broad backgrounds. I was proud of being part of a lab where ideas and expertize were shared and I believe it is because Matthieu never hesitate with providing people (sometime even competitors :)) with ideas. I hope to be able to keep this vision of Science as a world were ideas and expertize are shared without restrictions!! Thank you Matthieu!!!

Now, place for the rest of the lab. First, I would like to thank Pablo Vargas who, as I used to say, was for me a sort of second PhD supervisor. It took one year to be able to talk to him without wondering if he will answer but from then everything was great!!! Thank you Pablo for having been around to teach me how to handle (and sing :) for) dendritic cells. Thank you for sharing with me your cells, ideas, drugs ... And most of all thank you for all the discussion we had about my doubts. I really enjoyed being able to talk to you about everything and that you were able to tell me directly when I was exaggerating!!! Thank you Pablo Vargas!! I would like to thank Franzi for her kindness, her continuous availability particularly for post-labmeeting debriefings :). Most of all, thank you Franzi for believing in me!!! You were a great deskmate. Thank you Julie Janvore for all the time you spent with me on the Zeiss!!! Thank you for your availability and kindness even in the most stressful

moments of your PhD!! Thank you for your well written thesis manuscript which helped be a lot when I was writing mine!!! And thank you for your smile during my presentations!!! Many thanks to Manu who took the time to teach me lithography. I also enjoyed all the discussions we had!!! I would like to highly acknowledge Daria who made my life in (but also outside) the lab so much easier!!! Thank you for all the time we spent laughing about everything, saying stupid things, gossiping, dreaming, making the world and sharing personal things. You became someone very precious to me!!! Just stay as you are Bonazzi!!! Thank you Melanie, my co-PhD as you used to say!!! Thank you for your honesty. We took time to adapt to each other but this time was worth it!! It was great to be able to discuss about our doubts, our frustration and also our success (yeah, there were few of them!!!). Thank you Nico for your help with computers during all this time!!! Thank you for keeping saying "oui" after my 1000s " Nico... j'ai une question". Thank you Paolo (la force tranquille) for your help in image analysis!!! Many thanks to Mael for all the discussions we had. Thank you Ewa for your honesty and your enthusiasm!!! It was nice spending time analyzing, trying to improve our personalities!!! Many thanks Clotilde for your enthusiasm, your smile and your kindness!!! I enjoyed our after 7 pm discussions in our office and our jogging sessions!!! You were a cool deskmate!!! Thank you Sylvain, Camille and Yanjun for your kindness, Lyasmin for making me laugh so much!! Thank you Rafaele for splitting cells for me :).

I would also like to acknowledge Ana-Maria's lab members, starting from Ana for accepting to see me coming all the time in your lab, talking and thus distracting people, stilling reagents and protocols!! Thank you Melina for being the first one who showed me how to put cells in channels; Paola for all the protocol you shared with me; Marine for all the discussions we had; Dorian for you help in western blot; Heléne for the neutrophils; Paolo, Pablo Saez, Dan, Anita, Odil for your kindness. Thank you Matthieu Maurin for helping me so much with imageJ!!! Just try to stop complaining about everything !!! :) Many thanks to each members of the UMR 144, 932, 168 with whom I interacted as I believe that each interaction is a gift!!!

Now, time for my family.

Je voudrai d'abord remercier Mariame poolel baaba racine Thiam, ma soeur qui est devenue une mére et une amie. Merci d'avoir accueilli et accepté la jeune fille perdue, têtue de 17 ans que j'étais. Merci de m'avoir encouragé en tout, tout le temps. Et merci de m'avoir donné Hawa et Tidiane!!!! Un grand remerciement à mes parents qui sont allés à l'encontre de toutes les règles dictées par la tradition toucouleur en m'inscrivant à l'école, en me laissant partir de la maison si jeune pour poursuivre de si longues études. Merci d'avoir cru en moi, de m'avoir fait confiance et de m'avoir donné autant de liberté. J'ai pleine conscience de la chance que j'ai de vous avoir. Hon diaaraamaa!!! Merci à mes formidable fréres: Fadel pour le soutient inconditionel; Matthiam pour ta gentillesse; Tidiane mon chér Tidiou!!; Djiby Poulo, le premier Dr. Thiam; Oussou Bébé mon amour de petit frére ainsi que tous les autres. De même pour mes soeurs, les battantes. C'est grace à vous tous que j'ai appris à ne pas accepter les limites pré-definis!!! Hon Diaaraama onone fof!! I would also like to greatly

acknowledge Matthias Garten for being around during this last 3 years!!! Here again, I was really lucky to have found you!! Thank you for being so supportive and available, I particularly appreciated it as we both went through the same PhD-related issues, joys and others... I strongly hope we will keep understanding each other for longer!!! Many thanks to Kelly for your perpetual friendship and all the just Dance nights; Lauriane for your smile and helping me to escape from the lab from time to time; Aida, Henriette for everything!!!

Finally, I would like to thank all the people that help me to reach this point. The Senegalese society for giving me the opportunity to pursue my studies in France and providing me with financial support for 5 years, the French society for hosting me for 9 years, sharing with me this beautiful culture thus helping me to become the adult I am now. I am really proud of having experience the "enracinement et ouverture" that was so valuable to Leopold Sédar Senghor. I am grateful to M. Kébé, my Math teacher during the last year of secondary school, who made me discover the beauty of math with his expression " the only thing you need in maths is good eyes" :); to M. Konaté who triggers my love for physics; the MC Donald company that hired me for 3 years and half making me discover the beauty of social diversity!!!

Just **Merci, Dieureudieuf, Hon Diaaraamaa, Danke, Thank you ...**

0.1 Abstract

Cell migration has two opposite faces; necessary for many physiological processes such as immune response, it can also lead to the organism death by allowing metastatic cells to invade new organs. *In vivo* migration often occurs in complex 3D environments which impose high cellular deformability. Recently, the limit of cellular deformability during 3D migration has been shown to be limited by the nucleus [Wolf 2013]. For instance, cell migration can be increased by decreasing nuclear stiffness. However, below a given nuclear stiffness 3D cell migration can be reduced as a result of impaired cell survival [Harada 2014]. Cancer cells which display slow migration and have rather stiff nuclei have been shown to overcome the physical limits of 3D migration through adhesion combined to matrix degradation or high actomyosin contraction [Wolf 2013]. Immune cells such as neutrophils which are fast moving cells with soft nuclei have been reported to die at sites of infection. Interestingly, dendritic cells function as antigen presenting cells requires high migratory ability as well as high survival. They thus constitute an interesting model for studying nuclear deformation in fast moving and long lived cells. During my PhD, I studied the mechanism by which dendritic cells deform their nuclei to achieve proper migration in highly confining space while preserving a high survival rate. I used an original micro fabricated experimental set up [Heuzé 2011] consisting of microchannels with constrictions to mimic cellular transmigration. Those channels combined with genetic manipulation and live cell imaging followed by image processing were used to assess the mechanism dendritic cells use to deform their nucleus, which we found to be specific and not required for cell motility per se. I showed that dendritic cells overcome the physical limitation imposed by nuclear deformation through small gaps by nucleating an Arp2/3 based actin network around the nucleus. Surprisingly, the formation of this actin network is independent of myosin II based contraction. This actin accumulation around the nucleus co-localized with sites of nuclear Lamin A/C breakage. Moreover, Lamin A/C depletion in dendritic cells leads to the disappearance of this actin ring and the release of the need for Arp2/3 for nuclear deformation. We thus propose a new mechanism of nuclear squeezing through narrow gaps based on an Arp2/3 nucleated actin meshwork which, by transiently breaking the Lamin A/C network, releases the nuclear surface tension and allows nuclear thus cell passage through micrometric constrictions. Lamin A/C repolymerization around the nucleus at the exit of constrictions would then restore nuclear stiffness, allowing cell survival. Interestingly, this actin accumulation around the nucleus was also observed in vivo in migrating macrophages but not in HL-60 derived neutrophils. Taken together, our data suggest that the Arp2/3 based nuclear squeezing mechanism would be a general feature of highly migratory cells which need to survive long enough to accomplish their functions.

Contents

List of Figures

0.2 Foreword

Studying cell migration is necessary to have a minute understanding many physiological (e.g. embryogenesis, immune response) but also pathological (e.g. metastasis formation) processes. If the mechanisms of 2D cell migration have been extensively studied, only few models of cell migration in complex 3D environments have been proposed. Emerging evidences point towards the idea that well established mechanism such as the requirement of integrins based adhesion might not subsist in 3D environments. On the contrary, 3D environments by imposing new constrains (e.g. confinement) might require specific mechanisms (e.g. cell deformation) which can be neglected when studying cell migration on 2D substrates. Three components define cellular deformability: the cytoskeleton, the plasma membrane and the nucleus. while the roles of the cytoskelon and the plasma membrane in cell migration have already been addressed, the role of the nucleus in 3D cell migration is far from being known. My PhD project thus sought to investigate the role of the nucleus in 3D cell migration focusing on the mechanisms of nuclear deformation during immune cells migration under confinement.

This thesis manuscript thus presents the research work performed during my PhD under the supervision of Matthieu Piel at the UMR144 of the Curie Institute. It aims to pose the general context of this project, the main results obtained during this PhD and discuss the contribution of these results in the general context of 3D cell migration.

The first, introductory part of this thesis manuscript in composed of four chapters. In the first chapter, I will introduce the broad subject of cell migration. Starting with a brief description of the main *in vivo* events which require a minute control of cell migration, I will then illustrate the importance of this process in immune response by describing the migratory route of immune cells particularly dendritic cells. In the third chapter, I will introduce the physics of cell migration focusing on the mechanical properties of the cell important for cell migration. This chapter will end with a general review of the main models proposed for interstitial migration. In the fourth chapter, I will introduce the role of the nucleus in cell migration focusing, again, on the role of nuclear mechanical properties in this process. A last chapter presents the objectives of this PhD project.

In the second part of this manuscript, I will describe the main methods developed to address my questions during this PhD. I will particularly focus on describing the constrictions based setup I used to study nuclear deformation during immune cells migration under confinement.

In the results part of this manuscript, I will present the main results obtained during this PhD in form of a manuscript in preparation for submission. A last section in this chapter will list the

experiments I plan to perform before the submission.

In the last part of this manuscript, I will discussed the results presented in the manuscript in preparation before proposing a general model of nuclear deformation during immune cells migration under confinement. Toward the end, I will put the results obtained during my PhD in the broader context of 3D migration focusing on the emerging direction of the role of nuclear deformation in cell survival during 3D migration.

INTRODUCTION

Chapter 1

Migration: a multiscale process

Contents

1.1 Migration: a multiscales process

"Migration" originates from the latin verb *migrare* which means "moving/going away". It is a multistep biological process which consists of the displacement of organisms from an original location to a new one. This type of displacement occurs through different mechanisms that include walking, swimming, flying, drifting [DINGLE 2007] and is a well conserved capacity through different species ranging from prokaryotes (bacterias) to animals (Human, Birds, Fish).
Migration can occur at the individual as well as at the population level [DINGLE 2007]. We can talk about individual migration when, for example, young birds migrate *"away from their parents to avoid competition and inbreeding"* [DINGLE 2007]. An example of population migration is the general displacement of refugees during a war.
The term migration often implies the existence of either an internal of external cue. Many cues can lead to organism migration but the most recurrent ones are:

1. Change in local food availability
2. Climat changes
3. Reproduction
4. Safety

These four majors cues, all related to organism survival define a pattern of migration. Organisms can, for example, display periodic patterns such as the one observed in birds caused by seasonal availability of food in different regions.

Migration, which can thus be *"recognized to be an adaptation driven by the transitory availability and changing location of resources."* [DINGLE 2007] is a multiscale process that occurs at molecular, cellular and multicellular scales. Its profound understanding requires studies at each of those scales. During my PhD, I was interested in cell migration which can be seen as the mesoscale of the migration process.

1.2 Cell migration

One proposed definition of cell migration is cellular displacement toward chemical and/or physical cues. Cell migration is a fundamental process in different aspects of the organism generation and survival. It is indeed necessary for embryogenesis as well as morphogenesis. In an adult organism, it is required to maintain tissues homeostasis and for a proper immune response.
Cell migration can also participate to our death. When deregulated, it can lead to catastrophic consequences such as chronic inflammation, virus and bacterial infection, mental retardation, cancer formation and dissemination [Vicente-Manzanares 2005]. Dissecting the mechanisms underlying this process is then necessary for developing therapies against migration related disorders such as metastasis.

1.2.1 Cell migration in health and disease

1.2.1.1 Cell migration during embryogenesis

Embryogenesis is a multisteps process which leads to the formation of a multicellular organism composed of specialized tissues and organs. This fundamental process starts with the fertilization of an ovum by a sperm followed by a stage of intensive cleavages of the zygote before entering a gastrulation phase. Embryonic cell migration starts at gastrulation when epiblast cells migrate to reorganize themselves. This reorganization leads to the generation of the primary germ layers: the ectoderm, mesoderm and endoderm [Kurosaka 2008].
Each of those three layers will give rise to specific organs. The ectoderm will indeed generate the skin and nervous system, the mesoderm will generate muscle, respiratory system, the heart and bones while the endoderm will give rise the digestive truck. This morphogenesis process occurs through cycles of growth, division and migration of cells.
Although cell migration occurs during the whole embryogenesis, it is possible define two main post gastrulation migration periods: the early and the late embryonic migration. The early embryonic migration includes the migration of neural crest cells, of primordial germ cells and to some extend, the positioning of the blood cell precursors to the bone marrow and the fetal liver [Kurosaka 2008]. The late embryonic migration include neuronal migration during neuritogenesis [Flynn 2013] and endothelial cell migration during angiogenesis ([Schuermann 2014],[Kurosaka 2008]). To give a more

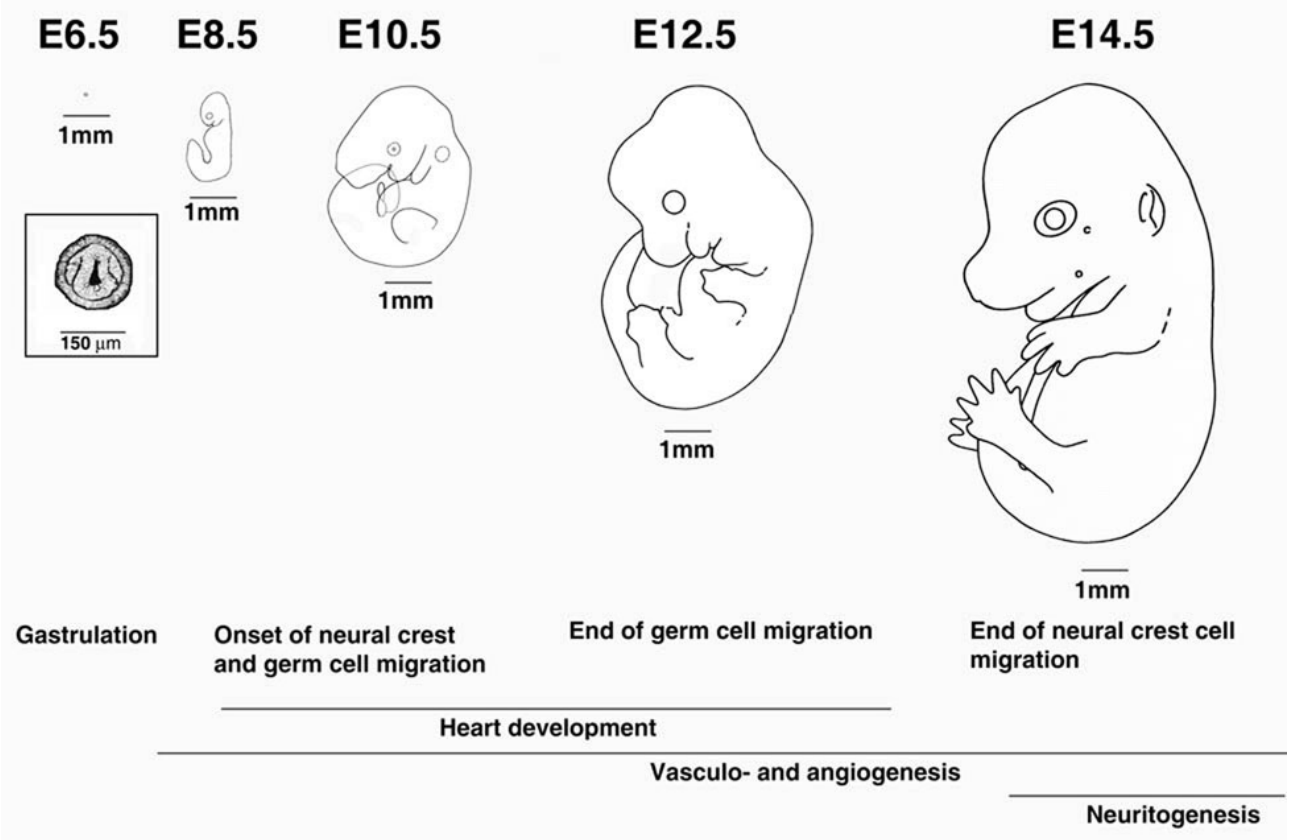

Figure 1.1: "**Timing of the major migratory events in mouse embryogenesis in relation to the embryo growth**. Letters and numbers on the top denote days postcoitum. 1*mm* scale bar of the same size is shown next to each embryo to enable the direct size comparison. Boxed image showed an enlargement of the gastrula shown above. The major migratory events corresponding to those shown in Table 1 are written for the appropriate stages underneath." From [Kurosaka 2008]

precise idea of how important migration is during development, I will describe the migration of neural crest cells lineage as they dominate early embryonic migration.

1.2.1.1.1 Neural crest cells migration: Neural crest cells originate at the interface between the neural plate and the embryonic ectoderm. They are the embryonic precursors of neurons and glia of the peripheral nervous system, and of pigment cells and connective tissues in the face, neck and heart[Tucker 2004]. Neural crest cells are classified according to their migratory routes (origin and destination) inside the embryo. Indeed, cranial and cardiac neural crest cells originate from the head and neck region of the embryo. They both migrate from their origin to give rise to tissues necessary for the face generation (cartilage, bone, cranial neurons, glia, connective tissue of the face, thyroid, teeth, bones of the middle ear, and jaw ...) ([Kurosaka 2008],[Trainor 2005]) or for heart formation (cardiac outflow, heart septae and parts of the ventricular myocardium) ([Kurosaka 2008], [Hutson 2007]).
"Vagal and sacral neural crest cells migrate from two opposite sides to populate the gastrointestinal

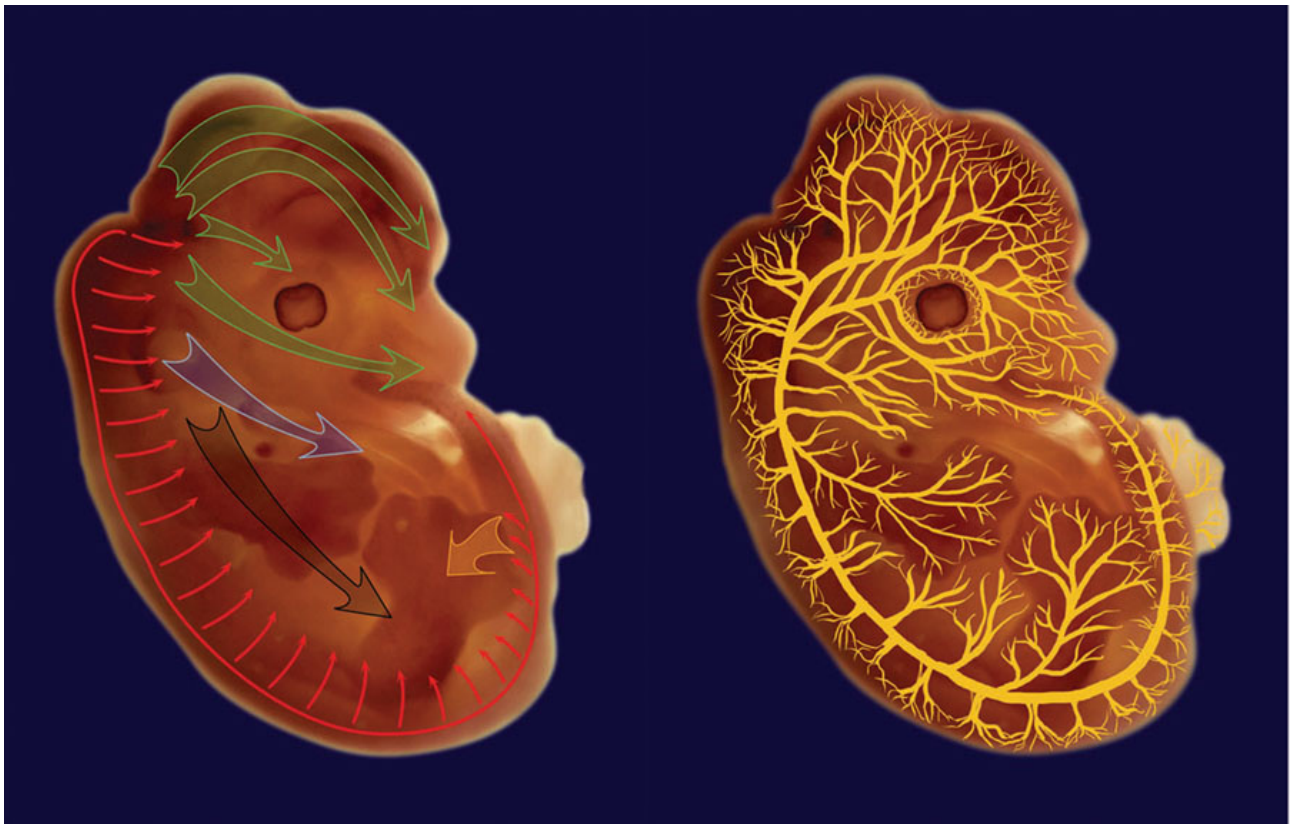

Figure 1.2: "**Pathways of neural crest migration, neuritogenesis, and angiogenesis during mouse development**Neural crest cells (left) generally migrate from the back area of the embryo, originating from different somite regions at the different embryonic stages. Large green arrows in the head area denote cranial neural crest, blue arrow (cardiac neural crest), black (vagal neural crest), orange arrow (secral neural crest) and thin red arrows (trunck neural crest). Neurites and blood vessels sprout from the structures laid out during earlier stages of development and reach to all the areas of the mature organism along the pathways illustrated on the right hand image. Illustrations were prepared by O. Karengina based on an image of a mouse embryo at E13.5." From [Kurosaka 2008]

system and differentiate into the neurons that innervate the digestive tract" [Kurosaka 2008] while the *"Trunk neural crest cells migrate from the back of the embryo to form sensory and sympathetic neurons, adrenal gland, Schwann cells, and pigment cells of the skin"*([Kurosaka 2008], [Hutson 2007]). Neural crest cell migration is thus a fundamental process in embryogenesis and morphogenesis.

1.2.1.2 Cell migration to maintain tissue homeostasis

Homeostasis is a property of a system to react and adapt in order to maintain some parameters constant/stationary. Temperature is, for example, a tightly regulated parameter in many organisms. This property is recurrent to most of the biological systems and plays a crucial role in organism development and survival.

Tissue homeostasis is maintained in multicellular organism through various processes including cellular division, growth, control of metabolic function and also control of cell migration. For instance, after a wound, the organism will deploy a set of machineries to repair the tissue. Cell migration is one of those machineries; it is used to fill the newly created free space.
Wound healing is, to my knowledge, the most well studied biological process related to cell migration for the maintenance of tissue homeostasis. In the following paragraph I will briefly describe the wound healing process in order to point out the importance of cell migration in tissue homeostasis.

1.2.1.2.1 Cell migration during wound healing Wound healing is a natural biological process which starts after a scar formation on an organ. This process occurs in four tightly regulated phases: homeostasis, inflammation, proliferation and remodeling ([Guo 2010], [Rs 1993]).
During the first homeostasis phase, the organism reacts to the scar by tightening the blood vessels around the wound to avoid blood flow. The wound will then be isolated from the external environment by platelet accumulation and fibrin clot formation.[Guo 2010]
After wound isolation, starts the second phase with the release of the blood vessels allowing leukocytes migration from the blood stream to the cite of injury [Rs 1993].
The proliferation phase is characterized by epithelial cell growth, division and migration, angiogenesis as well as extracellular matrix synthesis [Guo 2010].
The final remodeling phase consists of the reduction of the vascular density in the wound region followed by the remodelling of the extracellular matrix. The wound region returns to it's original state. This phase can last for years ([Guo 2010], [Rs 1993]).
The spatial and temporal regulation of each of the wound healing phases is necessary for a proper wound closure and the maintenance of tissue homeostasis.
Cell migration is crucial in two of the wound healing phase: the inflammatory and the proliferation phases. Indeed, the right achievement of the inflammatory phase requires leukocytes migration from the blood vessels to the site of injury while the closure of the wound require epithelial cell migration. Thus, the deregulation of cell migration can lead to a delay or failure of the wound healing process. This can induce catastrophic consequences such as viral/bacterial infection or chronic wound.

1.2.1.3 Metastasis formation: when cell migration goes out of control

Cancer is one of the leading cause of death in the world with 8.2 millions of deaths, 14.1 millions new cases and 32.6 million people living with cancer in 2012 *(Sources from World Health Organization)*. It is a common term for a group of diseases which can arise in different parts of the body and could require different treatments. One defining characteristic of cancerous cells is a rapid and uncontrolled burst of cell growth and proliferation which leads to tumor formation. Metastasis occurs when some cancer cells manage to escape from the primary tumor and colonize a new organ. Even though the triggering event which leads to metastasis formation is not well understood yet, five phases are

conserved during all metastasis formations: local invasion, intravasation, survival in the circulatory system, extravasation and colonization [Nguyen 2009]. Each of those phases requires cell migration. Because metastasis is the primary cause of cancer induced death, it is one of the most well studied case of the effect of cell migration deregulation.

1.2.1.3.1 Some history: Cancer has always been part of the human history. Indeed, some papyrus from the ancient Egypt (The Edwin Smith Papyrus, 3000 BC) was already describing tumors. The term "Cancer" is the latin translation from the Roman physician, Celsus (28-50BC) of the greek word *carcinos* credited to Hippocrates (460-370 BC). Cancer is the latin word for crab *"most likely applied to the disease because the finger-like spreading projections from a cancer called to mind the shape of a crab" (source from the American cancer society)*.
If the idea of invasion is already in the description of cancer, it is only in the first millennium that the term invasion arises with Avicenna (980-1037) who noticed that the tumor invades and destroys neighboring cells.
The term *metastasis* appears only after the eighteen century thanks to the development of microscopy. Indeed, in series of publication between 1871 and 1874, the English surgeon Campbell de Morgan rationally argued *"that cancer arise locally then spread first to the lymph nodes then further afield"* [Grange 2002].
Nearly three centuries after its discovery, crucial questions about metastasis formation remain to be elucidated. What trigger metastasis? Why do some tumors metastasize and others don't? Why do different tumors metastasize in the same organs? What defines the colonization of one organ instead of another? and more importantly, what makes a "regular" cancer cell become a metastatic cell? These are some of the main questions which need to be answered in order to control metastasis.
As all metastasis share a common feature of migration, I will describe in the following paragraphs some aspect of cell migration that are known to be important for metastasis formation.

1.2.1.3.2 Cancer cell migration: One of the most accepted idea of metastasis formation is that a cell will detach from the main tumor after loosening it's cell-cell adhesion, migrate toward the circulatory system, extravagate then invade a new organ. All this process occurs at the single cell level, and thus requires single cell migration. It is triggered by a process called epithelial to mesenchimal transition (EMT). EMT is a process that is also describe in development when epithelial cells start loosening their cell-cell adhesion then migrate to form new organs (Neural crest cells lineage formation [Nakaya 2013]). A more recent idea of metastasis formation is that it can not only occur at as a single cell migration process but also through a collective cell migration. Collective cell migration is a process by which a group of cells will migrate keeping the contact between them. During such migration, cell-cell adhesion maintain supracellular properties and cells move as sheets, strands, clusters or ducts [Friedl 2009a]. Both migration phenotypes are now well accepted to be used by cancer

cells to invade and metastasize. The choice of the migration phenotype is though to be determined by the stroma. The biochemical and physical properties of the extracellular environment was proposed to determine the type of motion single metastatic cells or collectively migrating cells will adopt [Friedl 2011]. Plasticity in the migratory mechanisms make metastasis hard to predict and to control. Whatever the extracellular properties are, cancer cells will adapt to it and keep migrating forward [Friedl 2010].

Because it is not the purpose of this thesis, I will not talk further about cancer cell migration. However, because single cancer cell migration shares many features with leukocytes migration, I will discuss later the mechanism of migration described for cancer cells (3.4).

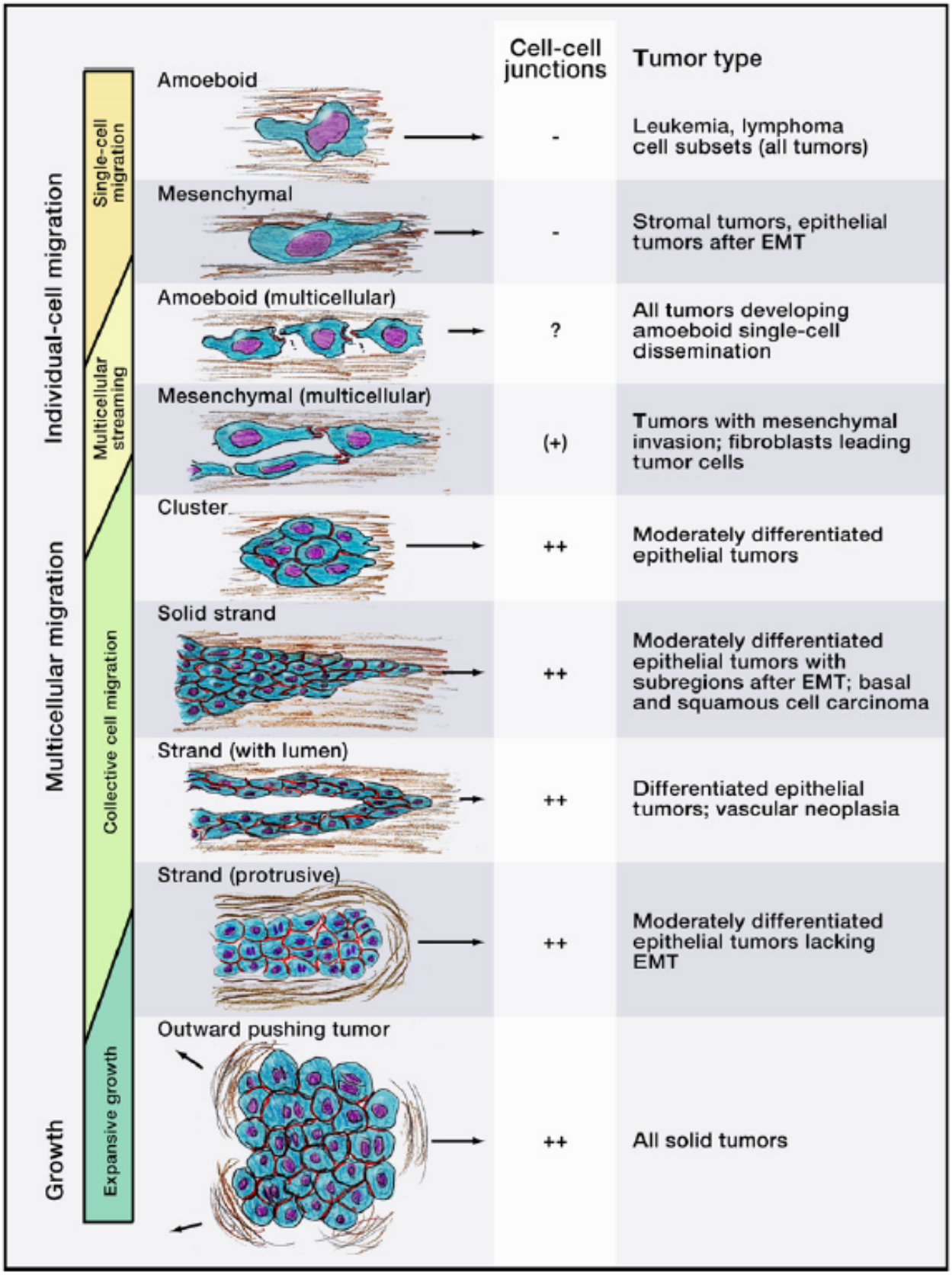
Individual-cell migration
Multicellular migration
Growth
Single-cell migration
Multicellular streaming
Collective cell migration
Expansive growth
Cell-cell junctions
Tumor type
Amoeboid
-
Leukemia, lymphoma cell subsets (all tumors)
Mesenchymal
-
Stromal tumors, epithelial tumors after EMT
Amoeboid (multicellular)
?
All tumors developing amoeboid single-cell dissemination
Mesenchymal (multicellular)
(+)
Tumors with mesenchymal invasion; fibroblasts leading tumor cells
Cluster
++
Moderately differentiated epithelial tumors
Solid strand
++
Moderately differentiated epithelial tumors with subregions after EMT; basal and squamous cell carcinoma
Strand (with lumen)
++
Differentiated epithelial tumors; vascular neoplasia
Strand (protrusive)
++
Moderately differentiated epithelial tumors lacking EMT
Outward pushing tumor
++
All solid tumors

Figure 1.3 *(facing page)*: "**Modes of cell movement implicated in cancer invasion and metastasis**. Single-cell and collective cell migration can be further partitioned based on the specific cell-cell junctions, contractility of the cytoskeleton, and the turnover of cell attachments to the extracellular matrix (ECM). These modes of migration can be unstable and change upon alterations of cell-cell interactions, cell-ECM adhesion, or cytoskeleton contractility, resulting in intermediate phenotypes." From [Friedl 2011]

Chapter 2

Cell migration in the context of the immune response

Contents

Cell migration is a central and crucial phase of an immune response. Indeed, because infection can occur anywhere at any time in an organism, the defense mechanism has to be omnipresent and dynamic. Without migration, any local injury would have to be overcome by cells that are already present in the area. Local cells would have to for example produce toxins or engulf the invader in order to kill it. Even though this strategy could work to a certain extend, one can then wonder if this strategy would resist to a high invasion. Another risk would be that invaders develop a resistance to such specific toxins as already seen in bacteria. Many organism have developed an immune system and vertebrate went even further by developing two: the innate and the adaptive immune systems. Both of those immune strategies rely on cell migration. In the following paragraph, I will give an overview of the immune system in vertebrates, describe the keys players before focusing on dendritic cells which are at the interface between innate and adaptive immune response.

2.1 Introduction to the immune system

The immune system represents a set of organs, and processes used by organisms to defend themselves against external invasion. It is thus a fundamental system in the protection of organisms against diseases.

2.1.0.4 Some history:

One of the oldest reference to immunity comes from Thucydides's text where he described that the survivors of the Athenian epidemic (430-426 BC) developed at least partial immunity [Retief 1998]. But it is only in the late nineteenth centurie that the existence of an immune system was proven by Ilya Mechnikov and Paul Ehrlich, the receivers of the Nobel prize in Physiology or Medicine in 1908. Hopefully, scientists did not wait for understanding the immune system to use it for preventing infection. Indeed, already in the eleventh centurie, Chinese were practicing variolation to get immunized against smallpox [Plotkin 2005]. Height centuries later (1880), Louis Pasteur, working on chicken cholera, showed that pathogens could be attenuated using environmental cues such as temperature or chemicals. Furthermore infection of an organism by such attenuated pathogens confers a resistance against the same, less attenuated (normal), pathogens [Plotkin 2005]; this was the starting point of vaccination.
The discovery of vaccination had opened the question of how an organism deals with pathogens. The initial idea of Louis Pasteur based on a differential biochemical environment that would permit or not the survival of pathogens in hosts was abandoned after the discovery of pathogens in the blood of immunized hosts *(Source from the Nobel lecture of Ilya Mechnikov)*.
Ilya Mechnikov and coworkers, while working on the origin of the digestive organs in animals, observed that some moving cells that are not part of the digestive system were able to sort foreign bodies. Years later, he defined those cells as phagocytes (devouring cells) which posses the phagocytosis function. Phagocytes would, anytime that the organism face infection, move to the site of infection to devour and destroy the pathogens by phagocytosis. This was the beginning of the understanding of the innate immunity *(Source from the Nobel lecture of Ilya Mechnikov)*.
If Mechnikov discoveries nicely explained how a host reacts to pathogen infection, the question which still remained was why and how hosts develop resistance to pathogens? Important elements of answers came from the work of Emil von Behring and Paul Ehrlich.
Behring, showed that the *" Blood fluid - or blood serum - from an individual who has been immunized with poisons from a certain bacterium, can, namely, when introduced into the organs of another individual, confer resistance upon him against the bacterium in question" (Source from the Nobel lecture of Ilya Mechnikov)*. This introduced the idea that upon infection, individuals produce chemicals to fight again toxins produced by the pathogen. Those chemicals where named antitoxins. Ehrlich brought the idea of an antigen (toxin) and antibodies (antitoxin) that would fit to each other like a

lock and a key. Those works are the precursors of our actual understanding of the adaptive immune response.

2.2 The immune system

As said earlier, the immune system consist a set of process and organs used by organisms to resist to pathogen invasion. This protection is set through different layers of defense. The first protective layer is the epidermis which confers a physical and also chemical barrier to invaders. Pathogens which manage to cross this first barrier will face the innate immunity in plants and animal. In vertebrates, a second layer of defense which consist of the adaptive immunity will arise after the innate immunity. In the coming sections, I will briefly describe the innate and adaptive immunity of vertebrates.

2.2.1 Innate immunity

In an healthy individual, pathogens will first encounter the innate immune system before the adaptive immunity is "called to help"[Alberts 2007, p. 1524]. For example, in the process of wound healing, the innate immune response occurs within hours right after the wound isolation. This fast reaction is one of the characteristics of the innate immunity and is required to prevent any infection as pathogens such as bacterias have a very fast cell division cycle. The innate immunity, contrary to the adaptive one, is common to all types of pathogens. The innate immune system consists of 3 lines of defenses [Alberts 2007, p. 1524]:

1. The epidermis and other epithelial surfaces such as the one covering the respiratory, digestive and urinary tracks which provide a physical barer to invasion. A mucus layer covering those surfaces and containing substances such as defensins will prevent the entrance of pathogens to sterile regions of the organism.

2. The epithelial barer where epithelial cells can engulf microorganisms and direct them to specific compartments such as lysosomes where they will be degraded. In addition, epithelial cells as well as any other eukaryotic cells have the ability to degrade double stranded-RNA, a hallmark of viral replication.

3. The phagocytes kill pathogens by engulfing and devouring them.

The two first lines of innate immunity are shared among plants and animal while the third one is specific to animal cells. It is thus really interesting to note the requirement for cell migration in the third line of innate immunity but not in the two first ones.
Indeed, the phagocytes are highly motile immune cells. Their motile capability allows them to patrol the whole organism and display a fast reaction to any injury. Four different cell types orchestrate

the innate immune response: macrophages, neutrophils, natural killer cells and dendritic cells. All descendent of the hematopoietic lineage (see figure 2.1), they work in tight cooperation to defend the organism. Phagocytes detect their pray using a common receptor, the germline-encoded pattern-recognition receptors (PRRs) [Akira 2006]. The PPRs recognize microbial components essential for pathogen's survival: the pathogen-associated molecular patterns (PAMPs). Examples of PAMPs are components of bacterial cell wall as well as viral envelope proteins or bacterial DNA. Part of the main PRRs are the Toll-Like receptors which are well conserved from plants to mammals. The binding of a PAMP to a PRR leads to the phagocytosis of the pathogen and also to the activation of many genes responsible for the innate immune response [Alberts 2007, p. 1528]. In the following section, I will give an overview of each of those cells.

2.2.2 Motiles cells in innate immunity

The macrophage, neutrophils, natural killer and dendritic cells are at the first line of the innate immune response. Indeed, upon invasion, those cells will move towards the site of infection to kill pathogens as well as infected cells. In vertebrate, the movement of those cells, particularly dendritic cells, is also essential to activate the adaptive immune response.

2.2.2.1 Macrophages: the long lived cells

In vertebrates, macrophages are the cells that first encounter invaders. They are indeed living in tissues all around the body with a particular concentration in sites where infection has a higher probability to occur: connective tissues, liver, spleen. They are rapidly recruited to site of infection where they will display a set of machineries to phagocyte and kill pathogens. Their activation at sites of infection, leads to the production of cytokines that can activate other phagocytic cells such as neutrophils but also triggers fever which by rising the body temperature inhibit the growth of pathogens. Macrophages often survive their first encounter with pathogens, they then keep patrolling the body waiting for the next invasion. They are thus the most long lived cells among the ones involved in innate immunity.(Adapted from [Alberts 2007])

2.2.2.2 Neutrophils: the short lived cells

Neutrophils are usually present in the blood stream and are rapidly recruited to sites of infection by activated macrophages, by molecules specific to the pathogens such as the formylmethionine-containing peptides or "by peptides fragments from the complement components" [Alberts 2007, p. 1528]. They are highly phagocytic cells which will usually die at the site of infection. As they are short lived cells, they can use their own DNA as nets to trap pathogens [Alberts 2007, p. 1532].

2.2.2.3 The natural killers cells

Natural killer cells target virus infected cells and trigger their apoptosis. They recognize infected cells through their levels of expression of a class of proteins called the Major Histocompatibility Complex (MHC) of class I. Indeed, many viral infections lead to the down regulation of the MHC class I as those proteins are used to present antigen to cytotoxic T lymphocytes during the adaptive immune response (see 2.2.3.1). By lowering the amount of MHC class I, viruses escape from the cytotoxic T cells but are then detected by natural killer cells. The apoptosis pathway will be activated in infected cells before viral replication [Alberts 2007, p. 1536].

2.2.2.4 Dendritic cells at the interface between innate and adaptive immunity

Dendritic cells are also phagocitic cells with a large variety of PRRs which allows them to detect a wide variety of pathogens. Once they encounter a pathogen, they will cleave it into peptide fragments which will be presented at their surface with MHC proteins. They will then carry such complexes toward the nearby lymphoid organ where they activate T cells. This will trigger the adaptive immune response. Dendritic cells are thus essential linkers between the innate and the adaptive immunity. (Adapted from [Alberts 2007])

2.2.3 Adaptive immunity

The adaptive immunity also called acquired immunity arose 500 millions year ago in vertebrates. While the innate immunity displays a common mechanism to fight against pathogens, the response gets more sophisticated and specific when the adaptive immune system comes to play. This highly specific response is carried out by Lymphocytes: the T and B lymphocytes.
Upon infection, activated dendritic cells migrate towards the nearest lymphoid organ where they activate T cells. T Cells activation occurs after the recognition of the antigen presented on the MHC proteins of the dendritic cells associated to some co-stimulatory molecules. This will lead to the onset of the migration of some T cells towards the sites of infection where they will participate to the destruction of pathogens and infected cells.
Other dendritic cells activated T cells will remain in the lymphoid organ where they will keep dendritic cells active in order to activate more T cells and help activating B lymphocytes which will produce antibodies against the pathogen. The adaptive immune response is then displayed in two phase: the humoral immunity based on B cells antibody production and the cell-mediated immunity based on T lymphocytes. In the following paragraph, I will describe the keys players of the adaptive immune response: the T and B lymphocytes. Even though they derive from the same common lymphoid progenitor cells (see figure 2.1), they display specific feature in their fight against infection.

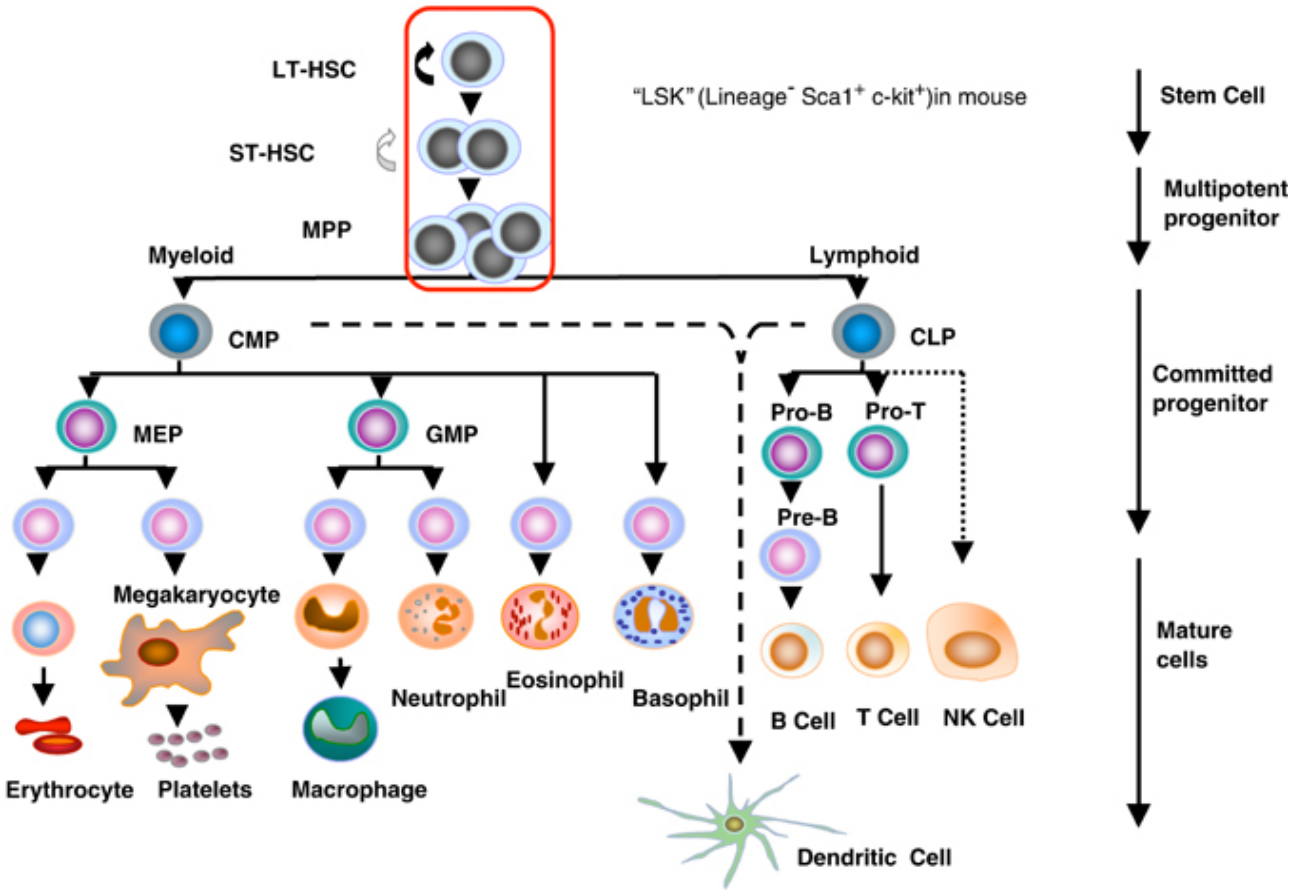

Figure 2.1: "**The hierarchy of hematopoietic cells**. Hematopoietic Stem Cells (HSCs). LT-HSC, long-term repopulating HSC; ST-HSC, short-term repopulating HSC; MPP, multipotent progenitor; CMP, common myeloid progenitor; CLP, common lymphoid progenitor; MEP, megakaryocyte/erythroid progenitor; GMP, granulocyte-macrophage progenitor. The encircled pluripotent population, LT-HSC, ST-HSC and MPP are Lin^{-}, $Sca-1^{+}$, $c-kit^{+}$ as shown." From [Larsson 2005]

2.2.3.1 The T lymphocytes

T cells develop from the lymphoid progenitor cells that migrate from the hematopoietic tissues to the thymus via the blood. After a set of selections for their affinity and specificity to antigen presenting cells, they leave the thymus as CD8+ or CD4+ T cells to migrate towards the peripheral lymphoid organs: the lymph nodes, spleen and epithelial associated lymphoid tissues in the digestive/respiratory tract as well as the skin. Their activation by dendritic cells occurs in these peripheral lymphoid organs and leads to their proliferation and maturation to effectors T cells. Three main classes of effectors T cells are described:

1. Cytotoxic T cells migrate to the site of infection to directly induce the apoptosis of infected cells.

2. Helper T cells stimulate the responses of other cells. They, for example, help to the stimulation of B cells for the production of antibodies.

3. Regulatory T cells suppress the activity of dendritic cells, cytotoxic and helper T cells. They play a crucial role in preventing the adaptive immune response from damaging host tissues.

T lymphocytes activity is thus tightly coupled to cell migration. Indeed, their activation relies on their specific interaction with dendritic cells which then implies first T cells migration from the thymus to the peripheral lymphoid organs and second dendritic cells migration towards the same organs. In addition, effector T cells action relies on their interaction with infected cells or other antigen presenting cells which then implies T cells migration towards the site of infection. Thus cell migration is necessary for T cells response.

2.2.3.2 The B lymphocytes

B lymphocytes are the main mediator to the humoral immunity. They develop from the lymphoid progenitor cells directly in the hematopoietic tissues (liver in fetuses, bone marrow in adults). Similarly to T cells, B cells are also controlled for auto-reactivity. Indeed, B cells with B cell receptors that bind too strongly to the host antigen will not mature. If they succeed at the central tolerance selection (control for tolerance in the bone marrow), mature B cells will then be released in the circulatory system before reaching the peripheral lymphoid organs. In those peripheral lymphoid organs, activation by an antigen give rise to effectors B cells which will secrete antibodies specific to the antigen they have been activated with.
Contrary to T cells, the action of B cells does not rely on cell migration. Although their activation requires migration of the antigen presenting cells, their action relies mostly on the diffusion transport of the produced antigen towards the sites of infection.

2.2.3.3 Generation of memory

One specificity of the adaptive immunity is its ability to generate memory. Indeed, upon activation of B or T lymphocytes, most of the mature cells give rise to effector cells, but a subset differentiates into memory cells. Those memory cells will then induce a faster reaction of the organism in case of a second infection.

2.3 Dendritic cells

Dendritic cells derive from the hematopoietic lineage. Despite the absence of a DC-specific phenotypic marker and the lack of-identification of a DC precursor in the bone marrow, all DCs share the common feature of being able to activate T cells [Merad 2013]. Dendritic cells are usually classified in 4 subgroups (See figure 2.2):

1. The langerhans cells which populate the epidermal layer of the skin have been first described in 1868 by Paul Langerhans who associated them to neuronal cells. Under homeostatic conditions, they continuously move to patrol their environment and upon infection, they become immobile and start engulfing parasites using their large and dynamic dendrites [Ng 2008]. One characteristic of langerhans cells is the presence of granules called Birbeck granules.

2. The classical dendritic cells which have been first describe in 1973 by Steinman and cohn [Steinman 1974]. This subset can be divided in two part: the lymphoid resident and the non-lymphoid resident classical dendritic cells. The lymphoid resident dendritic cells populate lymphoid organs such as the spleen and the thymus and are though to participate to the establishment of immune tolerance in T cells. The nonlymphoid resident dendritic cells are the one that would be sampling the tissues and would migrate towards the lymphoid organs after detection of a danger signal.

3. The plasmocytoid dendritic cells which have a characteristic low level of expression of the MHC class II proteins as well as co-stimulatory proteins and PRRs [Merad 2013]. Their role seems to be specific to viral infection as upon recognition of foreign nucleid acid, "they produce massive amount of type I interferon and acquire the ability to present foreign antigens" [Merad 2013].

4. The monocyte derived dendritic cells are dendritic cells which are differentiated from monocytes during an inflammation [Geissmann 2010].

As said earlier, dendritic cells are at the interface between innate and adaptive immunity. Indeed, naive T cells activation requires it's direct interaction with dendritic cells. Their crucial role in T cell activation requires different events. The immature dendritic cells must be able to engulfs the pathogen, to degrade it, to present it at their surface, to migrate then present the antigen to the T cells. This

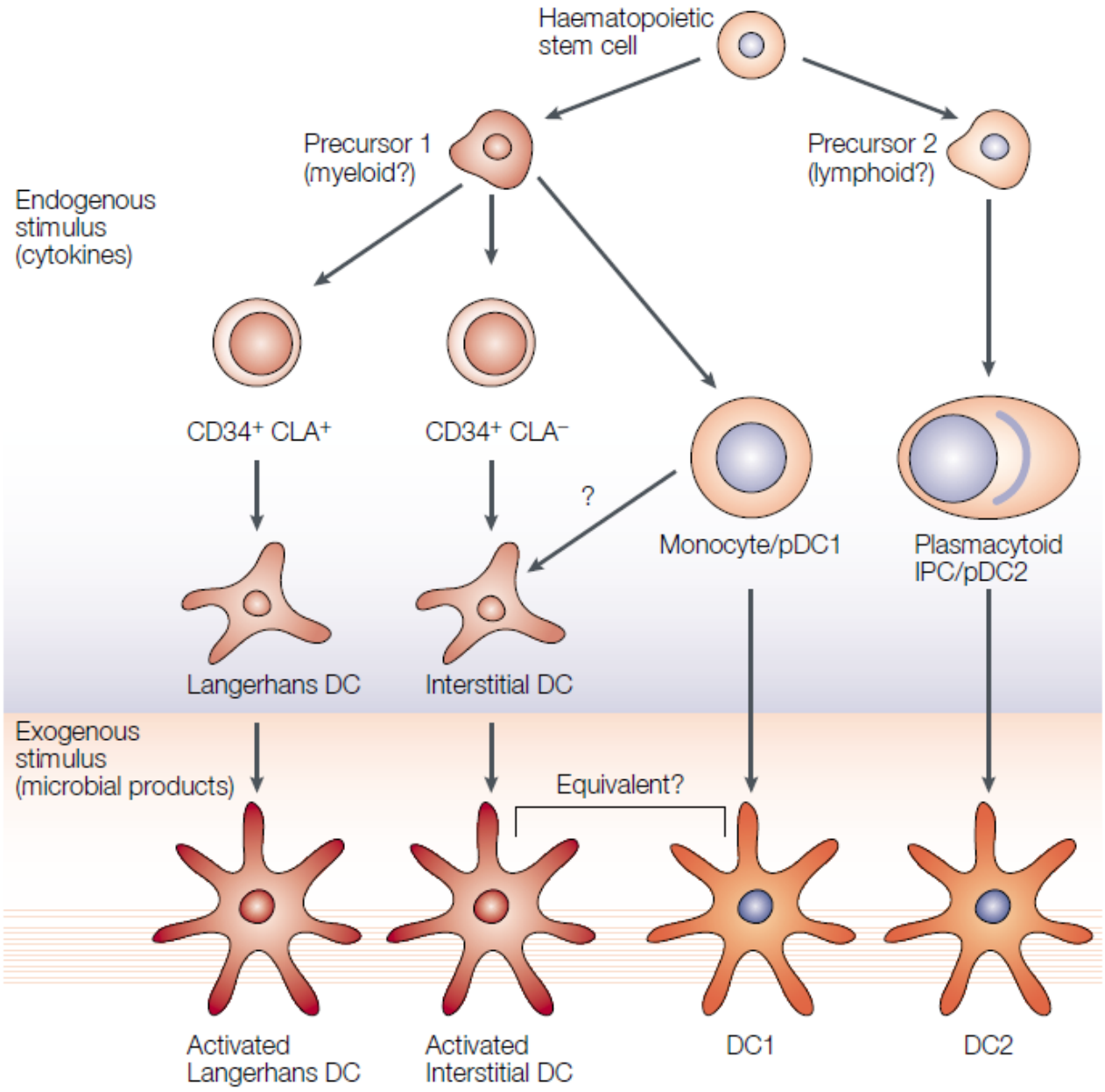

Figure 2.2: "**Pathways of human dendritic cell development**. These pathways were deduced from culture studies. Some dendritic cell lineages progress to a mature but quiescent state under the influence of cytokines alone, requiring exogenous stimuli only for full activation. Other dendritic cell lineages, however, probably remain at a precursor state in an uninfected individual, because they require stimulation by microbial products to produce mature dendritic cells. CLA for cutaneous lymphocyte-associated antigen; IPC for interferon-producing cell; pDC for presursor of dendritic cells." From [Shortman 2002]

succession of events requires the ability of the cell to process the information (pathogen detection and processing), and to move efficiently (environment sampling, migration towards the T cells regions) in order to transmit the information. In the following section, I will describe two important features of dendritic cells : their antigen uptake ability and their migratory ability.

2.3.1 Antigen uptake in dendritic cells

Antigen uptake is a fundamental process in the accomplishment of dendritic cells task during immune response. Indeed, its role as an antigen presenting cell requires the ability to engulf pathogens and present antigens at its surface. Different modes of antigen uptake have been describe in dendritic cells. According to the size of the element to internalize, the cell will perform either phagocytosis, endocytosis or, macropynocytosis. Indeed, particles bigger than 0.5mm will be internalized by phagocytosis while smaller particles will be internalized by endocytosis through specific receptors/cargo interaction. Macropanocytosis is used to internalize fluid, it does not requires receptor/cargo interaction which makes it unspecific.

After internalization, two routes can be taken by the particle. In the first case, the particle will be released from endosomes to the cytoplasm where it will be cleaved into small peptides before being transported towards the endoplasmic reticulum by the ABC transporter where it will bind to the MHC class I molecules [Alberts 2007, p. 1583]. In the second case, the particle will be released from the early endosome to the late endosome where it will be joined by the complex MHC class II/Invarian chain. The release of the invarian chain from the MHC class II allows its binding to the particle. The MHC/particle complex is then targeted to the plasma membrane where it will be recognize by the T lymphocyte. Note that the MHC class I is recognized by the cytotoxic T cells while the MHC class II is recognized by the Helper T cells [Alberts 2007, p. 1584]. The dendritic cell , by activating different subset of effector T cells will then define the type of adaptive immune response that will be displayed by the host.

The interaction between T cells and dendritic cells should lead to the activation of the T cell only if the dendritic cell is activated. Indeed, if the dendritic cell has not been activated, the activation of the T cell triggers apostosis. The activation of dendritic cells is thus an important process in the adaptive immune response.

2.3.2 From an immature to a mature state

Upon recognition of a so called "danger signal", the immature dendritic cell enters a differentiation process to become a mature dendritic cells. A global set of particles including PAMPs, cytokines produced by macrophages or neutrophiles can be recognized as danger signal [Reis e Sousa 2004]. The maturation of dendritic cells leads to the up-regulation of MHC-peptide complexes and co-stimulatory proteins as well as the production of immunomodulatory cytokines, all this has a major role in T cell

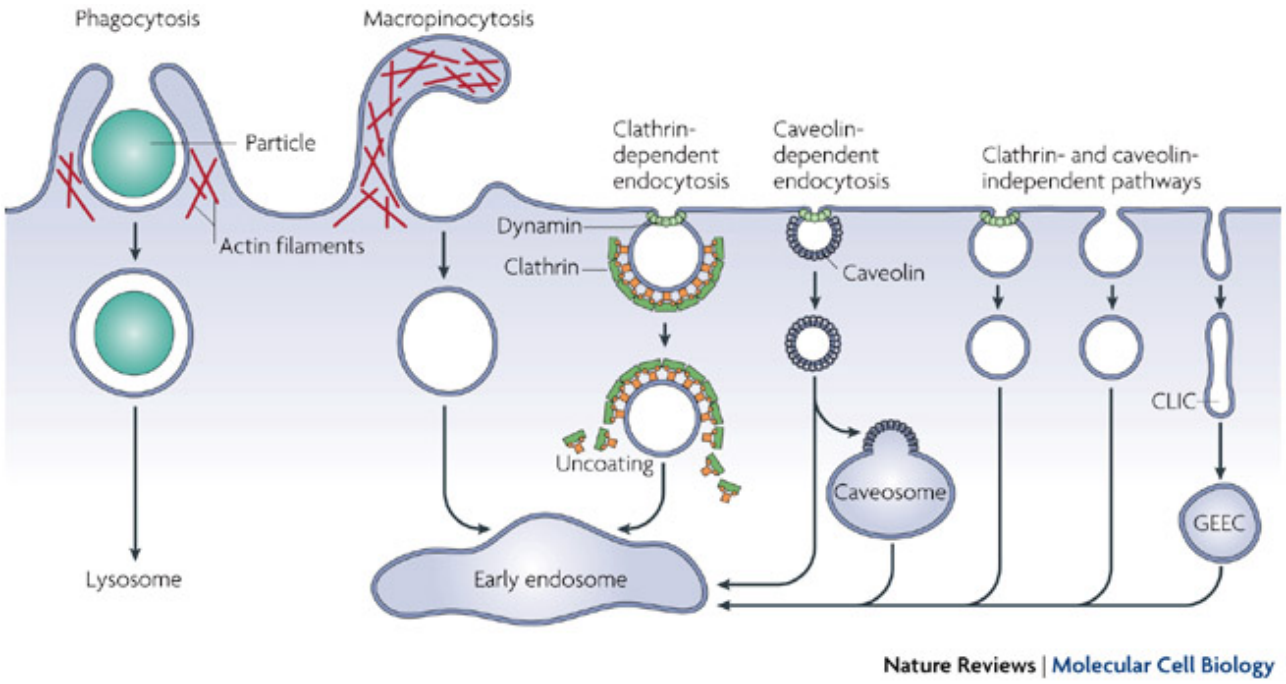

Figure 2.3: "**Pathways of entry into cells**. Large particles can be taken up by phagocytosis, whereas fluid uptake occurs by macropinocytosis. Both processes appear to be triggered by and are dependent on actin-mediated remodeling of the plasma membrane at a large scale. Compared with the other endocytic pathways, the size of the vesicles formed by phagocytosis and macropinocytosis is much larger. Numerous cargoes can be endocytosed by mechanisms that are independent of the coat protein clathrin and the fission GTPase, dynamin. Most internalized cargoes are delivered to the early endosome via vesicular (clathrin- or caveolin-coated vesicles) or tubular intermediates (known as clathrin- and dynamin independent carriers (CLICs)) that are derived from the plasma membrane. Some pathways may first traffic to intermediate compartments, such as the caveosome or glycosyl phosphatidylinositol-anchored protein enriched early endosomal compartments (GEEC), en route to the early endosome." Adapted from [Mayor 2007]

activation and differentiation. Another aspect of dendritic cells maturation is their upregulation of a chemokine receptor (CCR7) which through binding to the ligands CCL21, CCL19 directs mature dendritic cell migration towards the nearest lymphoid organs through the afferent lymphatic vessels [Weber 2013].

2.3.3 Dendritic cells migratory routes

From their birth until their death, migration is an intrinsic feature of dendritic cells. Hematopoietic stem and progenitor cells in the bone marrow give rise to many dendritic cells precursors including monocytes. Those precursors migrate from the bone marrow to the tissue or secondary lymphoid organs via the blood ([Alvarez 2008], [Geissmann 2010]). Fully differentiated dendritic cells are found in:

- tissues where they perform their role as sentinels. They accomplish their role by moving around and internalizing particles that will be processed for presentation.
- the blood stream from where they are recruited during inflammation or renewal of the tissue patrolling dendritic cells.
- secondary lymphoid organs such as the thymus where they performs their task in immature T cells selection.

Upon activation, mature dendritic cells migrate from the site of infection to the lymph node via the afferent lymphatic vessels.
The good performance of each of the cited task requires the ability of fully differentiated immature or mature dendritic cells to migrate as single cells in highly confining spaces such as peripheral tissues or lymphoid organs where the high density of cells and extracellular material imposes a high confinement. The success of dendritic cells migration then relies not only on chemical gradients but also on the cell as well as on the physical properties of the extracellular environment. The study of dendritic cell migration must then be put in the context of the physics of cell migration.

Chapter 3

The physics of cell migration

Contents

The study of the physics of cell migration raises two main questions:

1. How can a biological system such as a cell self organize and produce motion?
2. How is this motion modified by the physical landscape of the extracellular environment?

Answering to the first question requires to understand how a cell transfers its chemical energy to mechanical energy. While understanding the dynamic interaction between cells and extracellular environment can allow to answer to the second question. In both cases, it is important to understand the intrinsic physical properties of the cell as well as the extracellular space. Whole cell mechanics is the most well studied physical property of a migrating cell. Many techniques, ranging from micropipette aspiration to optical cell stretcher, have been developed to probe the cellular mechanical properties. We thus, begin to have a good understanding of this fundamental parameter of the cell. In the following sections, I will review our current knowledge on cell mechanics before describing some extracellular physical properties which can influence cell migration.

3.1 Cell mechanics in migration

At first glance, cells mechanical properties can seem contradictory. For instance, cells can maintain their shape under mechanical stresses (Leukocytes under flow), like solids, but also undergo reversible deformations (leukocytes during transmigration) like liquids [Starodubtseva 2011]. This fine tuning is possible through the remodeling of cellular components. A cell can be seen as a set of bio-polymers, organelles and proteins in an aqueous solution separated by a membrane from the extracellular space. Its mechanical properties are thus the result of the mechanical behavior of those components which comprise the plasma membrane, the cytosol, some big organelles such as the nucleus and the cytoskeleton ([Starodubtseva 2011], [Abu Shah 2013]).

3.1.1 The cytoskeleton as a load bearing structure

The cytoskeleton is a three dimensions network made of bio-polymers. Mechanical loads applied on the cell are supposed to be held by the cytoskeleton. As for other networks of bio-polymer, any deformation leads to a certain loss of energy in the form of heat [Starodubtseva 2011]. Therefore, the cytoskeleton is often described as a viscoelastic material meaning that it exhibits both elastic as well as viscous properties when it undergoes deformations.
Elasticity is a measure of the capacity of an object to come back to its original shape after deformation. The main elastic modulii used for the definition of cellular mechanical properties are the tensile modulus (Young's modulus E), the shear modulus (G), the bulk modulus (K) and the bending modulus (κ). The tensile modulus defines the response of an object under uniaxial tension while the bulk modulus describes the object deformation under compression. The bending modulus defines the

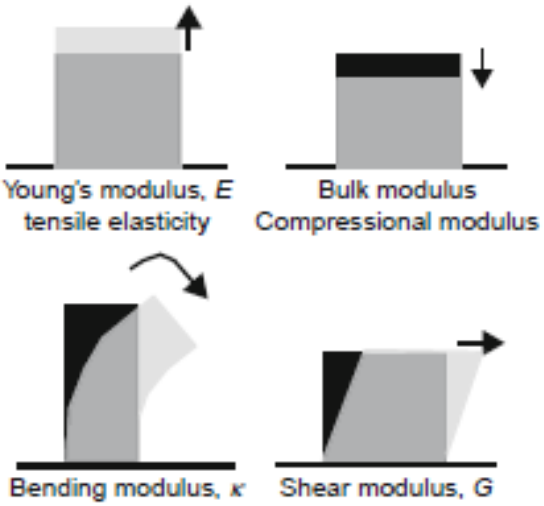

Figure 3.1: " **Main elastic modulii** Schematics showing the direction of the applied stress in several common measurements of mechanical properties; the light gray shape, indicating the sample after deformation, is overlaid onto the black shape, indicating the sample before deformation. The Young's modulus, or tensile elasticity, is the deformation in response to an applied tension whereas the bulk (compressional) modulus measures material response to compression. The bending modulus measures resistance to bending of a rod along its length and, finally, the shear modulus measures the response of a material to a shear deformation." From [Gardel 2008]

object resistance to bending along its length and the shear modulus sets the response of an object to a shear stress (illustrated in figure 3.1). Until now, most of the mechanical measurements of the cytoskeleton have focused on the shear elastic and on the shear viscous modulii. The shear elastic modulus measures how mechanical energy is store while the shear viscous modulus measures the dissipation of mechanical energy in a system. They are usually determined by the relation between the applied stress and the resulting strain. The cell contains three types of bio-polymers: actin filaments, microtubules and intermediate filaments. Their organization, dynamics and interaction plays an important role in the mechanical properties of a cell. In the following paragraph, I will describe the mechanical properties of those bio-polymers with a main focus on the actin cytoskeleton which has been at the heart of my PhD work.

3.1.1.1 The actin cytoskeleton

Actin is the most abundant protein in a cell where it can exist at as high concentration as 300 μM [Blanchoin 2014]. In most eukaryotic cells, globular monomeric actin (G-actin) assembles into dimers before polymerizing with a helical arrangement of the monomers [Pollard 2009] to form 5nm diameter filaments (F-actin) [Gardel 2008]. F-actin is a polar filament as actin subunits in the filament are oriented towards the same direction. It also has a fast growing end, the barbed end in opposition to the pointed end which elongates much slower [Pollard 2009]. ATP-G-actin dimers are added at

the barbed end, ATP is then hydrolyzed and releases a phosphate. ADP-G-actin is removed from the pointed end of the filament leading to depolymerization of the F-actin. ADP in the ADP-G-actin is exchanged for ATP making the G-actin available for another round of polymerization [Baum 2005]. F-actin length is regulated by capping proteins which through their binding to either the barbed or pointed end, prevent the adding or removal of G-actin. Severing proteins such as ADF/Cofilin, cleave actin filaments thus stopping the filament growth.

Because actin plays a central role in many cellular processes, it has been the subject of many studies. *In vitro* studies on single actin filaments measured a mean persistence length of 8-17 μm [Gittes 1993], a young modulus of 10^9 pascal ([Kojima 1994], [Gardel 2008]) and a buckling force (minimal force to apply for bending anactin filament) of 0.4 pN to 1.6 pN for a micrometer long filament [Berro 2007]. With such a persistence length of the order of magnitude of the cell diameter, actin filaments should behave like rigid rods inside the cell.

But inside cells, actin filaments exist in form of a network. By regulating the type of networks formed by actin filaments, cells are able to tune the local mechanical properties of the actin cytoskeleton. This regulation is achieved in cell by the regulation of the actin nucleators as well as actin crosslinkers.

In the following paragraph, I will describe the main actin nucleators and the resulting type of networks that have been describe in eukaryotic cells.

3.1.1.1.1 Actin polymerization: The main limitation to actin filaments formation inside cells is the nucleation step. Indeed, actin binding proteins such as profilin and thymosin-β4 which have a high binding affinity to G-actin, prevent the formation of actin dimers and oligomers thus the formation of filamentous actin [Pollard 2000]. The formation of actin filaments thus requires the contribution of other actin binding proteins called actin nucleators. Differents types of actin nucleators have been identified in the past twenty years: Arp2/3, Formins, Spire, cordon bleu and Leiomodin [Chesarone 2009]. They can be classify in three classes according to the way they induce polymerization. The first class of actin nucleators includes Arp2/3 which structurally mimics actin dimers to promote polymerization. The second class is composed of formins which stabilize already formed oligomers and thus promote their elongation. The third class contains Spire, cordon bleu and Leiomodin which, by recruiting and aligning actin monomers, induce polymerization [Chesarone 2009].

If the types of actin networks promoted by the first two classes of nucleators are well described, evidences are still lacking about the type of networks induced by the members of the third class of actin nucleators. In the following paragraphs, I will thus describe in more details the actin polymerization mechanism driven by Arp2/3 and formins as well as the type of network that result from this polymerisation.

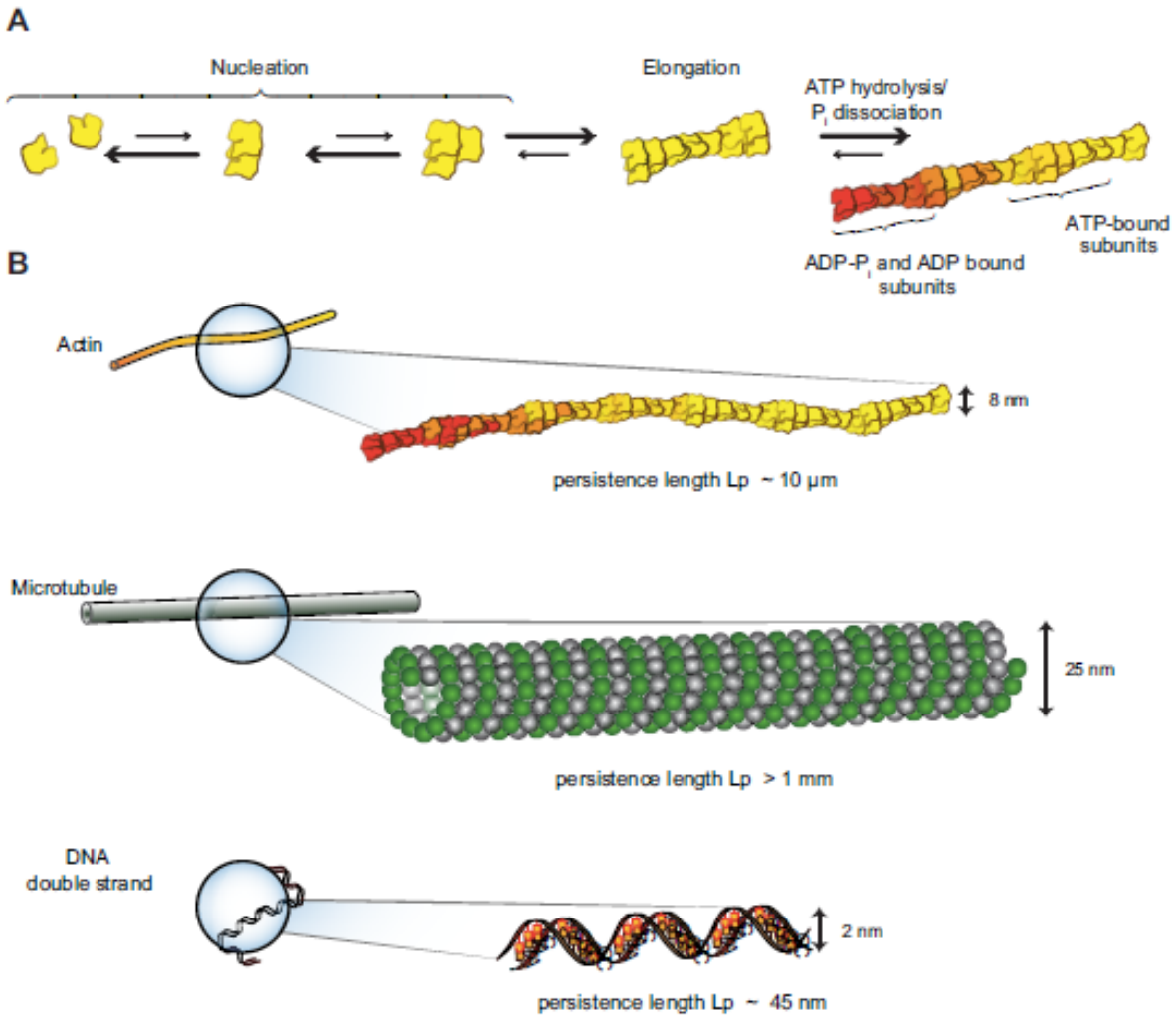

Figure 3.2: "**Single filament assembly and mechanics**.**A**) the kinetics of actin assembly. Actin polymerization from the pool of actin monomers happens in two phases. The thermodynamically limiting step for actin assembly, nucleation, is the formation of dimers and trimers. This is followed by rapid elongation at the more dynamic end, the barbed end, at $11.6\mu M.s^{-1}$, ATP hydrolysis in the filament at $0.3s^{-1}$, and phosphate dissociation at $0.0022s^{-1}$. **B**) persistence lengths of different cytoskeletal elements. Actin filaments are semi-flexible polymers with a diameter of $8nm$ and a persistence length of $10m$. Microtubules are rigid with a diameter of $25nm$ and a persistence length greater than $1mm$. For comparison, double-stranded DNA are flexible molecules with a $2nm$ diameter and a persistence length of $45nm$." From [Blanchoin 2014]

3.1.1.1.1.1 Arp2/3 based actin networks: Arp2/3 complex was first discovered twenty years ago [Machesky 1994] as a profilin (see 3.1.1.1.1) ligand. It consists of a complex of seven subunits (ARP2, ARP3 and ARPC1-5) with two of them being actin related proteins (Arp2 and Arp3). Once activated by a nucleators promoting factors (NPFs), the Arp2/3 complex catalyzes the polymerization of a new, "daughter" filament from the side of a "mother" filament with a characteristic $70° \pm 7°$ angle [Mullins 1998]. The newly formed filament is capped at its pointed end by the Arp2/3 complex while its barbed end is free to elongate. This is the first step toward a branched actin network.
The precise mechanism of actin nucleation by Arp2/3 is still unknown. Two main models are proposed according to the type of NPFs involved in Arp2/3 activation.

The best understood NPFs are the members of the family of the Wiskott-Aldrich Syndrome protein (WASP) and suppressor of cyclic AMP repressor (SCAR; also called WASP-family verprolin-homologous protein (WAVE)) [Goley 2006]. WASP, neural WASP (NWASP), WASH, WAVE are members of the class I NPFs family which possess a well conserved WCA domain composed of a WASP-homology-2 domain (WH2 or W), a central domain (C) and an acidic domain (A). The WH2 domain binds to G-actin while the CA domain mediates the binding to Arp2/3 [Goley 2006].
Even though many evidences are still lacking, the most common and well accepted model for class I NPFs-Arp2/3 actin nucleation is the following: the acidic region mediates binding to Arp2/3, the central region initiates an activating conformational change in the Arp2/3 complex that brings Arp2 and Arp3 closer to each other possibly to mimic a dimer, and the WH2 and central regions present an actin monomer to the complex, facilitating the formation of a nucleus for the polymerization of the daughter filament ([Goley 2006], [Chesarone 2009]).

The second class of NPFs includes cortactin and its mechanism of Arp2/3 activation is less well understood. Indeed, if these NPFs conserve the Arp2/3-binding acidic region, they lack the G-actin binging region. They instead contain an F-actin binding region. Moreover, cortactin fails to activate a conformational change in the Arp2/3 complex when it is bound to such NPF. Therefore, the role of the class II NPFs would be to stabilize the branching organization of the actin network generated by Arp2/3 [Goley 2006] rather than activating this actin nucleator.

The activation of Arp2/3 by NPFs requires another layer of regulation which goes through the activation of the NPFs. Indeed, the activation of members of the class I NPFs requires the action of members of the Rho-GTPases familly, kinases and/or phosphatidylinositols [Rotty 2013]. For instance, the most well studied NPF, WASP/NWASP exists in an autoinhibitory state where its WCA domain is tightly bound to its GTPase-binding-domain (GBD). This state can be overcome by the binding of the Rho-GTPases (RAC, CDC42) to the WASP-GBD domain which then releases the WCA domain thus allows the binding of WASP/NWASP to Arp2/3.

Interestingly, WAVE, another member of the class I NPFs does not posses a GDB which complicates the understanding of its regulation by GTPases. WAVE exists in a complex of five different proteins called the WAVE regulatory complex (WRC). WAVE stays inactive in the WCR where its C and A regions are sequestered by parts of the complex particularly the Specifically RAC1-associated protein 1 (SRA1). The actual model of WAVE activation is that the binding of RAC1 to the SRA1 domain of the WRC, would release the WCA domain of WAVE allowing its binding to Arp2/3 ([Rotty 2013], [Chen 2010]).
Even though many missing points exist in our actual understanding of Arp2/3 activation, the tight regulation of this process already indicates how important it is for the cell to be able to control the type of network which will be generated at a specific place.

3.1.1.1.1.2 Formins based actin networks Formins form a large family of several proteins whose role in actin polymerization was described in 2002 [Breitsprecher 2013]. They are characterized by their formin homology 1 and 2 domains at their C-terminus (FH1 and FH2 respectively). The FH2 domain has been shown to promote the nucleation of actin filaments *in vitro* ([Pruyne 2002], [Sagot 2002]). The proposed mechanism of actin nucleation by formins relies on the high binding affinity of the donut-shaped FH2 domain to the barbed end of F-actin [Chesarone 2009]. Because the FH2 domain lacks detectable binding affinity to G-actin, it has thus been proposed that formins promote actin polymerization by stabilizing spontaneously formed actin dimers or trimers. After polymerization, the formin FH2 domain stays at the barbed end of F-actin and moves progressively with the barbed end allowing rapid G-actin insertion ([Chesarone 2009], [Breitsprecher 2013]).
This current model of FH2 based actin nucleation is under controversy. Indeed the FH2 domain based actin nucleation was shown to be very inefficient with profilin bound G-actin which is the most available actin substrate *in vivo* [Chesarone 2010]. However, one hypothesis which would support the FH2 based actin nucleation theory is the recruitment of G-actin by sequences at the C-terminus of the FH2 side [Chen 2010] or by FH2 partners (in the same way than class I NPFs bind G-actin and Arp2/3). If there are some evidences of the existence of formins regulators which bind to G-actin (bud 6 a *Saccharomyces cerevisiae* polarity factor [Moseley 2004]) a direct proof of such a mechanism is still lacking. Therefore, the mechanism of Formin based actin nucleation is still far from being understood.
Another well studied role of Formins in actin polymerization involves filaments elongation. Indeed, the high affinity of the FH2 domain to the filament barbed end protects the filament from capping proteins which would stop the barbed end growth. In addition to this, the ability of the FH1 domain to recruit profilin-G-actin complex facilitates the insertion of G-actin in the growing barbed end. The combination of both interactions leads to an increase of the barbed end elongation rate by as much as 5-folds compared to free barbed ends ([Chesarone 2009], [Breitsprecher 2013]).
If the FH2 based actin nucleation is under debates, the role of Formins in F-actin elongation is very

well accepted. Thus the impact of formins on filament growth is also well accepted.

To nucleate or elongate actin filaments, Formins need to be activated. Indeed, Diaphanous-related formins (DRFs), the most abundant and well studied vertebrate Formins exist in an autoinhibitory state in the cytosol. This autoinhibitory state is achieved through the binding of the C-terminal Diaphanous autoregulatory domain (DAD) to the N-terminal Diaphanous inhibitory domain (DID) [Breitsprecher 2013]. This interaction which is proposed to sterically obstruct FH2 interaction with actin, inhibits the ability of the FH2 domain to nucleate actin assembly *in vitro* as well as *in vivo* [Chesarone 2010].
The exit from this autoinhibition state requires the activity of Rho-GTPases family members. Indeed, Formins such as DRFs contain a GBD which allows the binding of the DRFs to a GTPase and thus the release of the DID-DAD interaction. However, the complete release of the DID-DAD interaction by Rho-GTPases binding was shown *in vitro* to require high Rho-GTPases concentrations which may not be physiological [Chesarone 2010]. This suggests the existence of other co-regulatory proteins involved in formins activation.
Even though the details of Formin based actin network generation are not fully understood, many studies converge towards a major role of formins in the generation of bundled actin networks. Such networks play a critical role in force generation and in cell migration.

3.1.1.2 Actin networks and their mechanical properties

Actin networks are usually crosslinked in migrating cells. Indeed, the lammelipodium at the leading edge is made of branched actin networks, the contractile fibers (stress fibers and transverse arcs), are based on bundled actin filaments. The combination of branched and bundled filaments is found in the cortex and to some extent at the leading edge, between the lammelipodia and the filopodia (see figure 3.3).

The global effect of crosslinkers in an actin network is to link actin filaments together. Some crosslinkers such as Myosin II or Fascin will keep the filaments aligned creating a bundled network while others such as $\alpha-$actinin, Filamin and Fimbrin will entangle the filaments leading to a branched actin network. It is also interesting to underline the role of Arp2/3 in network generation.

Figure 3.3 *(facing page)*: "*Actin structures in moving cells.* Overlay of actin architecture and mechanics in the moving cell. **A**): schematic representation of the cell with the different architectures indicated: i) the cell cortex; ii) an example of a contractile fiber, the stress fiber; iii) the lamellpodium; and iv) filopodia. The zoom regions highlight architectural specificities of different regions of the cell. **B**): overlay of the actin architecture and its mechanical profile. The red rectangles are the shock absorbers (dashpots) that represent the actin network, while the green circles are active springs due to myosin motor activity." (From [Blanchoin 2014])

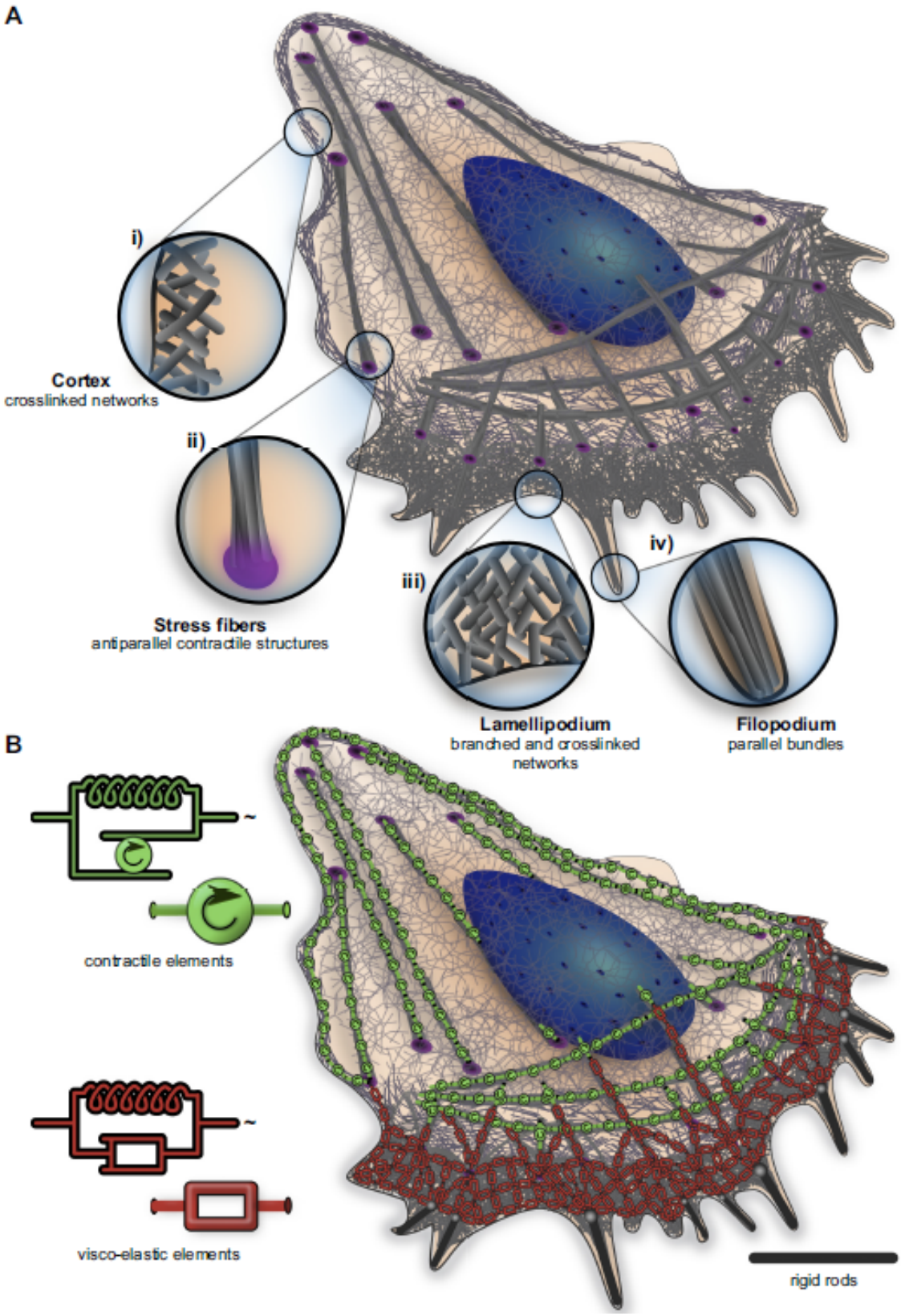
A
i)
Cortex
crosslinked networks
ii)
Stress fibers
antiparallel contractile structures
iii)
iv)
Lamellipodium
branched and crosslinked networks
Filopodium
parallel bundles
B
contractile elements
visco-elastic elements
rigid rods

[h]

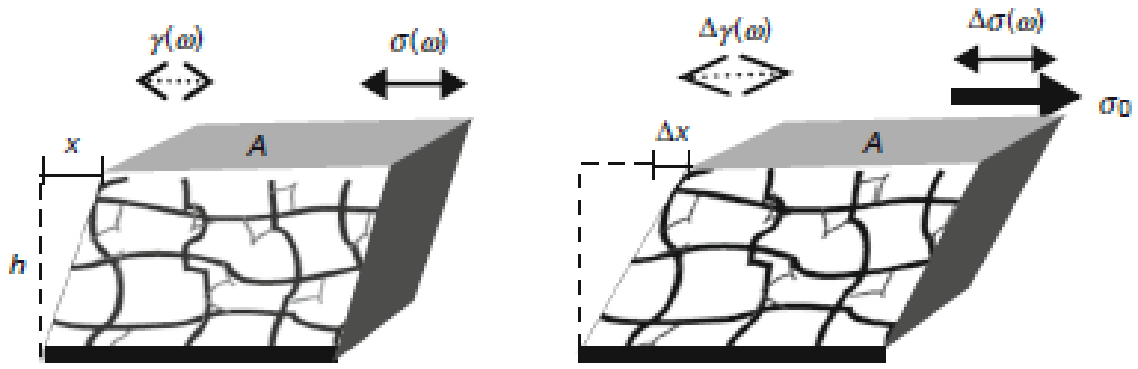

Figure 3.4: " **Determining viscoelastic properties of a polymer network**. (Left) To measure the shear elastic modulus, $G'(\omega)$, and shear viscous modulus,$G''(\omega)$, an oscillatory shear stress, $\sigma(\omega)$, is applied to the material and the resultant oscillatory strain, $\gamma(\omega)$ is measured. The frequency, ω, is varied to probe mechanical response over a range of timescales. (Right) To measure how the stiffness varies as a function of external stress, a constant stress, σ_0, is applied and a small oscillatory stress, $(\Delta\sigma(\omega))$, is superposed to measure a differential elastic and viscous loss modulus." From [Gardel 2008]

Arp2/3 based nucleation can induce either branched or bundled actin networks. Indeed, many *in vitro* experiments have shown that Arp2/3 based actin nucleation leads "by default" to the creation of "unbranched" networks in which freely growing actin filaments will self-organize in bundles ([Svitkina 2003], [Akin 2008], [Achard 2010], [Reymann 2010]). Arp2/3 based actin nucleation can also lead to branched actin networks formation. But in order to generate such a branching from Arp2/3 nucleation, capping proteins are necessary. Indeed, capping proteins, by inhibiting elongation of actin filaments promote branching of the network ([Akin 2008],[Blanchoin 2014]). Arp2/3 in synergy with capping proteins gives rise to highly dense branched networks [Blanchoin 2014] whose mechanical properties have been the subject of many studies.

3.1.1.2.1 Actin networks mechanical properties In order to define the mechanical properties of actin networks, various rheological as well as microrheological experiments have been designed since the 1980s. The classical rheological experiments consist in the application of a sinusoidal stress (periodic force per unit surface) on the overall network and the measurement of the resulting strain (a dimensionless parameter which measures the displacement divided by the displacement over which the deformation is applied). In microrheological experiments, the displacement of beads inside the network is measured.

From those experiments, the parameters G' and G" which define the rheological properties of the network are determined (see figure 3.4). G', the shear elastic modulus shows the elastic response of

the network by measuring how the mechanical energy is stored in the network. G", the shear viscous modulus measures the viscous properties of the network by measuring how the mechanical energy is dissipated in the network.

The mechanical property of crosslinked network is a function of the length and density of F-actin, the density of crosslinkers as well as their affinity to F-actin. According to those parameters, the network will store the mechanical energy in different ways. For example, a dense network with long actin filaments, containing a high concentration of static (high affinity to F-actin) crosslinkers will respond to a load by stretching the filaments in the network. The other extreme case is a loose network with short actin filaments containing a low concentration of static crosslinkers which would break the filaments under load [Gardel 2008].
For crosslinked actin network, G' and G" depend on the amplitude as well as the frequency of the load. At low amplitude, the response to an applied load is linear, dominated by G" at low frequencies (i.e. corresponding to short timescale) and by G' at higher frequencies (i.e. corresponding to long timescale). This means that a crosslinked F-actin network is viscous at high frequencies ($\prec$ 0.1Hz) and elastic at low frequencies. At higher amplitudes, the response of the network become nonlinear ([Storm 2005], [Stricker 2010]). Phenomena such as stress-stiffening or stress-softening can then occur [Stricker 2010]. In a stress-stiffening network, the elastic modulus G' will increase in a nonlinear manner when the applied stress exceeds a given value. In a stress-softening network, G' will start decreasing in a nonlinear manner above a given stress. The stress-stiffening property of a network arises from its entropic elasticity ([Storm 2005], [Pujol 2012]). Indeed, networks dominated by their entropic elasticity will resist to an applied stress by changing their configuration (rearrangement of filaments and crosslinkers). Above a given stress when no more configuration is available, the network will thus exhibit a high resistance to any deformation, which explain the drastic increase of G' with stress. When a network is dominated by its enthalpic elasticity, it will respond to a stress by stretching, compressing or bending the constituting filaments. Above a given stress, filament will buckle leading to a drastic decrease of the elastic modulus G' with stress thus stress-softening.
Many crosslinked actin networks have been shown to stress-stiffen in a manner qualitatively independent of the type of crosslinkers ($\alpha-$actinin, filamin, scruin) [Stricker 2010]. The transition between the linear and the nonlinear response occurs usually at $5-30\%$ of strain and with a typical two-fold increase in the shear elastic modulus before network dis-assembly. The elastic properties of the crosslinker can have an impact of the stiffness increase during the nonlinear response. Indeed, in the case of filamin crosslinked networks, a hundred-fold increase of G' has been measured. Filamin being a large protein, its compliance is believed to play a critical role in the network elasticity [Gardel 2008].
In the following paragraphs I will describe the mechanical properties of the two specific types of

crosslinked networks studied in migrating cells: the branched (dendritic) and the unbranched actin networks.

3.1.1.2.2 Mechanical properties of dendritic actin network The Arp2/3 branched actin network is a specific crosslinked network in which the crosslinker has an impact on the rate of growth of the network.

Arp2/3 branched networks are similar to other crosslinked actin networks: they are viscoelastic materials which undergo stress-stiffening [Chaudhuri 2007].

The typical measured linear shear elastic modulus (G') is on the order of 1kPa at 5 Hz [Chaudhuri 2007] for *in vitro* measurements in a cell extract. G', in the linear regime, can increase as a function of the Arp2/3 or capping proteins concentration [Pujol 2012], meaning that increasing the branching increases the stiffness of the network.

This linear regime persists until 15Pa of stress. Above such stresses, the network undergoes a stress-stiffening transition. This stress-stiffening regime persists for stresses up to 300 Pa.

Interestingly Arp2/3 branched networks exhibit a stress-softening regime following the stress-stiffening one (See figure 3.5). This stress-softening behavior was shown to be reversible which is in contradiction with the classical view of stress-softening materials. Indeed, because the softening is due to the enthalpic elasticity, it was believed to be associated to irreversible changes in the network such as filaments breakage or crosslinkers detachment. The reversible stress-softening behavior of dendritic network was then proposed to be due to filaments buckling. Under a critical stress, individual filaments would start buckling without leaving the network because of the dendritic organization. Thus when the load is remove, filaments would unbuckle giving rise to the reversible stress-softening behavior.

3.1.1.2.3 Mechanical properties of unbranched actin network Two types of bundled actin networks can be observed in migrating cells: the parallel actin bundles and the antiparallel actin bundles.

In the parallel actin bundles, all actin filaments have their barbed ends oriented in the same direction while in antiparallel actin bundles the barbed end of one filament will be in the opposite direction of the barbed end of the next filament.

Actin filaments in bundled networks are maintained in close contact via crosslinkers such as fascin or $\alpha-$actinin for parallel bundles and MyosinII for antiparallel bundles. Such networks are sensitive to two types of mechanical load: compression and stretching (shear stress). Bundled networks resist compression in a similar manner than single filamentous actin do. They possess a bending modulus which can be defined by their effective persistence length. This persistence length varies as a function of the number and length of filaments in the bundle but also as a function of the crosslinker

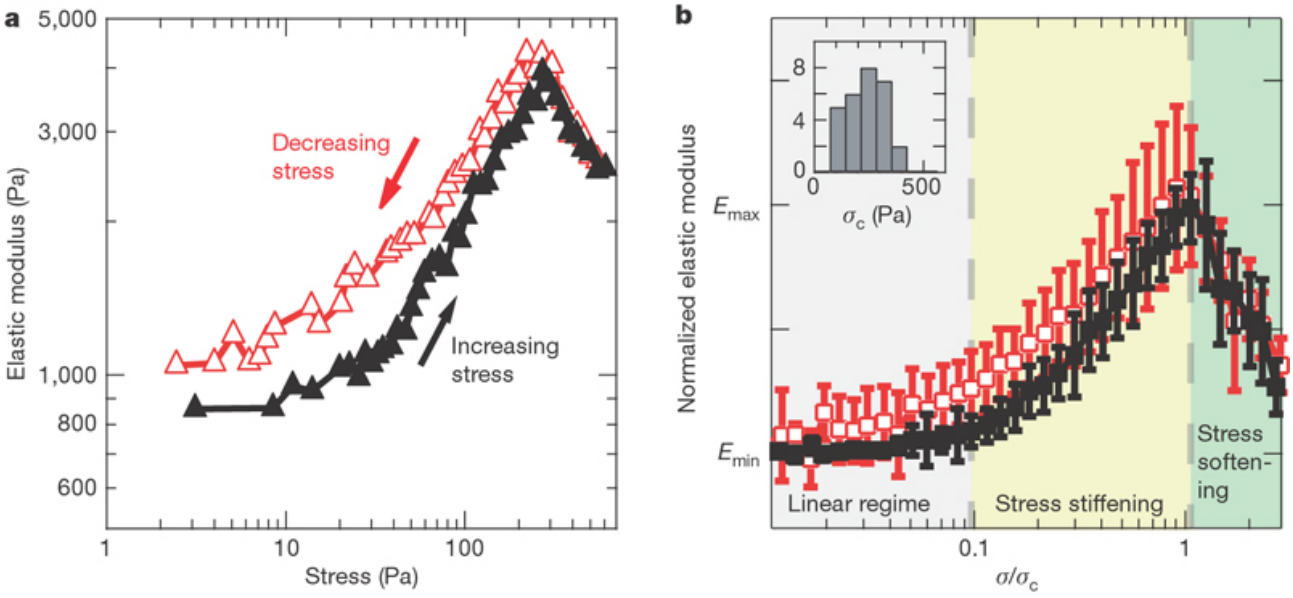

Figure 3.5: "**Dendritic actin networks exhibit stress stiffening and reversible stress softening**. a) In a typical nonlinear elasticity measurement, the stress on the network is first increased incrementally (black trace) to and then decreased incrementally from a maximum stress (red trace) of 600 Pa, with the elasticity measured at each stress at 5 Hz. The elasticity remains constant for stresses up to 15 Pa and then increases in a stress-stiffening regime. For stresses above the critical stress σ_c of 270 Pa, the elasticity decreases in a stress-softening regime that is reversible, as indicated by the overlay of the black and red traces. b) Averaged and normalized trace of the nonlinear elasticity of actin networks. Each individual measurement was normalized by the difference between the elasticity before the measurement Emin and the maximum elasticity for increasing stresses E_{max} and σ_c . The results of 28 different measurements from 12 separate experiments were averaged together (mean ± s.d. shown) and found to exhibit three distinct regimes of elasticity: linear, stress stiffening and stress softening. The stress softening is shown to be reversible. Note that the elasticity in b) is shown on a linear scale while the elasticity in a) is shown on a log scale. The inset shows a histogram of σ_c for which the mean value was 233 Pa." From [Chaudhuri 2007]

dissociation rate. Indeed, static crosslinkers, by inhibiting the sliding of filaments, leads to a network with higher effective persistence length than a network with dynamic crosslinkers [Blanchoin 2014]. Therefore the dissociation rate of the crosslinker defines the buckling force (the force above which the network will buckle) of the bundle as this force is proportional to the effective persistence length.

A bundled network subjected to shear stress behaves qualitatively like crosslinked network. They exhibit a linear viscoelastic response at low stress followed by a stress-stiffening behavior at higher stress ([Lieleg 2007], [Gardel 2008], [Stricker 2010]). This stress-stiffening regime is followed by a stress-softening regime. Above a given stress the crosslinker will be forced to detach leaving the actin filaments free to slide. Interestingly, the concentration of crosslinkers plays a crucial role in the transition between linear to non linear regime. Increasing the crosslinkers concentration decreases the stiffness variation during the stress-stiffening regime [Lieleg 2007]. On highly crosslinked bundles, a mechanical load will force the crosslinkers to unbind before the stress-stiffening regime occurs. A mechanical load can thus affect the dissociation rate of F-actin crosslinkers ([Lieleg 2007], [Gardel 2008], [Stricker 2010]).

3.1.1.2.4 Force production by actin networks Actin based force generation is a crucial process in cell migration. For instance, the membrane protusion at the leading edge is based on either branched actin networks generation for the lamellipodium or bundled networks in filopodia. Bundled networks are also found in stress fibers as well as in the transversal arcs which are important for the dynamic interaction between the migrating cell and its environment.
Two types of forces can be generated by the actin cytoskeleton: contractile and protrusive forces

3.1.1.2.4.1 Contractile forces Contractile forces are necessary for cellular retraction during migration. The best studied contractile force generation process is based on Myosin II action.
Myosin II is a hexamer with two long heavy chains, two regulatory light chains and two essential light chains. The two heavy chains dimerise through their coiled-coil rod domain forming the hexamer. Multiple hexamers assemble to form a minifilament which binds to actin through the head domain of the heavy chains. This minifilament organization is essential for high force generation as it converts the unipolar, non processive hexamer to a bipolar and highly processive machine.
The head domain of each heavy chain has an ATPase activity. ATP hydrolysis induces a conformational change in the head domain of the heavy chain which leads to F-actin displacement. After ADP release and replacement by ATP, the head domain detaches from the previous actin filament and is free to bind to another filament which will be displaced during the next cycle of ATP hydrolysis. Those cycles of head domain attachment and detachment leads to the general contraction of the network [Aguilar-Cuenca 2014].
The binding of Myosin II on actin filaments requires Myosin II activation. Myosin II exists in an au-

toinhibitory state during which a head-head and head-tail association inhibits the F-actin binding and the ATPase activity of the head domain. This autoinhibitory state can be overcome through biochemical as well as mechanical signals. The best known biochemical activation of Myosin II is through the phosphorilation of the regulatory light chain. Indeed, phosphorylation of the RLC in the residues serine 19 and threonine 18 induces the unfolding of the hexamer which releases the inhibition. Numerous kinases operate in different pathways to induce this phosphorylation. Amongst the best studied kinases involved in the RLC phosphorylation are the Rho kinase and citron kinase activated by the Rho-GTPase RhoA and the myotonia dystrophy-related Cdc-42-binding kinase (MRCK) activated by the Rho-GTPase CDC42 [Lecuit 2011]. Mechanical forces have also been shown to promote Myosin II activation by extending the motor interaction with actin filaments [Aguilar-Cuenca 2014].
Thus, using either chemical or mechanical energy, the cell might be able to tightly regulate the direction and amplitude of the contractile force exerted on the extracellular environment.

3.1.1.2.4.2 Protrusive forces Protrusive forces are at the basis of membrane protrusion and are usually generated by actin polymerization. Bundled/parallel actin networks can produce protrusive forces. This forces has been shown to be in the range of 1-3 pN for single filopodia [Cojoc 2007]. Branched networks such as found in the lammellipodium have been shown to generate higher protrusive forces than filopodia. Indeed, the comparative study of lamellipodia and filopodia pushing forces measured 20 pN for lamellipodia but not more than 3 pN for fillopodia [Cojoc 2007]. However, the measurement of forces generated by the lamellipodium are divergent. Some studies reported forces of the order of a few pN per micron [Bohnet 2006] while others reported high forces in the range of several hundreds of pN per micron [Prass 2006]. This high variability can be explained by the difference in experimental methods which would probe different adhesiveness of the cell to the experimental set up [Stricker 2010]. In vitro experiments have also shown that branched actin network can generate high forces which can be used for motility.

3.1.1.2.4.3 An exemple of actin based motility: actin comet tails One striking example of a motility machinery totally based on branched actin network is the one used by the pathogen *Listeria Monocytogenes*.
Listeria monocytogene as well as *Shigella flexneri*, and *Rickettsiae* hijack the host cell actin machinery to move and invade other cells. Listeria cells, in particular, use the Arp2/3 based actin nucleation machinery to propel through the cell by generating a comet tail at the back of their body. The listeria protein ActA by mimicking N-Wasp, activates the Arp2/3 complex at its surface leading to actin polymerization [Welch 1998].
Such machinery has been reconstituted *in vitro* using a minimal system [Loisel 1999] to study the physical properties of this actin based motility [Marcy 2004]. Indeed, using beads coated with nucleator promoting factors in solution with Arp2/3, actin, capping proteins, profilin and severing proteins

(depolymerizing factors such as ADF/Cofilin), many labs where able to induce beads motility qualitatively similar to Listeria propulsion in infected cells .
The generation of movement in such system goes through 3 steps [Akin 2008]:

1. Actin filament nucleation occurs around the bead with incorporation of new actin monomers at the surface of the bead. This leads to the assembly of dense spherically symmetrical actin shell around the bead.

2. Within minutes, the actin shell breaks leading to the formation of the polarized comet tail.

3. During the first 30 mns, the bead moves in the opposite direction of the comet tail at speeds around 5 $\mu m/mn$.

4. The system get's in a stationary phase during which the bead moves at a constant, lower velocity.

The symmetry breaking of the actin shell define the onset of beads propulsion. This process is based on the release of the gel elastic energy [Gucht 2005]. Indeed, because filaments elongation occurs at the surface of the bead, a strain is built up in the gel giving rise to a tensile stress at the surface of the gel [Gucht 2005]. Because of the nonlinear behavior of the dendritic network, the gel will stress-soften above a given stress leading to the symmetry breaking [Chaudhuri 2007], [Marcy 2004].
The resulting propulsive force will drive the high velocity motility. In the stationary phase, adding new filaments at the surface of the bead will just keep propelling it. The velocity would then be a function of the actin polymerization speed.
By hijacking the Arp2/3 based actin nucleation machinery, *Listeria Monocytogenes* found a sophisticated way to use the mechanical properties of the dendritic network for their invasion.

3.1.1.3 The microtubule network

Microtubules are the second major cytoskeletal components. They are formed after polymerization of $\alpha-$ and $\beta-$tubulins dimers in protofilaments. Thirteen protofilaments assemble in a hallow cylinder and form microtubules.
Microtubules are polar filaments. They posses a rapidly growing end called the plus end while the other end is called minus end. This polarity confers a direction to the microtubules associated motors such as kinesins which will bind/move either on/towards the plus or the minus end of the microtubules. In cells, the minus end is bound to structures called microtubule organizing centers (MTOCs). In interphase cells (such as dendritic cells), the MTOC is localized next to the nucleus. This MTOC-nucleus orientation is often used as marker of cell polarity.
Microtubules are very dynamic filaments which undergo multiple phases of growth and catastrophe. This alternation of polymerization and depolymerization at the plus end gives rise to the dynamic instability of microtubules [Mitchison 1984].

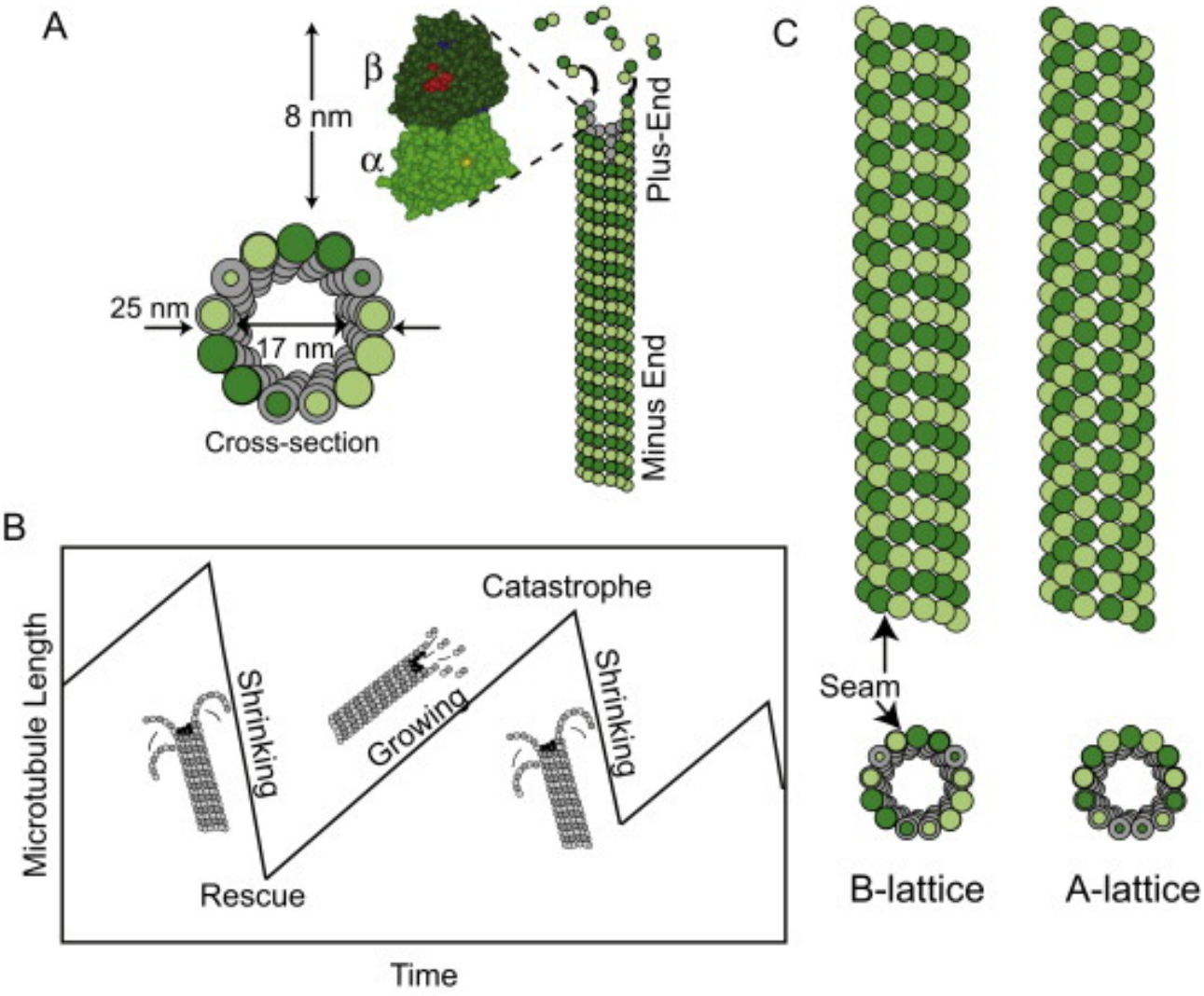

Figure 3.6: "**Microtubule structure and dynamics** (A) Microtubules are polymer filaments made from tubulin dimers. The tubulin heterodimer is made of a beta (dark green) and alpha subunit (light green). A few hundred dimers bind together to nucleate the polymer, and individual dimers add on to the ends to grow the microtubule. The plus-end is the more dynamic and rapidly growing and shrinking end. The minus-end is less dynamic. The microtubule is a tube with an outer diameter of 25 nm and an inner diameter of 17 nm. (B) Microtubules grow by the addition of dimers and shrink by the loss of dimers. Stochastic transitions from shrinking to growing are called "rescues." Stochastic transitions from growing to shrinking are called "catastrophes." Microtubules are more stable if they have reduced catastrophes and increased rescue frequencies. (C) Microtubule B-lattice and A-lattice. In B-lattice, the alpha (light green) touches a neighboring alpha except at the seam. In A-lattice, the alpha (light green) touches the beta (dark green) throughout the lattice. There is no seam in A-lattice." From [Hawkins 2010]

Many studies have been performed to measure single (or bundled) microtubules mechanical properties (see [Hawkins 2010] for a review). Most of those studies have focused on measuring the microtubules flexural rigidity (the bending rigidity multiply by the thickness). Different measurements using various experimental set-up estimated a mean microtubule flexural rigidity of 10^{-24}, similar to the carbon nanotubes [Hawkins 2010]. This measured rigidity corresponds to a persistence length of 1-10 *mm* which is much longer than the cell typical diameter. Because of their long persistence length combined to a high bending rigidity, microtubules are perceived as stiff filaments at the cell scale.
In vitro, microtubules networks are reported to exhibit a soft elastic gel behavior with a shear elastic modulus of few pascals ([Janmey 1991], [Lin 2007]). More recent works on crosslinked microtubule networks proposed a stiffening of the network at low stress followed by its softening at higher stresses [Yang 2013]. This behavior, characteristic of crosslinked networks, shows the rearrangement (disruption of previous bonds and formation of new ones) of the network under high stress.
In cells, microtubules form tracks on which motor proteins move to transport cargos. Their high binding rigidity might be necessary in this context. But a role of this high bending rigidity in the overall cellular mechanical properties is still unknown. Indeed, only few studies on the mechanical properties of microtubule networks *in cellulo* are available. This is primarily due to technical limitation as microtubules form a very dense network inside the cell which makes it hard to probe individual microtubules . On top of this, the crosstalk between the microtubule network and the actin cytoskeleton makes it more difficult to assess the specific impact of microtubules in cellular mechanics ([Hawkins 2010], [Gardel 2008]).

3.1.1.3.1 Crosstalk between microtubules and actin: In a living cell, microtubules are in a continuous cross talk with the actin cytoskeleton and the intermediate filaments (visualized in figure 3.7). Many proteins linking actin filaments to microtubules have been discovered and microtubules dynamics can also affect the mechanical properties of the actin cytoskeleton [Preciado López 2014]. Indeed, Formins, which have been described as actin nucleator/elongator are also known to regulate microtubules organization and dynamic. For instance, constitutively active mDia have been shown to regulate co-alignment of microtubules and actin fibers ([Ishizaki 2001]), to promote the targeting of microtubules to the cell periphery and to stabilize them [Breitsprecher 2013]. This Formin interaction with microtubules is actin independent as mutants of mDia which fail to polymerize actin can still bind to and stabilize microtubles [Chesarone 2010]. Thus Formins, by regulating both the actin cytoskeleton and the microtubule network, can change the whole organization of the cytoskeleton.
In a mechanical point of view, networks of actin and microtubules show very interesting behaviors. For example, the actin cortex have been shown to reinforce microtubules against buckling [Lin 2011]. *In vitro* reconstruction of composite networks of actin filaments and microtubules have shown that adding microtubules, even at very low concentration, to an actin network drastically changes the viscoelastic properties of the actin network [Lin 2011]. Indeed adding microtubules to an actin network

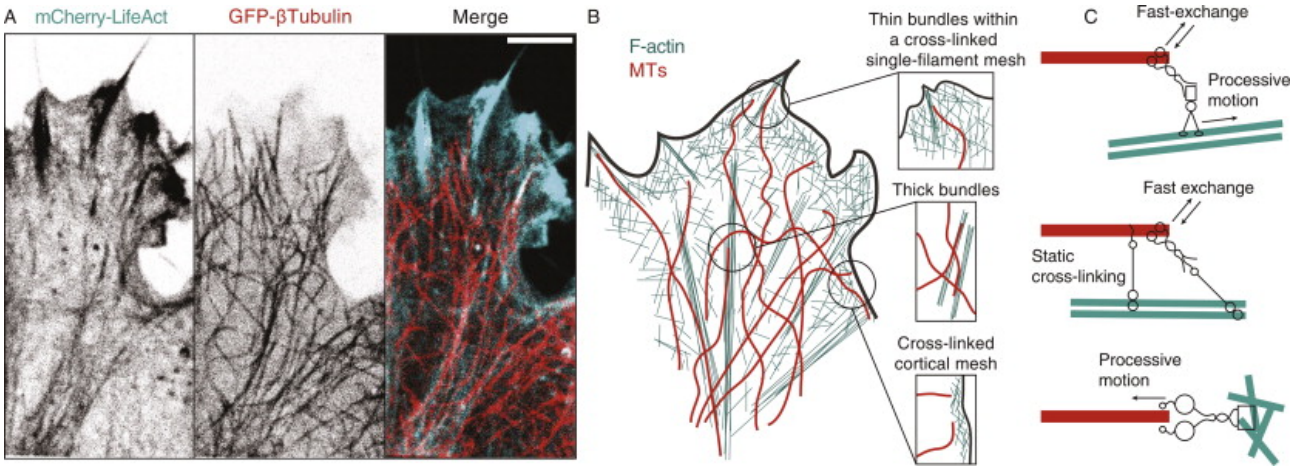

Figure 3.7: "*In vivo coorganisation of F-actin and microtubules*. A) Fluorescence micrograph of part of a 3T3 fibroblast with fluorescent labels showing the distinct organization of F-actin (cyan) and microtubules (red). Actin forms rigid stress fibers and dense networks underneath the plasma membrane (top), whereas microtubules grow toward the cell periphery and form a sparse network. B) Schematic showing how dynamic microtubules can encounter different F-actin architectures within a cell. C) Conceptual drawings of the different types of F-actin-microtubule cross-linking proteins and protein complexes, classified based on their activities (e.g., processive motion) and exchange properties (e.g., slow vs. fast). Scale bar: 5 μm." From [Preciado López 2014]

crosslinked with scruin (static crosslinker, the network behaves like and elactic solid [Stricker 2010]) changes the normal strain-softening behavior of the network to a strain stiffening network [Lin 2011]. It is interesting to observe that combining two networks with intrinsic strain-softening behaviors (microtubules in one hand and scruin crosslinked network in other hand) gives rise to a strain-stiffening network. Microtubules can also regulate actin networks in a more molecular scale. Indeed, the small GTPase RhoA which mediates Formins and Myosin II activation have been shown to be activated upon microtubules depolymerization. Indeed, a guanine exchange factor, GEF-H1, which activates RhoA normally binds to microtubules and upon microtubules depolymarization get released in the cytoplasm leading to RhoA activation [Krendel 2002]. This subsequent RhoA activation leads to an increase in cellular contractility. Thus microtubule dynamics can control, locally, the type of actin network in the cell.

Migrating cells, by controlling the crosstalk between the actin cytoskeleton and the microtubule network could refine their mechanical properties. They can indeed regulate the amount and the type of forces they will generate by controlling the stability of microtubules in an actin network. They can also modulate their response to a mechanical load by changing the non-linear response of the actin network through microtubules growth inside this network.

3.1.1.4 The intermediate filaments

The intermediate filaments are the third members of the cytoskeleton family. Their discovery dates back to the 1970s when Weber and coworkers visualized vimentin in mouse 3T3 cells [Franke 1978]. They were named intermediate filaments for geometrical reasons as their characteristic diameter of 10 nm is in between the one of actin filaments (6-7 nm) and of microtubules (25 nm) [Buehler 2013].The type of intermediate filament expressed is cell type dependent. Indeed, migrating cells such as fibroblasts and endothelial cells express vimentin while epithelial cells highly express keratin.
Intermediate filaments constitutes two intracellular networks: one in the nucleus is proposed to define the mechanical properties of nuclei, and a second one in the cytoplasm which is proposed to be a mechanical stress absorber [Herrmann 2007]. In this paragraph, I will focus on the mechanical role of the cytoplasmic intermediate filaments, the one of the nuclear intermediate filaments will be discussed later.
In *in vitro* studies, intermediate filaments appear to be soft, extensible and nearly unbreakable [Herrmann 2007]. Indeed, the estimation of vimentin persistence length of nearly 1 μm, which give rise to a dynamic shear modulus of few Pascal of a dilute suspension of entangled vimentins, shows that at similar protein concentrations a vimentin network is much softer than an actin network ([Mücke 2004], [Herrmann 2007]). Not only intermediate filaments are more flexible than microtubules and actin, they are also more extensible. Indeed, the neurofilaments, desmin and keratin can bear a 3.5 fold stretch before breaking [Kreplak 2005]. Intermediate filaments such as desmin have also been shown to resist to higher forces (1-2 nN) compared to actin (0.6 nN) ([Kreplak 2007], [Tsuda 1996]). They also exhibit an interesting property of strain hardening. Indeed, keratins have been shown to break at large stresses (150-180 MPa) and they would achieve so by stiffening their network at low and intermediate strain [Storm 2005]. From this set of measurement emerged the idea of the intermediate filaments as mechanical absorber [Herrmann 2007].
Data about the mechanical role of intermediate filaments *in vivo*are still sparse. The few available data are pointing toward a role of intermediate filaments in stabilizing microtubules [Brangwynne 2006] and actin networks [Esue 2006]. Previous studies have shown that vimentin integrity plays an important role in the establishment of cellular stiffness (Young modulus) [Wang 2000] but because of the mechanical feedback between intermediate filaments and the actin cytoskeleton, one could argue that this decrease in the cell stiffness is due to the disruption of the cell cortex. However, more recently, mouse embryonic fibroblasts (MEFs) from vimentin knock down mice have been shown to exhibit a lower cytoplasmic shear modulus compared to control MEFs [Guo 2013]. Interestingly, the authors further showed that the actin cortex mechanical properties is not affected by vimentin knock down suggesting that the observed effect of vimentin on cellular mechanical properties can be independent of the actin cytoskeleton [Buehler 2013].

3.1.2 Proposed model of the cytoplasm

In the previous paragraphs, I described the mechanical properties of each of the constituents of the cytoplasm. This description is necessary to understand how each part of the cytokeleton can contribute to the mechanical properties of the cell. Such a detailed description was also important for understanding how a specific part of the cytoskeleton can exert and respond to forces. However, the real understanding of the overall cellular mechanical properties requires an integrated view of the system. Indeed, in a living cell, actin, microtubules and intermediate filaments are in a continuous crosstalk and feedback. A cellular actin network cannot be describe as polymers in an aqueous solution but more as polymers in a net. More and more proteins are being described for linking actin filaments to microtubules or intermediate filaments. To understand the physical properties of this network, many mechanical models have been proposed.

The first integrative model is based on classical viscoelastic models. The cytoskeleton is thus view as an integration of springs (elastic) and dashpots (viscous) which are in parallel (Kelvin voigt model) or in series (Maxwel model). The most important parameter of this model is the relaxation time which defines the transition between the elastic and the viscous response.

In the context of structural-kinetic approach, the cytoskeleton can be viewed as a set of rods (for example microtubules) and flexible binding elements (actin filaments) or as a granular medium modelled as rigid spheres corresponding to intracellular cross-linking proteins and distant mechanical interactions to reproduce the cytoskeleton filament internal forces. [Starodubtseva 2011].

The combination of the classical viscoelastic model and the structural kinetic model gave rise to the 30-elements tensegrity structure of adherent cell cytoskeleton composed of six rigid bars compressed by a continuous network of 24 prestretched cables (stress-supported structures). This model determines the relationship between the viscoelastic properties of the tensigrity structure and the mechanical and geometrical parameters.

In the context of continuous media, the cytoplasm is modeled as a gel or a soft glassy material. In the gel model, the cytoplasm can be fluid-like (sol phase) or solid-like (gel phase) according to the circumstances. Moreover, the cytoplasm can then undergo sol-gel transitions. As a soft glassy material, the cytoplasm is composed of discrete, numerous elements which can aggregate through weak interactions. Each element exists in the energy well formed by the binding energy of neighboring cytoskeletal elements. The glassy state is characterized by the noise temperature which is related to the energy necessary for elements to hop out of the energy well.

The cytoplasm have also been described as a poroelastic material. In this model, the cytoskeleton and the organelles constitute a porous elastic solid and the cytosol a fluid. The interaction between the porous elastic meshwork and its interstitial fluid gives rise to a poroelastic material. This model is supported by some experiments showing that pressure equilibrates slowly within cells (10 s) [Charras 2005] giving rise to intracellular flows of cytosol which might be used by cells to pro-

trude their membrane [Charras 2008]. Interestingly, this poroelastic model takes into account not only shear forces but also dilatational effects (volume variation) [Moeendarbary 2013] as cellular rheological properties are predicted to change due to volume changes. The most important parameter for a poroelastic material is its poroelastic diffusion constant which measures how fast intracellular fluids get redistrubuted in response to a localized deformation. Recent experiments challenging this poroelastic theory showed that at short time scales ($\leq 0.5s$) the cell behave like a poroelastic material which transit to a viscoelastic material at longer time scales [Moeendarbary 2013].
The length scale and more importantly the time scale of the study define the model which will be used to define the cytoskeleton. In the context of cell migration, the cytoskeleton is usually viewed as an active viscoelastic gel: a viscoelastic gel with a constant energy input [Hawkins 2009]. In the specific case of blebbing migration 3.4.2.2.1 the representation of cells as a poroelastic material might be more accurate.

3.1.3 Contribution of the plasma membrane to the cell mechanics

The plasma membrane is a lipid bilayer in which trans-membrane proteins are imbedded. It is viewed as a continuous fluid in which proteins as well as lipid are almost free to diffuse along the bilayer. It thus does not contribute to the shear modulus of the cell. The plasma membrane confers a boundary to the cell which separates it form the extracellular environment. As a consequence, mechanical interaction between the cell and its environment occurs through the plasma membrane.
The main contribution of the plasma membrane to the mechanical properties of moving cells goes through the establishment of the membrane tension. This membrane tension is the resultant of the in-plane tension in the lipid bilayer combined to the membrane-cytoskeleton adhesion energy [Lieber 2013]. The in-plane tension, intrinsic to the inextensible nature of the lipid bilayer will resist to any membrane stretching which would tend to expose the hydrophobic tails of the lipids [Keren 2011]. The balance of the in-plane and the membrane-cytoskeleton adhesion generated tension is cell type specific. Indeed, while in cells such as the erythrocytes the first one dominates, in neutrophils [Zhelev 1994], this in-plane tension can be neglected compared to the membrane-cytoskeleton induced tension.
The membrane tension applies an opposing force to membrane extension [Sheetz 1996]. It thus has a high contribution in the establishment of the isotropic tensile as well as the bending stiffness of the cell [Starodubtseva 2011]. Because force transmission along the membrane is very rapid ($\approx$ms) [Kozlov 2007] any local change in the membrane tension (for example after front protrusion), leads to a global variation of the cellular surface tension.
The plasma membrane is in a continuous crosstalk with the cytoskeleton. Not only it can impose a load to the actin network thus directing polymerization, it can also impact the biochemical composition of the actin network . Indeed, many proteins such as the Rho-GTPases locates at the plasma

membrane and can affect actin polymerization [Diz-Muñoz 2013]. For instance, membrane tension has been shown to modulate front back polarity [Houk 2012].
In addition, transmembrane proteins such as ion channels can impact actin polymerization by activating specific motors. As an example, calcium channels located at the plasma membrane are stretch activated and upon mechanical load (either imposed by the actin network or by extracellular stimuli) can induce Myosin II activation and thus contraction. (See 3.3.1 for a more detailed description of stretch activated ions channels)

3.1.4 The nucleus in cell mechanics

Among all cellular organelle, the nucleus is the one that could more likely play a role in whole cell mechanical properties. Indeed, the nucleus is the most prominent organelle in the cell and different studies have shown that the nucleus is also the most rigid cellular organelle. The nuclear rigidity can be as large as ten time the cytoplasmic rigidity [Caille 2002]. In addition, the shape of the nucleus varies with the cellular shape. Indeed, cellular stretching induces nuclear extension, cellular compression leads to nuclear shrinkage and cellular contraction induce nuclear rounding [Caille 2002]. Moreover, it is now well accepted that the nucleus is physically connected to the cytoskeleton allowing possible nuclear-cytoskeletal force transmission. All this taken together indicates that the nuclear mechanical properties plays a big role in the overall cellular mechanical properties. More detailed description of nuclear mechanical properties is done in the section 4.1.

3.2 Physical properties of the extracellular environment

Migration is based on cell-extracellular matrix interactions. Beside chemical interactions, many physical interactions are also involved in cell migration. Among those, mechanical and electrical interactions are the best studied.
Defining the cell-substrate mechanical interaction requires knowing in one hand the mechanical properties of the cell and on the other hand the geometry as well as the mechanical properties of the extracellular environment. The best studied mechanical stimulii imposed by the extracellular space are strain, shear stress, substrate rigidity and topography.
If the usual migration assays are based on 2D flat and stiff substrates, a growing number of studies are made in 3D environments with various geometries as well as substrate rigidities.

3.2.1 *in vivo* environments

In vertebrate, at least two types of extracellular matrices can be found *in vivo*: the basement membrane and the interstitial connective tissues. The basement membrane is constituted by a dense and

flat protein meshwork underlying epithelial and endothelial cells. It confers an anchoring region to those cells. The interstitial connective tissue is made from a 3D meshwork of heterogeneous texture and composition. The main component of connective tissues is fibrillar type I collagen whose composition and structure define the physical stability of the tissue. Collagen fibers are crosslinked in different ways leading to different networks whose specific physical properties are defined by the fiber thickness, orientation, density, stiffness as well as pore sizes between fibers. Cells migrating in such a matrix can thus move on a single fiber (1D), on a sheet-like surface (2D) or inside a complex 3D network. The pore size between fibers is an important parameter of the geometrical constrain imposed by the extracellular matrices. This parameter turns out to be highly variable in a given connective tissue. For instance, in the mouse back dermis or mouse mammary tissues model, the diameter of pores in the network ranges from 1 to 20 μm (Adapted from [Wolf 2009]). Another parameter that must be consider when defining *in vivo* mechanical properties is the tissue stiffness. Indeed, tissue stiffness can vary from 100 kPa in bone to 1 kPa in the brain. Vascular endothelial cells encounter shear stress generated by the blood flow as well as cyclic strain due to blood vessel distension by transmural pressure [Ballermann 1998]. Body patrolling cells such as leukocytes will have to migrate through all those body compartments. They should then be able to respond to various mechanical stimuli including shear stress, tension, compression as well as geometrical constrains. Thus understanding of *in vivo* cell migration particularly the one of leukocytes requires the study of how those cells respond to extracellular induces mechanical stimulii.

3.2.2 *In vitro* assays for mimicking *in vivo* environments

Although *in vivo* measurements are desirable because they imply physiological relevance, they lack flexibility controlling physical parameters that are important to unravel mechanisms behind observations made *in vivo*. Many stimuli both physical and biochemical received by the cell lead to its migration. In addition, controlling the *in vivo* environment is a challenging task to achieve.
To overcome this problem, many *in vitro* setups were developed to study cell migration. Those setups ranging from 2D substrates with well defined stiffness to 3D matrices with defined pores section are now widely used to mimic the *in vivo* extracellular environment. In addition of providing a mechanically well controlled environment, *in vitro* systems are also permeable to chemicals thus allows a control of the biochemical properties of the extracellular environment. The figure 3.8 illustrates most of the actual *in vitro* setups.

3.2.2.1 The 2D migration assay

The most common *in vitro* system for cell migration is the 2D petri dish or glass bottom dish. This system, suits very well for studying molecular as well as fundamental mechanism involved in cell migration. Indeed, the simple geometry make visualization of proteins as well as the cytoskeleton

very accessible. In addition, the chemical properties of glass makes it very attractive to many surface chemistry. For instance, micropatterning on glass coverslips allows a very well control of the distribution of adhesive molecules on the substrate [Azioune 2010]. Using this technique allowed Maiuri *et al* to perform the first world cell race and propose a general correlation betwenn cell speed and persistence [Maiuri 2012]
This 2D geometry is relevant for many physiological processes including wound healing and cell migration on thin collagen layer as described above (see 3.2.1). However, this system have been criticized a lot for the non physiological rigidity of the substrate . Indeed, the stiffer *in vivo* tissue (bones) has an elastic modulus of 100 kPa while glass is at the giga pascal order. Recent chemical improvements made this system more suitable. Indeed, glass coverslips can now be covered by soft hydrogels with well controlled mechanical properties such as polyacrilamide gels. Using this system allowed Engler *et al* to show that stem cells lineage speciation is driven by matrix elasticity [Engler 2006].

3.2.2.2 3D collagen gels

Opposite, in the scale of complexity, to the 2D setup is the 3D collagen setup. 3D collagen systems are obtained after in vitro polymerization of collagen. Cells can be embedded inside the gel resembling to the *in vivo* interstitial tissue context. This set up is thus used a lot for cancer cell migration and invasion as well as leukocytes extravasation [Wolf 2009]. For many years, this 3D collagen field was facing controversial results. Indeed, some groups were showing that cancer cells migration in collagen gels requires matrix remodeling while others where supporting a non proteolytic migration mechanism. New data from the Friedl lab proposed surprisingly a technical explanation which might stop the debate. They indeed show that the matrix remodeling dependance of cancer cell migration varies as function of the geometry, particularly the pore sizes of the collagen gel. Using a fixed concentration of collagen, they showed that the topology of the gel varies a lot as function of the rate of polymerization, i. e. faster the polymerization is denser the collagen will be. This groundbreaking work released all the tension accumulated for years in the field of 3D collagen setup.
3D collagen setup are well adapted for global chemical treatment, but become limiting when studying chemical gradient induced cell migration. Indeed, long time control of external gradient is very challenging in such systems as molecules are freely diffusing inside the gel. However, even if the pore size as well as the biochemical environment can be fairly well controlled, this system is not always suitable for protein visualization, because the thickness of the sample limits the choice of suitable imaging techniques, e.g. two photon microscopy. Because the cell in embedded in the collagen gel, its visualization requires specific microscopes such as multi-photon microscopes. In addition, the geometry (e.g. pore size and length) of the environment is not well controlled which then make impossible to study the effect of geometrical constrains in cell migration.

3.2.2.3 1D/3D migration assays

In order to overcome this limitation, new techniques called 1D/3D emerged. Taking advantage of the development in microfabrications, scientists developed divers systems where the geometry of the environment is very well controlled.
The 1D/3D setup can be separated in 2 groups [Lautenschläger 2013].
In the first one, are systems such as the 'under agarose' system and the two gels 'sandwich' setup. Such systems can be viewed as the combination of the 2D system and confinement. Cells are usually confined in the Z direction but not in the X and Y directions. Because cells are usually in close proximity with the glass coverslip, high resolution video microscopy can be performed. Substrate rigidity can be controlled by controlling the mechanical properties of the gel. However, the level of confinement is not well controlled. Indeed, the cell underneath the gel will deform it in a not completely controlled way giving rise to different geometries according to the cellular mechanical properties.
The second group of 1D/3D is composed of the 1D micropatterned lines and the microchannels (see figure 3.8). Here, scientists focused on controlling the geometry of the extracellular matrix. In the 1D lines, adherent cells are confined in the X direction but not on the Y and Z one. This setup mimics very well the above mentioned cell migration on a single collagen fiber. Here again, in addition of the geometry, the mechanical property of the substrate can be controlled by using hidrogel. An improvement of this 1D lines is the microchannel based system. This setup allows the tight control of the geometry as well as the level of confinement. Indeed, in microchannels, cells are confined in both X and Z directions. The level of confinement can be controlled down to a micrometer. Microchannels are made out of a silicon elastomer, Polydimethylsiloxane (PDMS) which is permeable to gas as well as nutrients. Placed on top of a glass coverslip, it allows high resolution microscopy. By changing the geometry of the channels wall, one can challenge the ability of cells to deform in order to migrate. This setup is thus very well designed for studying leukocytes migration [Lautenschläger 2013].

3.3 Mechanotransduction in cell migration

Mechanotransduction defines the process by which cells read mechanical stimuli and translate them to biochemical signals. This process enables cells to sense their physical environment and adjust their structure and function accordingly [Isermann 2013]. In the early studies, only sensory cells were reported to be able to read mechanical signals. However, it became soon clear that all cells are mechanosensitive. For instance, stem cell differentiation can be controlled by mechanical signals including substrate stiffness and geometry. Cardiac as well as skeletal muscle cells respond to tension by increasing their volume. It also became clear that cells use a variety of elements to sense extracellular mechanical stimuli. Those elements can be localized at the plasma membrane (for example

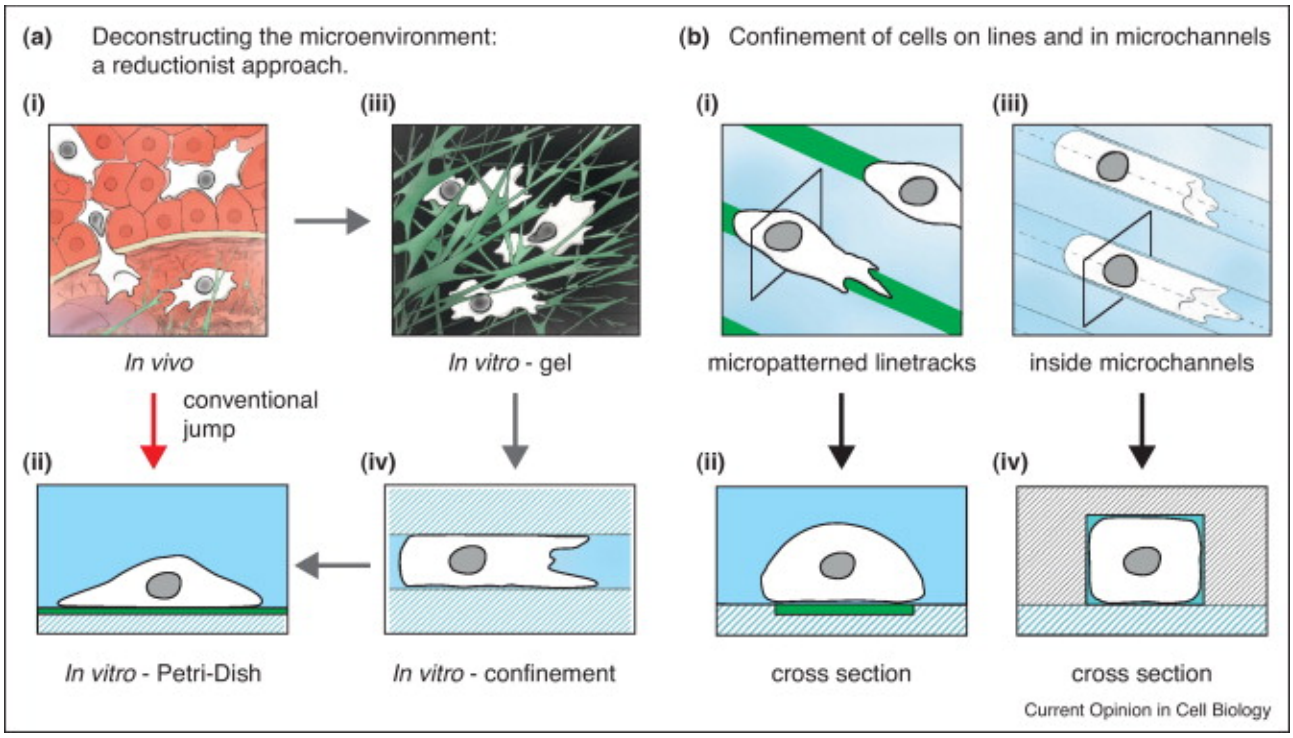

Figure 3.8: "**Quantitative control of the cell microenvironment *in vitro*.** (a) (i) Immune cells (in white) migrating in tissue (red) through a basal membrane (yellow) showing the many layers of complexity of the *in vivo* environment. This is in sharp contrast to the conventional approach for studying cells *in vitro* (ii) in a 2D uniform, flat Petri dish coated with adherent material (green). (iii) 3D matrix of ECM (green); closer to *in vivo* but still complex. (iv) A single parameter, here confinement, relevant for *in vivo* migration is implemented *in vitro* (e.g. in between two plates). (b) Simple methods for confinement of cells *in vitro*. (i) Schematic of cells on micropatterned, adhesive lines (green) on a 2D surface. Cells can only migrate along these lines, but the cell body can surpass the adhesive area. (ii) Cross sectional view of the rectangle in (i) showing the cell adhering to the linetrack. (iii) Schematic of cells inside microchannels confining the entire cell body. (iv) Cross sectional view of the rectangle in (iii) showing the cell confined within the microchannel." From [Lautenschläger 2013]

the ions channels), or in the cytoskeleton and even inside the nucleus. They are commonly called mechanosensitive proteins. (Adapted from [Isermann 2013]).
Mechanosensitive proteins change conformation and thus their functional role when sensing an applied force. For instance, mechanosensitive ion channels would open or close when a tensile stress is applied at the plasma membrane, some transmembrane proteins would unfold revealing cytoskeletal binding sites, this overall change in protein conformation would lead to the activation of a specific signaling pathway [Jaalouk 2009]. Disruption of mechanotransduction mechanisms can lead to several consequences including developmental defects, premature aging and cancer [Jaalouk 2009].
In the context of cell migration where cells are continuously in contact with the extracellular space and thus probe various mechanical properties, mechanotransduction is crucial for adapting to the corresponding mechanical stimuli. A cellular property which drives, for example, cell directed motion in durotaxis [Lo 2000]. The type of motility can also be determined by the mechanical properties of the extracellular matrix. Indeed, the extracellular geometry can drive the cell switch from an ameboid type of motion driven by contractility to a mesenchymal one driven by lamellipodium [Friedl 2010], see section 3.4.2.3.
In a migrating cells, many elements contribute to cellular mechanotransduction:

- Adhesion molecules at the interface between the cell and the extracellular matrix (ECM) sense and transduce mechanical signals
- ions channels at the plasma membrane can regulate ions flux upon mechanical load
- the cytoskeleton remodels when mechanically stressed (see section 3.1.1)
- the nucleus can receive mechanical signal which will induce gene expression (see section 4.4.2)

Because the role of the Cell-ECM adhesion molecules in mechanotransduction during cell migration will be addressed in section 3.4.1.1, I will now describe the role of ions channels.

3.3.1 Ions channels in mechanotransduction

Mechanical sensitivity is a common feature of proteins. Mechanosensitive channels (MSC) also called stretch-activated channels (SACs) or mechanogated channels are transmembrane channels which change their conformation between an open and a close state upon mechanical stimulus. This change in conformation induces ion flux which can then change membrane potential [Sachs 2010]. Two types of mechanical stimuli have been proposed to induce the conformation change of SACs: the bilayer and the tether model (see figure 3.9. In the bilayer model, channels would be activated by membrane tension while in the tether model, the gating force would be transmitted by the ECM or elements of the cytoskeleton bound to the channel [Nilius 2012]. If the bilayer model is now well accepted, the tether one is less. However, as some ions channels including the Na^+/H^+ exchange NHE1 has been

reported in focal adhesion, this tether model is not obsolete. Thus a local mechanical load, by either changing the membrane tension or locally pulling on channels, can induce channels opening which at first leads to ions flux throughout the plasma membrane. Ion flux can induce many changes in cells among which, variation of membrane potential (due to local charges accumulation across the membrane), changes in cell volume (due to water flux accompanying the ion flux and/or changes in osmotic pressure), changes in calcium (Ca^{2+}) concentration and changes in pH have been implicated in cell migration [Schwab 2012]. In the following paragraphs, I will briefly describe how membrane potential, cell volume, calcium signaling and pH can impact cell migration.

3.3.1.0.1 Role of membrane potential in cell migration Membrane potential can affect cell migration by regulating cell volume as well as intra- and extracellular pH. It can also induce calcium influx through an electric transport of the ion or the opening of voltage-dependent Ca^{2+} channels. Such a tight control of Ca^{2+} influx can impact the cell cytoskeleton. The electric field resulting from the membrane potential can further control actin polymerization by, for example, recruiting Rac1 which can thus activate some actin nucleators. Furthermore, this electric field can induce the opening of other voltage gated ions channels such as the K^+ which have been shown to be important for cell migration. For example inhibition of K_v1 a subgroup of the K^+ family is invariably followed by inhibition of cell migration. [Schwab 2012]

3.3.1.0.2 Role of cell volume in cell migration Many proteins involved in actin regulation has been shown to be sensitive to volume perturbations. Those proteins include Rho, Rac, Cdc42 and $PI(4,5)P_2$. Thus perturbing cell volume can perturb actin polymerization as illustrated by the rapid and pronounced polymerization of the actin cytoskeleton upon osmotic shrinkage. Another illustration of the importance of cell volume regulation is the observation that cell migration is abrogated when aquaporins as well as NHE1 are downregulated [Schwab 2012].

3.3.1.0.3 Calcium signalling in cell migration Change in calcium concentration can have drastic impact on cell migration. Indeed, many proteins involved in cell migration are regulated by calcium. Those proteins include myosin II which plays a big role in force generation and integrins which are important for force transduction. Migrating cells maintain a front-rear gradient of calcium crucial for cell polarity. Furthermore, the local control of calcium concentration through calcium "Flickers" (short-lived calcium pulses at the leading edge of migrating cells) has been shown to be important for directional migration. Calcium signaling has also been shown to regulate rear retraction by triggering actomyosin contraction following myosin light chain phosphorilation. In addition, calcium signalling has also been shown to regulate gene transcription. [Schwab 2012]

3.3.1.0.4 pH in cell migration pH variations can affect cell migration in many ways including integrin conformation changes as well as focal adhesion dynamics. Indeed an acidic extracellular pH has been shown to facilitates the activation of the $\alpha_v\beta_3$ integrins. In addition, alkaline intracellular pH has been shown to lower talin binding affinity to actin filaments. Thus by regulating the pH, stretch activated ions channels can regulate the turnover of focal adhesion. (Adapted from [Schwab 2012]).

In many ways, ions transport regulates cell migration. By using ion channels to sense the extracellular environment, the cell allows itself to rapidly respond to mechanical stimuli.

3.4 Mechanism of cell migration

Cell migration is a highly integrated multistep process which can be described as follows [Ridley 2003]. At first, the cell need to break its symmetry and establish a front-back polarity. This asymmetry enables cells to turn intracellularly generated forces into a net cell body translation [Lauffenburger 1996]. This symmetry breaking can occurs either spontaneously (due for example, stochastic local decrease in a polarity protein) or be driven by external cues (chemical, mechanical or electrical gradients). Once this is achieved, the cell will 'elongate' its front then retracts its back which will lead to a net movement. Said this way, the process seems to be simple, however, each of these steps requires a complex cellular machinery and a continuous crosstalk between the cell and its extracellular environment. Indeed, cues from the extracellular environment will be received, processed and the reaction of the cell to those cues will drive directional cell migration. One striking property of cells is their plasticity. So to say, their ability to adapt to the extracellular environment and modify their migration behavior [Zaidel-Bar 2007]. One extracellular cue which has been shown to have a high impact on cell migration is the geometry. Indeed, same cells, placed on 2D, 3D or 1D spaces will display a variety of migration phenotypes. In the following, I will discuss the mechanism of cell migration in 1, 2 and 3D.

3.4.1 2D/planar migration

Most of our current knowledge in cell migration was obtained using 2D/planar substrates. As said earlier, the simple geometry of these substrates allows a high resolution visualization of molecules implicated in cell migration. In 2D, most of cells display a mesenchymal type of migration. Such migration is characterized by a large protrusion, the lamellipodium, cell-ECM adhesion trough focal adhesions and stress fibers at the cell edges.
The lamellipodium, at the leading edge of migrating cells, is made of branched actin networks nucleated by Arp2/3 which extend ≈3-5 μm from the cell edge. Arp2/3 and its activators are located at the cell membrane where new actin monomers are added. The mechanism by which actin polymeriza-

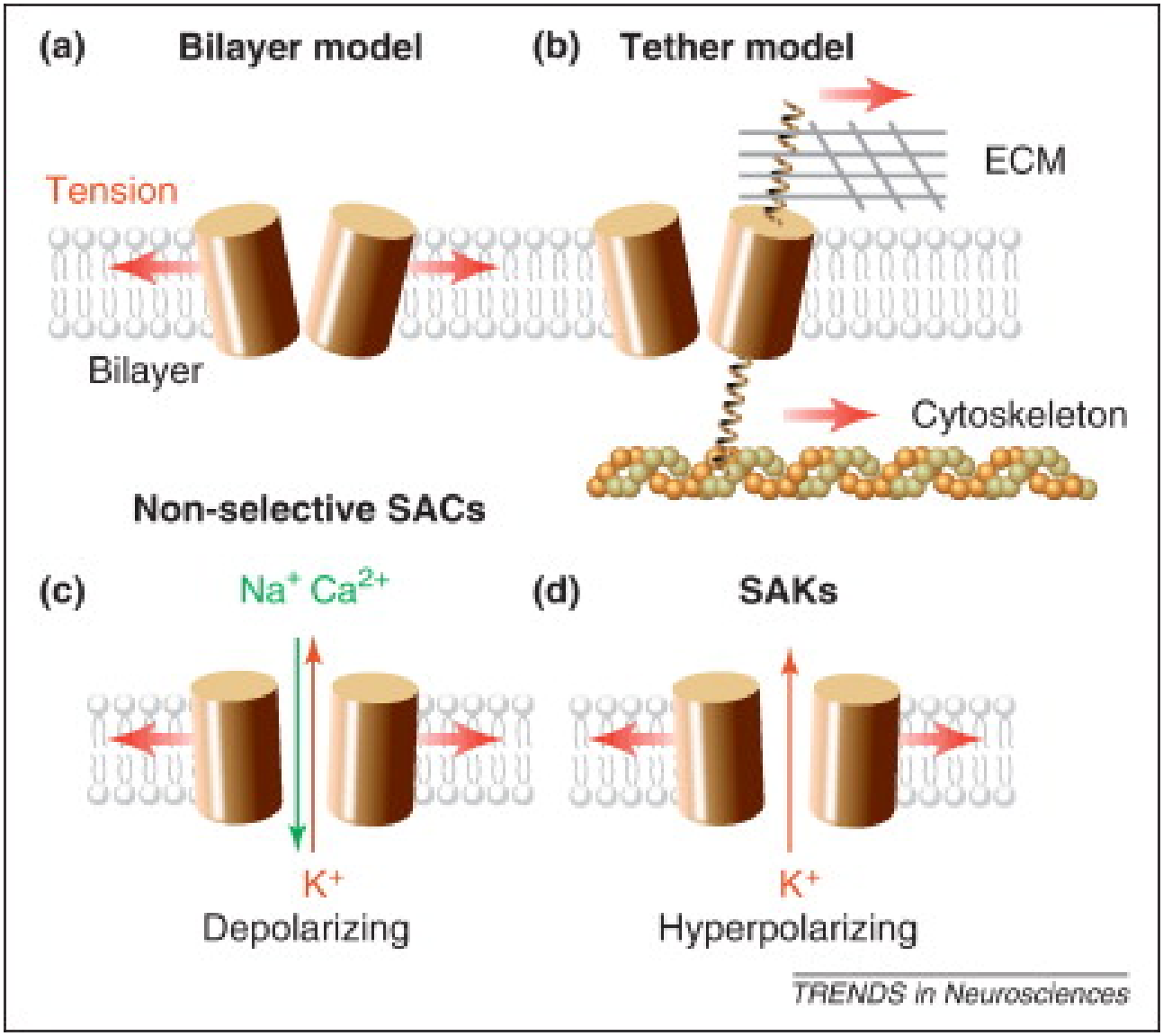

Figure 3.9: "**Gating models for Stretch Activating ion channels**. (a) Stretch Activating ion channels (SACs) may be directly gated by tension in the membrane. This bilayer model has been put forward for the bacterial MscL channel. (b) Tethered elements of the ECM or of the intracellular cytoskeleton (dual-tether model) may transmit force to the channel. Although initially put forward to model the C. elegans mechanoreceptors sensitive to light touch (where intracellular tubulin instead of actin interacts with the channel), it is now demonstrated that there is no direct connection between the microtubule cytoskeleton and the channel and, moreover, the cytoskeleton is dispensable for channel activation. Nevertheless, whether such a dual-tether mechanism is at play in other cell types, such as the hair cells, cannot be entirely ruled out. An alternative single-tether model involves the ECM which is proposed to move the channel into or out of the plane of the membrane, thus controlling channel opening. (c) SACs (including Piezo1 and Piezo2) are non-selective channels permeable to Na^+, Ca^{2+} and K^+. (d) SAKs (i.e. TREK-1, TREK-2 and TRAAK) are selective for K^+. Surprisingly, an N-terminal variant of TREK-1 has been shown to be permeable to Na^+." Adapted from [Nilius 2012]

tion leads to membrane protrusion is believed to be based on an elastic molecular ratchet mechanism. According to this theory, thermal fluctuations induce the bending of the growing filament which will then store elastic energy. The unbending of this filament which have been elongated in the mean time, provides enough force to deform the membrane [Ridley 2003]. The rate of global protrusion is regulated by the rate of actin polymerization as well as the organization of the actin network at the leading edge. Indeed, fast actin polymerization leads to fast protrusion which can induce high strain on the cell. This rate of polymerization at the leading edge is tightly controlled by different actin binding proteins. For instance, profilin, by binding to actin monomers prevents self-nucleation and regulates the target of actin monomers to F-actin barbed end. Capping proteins by terminating actin filament elongation restrict polymerization to the plasma membrane. ADF/Cofilin, by disassembling older filaments regulates the renewal of the pool of actin monomers which will be used for filament elongation at the leading edge. [Ridley 2003] Thus by controlling the generation of a broad, dendritic like network, the cell is able to push the membrane on a long distance. At the edge of lamellipodia, migrating cells exhibit filopodia; elongated structures made of bundled actin filaments. Their structure and their position are well designed to explore and sense the environment of the cell. [Ridley 2003] Opposite to filopodia and at the interface between the lamellipodia and the lamella are actin transverses arcs which results from the contraction of the dendritic actin network polymerized at the cell front. In the lamella bundled actin filaments crosslinked by myosin II motors are though to mediate high forces generation for migration. The current model of actin transverses arcs and lamela formation is illustrated in figure 3.10. [Burnette 2011].

A net movement occurs if the cell is able to transmit forces to the substrate. Indeed, the stabilization of the protrusion needs cell-ECM attachment thus force transmission to the substrate. This cell-ECM force transmission can be done through small, sub-micrometric adhesions as reported in leukocytes or keratinocytes which are rapidly moving cells. In other cell types such as fibroblast, focal complexes induced by Rac activation form at the leading edge of migrating cells. Formed at the cell edge as nascent adhesions, they maturate in the lamella as focal complexes and detach at the cell rear. Adhesion complexes are thus dynamic structures which regulate cell migration.

3.4.1.1 Adhesion dynamics

The best studied adhesion receptors are integrins. Integrins are heterodimeric receptors composed of various α and β chains with a large ligand-binding extracellular domain and a short cytoplasmic domain. Upon binding of ligands to the extracellular domains, integrins change their conformation by changing the interaction between the α and β chains. This conformation change is followed by integrin clustering and recruitment of more proteins complexes including talin, vinculin, paxilin, kindlin and focal adhesion kinase (FAK). Those proteins complexes particularly vinculin, talin and $\alpha-actinin$ will link integrins to the actin cytoskeleton thus allowing force transmission to the ECM. For instance, focal complexes are connected to dorsal stress fibers at one of their ends while mature focal adhesions

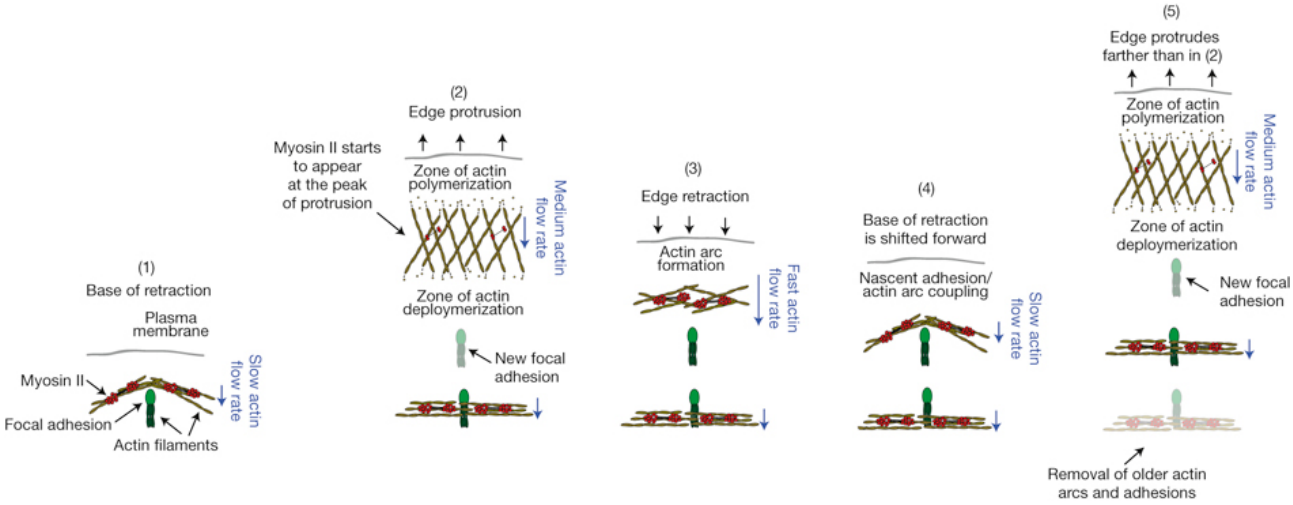

Figure 3.10: "**Leading-edge advance is broken down into discrete steps**. Step (1) shows the base of a previous retraction where a newly created actin arc is coupled to a focal adhesion. Hypothetically, the new lamellipodial protrusion could push off the arc to drive the membrane forward. During protrusion (2), actin-filament polymerization occurs behind the plasma membrane and depolymerization occurs a few micrometres away from the edge. Actin filaments treadmill through the lamellipodium during protrusion, and nascent adhesions form. At the peak of protrusion (2), myosin II filaments form in the lamellipodium and a local network contraction (similar to that proposed for keratocyte cell body translocation3) occurs that drives actin-arc formation and edge retraction (3). In cells that show net advance, the new actin arc slows at the nascent adhesion (4), most likely owing to strong coupling between the arc, adhesion and growth substrate. The base of the retraction in (4) is shifted forward when compared with (1). As a consequence, the start of the new protrusion in (5) is also shifted forward and the edge protrudes farther than in (2). In cells that do not show net advance, the actin arc and adhesion slip rearward during edge retraction. This indicates that there is still strong coupling between the actin arc and the adhesion, and also indicates a weak coupling between the adhesion and the growth substrate. Actin-arc addition to the front of the lamella is balanced by actin-arc removal at the back of the lamella (5). Lamellipodial and arc actin filaments are yellow. Focal adhesions and associated actin filaments are green. Myosin II filaments are red. Relative actin-rearward-flow rates are represented by blue arrows." From [Burnette 2011]

are present at either one or both ends of ventral stress fibers [Burridge 2013] . These stress fibers, cross-linked by $\alpha - actinin$ and myosin II will generate the necessary force for counteracting the force applied by the ECM to the cell. (Adpted from [Jahed 2014]). Figure 3.11 illustrates the events leading to focal adhesion formation. Focal complexes are believed to be mechanosensitive. Indeed, they have been shown to maturate upon tension. The mechanism which leads to focal adhesion maturation is not really understood but some emerging ideas point towards a mechanically induced maturation. Many proteins at the adhesion sites are mechanosensitive. For instance, talin which is recruited at the early times of adhesion complex formation has been shown to unfold upon stretch revealing more actin as well as vinculin binding sites ([del Rio 2009], [Margadant 2011]). Vinculin recruitment to focal adhesions has been shown to be force dependent ([Carisey 2013], [Hirata 2014]). Moreover, vinculin recruitment has been proposed to be necessary for focal adhesion maturation [Jahed 2014]. Stress fibers which terminate adhesion complexes have also been proposed to be mechanosensitive as they have been shown to reorganize, reinforce and repair under mechanical load [Burridge 2013]. Thus, mechanical load applied by the extracellular matrix can regulate focal adhesion maturation as well as force generation and transmission to the ECM.

In the context of force transmission to the ECM, it has been surprising to discover that the most traction forces in rapidly moving cells are generated by focal complexes (at the lamellipodia) [Webb 2002]. This goes very well with observed correlation between cell velocity and size of adhesion complexes [Gupton 2006]. Mature focal adhesions which have been extensively studied inhibit cell migration by immobilizing the cell on the substrate. However, such focal adhesions have been shown to be important for durotaxis. Moreover, a recent study from Waterman's Lab proposed that dynamic fluctuation of the force exerted by mature focal adhesions might be important in rigidity sensing and more importantly to durotaxis [Plotnikov 2013]. Durotaxis is one of the most striking examples of cellular mechanotransduction which have a direct impact on cell migration. Durotaxis is the process by which a cell migrates toward stiffer substrates [Lo 2000]. First proposed in 2000 by Lo et al in NIH3T3 fibroblast, the mechanism by which cells keep their persistence towards stiffer substrates is still unclear. On general idea, is that cells should be able to locally sense the force exerted by the ECM and dynamically respond to it. Plotnikov et al proposed a mechanism by which mature focal adhesions could drive durotaxis. Measuring traction force dynamics at the single focal adhesion scale, they proposed the existence of two populations of focal adhesions in migrating cells: static ones and fluctuating ones. The static ones would generate an uniform and constant traction field on the substrate while the dynamic one exhibit a pattern of traction fluctuations which was reminiscent of repeated, centripetal tugging on the ECM. Plotnikov et al proposed that this sub-population of tugging focal adhesions drive cellular rigidity sensing by allowing a regular testing of the local ECM rigidity landscape over time (see figure 3.12)[Plotnikov 2013]. Even though focal complexes have been shown to exert traction forces on the substrate, to modulate rigidity sensing and to mediate durotaxis, the mechanism by which forces are produced and transmitted to the substrate resulting in a

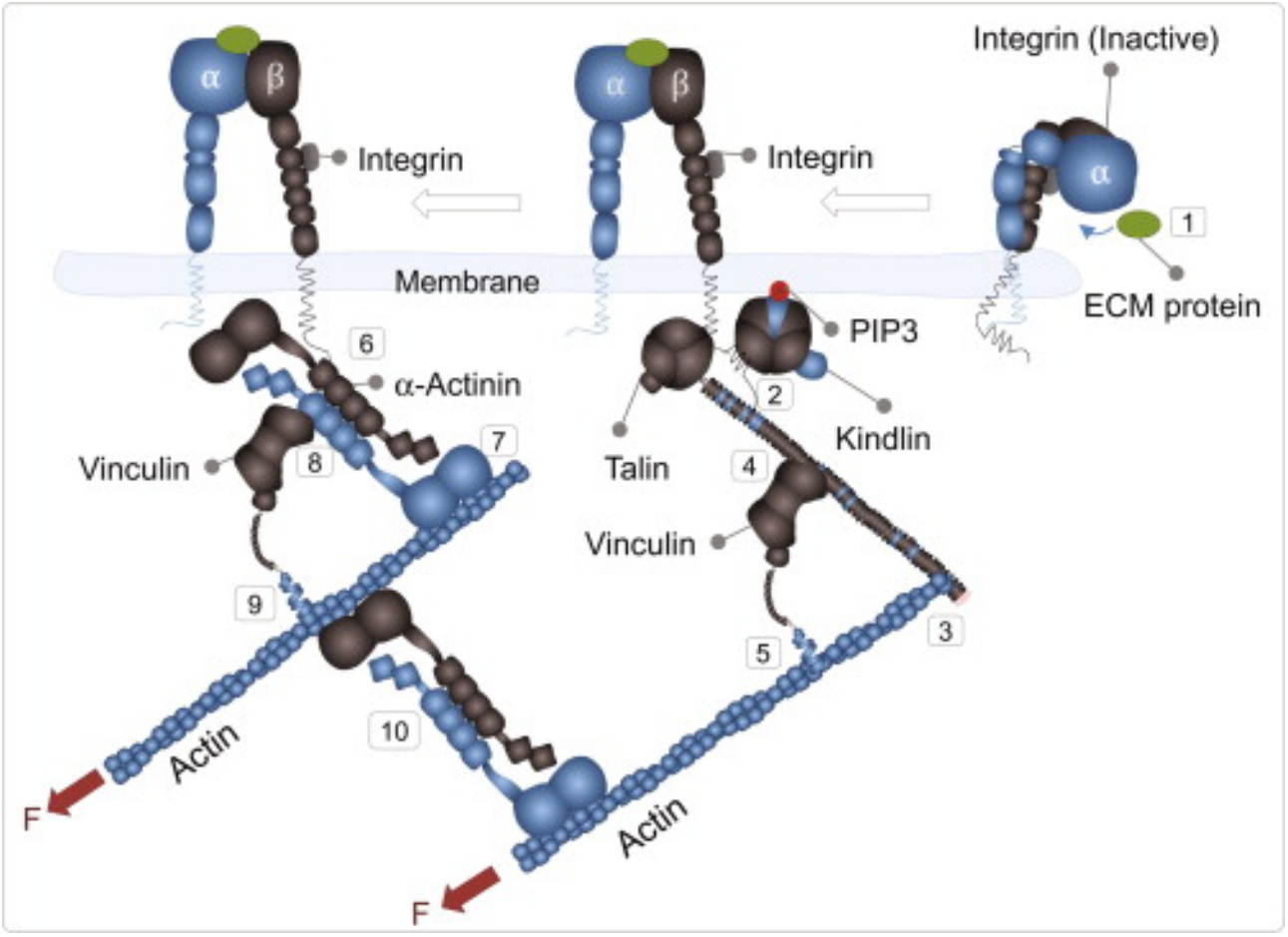

Figure 3.11: "**Proposed model for binding events at initial stages of focal adhesion formation**, starting with (1) the weakening of electrostatic bonds between integrin α and β TM domains upon ECM molecule binding; (2) activation of integrin through the binding of kindlin and talin to the NxxY motifs on integrin β cytoplasmic tail; (3) talin cross-links integrins and the cytoskeleton by binding actin, subsequently tensile actomyosin forces result in the exposure of cryptic vinculin-binding sites on talin; (4) consequently, vinculin head weakly binds talin, acquiring an intermediate conformation which promotes actin binding. (5) Vinculin binds actin and fully extends under tensile forces, reinforcing the talin-actin link. (6) $\alpha - actinin$ binds previously activated integrin by replacing talin and (7) subsequently binds actin, cross-linking integrin and actin. (8) $\alpha - actinin$ can bind vinculin head and (9) activate it for actin binding. (10) Finally, $\alpha - actinin$ acts as an actin crosslinker and is involved in actin reorganization." From [Jahed 2014]

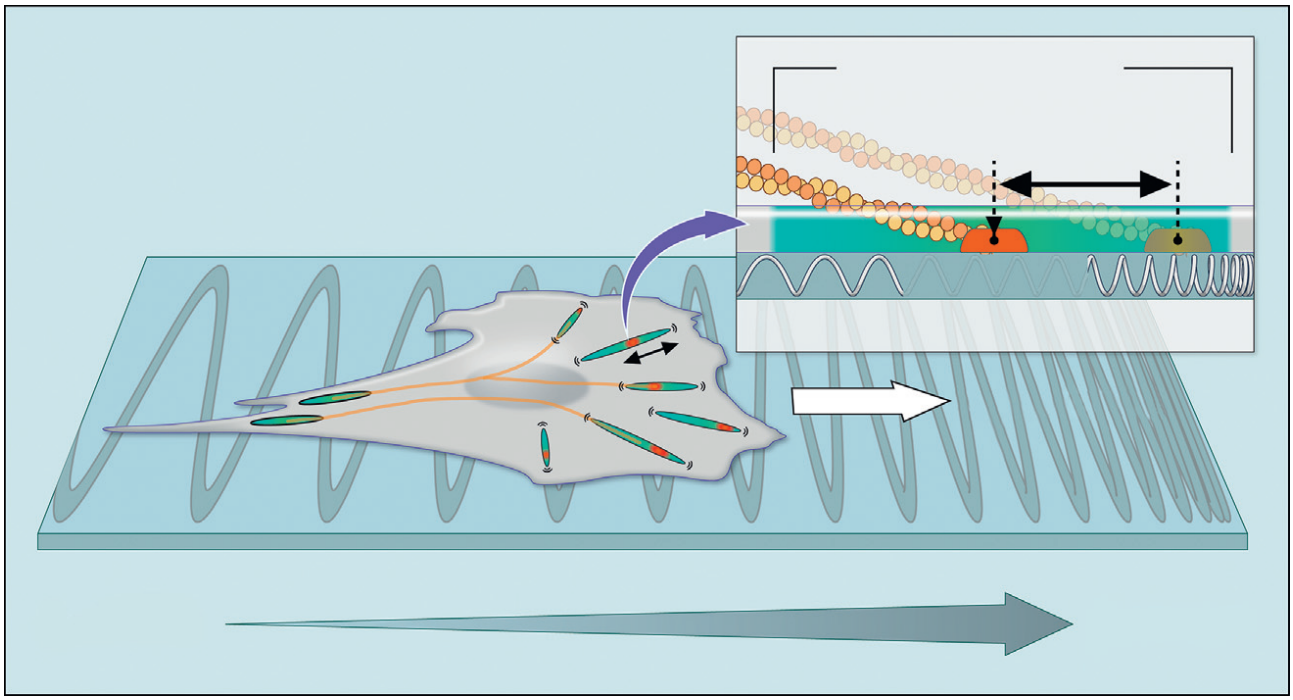

Figure 3.12: "**Model for durotaxis**. Nanoscale fluctuations of traction forces mediate ECM rigidity sensing and guide directed cell migration. Dynamics of traction forces within individual FAs are essential to direct cells toward stiff ECM. Zoomed insert depicts repetitive movement of force peak along individual FA (shown in green)." From [Plotnikov 2013]

movement on 2d substrates is still poorly understood. Twenty five years ago, emerged a model called molecular clutch which is trying to explain such mechanism.

3.4.1.2 The molecular clutch model

The molecular clutch is proposed to be composed of a set of proteins at the adhesion complex which modulate the strength of the connection as well as interaction between the cytoskeleton and the substrate [Giannone 2009]. Through this interaction, the clutch modulates the force transmission from the cytoskeleton to the substrate as well as the rate of translocation. The engagement state of the clutch determines the level of force transmission. Indeed, when the clutch is engaged, tight cytoskeleton-substrate linkage allows an efficient force transmission while a not engaged clutch is not able to transmit forces [Ananthakrishnan 2007].
The engagement state of the clutch and the amount of transmitted forces can be modulated by the retrograde flow. This retrograde flow is a result of pushing forces generated by the plasma membrane on the dendritic actin network at the leading edge and pulling forces generated by myosin II contractility in the lamella [Bangasser 2013]. With a too fast retrograde flow, actin filaments will slip on the clutch resulting in no clutch engagement (see figure 3.13 a anb b). An optimum retrograde flow is thus necessary to allow efficient and dynamic force transmission to the substrate [Ananthakrishnan 2007]. In addition the clutch engagement induces the slowing down of the retrograde flow which allows leading edge advance (see figure 3.13 c) [Bangasser 2013]. The molecular clutch model, thus predict that slow moving cells have a high retrograde flow and generate less traction forces while fast moving cells having smaller retrograde flow will generate higher traction forces.([Giannone 2009], [Ananthakrishnan 2007])
However, slow moving cells have been observed to generate high traction forces which is inconsistent with the molecular clutch model as presented here. Interestingly, most of the moving cells including neutrophils, NIH 3T3 fibroblast and U87 glioma cells display a biphasic distribution of their velocity as function of the substrate stiffness [Bangasser 2013]. A modification of the model proposing a tension dependent rate of clutch disengagement could explain this biphasic behavior. Indeed, on stiff substrates the molecular clutch engagement on F-actin leads to a rapid tension build up on the clutch due to the lack of substrate compliance. The resulting high tension will lead to a rapid clutch disengagement as the rate of clutch disengagement increase exponentially with tension [Chan 2008]. On soft substrates, the slow tension build up leads to an initial high retrograde flow which will be slowed down once the tension will reach a critical value. At this critical value, single clutches will start disengaging in cascade leading to a high tension on the remaining engaged clutches which will in turn disengage causing a snap back of the cell to its initial position. This phenomenon, named load-and-fail is characterized by a protracted period ($\approx$ 10 to 100s) of increasing tension followed by a rapid coupling failure [Chan 2008]. The optimal stiffness for migration is predicted to be the one where the the clutch binding time equals the load-and-fail cycle time. Indeed, in this configuration,

cluthes engaged long enough to allow force transmission without being blocked at their engaded state (which would prevent forward movement) [Bangasser 2013].
This molecular clutch model also predicts force fluctuations at the level of the focal adhesion which has been proposed to drive durotaxis [Bangasser 2013]. It also provides a possible explanation of the optimum of velocity which can be obtained by coordinately changing parameters of the model. Among those parameters, a coordinated change in motors activity and clutches is of particular interest for cell adaptation to stiffness variations [Bangasser 2013].

3.4.2 3D cell migration

In here, I refer to 3D migration as single cell migration in collagen gels or interstitial migration. In such environments, two types of locomotion have been reported: mesenchymal migration and amoeboid migration. In 3D environments, mesenchymal cells are characterized by an elongated shape with a well defined front-back polarity while amoeboid cells are more roundish with a much less difined polarity [Friedl 2010]. Various cells including fibroblast, neural crest cells and cancer cells, have been reported to adopt mesenchymal migration is 3D collagen gels [Friedl 2009b] while leukocytes are more prompted to migrate in an amoeboid manner.

3.4.2.1 3D mesenchymal migration

During 3D mesenchymal migration, cells display a specific spindle-like shape, elongated morphology [Wolf 2003] characterized by an actin-polymerization dependent pseudopod protrusion at the leading edge and a tensed rear defined as uropod. Such migration occurs in five steps. At first (1),

Figure 3.13 *(facing page)*: **Three potential states of the molecular clutch.** Side view of a lamellipodium moving on a rigid or flexible substrate coated with extracellular matrix molecules (red). The cell expresses the appropriate membrane counter-receptors (blue). Specific ligand-receptor recognition allows formation of adhesion complexes at the ventral surface. Actin filaments are flowing rearward, due to a combination of polymerization at the tip (+ sign), depolymerization at the rear (- sign), and the pulling action of myosin motors (green heads). Dynamic connection between F-actin and adhesion complexes is provided by a clutch module made of adaptor proteins (orange circles), specific for each adhesion type. The force exerted at adhesion sites translates into deformation of the matrix (wrinkles). (a) Unengaged clutch, no coupling between F-actin and ligand/receptor complexes. (b) Slipping clutch, where transient weak connections are formed between the F-actin flow and ligand/receptor complexes through clutch proteins. (c) Engaged clutch, where a strong coupling between F-actin and ligand/receptor complexes slows down F-actin flow downstream and allows polymerization forward. (From [Giannone 2009])

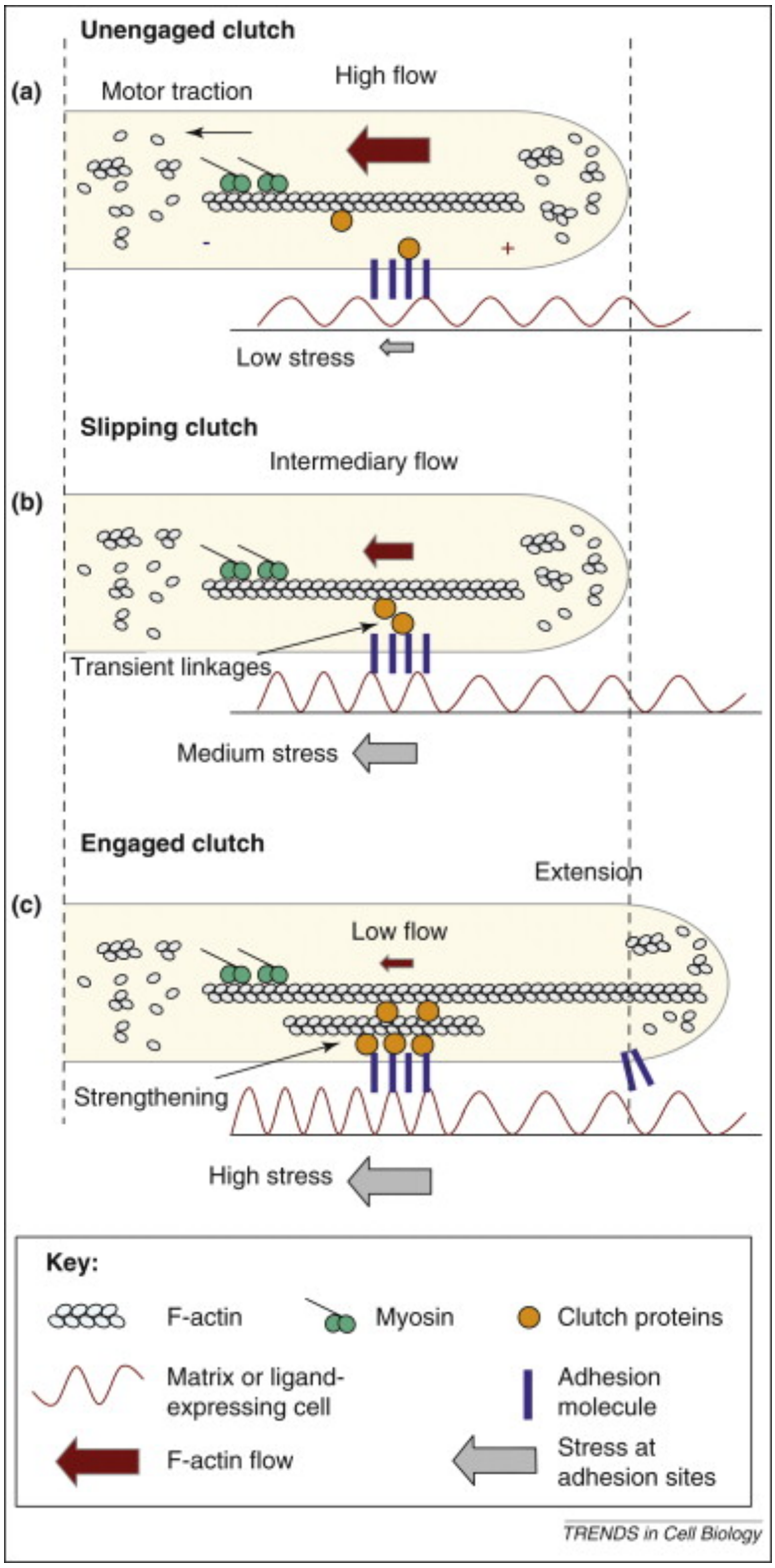
Unengaged clutch
(a)
Motor traction
High flow
-
+
Low stress
Slipping clutch
Intermediary flow
(b)
Transient linkages
Medium stress
Engaged clutch
Extension
(c)
Low flow
Strengthening
High stress
Key:
F-actin
Myosin
Clutch proteins
Matrix or ligand-expressing cell
Adhesion molecule
F-actin flow
Stress at adhesion sites
TRENDS in Cell Biology

the cell front protrude in an actin polymerization dependent manner. Following this protrusion, (2) integrins mediated adhesion to the substrate occurs allowing the stabilization of the protrusion as seen in 2D. Several micrometer from the leading edge, the ECM is remodeled by the cell during the third step (3). The fourth (4) step is characterized by the actomyosin driven contraction which increases longitudinal tension of the cell body and in the fifth (5) and last step, the cell rear retracts leading to cell body translocation ([Friedl 2009b], [Wolf 2013]) During 3D mesenchymal migration force transmission to the substrate is based on cell-ECM adhesion through integrins [Friedl 2010]. However, whether mesenchymal cells form stable adhesions is still under debate. Clear focal adhesions such as the ones described in 2D mesenchymal migration have not been reported in 3D environments ([Cukierman 2001]). Moreover, stress fibers which are the characteristic for 2D migrating cells, disappear in 3D matrices. However, the dependance of cell migration to integrins ([Wolf 2013]) suggests that some type of focal adhesion might exist in 3D environments.
3D mesenchymal migration displays another characteristic which is cellular proteolytic activity ([Aimes 1995], [Wolf 2003]). Indeed, most of the mesenchymal cells migrating in highly confining spaces posses a high ECM remodeling capability [Wolf 2013]. Cells such as cancer cells express specific matrix metalloproteinases (particularly membrane-tethered (MT)1-MMP/MMP-14) which by cleaving, remodeling or bundling the collagen fibers, enlarge the space for the cell [Wolf 2007].
3D mesenchymal cell migration can thus be described as a 2D mesenchymal migration in term of force generation and transmission. Indeed, the requirement of integrin suggests that force transmission for leading edge propulsion is based on a molecular clutch model. The requirement of Rac signalling through Wave2 [Sanz-Moreno 2008] which is known to activate Arp2/3 suggests that as shown in 2D substrates, force generation is based on actin retrograde flow originated at the leading edge. Interestingly, mesenchymal cells when put in a 3D environment get rid of the third dimension by degrading the matrix. This matrix degradation capability is intrinsic to such migration as its inhibition leads to a cell switch to an amoeboid type of migration ([Wolf 2003], [Wolf 2013]).

3.4.2.2 3D amoeboid migration

Amoeboid cells migrating in 3D collagen gels display mainly two shapes: a rounded, blebby migrating cells or a slightly more elongated shape with a filopodia at the leading edge [Friedl 2010]. Amoeboid cell migration is characterized by low to null adhesion as well as stress fibers. Such cells do not show any ECM remodeling activity, they tend to deform the cell body in order to move forward. Moreover, amoeboid cells tend to have a higher RhoA activity which is believed to increase the cellular tension and mediate force generation. One struggling question in the field of amoeboid migration is how are forces transmitted to the substrate to allow migration. Many models of amoeboid migration have emerged in the past decade. Form the best known blebs driven motility to the myosin II independent motility of dendritic cells, I will describe the proposed mechanisms of force generation and transmission during amoeboid migration.

3.4.2.2.1 Mechanism of blebbing migration Blebbing migration is characterized by the roundish shape of the cell. This round shape is proposed to be driven by a high cortical contractility mediated by myosin II. The proposed model for blebbling migration is as follows. The high cellular contractility induces a high hydrostatic pressure inside the cell which leads to a high cortical tension. This high tension will be released by formation of a membrane protrusion devoted of actin filaments called bleb. The cytoplasm will then flow in this newly formed bleb which will inflate much faster than a protrusion driven by actin polymerization [Renkawitz 2010]. After stabilization of front protrusion (through adhesions) in a form of bleb, rear retraction leading to a net cellular movement. [Paluch 2013]

3.4.2.2.1.1 Myosin II as force generator A hallmark of blebbing migration is the requirement of myosin II based contraction [Charras 2008]. Indeed, Myosin II overexpression has been reported to promote blebbing [Paluch 2013] and Myosin II accumulation has been correlated to sites of bleb formation in zebrafish primordial germ cells [Blaser 2006]. High contractility seems to be necessary for the establishment of high hydrostatic pressure driving bleb formation and expansion .

However, how this increase in hydrostatic pressure leads to bleb formation is still unkwown. Two models are proposed : the cortex-membrane detachment and the cortex breakage. Indeed, local breakage of the bounds between the membrane and the cortex has been shown to promote bleb formation supporting the cortex-membrane detachment theory [Paluch 2013]. At the same time, local rupture of the cortex using laser ablation has also been shown to promote bled formation [Paluch 2013]. It is thus likely that this high hydrostatic pressure will take advantage of a local weakening of the membrane tension to induce bleb formation. Another possible mechanism for bleb initiation is through osmotic swelling. Indeed, a polarized distribution of aquaporins could induce membrane swelling in regions where the cortex is transiently disrupted [Loitto 2009]. In order for directional migration to occur, a bleb should grow in the direction of migration. Indeed, non polarized blebbing will lead to a stationary movement. Cells migrating with blebs seem to form their bleb primarily at the leading edge [Charras 2008]. Even though the mechanism by which cells achieve this polarized blebbing remains unknown data from walker carcinoma cells which can display a blebbing migration, suggest a controlled polarized blebbing though an asymmetric distribution of the cortex-membrane linker ERM (ezin, radixin, meosin) proteins ([Charras 2008], [Rossy 2007]). Polarized blebbing can also be mediated by preferential tearing of the actin cortex at the leading edge [Charras 2008]. This could be achieved by imposing at the leading edge a locally high contractilitity close to the cortex rupture point ([Paluch 2005], [Charras 2008]).

3.4.2.2.1.2 Models for force transmission in blebbing motility In order for migration to occur, cells need to exert forces to the extracellular environment. As said earlier, mesenchymal cells achieve this task by forming strong adhesions to the ECM. However, such focal adhesion have not

been observed during blebbing migration giving rise to the question of how are blebs transduced to movement. Two hypothesis are emerging:

- The first hypothesis proposed that some small adhesions still exist between the cell and the ECM ([Grebecki 2001], [Sroka 2002]) allowing force transmission in a molecular clutch manner. See illustration in section c of the figure 3.14.

- The second hypothesis, only relevant for confining environments, (2D plus confinement or 3D matrices) propose no requirement for specific adhesions to the ECM ([Paluch 2013],[Charras 2008]). Because of the confinement, the cell would exert forces perpendicular to the substrate and squeeze itself forward in a mechanism known at chimneying illustrated in figures 3.17 and 3.14-d ([Lämmermann 2008], [Hawkins 2009]). A theoretical description of such migration proposed that actin polymerization against the ECM could produce enough pushing force allowing cell forward movement at velocities higher than the actin polymerization speed ([Hawkins 2009], [Paluch 2013]). Another possible mechanism for cell propulsion in confined spaces is through the coupling of a backwards flow of the actin cortex along the sides of the cell and friction between the cell and the substrate ([Hawkins 2011], [Poincloux 2011]). This friction can occur through specific adhesions or nonspecific interactions between the cell and the ECM [Paluch 2013]. In addition, blebbing cells in 3D matrices could use the pores of the ECM to entangle the bleb which after growth will allow the generation of local friction at the interface between the bleb and the pore section (illustrated in section e of the figure 3.14). This asymmetrical friction can be used by a cell to push itself forward ([Renkawitz 2010], [Paluch 2013]). This mode of blebbing migration has recently been predicted to be particularly more efficient in low or no adhesion conditions [Tozluoğlu 2013].

Thus amoeboid cells, could use actomyosin contraction to generate actin free membrane protrusion which by pulling, pushing or gliding on the extracellular matrix assure efficient cell migration

3.4.2.2.2 Polymerization driven amoeboid migration As said earlier, blebbing migration requires myosin II driven contractility and can be independent of adhesion. Leukocytes including dendritic cells, B cells, granulocytes and Drosophila haemocytes have been shown to migrate in 3D with low adhesion in an myosin II independent manner ([Lämmermann 2008], [Renkawitz 2010]). In addition, those leucocytes exhibit an actin-rich cell protrusion which bring them out of the group of blebbing cells (where the front protrusion is devoted of actin). This non blebbing amoeboid migration mode is supposed to be entirely based on actin polymerization. Indeed, the unique force of actin polymerization is believed to drive continuous cell front protrusion. The rear will retract following the front without any requirement of high forces as no strong adhesion needs to be 'broken' [Renkawitz 2010]. In the same way than for blebbing amoeboid migration, force transmission to the ECM can be done by friction without any requirement for strong adhesions.

In the context of chimneying migration (see figure 3.17), such actin polymerization based and myosin II/adhesion independent migration mechanism has been shown to be possible in a theoretical study [Hawkins 2009]. Indeed, in this study, Hawkins *et al* proposed that myosin II based contraction would just enhance the translocation rate of the cell but does not give the base of cell migration.
More experimental as well as theoretical studies are required to understand how leukocytes in a non blebbing migration produce forces for their translocation. Moreover, it would be really interesting to understand how produced forces (either by actin polymerization or blebbing) are transmitted to the substrate to allow efficient migration in 3D environments.

3.4.2.3 Switching migration mode as function of the ECM physical and chemical properties

Many cells, including cancer cells, dendritic cells and HL-60 derived neutrophils have been shown to change their migration mode as function of the biochemical and physical properties of the extracellular matrix. For instance, cancer cells which normally display a mesenchymal migration can move in an amoeboid manner when their proteolytic activity is inhibited ([Wolf 2003], [Wolf 2013]). Dendritic cells have also been shown to switch between an integrin-mediated to an integrin-independent migration mode in vitro as well as *in vivo* [Renkawitz 2009], [Lämmermann 2008]. At last, HL-60 derived neutrophils have recently been proposed to switch between an actin-polymerization driven migration mode to a blebbing migration [Wilson 2013]. Thus, different cells, can adapt to constrains

---

Figure 3.14 *(facing page)*: **a**) A tumour cell (blue) migrating through a collagen matrix (orange). Contraction of the uropod (arrowhead in all images) moves the cell body through the collagen mesh and, subsequently, a new protrusion is created (in the direction of the arrow, right image). Time between images 7 minutes. Scale bar, 20μm. Reproduced, with permission, from ([Wolf 2003]). **b**) Bleb migration of a deep cell in a mid-blastula fish embryo. The cells in the top part of the image are part of the periblast. A bleb can clearly be distinguished at the leading edge of the lowest cell (arrow, left image). This bleb broadens and possibly adheres to the periblast (middle image) before elongating into a lobopodium (right image). Time between images is 4 seconds. Scale bar, 50μm. Reproduced, with permission, from [Kageyama 1977]. **c**) In two-dimensional (2D) cultures, in order to translate polarized blebbing into movement, the cell must adhere to the substrate. When a new bleb is formed and comes in contact with the substrate, new cell-substrate adhesion are formed and the cell mass can stream forward. The pink dots indicate cell-substrate attachment points. **d**) When the cell is in a confined environment (for example, between two glass coverslips or in a thin microfluidic channel), it can move in the absence of cell-substrate adhesion. Instead, the cell exerts forces perpendicularly to the substrate and can squeeze itself forward; this mechanism is known as chimneying [Malawista 2000]. **e**) When the cell is migrating in an extracellular matrix (ECM) gel (three-dimensional (3D) matrix), it can move by a combination of the mechanisms described. The fluid nature of growing blebs enables the cell to squeeze through the ECM network mesh. The dashed line indicates the position of the leading edge before bleb nucleation, arrows indicate the forces that are exerted by the cells on the extracellular environment and dashed arrows indicate the streaming of cytoplasm. [Charras 2008]

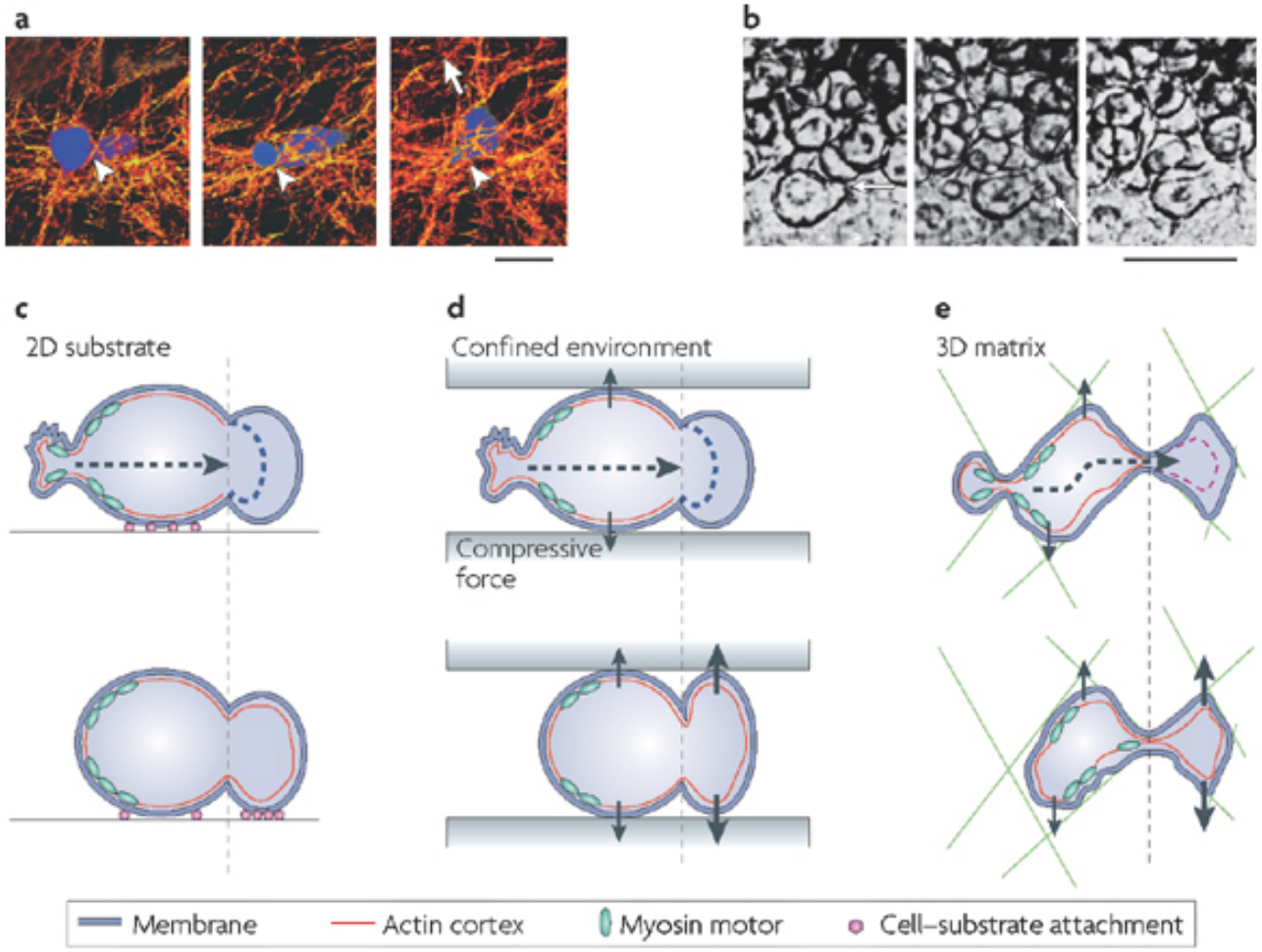
a
b
c
2D substrate
d
Confined environment
Compressive force
e
3D matrix
Membrane
Actin cortex
Myosin motor
Cell–substrate attachment
Nature Reviews | Molecular Cell Biology

imposed by the ECM to conserve their migration ability (resumed in figure 3.15). Many constraints including biochemical, topological and physical constraints can induce transition in cellular migration modes [Friedl 2010]. Among those, the effect of substrate adhesiveness, the ECM mechanical and geometrical properties have been the best studied. For instance the availability of extracellular binding partner for integrins can induce transition from blebbing migration to mesenchymal, lammelipodia based migration in walker carcinoma cells [Bergert 2012]. Fibroblast have been shown to favor lobopodia-based migration in linear 3D extracellular matrices and lamellipodia based migration in non linear elastic 3D extracellular matrices [Petrie 2012]. Various cells including Hela cells, fibroblast and RPE1 cells have been induces to amoeboid migration using geometrical confinement (Unpublished data from Le Berre *et al*). In order to perform such transition, the cell drastically adapts its cytoskeleton to produce the required forces for migration. Indeed, when Cell-ECM adhesion is blocked, confined cells move in a friction based mechanism [Renkawitz 2009]. When the pore sizes of the ECM are too small and the cell is not able to enlarge them, it will increase its contractility to generate the required forces for squeezing through the narrow gaps [Wolf 2013]. The cell mechanical properties, which display interesting properties such as strain/stress-stiffening allows the cell to rapidly adapt to the extracellular environment. This plasticity in cell migration is summarized in the tuning model of cell migration proposed by Friedl and Wolf (see figure 3.15). In this model the ECM architecture such as the geometry and the stiffness combined with cellular determinants, for example Cell-ECM adhesion, cellular proteolytic activities define the migration mode adopted by the cell [Friedl 2010].

Such plasticity in cell migration allows leukocytes to patrol the entire organism despite local biochemical and mechanical disparities. Unfortunately, this plasticity is also used by metastatic cells to invade the entire organism. Thus, understanding the transitions in cell migration is required to understand cancer metastasis and to drive immunotherapies.

3.4.3 1D-3D cell migration

I here, refer to 1D-3D migration as microchannels based migration. This type of migration is relevant to *in vivo* interstitial migration when for example cells have to crawl in between thick bundles of collagen fibers or in between two cells [Wolf 2003]. As said earlier, cells migrating in 3D matrices in a non-blebbing mode exhibit an actin rich protrusion named pseudopod. However, the complexity of the 3D space makes the full characterization of the shape, component and specificity of such protrusion harder. Microfabricated devices were introduced to tackle this issue. Indeed, with such systems, the condition of confinement is fulfilled without introducing any limitation for high resolution, live cell imaging [Irimia 2007]. Moreover, the simple geometry provided by microfabricated devices particularly microchannels makes theoretical modeling required to understand interstitial migration simpler. In the following paragraphs, I will describe how, using microchannels, Wilson *et al* were able

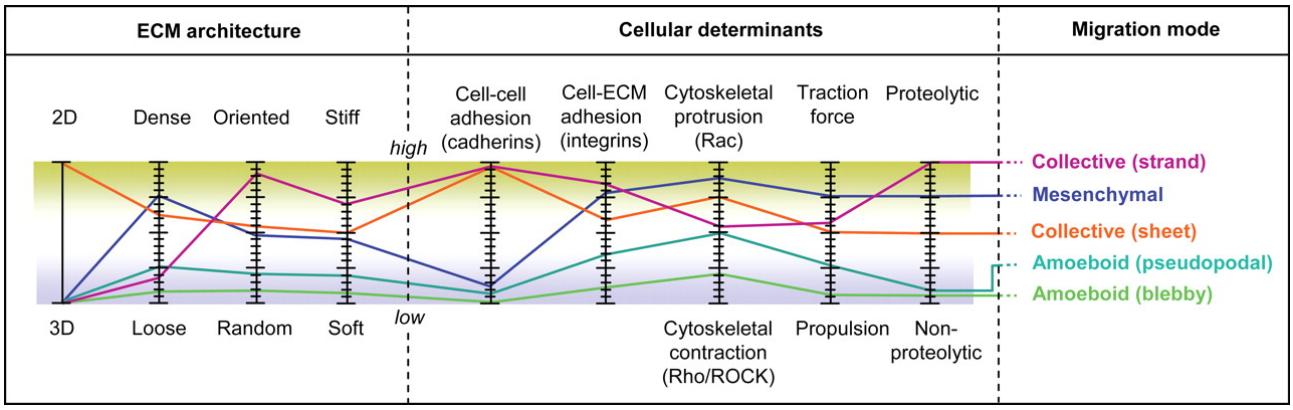

Figure 3.15: "**The tuning model of cell migration**. An integrated multiscale model to combine multiple interdependent parameters that impact migration mode. Each parameter is experimentally testable individually; however, in most cases they are interconnected with others. Approximated parameter profiles of selected migration modes are indicated (colored lines). Modulation by increasing or decreasing the magnitude of any parameter may impact the resulting migration mode as well as the input strength of coregulated parameters. The format of the tuning model mimics the popular display of a graphic equalizer, which is integral to modern media display programs (e.g., Windows Media Player or QuickTime); the graphic interface serves to adjust the intensity of different wavelengths of the phono output independently to modify the sound profile. [Friedl 2010]

to propose a detailed description of neutrophils "pseudopod". The simple geometry of microchannels allowed Hawkins *et al* to propose a theoretical model of chemnying migration and to Stroka *et al* to carry out an experimental and theoretical studies of actin-independent migration giving rise to the osmotic engine model.

3.4.3.1 Actin slab at the leading edge of neutrophils undergoing interstitial migration

Using microchannels allowed Wilson *et al* to propose a precise description of neutrophils leading edge during interstitial migration (see figure 3.16) [Wilson 2013]. This protrusion,in lack of high resolution imaging, called pseudopod [Irimia 2007] turns out to be quite complex with two zones of actin polymerization. Indeed, using Fluorescence Recovery After Photobleaching (FRAP) experiments, Wilson *et al* could show that at the interface between the cell and the channel wall, a dense, slowly polymerizing actin network, nucleated by Formins, is directed outwardly and perpendicularly to the channel wall while at the free cell edge, a much faster polymerizing actin network nucleated by Arp2/3 pushes the membrane forward, in the direction of motion. The adherent (cell-channel wall) and the free (free cell edge) actin network were shown to mechanically interact. The authors indeed proposed that the adherent actin network exerts compressive forces on the free network, preventing its retrograde flow and thus allowing a complete transmission of polymerization to forward leading edge protrusion.[Wilson 2013]

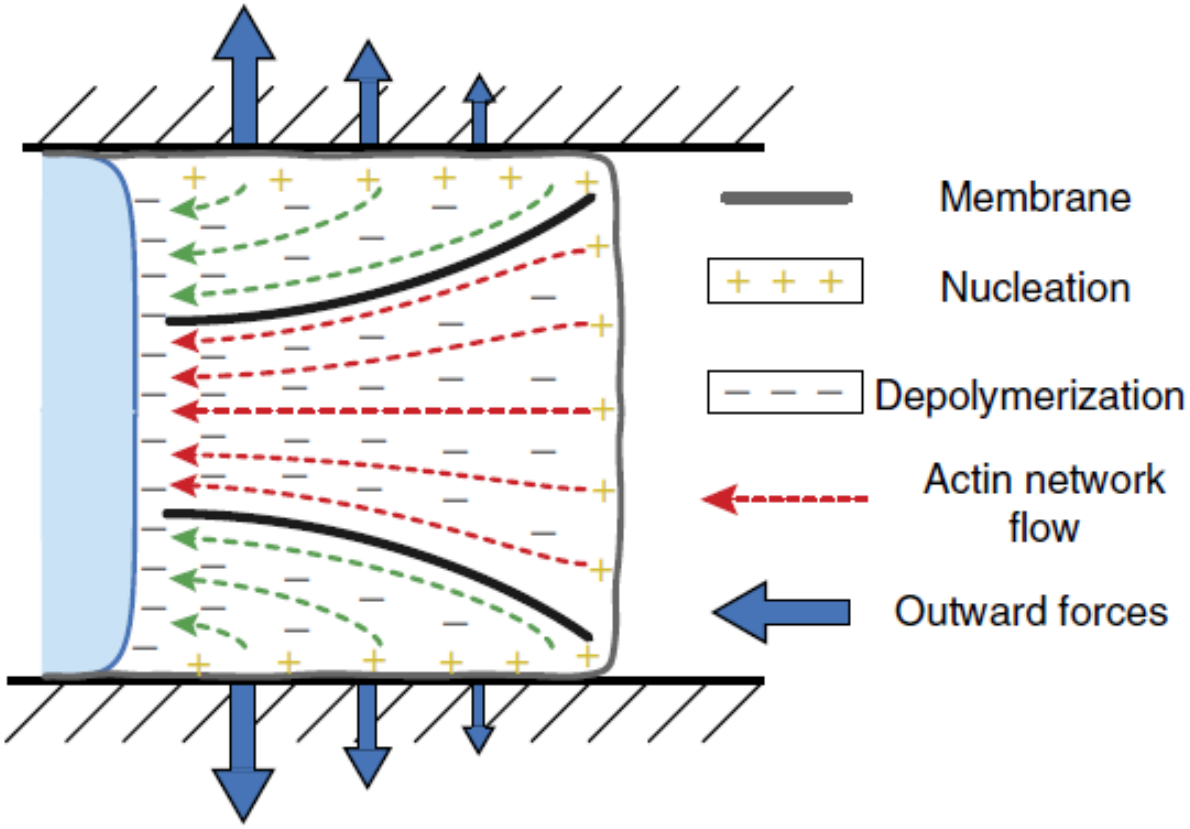

Figure 3.16: "**Conceptual model of F-actin dynamics in leading edge protrusion during interstitial migration**. In confined environments, leading edge protrusion results from the interaction between the adherent and the free F-actin networks. Nucleation of the adherent network (green) is directed perpendicular to the channel walls and its thickness increases from front to rear creating a constriction that compresses the free F-actin network (red). This constriction prevents rearward movement of the free F-actin network enabling new polymerization under the front membrane to create forward protrusion. Compression of the free network by the adherent network creates an outward pressure on the channel walls (arrows) as well as a protrusive force at the free membrane." From [Wilson 2013]

3.4.3.2 Pushing on the walls to move forward

Microfabricated devices were also used to tackle the struggling question in amoeboid migration of how are forces transmitted to the substrate. Indeed, the control of the geometry of the environment enabled by such devices allows theoretical studies of amoeboid cell migration to be performed. Using microchannels allowed Hawkins *et al* to propose a model for chimneying migration illustrated in figure 3.17 [Hawkins 2009]. This model is based on actin polymerization which by pushing the cell membrane along the channel walls allows force transmission to the substrate without requirement for specific adhesions. In this model, the cell is assumed to be an incompressible viscoelastic material confined by the channel. Such confinement induces a pressure build up in the gel which will enhance the cell-substrate friction and thus produce a forward movement of the gel. Such pressure gradient in microchannels was indirectly visualized using RICM (Reflexion Interference Contrast Microscopy) which visualizes the gradient of cell-substrate proximity. Hawkins *et al* indeed showed that the cell back is much closer to the substrate than the cell front which was interpreted as a sign of higher pressure at the cell back compared to the cell front. Interestingly, this model did not require myosin II based contraction which when present, could increase cell translocation rate [Hawkins 2009]. Even though further direct measurements of the required pressure gradient are needed, this model moved the field of amoeboid migration a big step forward. Moreover, the visualization of the adhesive network in HL-60 derived neutrophils which exert outward forces on the wall and compressive forces to the free network [Wilson 2013] is an evidence that confinement of an active gel can induce by itself a front-rear pressure gradient required for cell migration.

3.4.3.3 Interstitial migration independent of the actomyosin system: the osmotic engine model

One general idea is that in order for cells to move forward, they need to define an asymmetry. If until now, most of the studies have focused on the asymmetry of actin generated forces, a recent, ground-breaking work proposed a new model purely based on osmotic forces. Using again microchannels which allows a systematic polarization of migrating cells, Stroka *et al* proposed an integrated experimental and theoretical approach to provide the field with a new view of interstitial migration based on osmotic pressure gradient [Stroka 2014]. This model is illustrated in figure 3.18.

This study started by showing that the cancer cell lines MDA-MB-231 and S180 are able to migrate in microchannels without actin polymerization, myosin II based contraction as well as integrins based adhesions ([Balzer 2012], [Stroka 2014]). Interestingly, the interstitial migration of those cells requires aquaporins as well as the Na^+/H^+ exchanger. Aquaporins and Na^+/H^+ exchanger have been known for years to be essential for cell migration ([Papadopoulos 2008], [Schwab 2012]). The new contribution of Stroka *et al* was to visualize a polarized distribution of those channels. Indeed, aquaporins as well as the Na^+/H^+ exchanger were shown to be more concentrated at the cell front that the rear (see section a of figure 3.18). The authors, thus proposed an osmotic pressure based migration

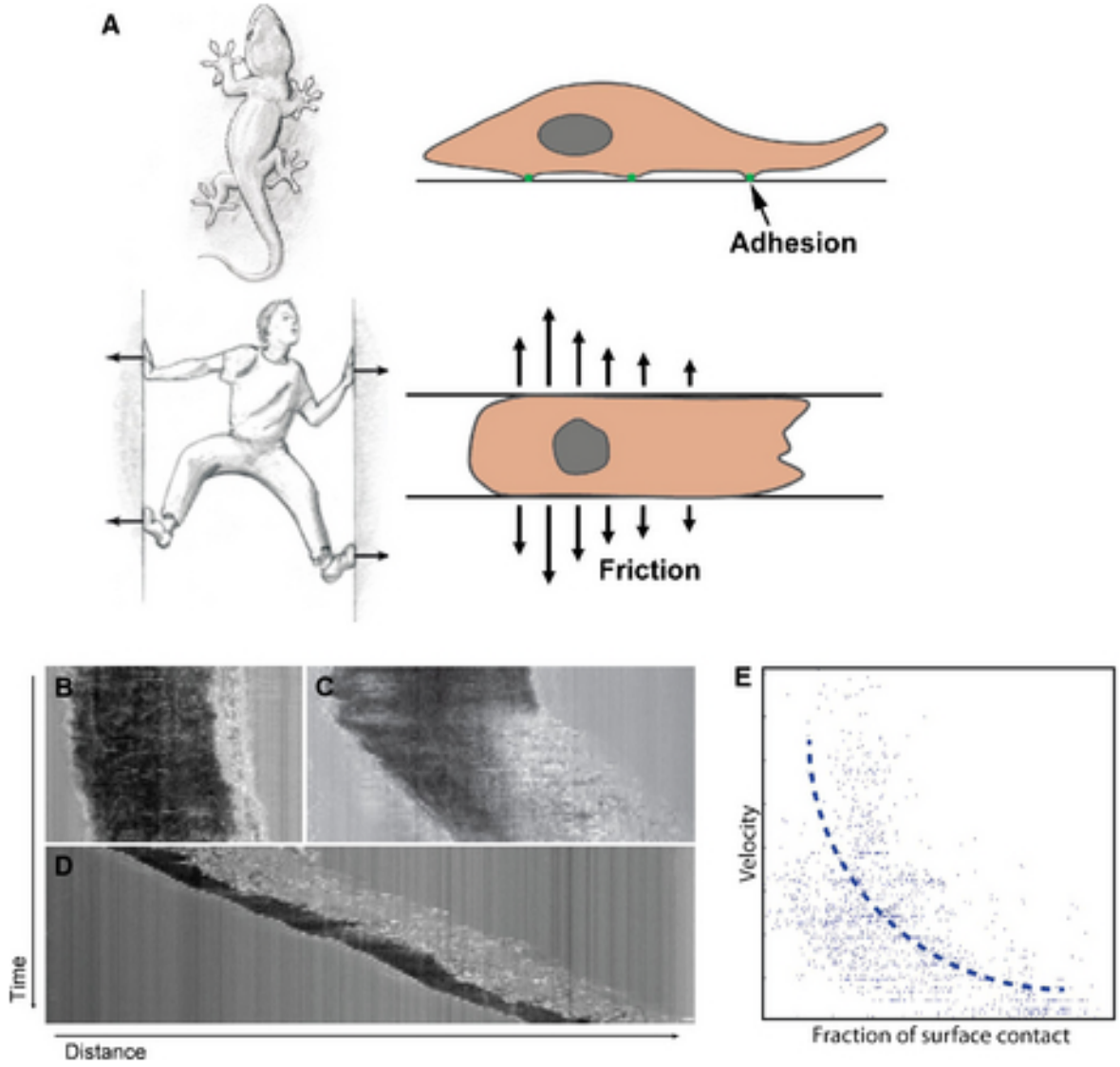

Figure 3.17: "**Pushing on the wall to move forward**. A) Schematic representation of forces required for cell movement in 2D and under confinement. 2D motility requires adhesion to the substrate, whereas, under confinement, it can be compensated by forces exerted by the cell body when pushing laterally on the substrate. B-E) RICM (reflection interference microscopy) measurements of dendritic cells migrating along fibronectin-coated microchannels show an inverse correlation between cell speed and surface of contact with the substrate (contacts appear in dark). B) Slow cells exhibit large contacts. D) Fast cells present minimal interactions, mostly restricted to the back. C) During bi-phasic migration, slow phases are associated with increased surface contact at the front. E) Correlative graph of cell speed versus fraction of surface contact." From [Hawkins 2009]

model called the osmotic engine model. The cell, by regulating the net inflow of water at its leading edge and a net outflow of water at its trailing edge would control its migration. This difference in water flow between the leading and the trailing edge is regulated by the extracellular osmotic pressure. Stroka *et al* indeed showed that they could induce the cell to change direction by putting and hypotonic medium at the leading edge or a hypertonic medium at the trailling edge. The osmotic engine model thus proposes that the cell can move forward in microchannels as a result of different extracellular osmolarities at the leading and/or trailing edge and/or front-rear polarization of ions channels and aquaporins. Both the differential osmolarity and the polarization of ions channels and aquaporins will induce a differential water flow through the cell resulting in a ions concentration gradient which in turn induces a gradient of osmotic pressure along the cell. Even though actin polymerisation is not required for a nonzero velocity of polarized cell, changing direction requires actin polymerization. Indeed, repolarization of the ion transporters and aquaporins upon osmotic shock requires actin polymerization presumably for their transport. [Schwab 2012] One can thus imagine that during interstitial migration, the cell might use a gradient of osmotic pressure to move forward but in presence of an obstacle, actin polymerization will be used to change direction.

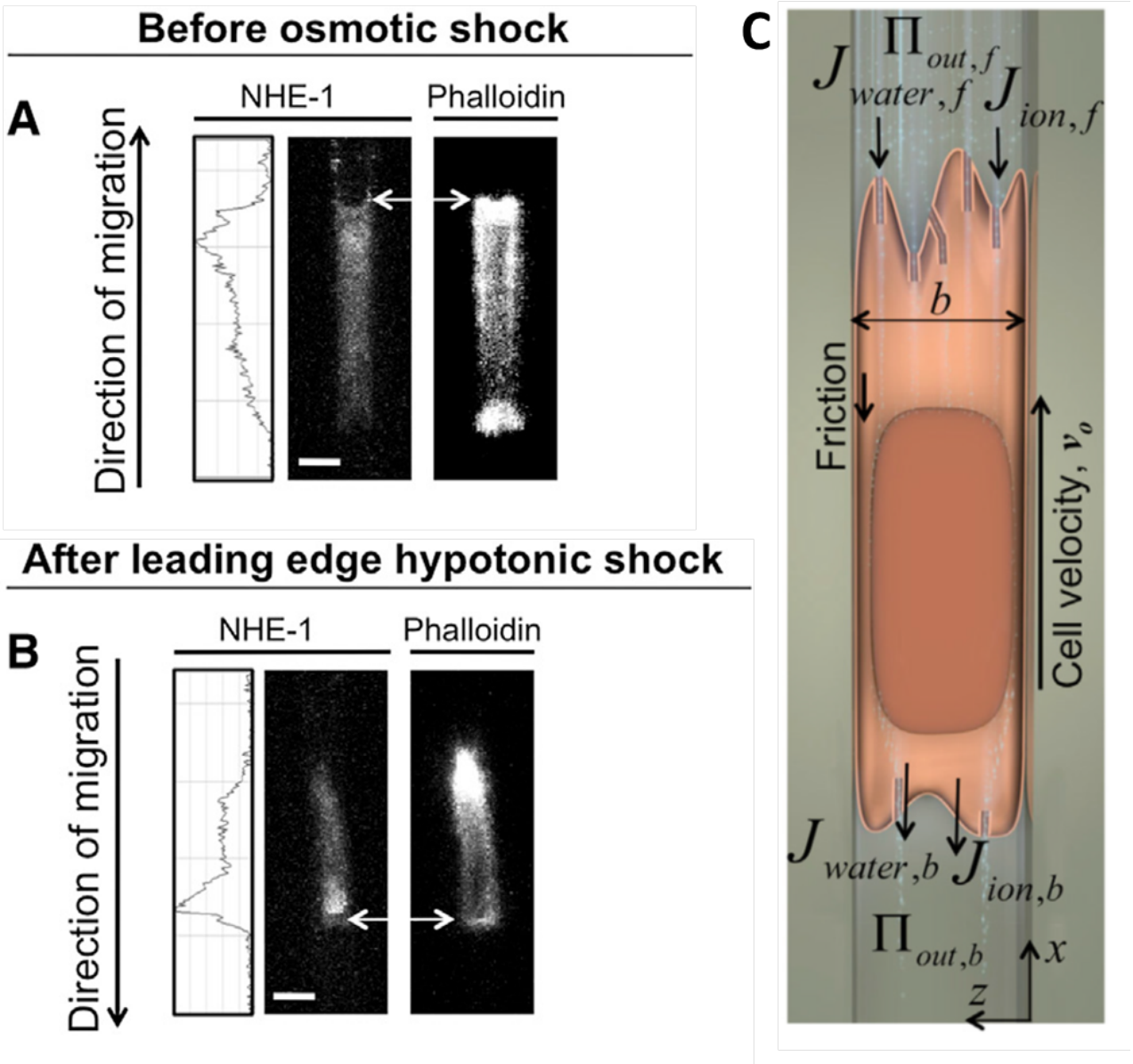

Figure 3.18: "**The Osmotic Engine Model**.A) and B) Confocal images and corresponding NHE-1 plot profiles of S180 cells stained for NHE-1 or for actin by phalloidin-alexa 488, A) in isotonic medium, B) after a hypotonic shock at the leading edge. White scale bars represente 3 μm. White arrows point to the cell leading edge. C) Schematic of the Osmotic engine Model, based on water permeation through the cell membrane at leading and trailling edges." Adapted from [Schwab 2012]

Chapter 4

Nuclear mechanics in cell migration

Contents

The nucleus has a preferential position in eukaryotic cells. As genetic material container, its integrity is necessary for the survival of many cells. Mammalian nuclei are highly organized structures. They are composed by the nucleoplasm, surrounded by the nuclear lamina and two lipid bilayers: the inner nuclear membrane and the outer nuclear membrane (see figure 4.1). The outer lipid bilayer is an extension of the endoplasmic reticulum membrane and is connected to the inner nuclear membrane by the nuclear pore complexes (NPCs) which are large structures that control protein transport across the nucleus. As a lipid bilayer, the nuclear membrane can be considered as a 2D fluid which thus does not impact the nuclear mechanical properties [Rowat 2006]. However, the inner nuclear membrane is tightly coupled to the lamina network which can then induce membrane tension as observed on the plasma membrane. Indeed, the lamina has been shown to interact with variety of nuclear envelop proteins including emerin, lamin B receptor, nesprins and sun proteins [Isermann 2013]. More data on the mechanical coupling between the lamina network and the nuclear membrane would be necessary to determine the existence of nuclear membrane tension ([Rowat 2005], [Rowat 2006]).
In the past decade, the role of the nucleus in cell architecture and mechanical properties became of high interest because of the identification of a growing number of diseases associated to the nucleus.

Its role in cell migration is also becoming more and more addressed. Indeed, the nucleus has been implicated in cell polarity as well as in the ability of cells to move under confinement. In the following paragraphs, I will describe the role of the nucleus in cell migration focusing on the mechanical properties of the nucleus.

4.1 Nuclear mechanics

As said earlier, the nucleus is often the biggest (≈5-20 μm) cellular organelle with an elastic modulus that can be ten times higher than the cytoplasmic one (see section 3.1.4). For several years, the nucleus has been predicted to play a major role in cell mechanics [Maniotis 1997].However only 14 years ago, in 2000, it was realized that the nucleus has mechanical properties that can be distinguished from the overall cellular ones. In their paper, Guilak *et al* used micropipette aspiration to show that the nuclear mechanical property is significantly higher than the cellular one. Using a classical viscoelastic model, they showed that the nucleus behaves like a viscoelastic solid with a mean elastic modulus of 1-5kPa [Guilak 2000].
New technological developments, such as micropipette aspiration of the nucleus , were applied to the nucleus and allowed scientists to decompose the contribution of each part of the nucleus in this viscoelastic behavior. Even though many components as well as scales can be found in the nucleus most of the studies in nuclear mechanics focused on the nucleoplasm and the nuclear lamina.
A decade of intensive studies gave rise to a common mechanical view of the nucleus as a viscoelastic solid embedded in an elastic shell [Verstraeten 2008]. The viscoelastic solid being the nucleoplasm and the elastic shell the lamina. In the following paragraph, I will review our current knowledge on the mechanical properties of the nucleoplasm as well as the lamina network.

4.1.1 The nucleoplasm define the nuclear rheological properties

In many ways, the nucleoplasm is similar to the cytoplasm (bio-polymers in aqueous solution). The nucleoplasm is composed of DNA, arranged in chromatin which can be modeled as bio-polymers. Those bio-polymers are embedded in a solution containing several proteins and even filaments [Zwerger 2011]. Recently, actin filaments have been shown to assemble inside the nucleus [Belin 2013]. Even though the mechanical interaction of the different polymers constituting the nucleoplasm is not well understood, many studies performed at the level of the overall nucleoplasm are revealing details of its mechanical properties.
In my knowledge, the first study on the viscoelastic properties of the nucleaoplasm was performed in 2004 when Tseng *et al* performed nanorheological experiments in nuclei. By studying the trajectories of 100nm diameter particles, they proposed that the nucleoplasm is a highly viscous and elastic solid. They measured a mean shear elastic modulus of 18 Pa and a shear viscous modulus of 52 Pa. They

were also able to detect the presence of microdomains (domains with higher elastic moduli) which they proposed to preserve nuclear structural coherence [Tseng 2004].
But this viscous material (i.e. the nucleoplasm) can undergo a transition to a more condensed network. Indeed in 2006 Rowat *et al* showed that the nuclear volume decreases by 60-70% during micropipette aspiration. Following this volume decrease, the nucleoplasm become resistant to further deformation [Rowat 2006]. They explained this lost of volume and compliance by water lost upon aspiration. In 2007 Pajerowski *et al* using also micropipette aspiration, showed that the nucleus undergoes a phase transition between a viscoelastic to a viscoplastic material. Using various not fully differentiated or lamina depleted epithelial cells, they showed that the nucleus has a fluid-like behavior at short time scales (less than 10s) but exhibit irreversible deformations at longer time scales. They also reported a stress-stiffening behavior of the nucleus in TC7 epithelial cells subjected to increased pressure. This stress-stiffening was mainly attributed to the chromatin so the nucleoplasm [Pajerowski 2007]. The long time scale plastic behavior being independent of the lamina network was also attributed to the nucleoplasm. Taken together, these studies point towards a mechanical description of the nucleoplasm as a viscoplastic material which define the rheological behavior (ability to flow) of the nucleus.
Interestingly, a recent study has proposed that the nucleoplam can behave like auxetic materials (i.e. materiels which decrease size perpendicular to the applied compression,). Indeed, Pagliara *et al* have shown that embryonic stem cells in their metastable state (transition between naive pluripotency and differentiation proming states) become smaller in their cross-sectional area under compression which is the characteristic of auxetic materials. As auxetic materials, the nucleoplasm of transition embryonic stem cells stiffen under compression [Pagliara 2014].
Although many different mechanical models (viscoelastic, viscoplastic, auxetic) of the nucleoplasm are emerging, one constant feature is the stress-stiffening behavior of this material. The observed differences in the intrinsic nuclear mechanical properties can be due to the differentiation state of the studied cells. Further characterization of the composition of the nucleaoplasm and the interaction between its different components (chomatin, F-actin, Myosin motors) is necessary for a better understanding of the mechanical behavior of the nucleus.

4.1.2 Mechanical properties of the lamina network

As a polymer network the mechanical property of the lamina relies on the structure of the network (aligned, entangled, crosslinked) combined with the mechanical properties of single filaments. However, difficulties in precisely defining the type of network forming the lamina motivated the study of the lamina network mechanical properties as a whole system. In the following paragraph, I will describe our current knowledge about the structure of the lamina as well as the mechanical properties of this network.

4.1.2.1 Structure of the lamina network

The nuclear lamina is composed of lamin filaments. Lamins are type V intermediate filaments found predominantly in the nucleus with a particular concentration in the nuclear periphery. In vertebrates, two groups of genes, LMNA and LMNB1/2, code respectively for the A- and B-types lamins. The LMNA gene gives rise to the splice variants Lamin A, Lamin C and the less abundant lamin $A\Delta 10$ and lamin C2 proteins. The B-type lamins are coded by the LMNB1 and LMNB2 genes and are found in all cell types [Ho 2012]. A-type lamin expression depends on the level of differentiation of the cell and has recently been shown to scale up with tissue stiffness [Swift 2013].
The nuclear lamina is the result of the A and B type lamins interaction. As a type V intermediate filaments, lamins are composed of a short N-terminal domain, a central rod domain and a long C-terminal domain. Coiled-coil formation of two central rod domain drives lamin dimerization. Head to tail interaction of dimers leads to a polar filament formation. Two filaments assemble then in an anti-parallel fashion into non-polar filaments [Ho 2012]. In *Caenorhabditis elegans* and *Xenopus oocytes* lamins have been shown to form thick, approximately 10-nm-diameter filaments. In the large NPC-free areas of *Xenopus oocytes* nuclei, lamins networks are seen as a two-dimensional set of parallel filaments with distinct regular cross-connections [Goldberg 2008]. Such regular network has not been described in somatic nuclei. Indeed, the electron micrographs of somatic nuclei lamins usually shows a dense, poorly defined protein network [Zwerger 2011]. The A- and B-type lamin proteins are proposed to form two distinct but interconnected layers ([Goldberg 2008],[Shimi 2008]). Expression of somatic lamins in the big *Xenopus oocytes* nucleus allowed Goldberg *et al* to propose a model for the A and B-type lamins structure in somatic cells. Closer to the nuclear membrane, B-type lamins form thin, highly organized layers whereas A-type lamins form thick bundles and a compact layer which leaves the NPC clear [Goldberg 2008]. This model still needs to be validated in somatic cells. Thus more evidences of the detailed structure of the lamin A/C network in somatic cells are necessary for the understanding of its mechanical properties.

4.1.2.2 Lamina mechanics

In a mechanical point of view, the lamina network in somatic cells was initially viewed as a two-dimensional solid-elastic material which resists forces like a solid ([Rowat 2005], [Rowat 2008]). However, the studies from which this model emerged were performed in LMNA overexpressing cells, it was thus necessary to determine the lamina mechanical properties in cells expressing a basal level of the LMNA and LMNBs genes. A recent work has proposed a viscoelastic model of the lamina network where A- and B- type lamins would have a distinct mechanical role [Harada 2014]. According to this model, the A-type lamin network is a viscous material which would flow under deformation while the B-type lamins constitute is an elastic material which can be represented by a spring.

From a solid-elastic representation to a viscoelastic model, the mechanics of the nuclear lamina has evolved considerably in the past ten years. Further studies on the differential contribution of the lamina components are needed to confirm this new and interesting model proposed by Harada *et al*.

Many studies have been performed to determine the role of the lamina network in global nuclear mechanical properties. Lamins are seen as shock absorber of the nucleus where it can bear up to 50% of the applied stress. Experiments performed in 2004 have shown that lamins downregulation decreases nuclear stiffness [Lammerding 2004]. Recently, A-type lamins have also been shown to be important in nuclear stress adaptation [Guilluy 2014]. Indeed, in this studies, Guilluy *et al* reported that upon periodic stresses, lamin A/C is recruited at the site of stress application leading to nuclear stiffening . This lamin A/C dependent nuclear stiffening was shown to go through emerin phosphorilation by the SRC family kinase. Interestingly, Src-family kinase also mediates cellular mechanotransduction through integrins [Hoffman 2011]. Until the last year, only lamin A/C has been implicated in nuclear mechanical properties. Indeed, in 2006, Lammerding *et al* have shown that lamin A/C but not Lamin B1 downregulation is responsible for the lamins dependent nuclear stiffness. However a recent study performed in fibroblasts reported that LaminB1 overexpression also leads to an increased nuclear stiffness [Ferrera 2014].

Thus, even though a detailed description of the structural and also mechanical properties of the lamina network are still required, the role of this network in nuclear mechanical properties is now well accepted. However, more studies will be required to further understand the role of the lamina network in nuclear mechanics.

4.2 Linking the nucleus to the cytoplasm

In addition to chemical interactions, mechanical interactions between the nucleus and the cytoplasm are now well accepted. In 1997, Maniotis *et al*, demonstrated the existence of a direct, physical connection between the nucleus an the cytoskeleton [Maniotis 1997]. They indeed show that force exerted on the cytoskeleton (Actin, Microtubules, Intermediate filaments) is transmitted to the nucleus through a mechanical coupling. Since then, many studies have been performed in order to identify which protein mediates this nucleo-cytoskeleton interaction. Thirteen years later, we have a good view of the structure of the LInkers of Nucleoskeleton and Cytoskeleton (LINC) complex. We also start having a good understanding of how forces can be transmitted from the cytoskeleton to the nucleus.

4.2.1 The LINC Complex

At the moment, best accepted model of the LINC complex is based on the SUN-KASH interaction at the perinuclear space (PNS) (see figure 4.1). As said earlier, the nuclear membrane is composed of two lipid belayers, the inner nuclear membrane (INM) and the outer nuclear membrane (ONM). To form a nuclear envelop bridge, proteins are transported from the endoplasmic reticulum either towards the INM to interact with the Lamina or the ONM for cytoskeletal interaction. The bridge is complete when proteins in the INM interact with the ones in the ONM through the PNS. In the actual LINC complex model, Klarsicht, ANC-1, and Syne/Nesprin (KASH) homology proteins at the ONM interact with Sad1 and UNC-84 (SUN) proteins located at the INM thus make the connection between the inner and the outer nuclear area (see figure 4.1) [Starr 2010]. Sun and Kash are well conserved domains that define two protein families: the sun-domain proteins and the Kash domain proteins.

4.2.1.1 The SUN-domain proteins:

Sun proteins are conserved across all eukaryotic cells. They are defined by a stretch of $\approx$ 175 amino acids at their C-terminus termed the "SUN domain". This sun domain is also found at the C-terminus of the C. elegans protein UNC-84 and the S. pombe protein Sad1. The number of Sun proteins scales up with the level of complexity of the organism [Sosa 2013]. While single cell organisms carry out only one sun protein variant, 5 sun protein variant are found in the mammalian genome. The expression of different isoforms is cell type dependent. If Sun1 and Sun2 are usually ubiquitous, Sun3-5 show a more restricted , testis-specific expression pattern [Sosa 2013]. The expression pattern of sun proteins also vary during development [Starr 2010].
All sun proteins have at least one trans-membrane domain which position them at the nuclear membrane. But the mechanism which leads to their localization at the nuclear membrane is still poorly understood. Indeed, many sun proteins contain a nuclear localization signal (NLS) which however, has been shown to not be required for INM localization. The other possibility would be a sun protein positioning via lamina interaction. But only some sun proteins require a functional lamina for their localization at the inner nuclear membrane [Starr 2010]. Thus more studies are required to understand the dynamic of the nucleo-cytoskeleton formation. Understanding this dynamic of formation is necessary to understand how forces are transmitted through the LINC complex. The most accepted picture, at the moment, for the LINC complex formation is that sun proteins localization at the perinuclear space drives the recruitment of Kash proteins ([Starr 2010], [Sosa 2013]).

4.2.1.2 The Kash-domain proteins

So far, Kash proteins have been exclusively found in the ONM (see figure 4.1). They are defined by a C-terminal conserved KASH domain which is a membrane-spanning region followed by 8-30 residues before the C terminus. Kash proteins are supposed to be tail-anchored in the ER where they

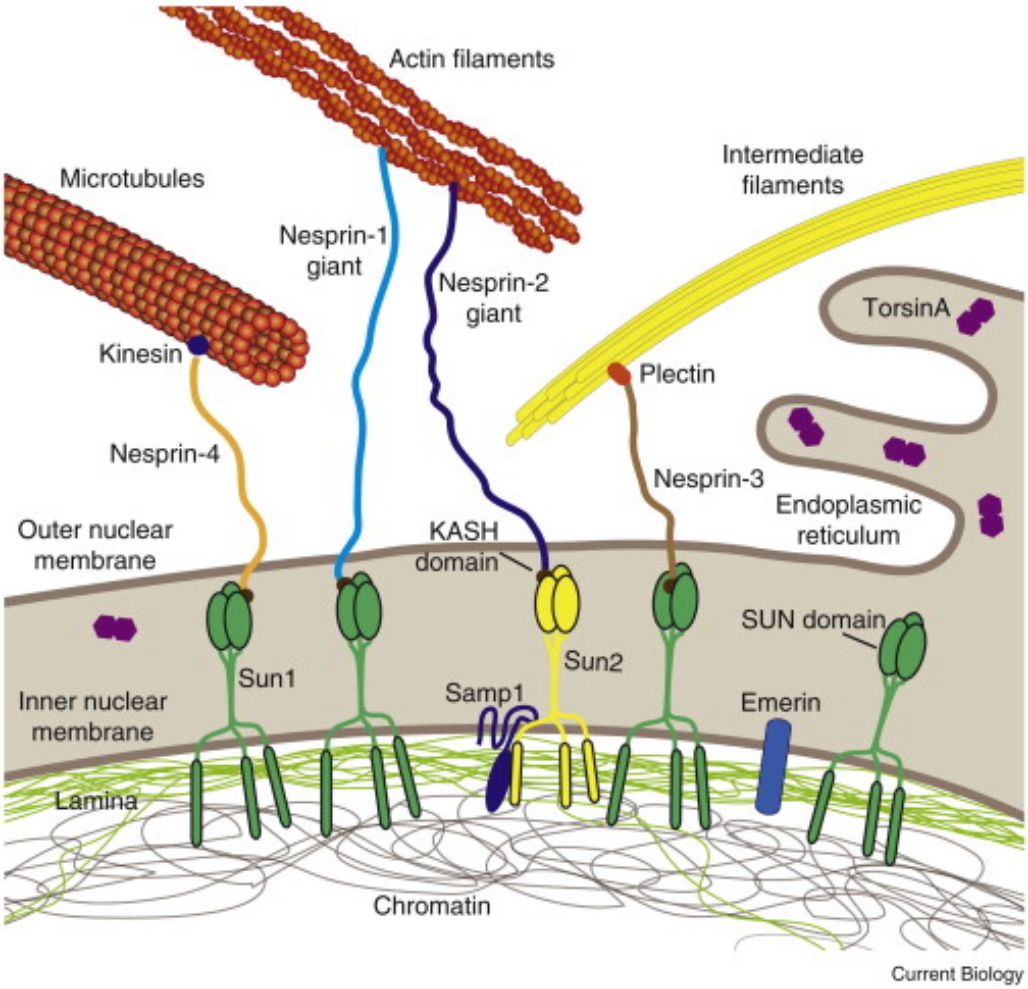

Figure 4.1: "**Schematic overview of LINC complex proteins and their connections to the cytoskeleton and nuclear interior.** SUN proteins at the inner nuclear membrane bind to the nuclear lamina and other nucleoplasmic proteins while interacting with KASH domain proteins at the outer nuclear membrane. KASH domain proteins directly or indirectly interact with cytoskeletal filaments, thereby forming a physical connection between the nuclear interior and cytoskeleton. Please note that SUN and KASH domain proteins can exist in multiple isoforms encoded by several genes. In human somatic cells, the most predominant KASH domain proteins are nesprin-1, -2, and -3 and their various isoforms, and Sun1 and Sun2 are the predominant SUN proteins. Illustrated are only the largest isoforms for nesprin-1-4; cells express many additional shorter nesprin isoforms, including some lacking the KASH domain. Smaller nesprin isoforms may also be located on the inner nuclear membrane. Note that nesprin-1, -2, -4 and KASH5 can also interact with kinesin and/or dynein. Samp1 and torsinA are involved in the regulation of the LINC complex. Not depicted are KASH5 and the SUN protein isoforms Sun3-5, as their expression is restricted to germ cells. The nuclear lamina comprises A-type and B-type lamins. Note that torsinA can be localized in the endoplasmic reticulum and the perinuclear space, with the distribution varying depending on expression levels." From [Isermann 2013]

are post-translationally inserted by Asna1-GET3 [Starr 2010]. They localized in the ONM with their conserved Kash domain into the perinuclear space. Interestingly, inserting a Kash domain in a given protein is sufficient to target it to the ONM [Starr 2010]. The N-termini of Kash proteins are highly variable in length and domain composition [Cartwright 2014].

As said earlier, the central hypothesis of the LINC complex model is that Kash proteins recruitment at the ONM requires Sun proteins. Even though the dynamic of this interaction is not yet known, the recently published crystal structure of the sun-kash complex showed that the sun-kash interaction is stable and strong. Indeed, three Sun proteins form a homotrimer with three deep grooves in which three Kash peptides are inserted (see illustration in figure 4.2) [Sosa 2013]. As the trimerization of sun proteins is a prerequisite for kash binding [Sosa 2012], the central hypothesis of the LINC complex formation is still valuable.

What initiates Kash and Sun interaction is still an open question. Both proteins have diffusional mobilities similar to other nuclear membrane proteins suggesting that they are more likely in dynamic complexes. TorsinA, an homologue to AAAATPases which is localised at the ER lumen and shows a binding affinity for Kash domains is a potential regulator of the LINC complex assembly and disassembly [Gundersen 2013]. To date, six Kash proteins have been reported in mammals, each of them has a distinct role in binding the cytoskeleton. Four of the human Kash proteins have multiple spectrin repeats and are thus called nesprins for NE spectrin repeat proteins [Sosa 2013].

Nesprins 1 and 2 are giant proteins (between 800 and 1000 kDa) coded by the SYNE1 and SYNE2 genes. They exhibit a large cytoplasmic domain which is predicted to be composed by their spectrin repeat motifs. They are thus supposed to form flexible and extensive fibers into the cytoplasm. Near the nesprin-1 and 2 N-termini is a domain homologous with Calponin (calcium binding protein) which mediates their binding to actin [Starr 2010]. In addition Nesprins 2 binding to F-actin has been shown to drive nuclear positioning in fibroblasts [Luxton 2010]. Nesprin-3 is shorter than nesprin1-2 and binds to intermediate filaments through plectin. Nesprin-4 coded by the SYNE4 gene is a cell type specific nesprin (it has until now been seen in highly secretory cells and hair cells) and binds to kinesin which in turn binds to microtubules. KASH5 binds to Sun1 in the PNS and to the dynein regulator dynactin. KASH5 is germ-cell specific and is involved in meiotic homologue pairing. The latest characterized KASH protein, the Lymphoid-restricted membrane protein (LRMP) has been reported to be necessary for pronuclear congression in fertilized egg. Even though its binding to sun proteins is not yet shown, its involvement in nuclear positioning makes it appear as a KASH protein family [Sosa 2013]. More and more attention is now put on identifying the proteins composition of the LINC complex. Emerin, Samp1 and others are emerging as component of this complex which complete identification is at high interest for different communities in biology. Indeed, defining how the nucleus is connected to the cytoskeleton is important for understanding how this organelle is positioned in many cellular processes including cell migration. A nucleo-cytoskeleton physical link can be also important to organize the nuclear interior and to regulate the force transmission from the ex-

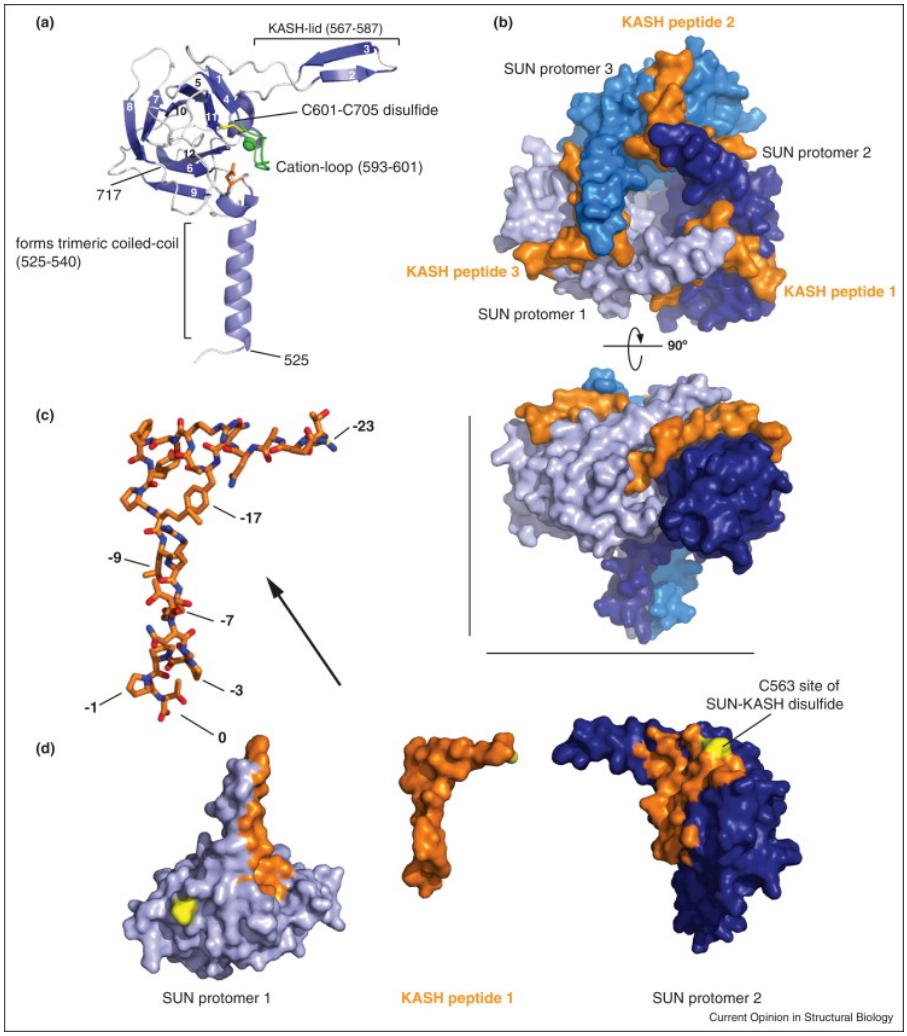

Figure 4.2: "**Sun-Kash crystal structure** a) Overview of a human SUN2 protomer isolated from its Nesprin-2 binding partners in the trimeric SUN/KASH complex. The protein is organized around a compact β-sandwich core, decorated with features important for function (labeled). Bound cation depicted as a green sphere. b) View from the ONM facing the bottom of the trimeric SUN2 arrangement (blue colors) with three individual KASH peptides (orange) bound. c) Side view of the SUN2/KASH2 complex. It is easy to recognize how deeply the three KASH peptides are buried in clefts formed between neighboring SUN2 protomers. d) Explosion view of the KASH peptide interacting with neighboring SUN domains in the SUN2 trimer. Areas on the SUN domains in close contact with the KASH peptide are highlighted in orange. Note the L-shaped, extended conformation of the bound KASH peptide. Important residues for SUN interaction are labeled in the zoomed, stick representation of KASH2." From [Sosa 2013]

tracellular environment to the nucleus. This could ultimately allow us to understand how a possible mechanco-genetic feedback can be controlled at the level of the cell.

4.3 Nuclear mechanics in health and disease

As said earlier, the interest in defining a physical link between the nucleus and the cytoskeleton was triggered by the discovery of diseases related to lamins or LINC complex mutations. In 1994 Bione *et al* identified emerin as the gene which mutations give the hallmark of the Emery-Dreifuss muscular dystrophy (EDMD) pathology [Bione 1994]. Five years later, in 1999, Bonne *et al* followed showing that mutations in the LMNA gene also leads to the EDMD pathology [Bonne 1999]. Nowadays, a growing numbers of diseases are associated with mutations in genes encoding for the lamina proteins (LaminA/C, LaminB1/LMNB2) as well as lamins associated proteins including Nesprins 1, 2, Emerin, Lamin B receptor, Luma, $Lap2-\alpha$, Man1, BAF ([Schreiber 2013], [Méndez-López 2012]). To date, more than 400 mutations have been identified on the LMNA gene. These mutations, related to at least 15 known diseases called laminopathies and position the LMNA gene as the most mutated gene known to date [Ho 2012].

4.3.1 Laminopathies

Patients affected by laminopathies show a wide range of symptoms but the most recurrent one is muscular dystrophy which affects cardiac or skeletal muscle [Schreiber 2013]. Cells from laminopathies patients often carry out abnormal nuclear morphology and altered distribution of nuclear envelope proteins such as lamins, nesprins and sun proteins. This phenotype might result from impaired nucleo-cytoskeleton force transmission, a process important in cell migration. For example, depletion of LMNB1,2 in mice result in neuronal migration defect and causes lissencephaly-like phenotypes (severe psychomotor retardation, seizures, muscle spasticity, and failure to thrive) [Schreiber 2013]. Moreover, changes in lamin expression level have been reported in a variety of cancer including skin and ovarian cancer, leukemia, lymphomas, breast cancer and others. Interestingly, the changes in lamin expression correlated with the tumorigenic potential and malignant transformation. For example, the LMNA gene is upregulated in skin and ovarian cancer but downregulated in leukemia and breast cancer [Ho 2012].

Even though the molecular mechanisms of those pathologies are not well understood, many theories are emerging trying to explain how mutations in the LINC complex can lead to such pathologies. Firstly, by disrupting the LINC complex, those mutations might change the force transmission between the nucleus and the cytoplasm. Secondly, because the lamina plays a major role in nuclear mechanics, disrupting this meshwork can 'weaken' the nucleus. Lastly, lamins being implicated in

many gene transcription pathways, mutations in the Lamin genes can impair many signaling pathways. Those possibilities are now converging towards two theories for explaining tissues specific aspect of laminopathies: the structural hypothesis and the gene regulation hypothesis [Ho 2012].

4.3.1.1 The structural hypothesis

This hypothesis is based on the assumption that LMNA mutations weaken the nucleus which is thus more sensitive to mechanical stresses. This higher mechanical stress sensitivity would lead to cellular death and thus progressive disease. This theory is supported by the fact that skeletal muscle cells from patients with Emery Dreifuss muscular dystrophy (EDMD) as well as mouse models of this disease contain fragmented nuclei. Moreover, downregulation of Lamin A/C has been shown to decrease nuclear stiffness [Ho 2012]. However, establishing a clear correlation between structural defects and associated phenotypes in LMNA mutations is not straight forward.
In one hand cells lacking lamin A/C have softer and more fragile nuclei than the control cells [Lammerding 2006]. On the other hand, cells from patients with the Hutchinson Gilford progeria syndrome (HGPS) exhibit much stiffer nuclei which are still more susceptible to mechanically induced cell death [Verstraeten 2008]. A recent publication from Denis Discher's lab brings new data which could explain this apparent antagonism. Harada *et al* showed that lamin A/C downregulation has a biphasic effect in both cell migration and cell survival in 3D environments. Indeed, partial knockdown of the LMNA gene resulted in an increase in cell passage through narrow pores while higher knockdown as well as overexpression of LMNA impaired cell migration in 3D. They also showed that decreasing LMNA expression increases the number of dead cells after passage through the narrow pores. They thus proposed that Lamins would impede 3D migration but also promote survival against migration-induced stresses [Harada 2014]. One could thus think that Hutchinson Gilford progeria syndrome disease might be caused by defects in cell migration as nuclei are stiffer while Emery Dreifuss muscular dystrophy would be caused by stress induced cell death of muscle cells. One important point is still why are cells from patients with progeria susceptible to mechanical stress induced death. The structural hypothesis alone is then insufficient to explain the diverse phenotypes observed in laminopathies.

4.3.1.2 The genome regulation hypothesis

This theory postulates that the development of different disease phenotypes observed in lamminopathies is due to a perturbed interaction with tissue specific transcription factors. In favor of this theory, lamminopathies are always associated with misregulation of common signaling pathways including the mitogen activated protein kinase (MAPK), the transforming growth factor beta ($TGF-\beta$), $Wnt-\beta-catenin$ and the Notch pathways which are crucial regulators of proliferation, differentiation and apoptosis [Ho 2012]. This might be related to the role of lamins in gene expression. In

addition, many laminopathies including HGPS, familial lipodystrophy and mandibuloacral dysplasia are associated with lost in heterochromatin. This phenotype is also observed in cells lacking A-type lamins. Changes in chromatin organization could thus modulate gene expression, the frequency of DNA damage as well as the efficiency of DNA repair [Ho 2012].

The genome regulation hypothesis and the structural hypothesis are actually not exclusive. Indeed, several other pathways including some involving mechanosensitive proteins such as the one coded by Egr1 and Iex1 are also impaired in cells and mice lacking A-type Lamins. One could imagine that the observed defects in signaling pathways is due to the mechanical uncoupling between the cytoskeleton and the nucleus. Indeed, a defect in mechanical force transmission can lead to the rupture of the connection between the lamina and the chromatin and thus a misregulation of gene transcription. In one way or another, disrupting the LINC complex can lead to many consequences among which defects in cell migration. In the following section I will focus on the importance of the nucleus in cell migration. In one hand, the nucleus can facilitates cell polarization but on the other hand, having to drag such a huge and stiff organelle can limit cell migration.

4.4 The nucleus during cell migration

One specific cellular process where both nuclear mechanics and nucleo-cytoskeleton connection play an important role is cell migration. Indeed, cell migration is based on mechanical force transmission between the extracellular environment and the cell. Because the nucleus is the stiffest and most voluminous organelle in the cell it may have special requirements to force transmission. Moreover, recent publications are pointing towards the idea that the nucleus might be the limiting factor during cell migration. Indeed, when a cell has to move in a highly confined space, deforming and transporting its nucleus might require additional forces ([Le Berre 2013], [Wolf 2013]). In this line of understanding how forces are transmitted from the cytoskeleton to the nucleus, a lot of efforts were put in identifying specific perinuclear structures involved in nuclear deformation, transport and/or positioning. In the following section, I will describe how, in migrating cells, the nucleus is well positioned.

4.4.1 Nuclear positioning

In textbooks, the nucleus is usually represented at the center of the cell. However, more and more data are now showing that its position inside the cell is tightly regulated (illustrated in figure 4.3). A molecular toolbox, which detailed identification is rapidly growing, is used by cells to either maintain the nucleus at a given position or move this organelle whenever it is needed [Gundersen 2013]. This molecular toolbox is though to contain in one hand elements of the cytoskeleton and on the other hand proteins of the nuclear envelope. Actin filaments, microtubules and some motors proteins such as kinesin and dyneins are the main cytoskeletal elements found in the nuclear positioning tool-

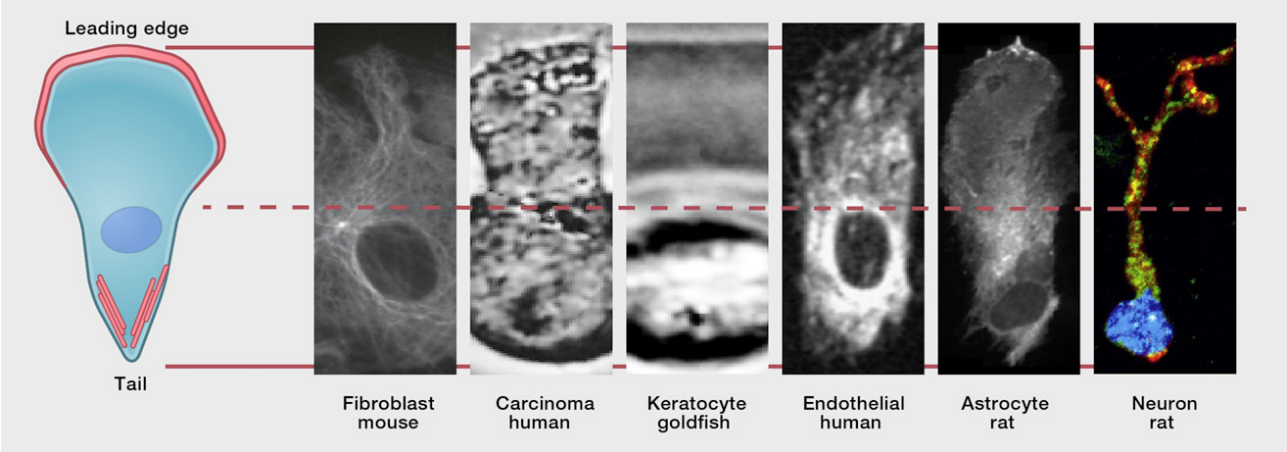

Figure 4.3: " **Diversity in nuclear positioning.** Rearward nuclear position is typical of migrating cells. (Left) Schematic of a migrating cell with protruding leading edge and contracting tail. (Red) Actin filaments. (Right) Montage of migrating cells with front-back dimensions normalized. Dotted line represents the midpoint between the front and back. Nuclei are positioned along the front-back axis but always rearward of the cell center. From [Gundersen 2013]

box. Intermediate filaments have also been implicated in nuclear positioning and nucleo-cytoskeleton force transmission but their requirement remains elusive particularly in the context of cell migration ([Dupin 2011], [Maniotis 1997]). Thus, microtubule and actin filaments working either in coordination or independently mediate most of the described nuclear positioning events. The LINC complex is so far the protein complex at the nuclear envelope which has been implicated in nuclear positioning [Gundersen 2013].

Nuclei are positioned for specialized cellular function. For example, after fertilization, the male pronucleus nucleates microtubules from its centrosome to move towards the middle of the cell where it will be joined by the female pronucleus. This central positioning of the male and female pronuclei is required for zygote formation. In drosophila, a proper cellurization of the embryo requires the positioning of nuclei towards the cortex of the embryo before the invagination of the plasma membrane. In the developing retina of the zebrafish, a proper nuclear positioning during interkinetic nuclear migration regulates cell-cycle as well as cell fate determination [Dupin 2011].

In the context of cell migration, a proper nuclear positioning has been implicated in cell polarization which is a crucial step for this process. In the following section, I will review our current knowledge of the mechanism of nuclear positioning during cell migration.

4.4.1.1 Microtubules based nuclear positioning

Many nuclear positioning processes are based on microtubules driven forces [Dupin 2011]. However, only one of those processes is implicated in cell migration: nucleokinesis during neuronal migration.

Newly created neurons leave the proliferative epithelium to disperse throughout the central nervous system. This migratory process occurs through three, well synchronized steps. At first, the neuron extends a protrusion at its leading edge, then the nucleus translocates into this protrusion and finally, the trailing edge is retracted. The process of nuclear translocation into the leading edge is named nucleokinesis and exhibits a two-stroke form of migration. At first a cytoplasmic swelling is formed at the leading edge then the centrosome as well as other organelles including mitochodria, the golgi apparatus and the endoplasmic reticulum move into the swelling. During the second step, the nucleus follows the centrosome [Marín 2010].
To achieve such a movement, microtubules as well as many microtubules associated motors are required [Marín 2010]. The displacement of the centrosome towards the swelling is mediated by dynein and its regulator lissencephaly 1 (Lis1). Following centrosome movement, the nucleus is pulled by dyneins associated with the microtubule network. The nucleus is believed to be transported on microtubules by dyneins as any cargo would be [Gundersen 2013]. It is necessary to note that this nucleokinesis event also requires actomyosin contraction which drives the nucleus forward (illustrated in figure 4.4) [Marín 2010].

4.4.1.2 Actin based nuclear positioning

Many migrating cells exhibit a nucleo-centrosome axis which is aligned with the front-back cellular axis. Actin-based nuclear positioning has been implicated in maintaining this polarity during cell migration ([Gomes 2005], [Luxton 2010]). Studies from the Gundersen lab have shown that the rearward movement of the nucleus prior to the nucleo-centrosome axis formation requires an active mechanism based on the actin cytoskeleton. In 2005, Gomes *et al*, identified a pathway involving the small GTPase Cdc42, its effector MRCK, which phosphorilates myosin II, as the molecular pathway required for nuclear positioning prior to fibroblast polarization. They proposed that the actin retrograde flow induced by myosin II contraction upon activation by MRCK is generating the required force for moving the nucleus backward [Gomes 2005]. A mechanism proposing how this force is transmitted to the nucleus arose five years later. In 2010, Luxton *et al* identified a linear array of nuclear envelope proteins called TAN lines which harness retrograde actin flow for nuclear movement [Luxton 2010].

4.4.1.2.1 The Transmembrane Actin-associated Nuclear (TAN) lines TAN lines are a set of transmembrane proteins which connect the nucleus to the nucleoskeleton in migrating fibroblasts. Those lines have initially been shown to contain nesprin-2 and sun2 and more recently, Samp1, a nuclear envelope protein has also been shown to be a member of the TAN lines ([Luxton 2010], [Borrego-Pinto 2012]). TAN lines form linear arrays which co-localize with actin filaments at the dorsal surface of the cell. During fibroblast migration, the TAN lines move with the nucleus and are supposed to transmit forces from the retrograde actin flow to the nucleus. Interestingly, the formation

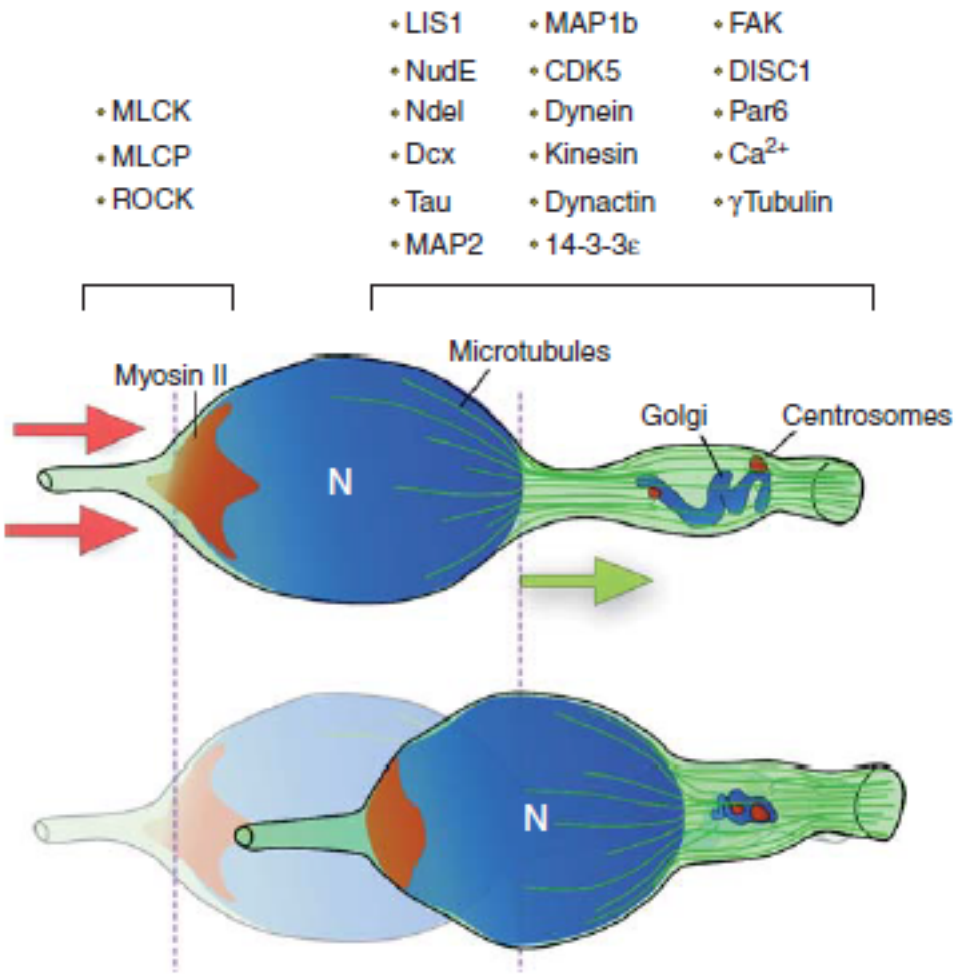

Figure 4.4: "**Nucleokinesis in migrating neurons**. Nucleokinesis involves both perinuclear and nucleus translocation. First, the perinuclear dilatation containing the centrosome and the Golgi apparatus move forward. The perinuclear microtubular cage (in green) pulls the nucleus forward until reaching the swelling. Forward pulling forces (green arrow) are complemented by myosin II at the rear, which generates pushing forces (red arrows) to move the nucleus in its characteristic saltatory pattern of nucleokinesis. Many motor proteins and other proteins related to the cytoskeleton are implicated in the process. (N) nucleus." From [Marín 2010]

of those actin bundles requires Myosin II activated by CDC-42 through its associated kinase the myotonic dystrophy related kinase Cdc42-binding kinase (MRCK). In addition, the TAN line mediated nuclear movement requires the A-type lamins for efficient force transmission from the actin retrograde flow to the nucleus [Luxton 2011].
Thus the TAN lines, by transmitting forces from the Myosin II-dependent actin retrograde flow to the nuclear lamina allow an efficient nuclear positioning followed by an efficient migration ([Gomes 2005], [Luxton 2010], [Luxton 2011]).
In astrocytes, a similar actin flow dependent nuclear positioning has also been observed. However, this system does not require myosin II but nesprins as well as intermediate filaments. In this system, actin retrograde flow is proposed to drive the accumulation of intermediate filaments around the nucleus and therefore transmits forces to the nucleus [Dupin 2011].

4.4.2 The nucleus in mechanotransduction

As said in section 3.3, the nucleus might have an important role in cellular mechanotransduction during migration. During cell migration, forces exerted by the extracellular matrix must be transmitted to the cell to promote motion [Maniotis 1997]. Given the central role of the nucleus in transcriptional regulation, it has long been proposed that the nucleus can act as a cellular mechanosensor. However because forces are usually applied at the cell periphery, they must reach the nucleus to be sensed by this organelle.

4.4.2.1 Can the nucleus feel the force?

The main argument against nuclear role in mechanotransduction is that if we consider the cell as a viscoelastic cytoplasm filled with dynamic cytoskeletal elements and surrounded by an elastic plasma membrane, mechanical stresses would dissipate rapidly throughout the cytosol. The nucleus would thus not feel a force applied on the cell [Wang 2009].
However, already in 1997, nuclei have been shown to respond to mechanical stresses applied on the cell [Maniotis 1997]. Moreover, even though cytoskeletal elements are rapidly polymerizing and depolymerizing, they have been shown to bear significantly high tensile and compressive forces. Indeed, actin as well as microtubules or intermediate filaments have been shown to possess the ability to either stress-stiffen or stress-soften under mechanical load (see section 3.1.1). The cell could then locally tense cytoskeletal filaments to regulate force transmission. If we consider the cell in the context of the tensigrity model (see section 3.1.2), long distance force transmission can occur in time scales much shorter than the diffusion one. Thus, one can imagine that forces exerted at the surface of the cell might reach the nucleus before vanishing. Many recent evidences support this tensigrity model. For example forces applied on integrins can induce mitochondria as well as nuclei displacement up to 20 μm away from the site of force application [Wang 2009]. This tensigrity model, combined with our

actual understanding of the physical link between the cell and the nucleus can then explain how forces could be transmitted to the nucleus ([Wang 2009], [Isermann 2013]).
LINC complex disruption has been related to defects in intracellular force transmission. For instance, LINC complex disruption can interfere with stretch-induced proliferation. In endothelial cells, nesprin3 downregulation impairs the shear flow induced cell polarization of the centrosome as well as flow induces migration [Morgan 2011]. Moreover, cells lacking lamin A/C or emerin have impaired activation of mechanoresponsive genes such as the one involving the myocardin-related transcription factor-A [Isermann 2013].
In the past decade an actin structure named actin cap has been proposed to directly mediate force transmission to the nucleus.

4.4.2.1.1 The actin caps The actin cap is a perinuclear actin structure which has been characterized in 2009 by Khatau *et al* as a regulator of nuclear shape in fibroblasts [Khatau 2009]. It is composed of stress fibers in the apical region of the cell (on top of the nucleus) which terminate at specific focal adhesions (i.e. these focal adhesions contain zyxin at earlier stages of their formation) [Kim 2012] and are connected to the nucleus through nesprins-2-giant and nesprins-3. The formation of this actin cap has been shown to be acto-myosin contractility and LINC complex dependent [Khatau 2009]. For instance, the organization of this dome-like structure is disrupted in cells from mouse model of progeria or muscular distrophy [Khatau 2009]. Note that this actin structure if different from the actin cables connected to the nucleus by the TAN lines. They are indeed, perpendicular to each other. Moreover, TAN lines have not been reported to be linked to focal adhesion [Luxton 2011].
The actin cap has recently been implicated in mechanotransduction. Indeed, it has been shown to be more sensitive to substrate stiffness than conventional stress fibers. The actin cap disappears as surface compliance decreases while the conventional stress fibers stay much longer (see figure 4.5) [Kim 2012]. Thus this structure through its specific focal adhesions seems to respond to higher traction forces than conventional stress fibers. However, actin caps respond to lower shear forces than basal stress fibers. Indeed, last year, Chambliss *et al* proposed that upon shear stress, the actin cap forms rapidly (within two minutes) in previously serum-starved mouse embryonic fibroblasts (MEFs) much faster than the basal stress fibers (which form thirty minutes after shear flow) [Chambliss 2013]. Moreover, this actin cap forms at lower shear stresses (0.01 $dyn/cm^2 = 10^{-3}$ Pa) than basal stress fibers (1 $dyn/cm^2 = 10^{-1}$ Pa). In addition, actin cap formation was mediated by zyxin (which is recruited to focal adhesions at high traction forces) at low shear stress and by talin (which in contrary is one of the first proteins recruited at focal adhesions) at higher shear stresses. It was thus proposed by Chambliss *et al* that the actin cap is involved in force transduction from the extracellular space to the nucleus and this force transduction is ultrafast (within 30s), ultrasensitive (low shear stress) and mediated by zyxin [Chambliss 2013]. More evidence about the involvement of the actin cap in mechanotransduc-

tion pathways (such as the MAPK pathways) would be required to assess its role as force transducer.

4.4.2.2 How could the nucleus react to forces?

Because the general definition of mechanotransduction is translation of mechanical force into biochemical signaling, it is important to understand how nuclei biochemically react to forces.
The number of possible mechanisms is huge [Wang 2009]. Indeed, forces applied at the nuclear membrane can induce a conformational change in nuclear membrane proteins such as the ions channels. Supporting this theory, nuclear membrane ions channels have been shown to respond to mechanical forces. Indeed, when nuclear membrane distortion is induced by a mechanical load, the calcium entry inside the nucleus is stimulated which induces gene trancriptions [Wang 2009]. On the other hand, the ion flux through nuclear membrane can be modulated by altering the actin cytoskeleton. One can thus imagine that because the channels are mechanically coupled to the nuclear lamina and presumably to the cytoskeleton, pulling on the cytoskeleton can induce channels distortion which can promote ions influx.
The lamina network can be affected by mechanical loads which can induce its stretching and weakening ([Rowat 2005], [Swift 2013]). It has also been shown that the expression level of the A-type lamins relative to the B-type one scales up with tissue stiffness [Swift 2013]. Moreover, applying a mechanical load on the nucleus has been shown to induce nuclear stiffening through lamin A/C recruitment at the site of force application [Guilluy 2014].
Because the A-type lamins bind transcription factors as well as emerin which in turn interacts with splicing factors, mechanical deformation of the lamina network can result in altered gene expression and protein isoform expression through sequestration or modification of the transcription or splicing factor [Wang 2009]. Forces could also transfer to the DNA backbone which could induce DNA conformational change thus modulate gene expression by changing for example the binding kinetic of transcription factors.

In the context of cell migration particularly 3D migration, the role of the nucleus in mechanotransduction is more than important. Indeed, cells having to crawl through narrow spaces will deal with quite high forces. In addition, deforming the nucleus through spaces which are smaller than the characteristic nuclear diameter can require additional forces. Understanding how forces are transmitted to the nucleus and what are the consequences of mechanical loads on the nucleus can improve our understanding of *in vivo* migration processes in immune cells as well as in cancer metastasis. It can also provide new insight in our understanding of laminopathies.

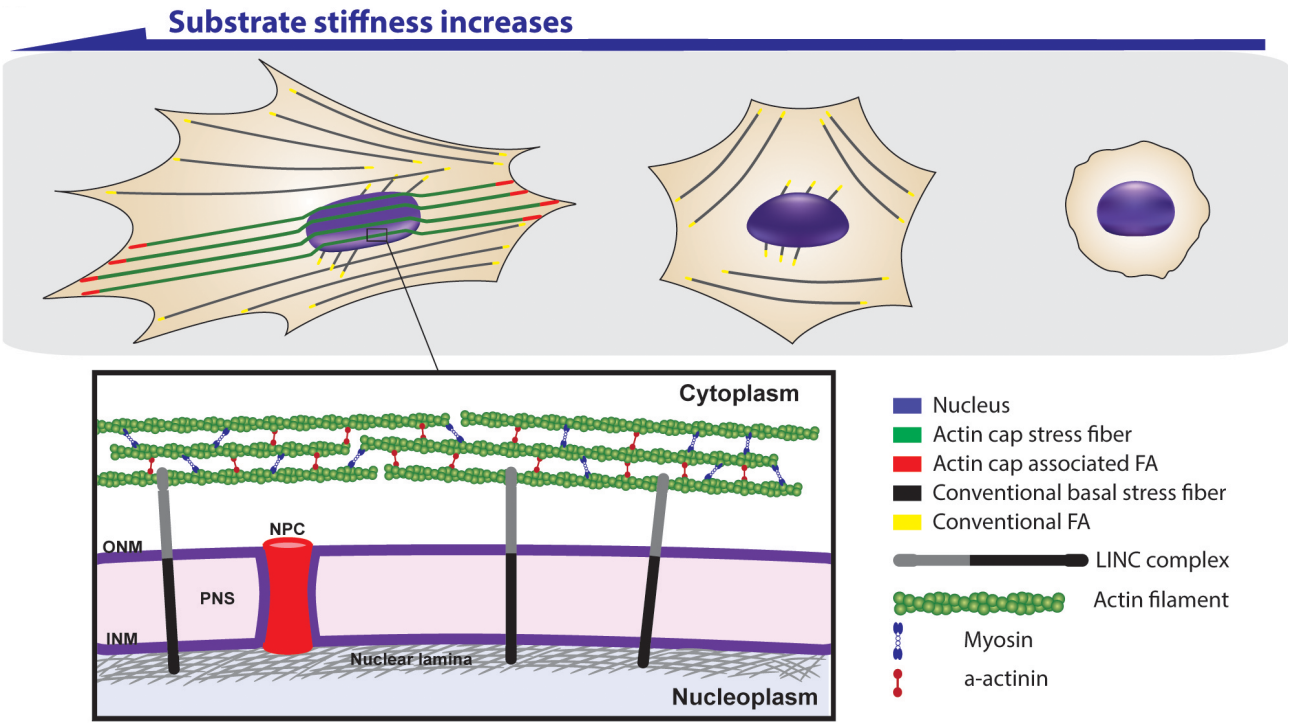

Figure 4.5: "**Actin caps in mechanotransduction**. Schematic of the cellular mechanosensing in response to substrate compliance. Well-organized actin cap fibers (green) on top of the nucleus are terminated by actin caps associated focal adhesion (ACAFAs, red) at the pheripery of the adherent cell and nucleus (blue) is elongated in the same direction as actin cap fibers (Left). As substrate compliance increases, ACAFAs and actin cap fibers disappear, but conventional focal adhesion (CFAs) (yellow) and basal actin fibers (black) remain and the nucleus becomes rounded (Middle). On extremely soft substrates, most actin stress fibers and focal adhesions disassemble and the nucleus is more rounded (Right). Inset. Physical connections between actin cap stress fibers and nucleus through the linker of nucleoskeleton and cytoskeleton (LINC) complexes. PNS: perinuclear space; INM: inner nuclear membrane; ONM: outer nuclear membrane. By disrupting LINC complexes, actin cap fibers become disorganized and mechanosensing controlled by actin cap associated focal adhesions is suppressed." From [Kim 2012]

4.4.3 The nucleus as limiting factor for cell migration

In the context of 3D migration which has been at the center of my PhD project, the nucleus plays a major role. Indeed, the deformability of the nucleus can in one hand impose a physical limitation to cell migration but on the other hand, having the nucleus anchored to the cell can be exploited for cell polarization. Even though the idea that 3D migration can differ in many points from the well known 2D migration is well accepted, the idea that the main difference might come from the nucleus only recently emerged.

For example, having less lamin A has been shown to promote 3D cell migration ([Harada 2014], [Rowat 2013]). During the last year, Le Berre *et al* proposed that the nucleus can define the cell persistence during migration under geometrical constrains [Le Berre 2013]. During the same period, Wolf *et al* proposed that when cancer cells encounter constrictions smaller than their nuclei while moving a dense collagen gels, they will either degrade the matrix or deform their nuclei to move forward. Indeed, when the proteolytic activity of those cells were inhibited, the large and stiff nucleus which requires substantial deformation imposed limitations to cell migration. Forward movement became completely inhibited when a cell encounter constrictions cross-section smaller than 10% of the initial nuclear cross-section [Wolf 2013]. They also proposed that in non-proteolytic migration, the displacement of this organelle requires specific forces provided by acto-myosin contraction.

This substantial work, focused on cancer cells, illustrates the plasticity of the migration mechanism of those cells and at the same time raises many questions. Indeed how does the acto-myosin contraction transmit forces to the nucleus? What are the directions of these forces (pushing or pulling forces)? Which nuclear property or component sets this limit of 10% of the nuclear cross-section? And also what are the effects of those forces on the nucleus? These are some of the questions which might be asked. One can also wonder to which extend is this mechanism shared among cells. Indeed, immune cells are other cell types which have been shown to migrate in highly confining spaces. Dendritic cells, in particular, are found in many dense tissues in which they have to continuously migrate. Dendritic cells do not exhibit high proteolytic activities and moreover do not require adhesion to migrate in vivo [Lämmermann 2008]. Thus the question of what is the role of the nucleus in dendritic cell migration is important for a detailled understanding of the immune system.

Chapter 5

Objectives

When I started my PhD, relatively few evidences on the role of the nucleus in cell migration existed. For instance, nuclear positioning was shown to be important for cell polarization prior to wound healing driven fibroblasts migration ([Gomes 2005], [Luxton 2010]). The contribution of the nucleus in cellular mechanical properties had driven the hypothesis that this organelle would limit cell migration particularly in 3D environments (see the section 4 of the Introduction). In 2008, Lammermann *et al.* had proposed that nuclear deformation in mature dendritic cells migrating through dense collagen gels requires myosin II based contraction [Lämmermann 2008].

Beside these evidences, direct proof of the limiting factor of the nucleus during 3D migration was still lacking. In addition, a mechanism of nuclear deformation during migration under confinement was far from being proposed. Moreover, the question of the effect of nuclear deformation during 3D migration on genome integrity and cell fate was not addressed.

It is in this emerging, interesting and challenging context that I started my PhD aiming to understand, at its end, how does the nucleus regulate cell migration in highly confining spaces. Is the nucleus imposing a physical limitation to cell migration under confinement and how are necessary forces generated and transmitted by the cell to allow migration in highly confining spaces were the two main questions I asked during this PhD.

I used a set of approaches at the interface between engineering/physics, cell/molecular biology and image analysis to address my questions. I optimized the constrictions based setup, which was designed before my arrival in the lab, to be able to visualize and quantify the kinetic of cellular migration through narrow pores and the subsequent nuclear deformation. Mouse Bone Marrow derived Dendritic cells (mBMDCs) were chosen as model system for their high motility and their *in vivo* relevance to cell migration under confinement.

Combining those interdisciplinary approaches allowed me to propose a model for dendritic cells migration in highly confined spaces. In this model, cells would overcome the physical limit imposed by nuclear deformation by nucleating an Arp2/3 based actin meshwork around the nucleus which, by breaking the lamin A/C network, facilitates dendritic cells passage through narrow pores. We proposed that this transient nuclear softening allows cells to efficiently pass micrometric constrictions while surviving long enough to accomplish their functions.

METHODS

Chapter 6

Methods

Contents

This chapter describes the main methods used during my PhD.
The aim of my PhD project being to study the mechanism of cell migration through narrow pores, it thus required to set up a well defined protocol. The first step towards this final protocol is the choice of the right cell type which will be used. In this study, I mainly focused on dendritic cells because of their *in vivo* relevance to cell migration.
Once the cell type chosen, the type of extracellular environment must be defined. This extracellular environment must provide cellular confinement with a well controlled geometry and should allow high resolution microscopy. Microchannels, which fulfill these three requirements were chosen in this study.
Combining microfabrication to live cell imaging of dendritic cells which can be genetically modified I was able to tackle this question of cell migration through highly confined spaces. In the following sections, I will describe the details of the experimental setup from the generation of the subset of dendritic cells which we use in the lab to the final visualization and analysis of cells transmigration through constrictions.

6.1 Cellular models for cell migration

The study of transmigration requires the choice of transmigrating cells such as leukocytes and metastatic cells. However, most of the metastatic cells have been reported to display a collective migration phenotype [Friedl 2010] in which single cell force generation leading to forward movement can hardly be uncorrelated from forces generated by neighboring cells. Moreover, cancer cells are slow moving cells compared to leukocytes with, for example, 10 order of magnitude between the mean velocity of MBA-MB-231 breast cancer cells and polymorphonuclear cells [Wolf 2013]. Because, I was mainly interested in rapid single cell transmigration, leukocytes were then the ideal cell type. As said in the chapter 2 of the introduction, different types of leukocytes exist in vivo. Among those leukocytes, neutrophils and dendritic cells are of high interest. Indeed, they are highly motile cells migrating in an amoeboid manner in highly confining spaces such as dense connective tissues. In the following, I will describe the way we generated dendritic cells as well as neutrophils.

6.1.1 Dendritic cells as model system

Dendritic cells are obtained from mouse bone-marrow cells using a protocol first described by [Inaba 1992]. Mouse bone-marrow cells are maintained in culture for 10 days in IMDM medium supplemented with 10% fetal calf serum and 50 ng/mL of granulocyte-macrophage colony stimulating factor (GM-CSF). This medium supplemented with 1% of a penicillin/streptomycin cocktail to avoid bacterial contamination will be refers to as differentiating medium. As previously described in [Faure-André 2008], GM-CSF is provided in a supernatant of J558 cells transfected with a GM-CSF-coding plasmid. At days 4 and 7 of culture, cells are detached with PBS-EDTA(5 mM) and replated at 5.10^5 cells per milliliter of differentiating medium. At day 10, 90% of adherent cells express CD11b, an integrin family member, as well as MHC class II at high levels. If CD11b is widely expressed in most of the leukocytes (monocytes, neutrophils, natural killers, granulocytes ans macrophages), high level of MHC class II expression is specific to dendritic cells [Inaba 1992]. This protocol, which will be detailed in the annexes of this manuscript, allowed the production of a high amount of dendritic cells ($> 4.10^7$ cells from one leg of a 6 weeks old mouse). The so obtained dendritic cells can be used at day 10 and 11 as immature dendritic cells.

6.1.1.0.1 Dendritic cells maturation When studying mature cells transmigration, D-10 dendritic cells (immature dendritic cells at day 10 of culture) are treated with 100 ng/ml of lipopolysaccharide (LPS). LPS is a component of bacterial cell wall which, upon binding to dendritic cells' TRLs is recognized as a danger signal leading to dendritic cells activation. Activated dendritic cells increase their expression of the costimulatory molecules CD86 and CD40 as well as the chemokine receptor CCR7. This increased expression of CCR7 has been shown to mediate dendritic cells migration toward the lymph vessels and lymph node [Weber 2013]. Moreover, activated dendritic cells display a transient

decrease, followed by an increase in cell velocity ([Faure-André 2008], [West 2008]). During my thesis, I used two protocols of LPS mediated dendritic cells activation. The first one, which is the most commonly used, consists of an overnight treatment with LPS at 100 ng/ml while the second one consists of a short (20 minutes) pulse of LPS. Both treatments lead to the same extend of cell activation however, the cells migratory behaviors are different. Indeed, with the overnight treatment, cells are much bigger, strongly adherent while cells treated with the short pulse are much smaller and more motile. I used the overnight LPS treatment in transwell experiments (see below) as this protocol is commonly used. However, because overnight treated cells were not entering the microchannels I decided to switch to the short pulse treatment.

6.1.1.0.2 Genetic manipulation of dendritic cells A common approach when studying a mechanism is to perturb the system and observe the readout. Genetic manipulations allow such approach. Indeed, by increasing or decreasing the expression of a given protein, we can understand the role of this protein in the studied mechanism. Protein overexpression is for instance extensively used to study protein localization while protein silencing is a great tool to study protein function.
During my PhD, I performed both approaches. I indeed, used small interferent RNA transfection (siRNA) to silence some proteins such as Arp4C a subunit of the ARP2/3 complex or LMNA which code for the A-type lamins. The detailed protocol for siRNA transfection will be given in the annexes. Illustrating images of the siRNA based protein silencing will be provided in the result chapter of this manuscript.
In order to visualize the localization of Arp2/3, I also transfected immature dendritic cells with Arp3. However, the faint signal combined to the localization of the protein in cellular compartments which resemble to lysosomes make us conclude that classical electroporation does not allow proteins overexpression in mouse bone-marrow derived dendritic cells. Nevertheless, I will report, in the annexes, the protocol I used for plasmid transfection for future users.

6.1.2 Neutrophils as a second model

I here refer to neutrophils as HL-60 derived neutrophils. HL-60 cells originated from a female patient with acute myeloid leukemia. 'Culture of peripheral blood leukocytes from this patient in conditioned medium resulted in the development of a growth factor independent immortal cell line with distinct myeloid characteristics' [Birnie 1988]. Over decades, HL-60 cells have been extensively used to study cellular differentiation. At steady state, an HL-60 culture contains 90% of differentiation arrested cells and 5 to 10% of cells with a more mature myeloid characteristics. The most striking and interesting feature of HL-60 colonies is the ability of a variety of chemical agents including dimethyl sulphoxide (DMSO), retinoid acid and phorbol ester, to increase the proportion of differentiating cells *in vitro* to as great as 90%. Moreover, the obtained lineage can be modulated according to the chemi-

cal agent. For instance, HL-60 cells can be induced to differentiate *in vitro* into granulocytes-like cells using DMSO or monocytes/macrophages-like cells using phorbol ester [Birnie 1988]. Even though the molecular mechanism leading to HL-60 differentiation is still incompletely understood, a well defined protocol have emerged over the last two decades allowing a reproducible induction of HL-60 differentiation into neutrophils-like cells.

The HL-60 used during my PhD were kind gifts of Guillaume Charras, at the ULC, England and Dyche Mullins from the USCF, USA. As previously reported in this detailed protocol of Milius *et al* ([Millius 2010]), HL-60 cells were maintained in culture in RPMI 1640 medium with L-glutamine (Life technologies), supplemented with 10% fetal bovine serum, 25 mM of HEPES, 1% of penicilin/streptomycin. HL-60 are passaged when they reach the density of $10^6 cells/mL$ and split to $0.15^6 cells/mL$ in a fresh, prewarmed culture medium. Cells are maintained in 10ml in a $25cm^2$ cell culture flask at 37°C and 5% CO_2.

To induce HL-60 differentiation into neutrophils, cells are counted and samples containing $1.5^6 cells$ are centrifuged at 1500rpm for 5mn. The pellet is resuspended in 10ml of prewarmed culture medium supplemented with 1.3% of dimethyl sulphoxide (DMSO), endotoxin, and hybridoma tested (Sigma). Such DMSO treated HL-60 are maintained in culture in a 25 cm^2 cell culture flask at 37°C and 5% CO_2 for 5-6 days prior usage [Millius 2010]). After 5 days of differentiation, HL-60 cells exhibit a polarized morphology which is accompanied by a highly migratory ability. Moreover, the upregulation of the Lamin B receptor leading to a polylobulated nucleus as well as LMNA dowregulation have been reported in retinoid acid induced HL-60 differentiation [Rowat 2013]. HL-60 was thus a convenient model system for studying the effect of nuclear mechanical properties in transmigration.

6.2 Microchannels as an original setup for transmigration

Once the right cell type chosen, one must define the right extracellular space which fit to the problematic. Because I am studying transmigration, I had to chose an extracellular environment where the chemical, mechanical and geometrical properties are well controlled. Transmigration often implies that the cell crawls through a pore smaller than its diameter. Many setups would fulfill those requirements among those, transwells are the most commonly used. However transwells do not allow the dynamic visualization of transmigration which made me switch to microchannels. The originality of the microchannels we used is the positioning of a constriction in the middle of the channels which acts as a narrow pore through which a cell should crawl. In the following paragraphs, I will describe the two techniques that I used to study dendritic cells transmigration: the transwells and microchannels with constrictions.

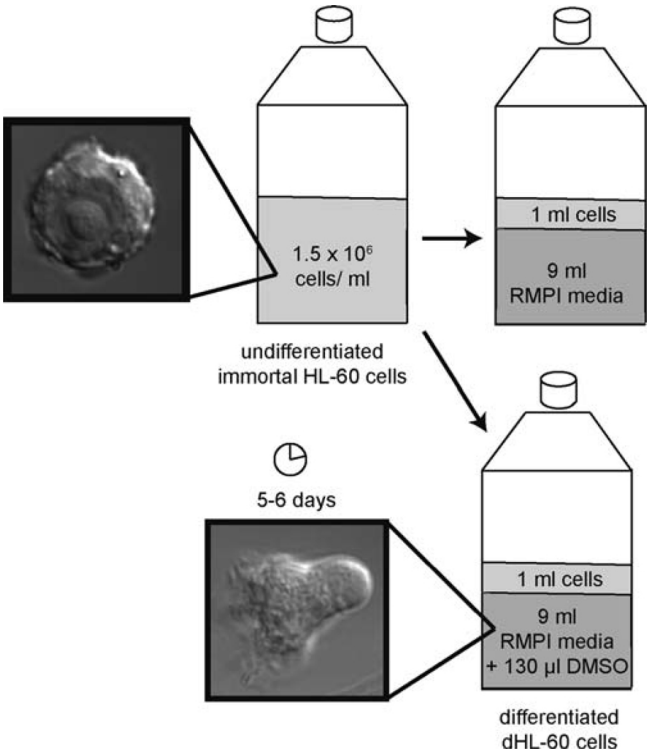

Figure 6.1: "**Passaging and differentiating HL-60 cells**. When cells reach a density between 1 and 2 million cells/mL, split to 0.15 million cells/mL in a total volume of 10 mL prewarmed culture medium. Differentiate cells in culture medium plus 1.3% DMSO; cells take ≈5 days to become migratory." From [Millius 2010]

6.2.1 The common setup: transwells

As said earlier, transwells are extensively used to study cell transmigration. The principle is fairly simple and consists of placing cells on top of a membrane containing pores of known sizes and to let them migrate for several hours before counting the number of cells which reached a bottom plate. This technique allows the study of chemical agents induced migration. For instance, chemokines can be placed at the bottom of the chamber allowing the establishment of a gradient for several hours. The membrane can be coated with extracellular matrix proteins such as fibronectin and collagen allowing a good control of the chemical environment of migrating cells. During my PhD, I used transwells to study the requirement of myosin II in mature versus immature dendritic cells transmigration. I thus used 96-wells transwells with polycarbonate membrane containing 10 μm long pores with 3 μm of diameter. In this study, 96-wells transwells were coated with fibronectin at 10 $\mu g/mL$ during an overnight incubation. The day after, cells were counted and placed at 10^5 cells/50 μL on each membrane and let to migrate for either 5 hours or overnight. The bottom chamber was filled with 200 μL of medium containing ± chemokines (CCL21 or CLL19 or a mix of both) at a given concentration. After transmigration, cells from the upper and bottom chambers are separately collected using PBS-EDTA at $5mM$, centrifuged at 2000rpm for 5 minutes then resuspended in PBS supplemented with 2%

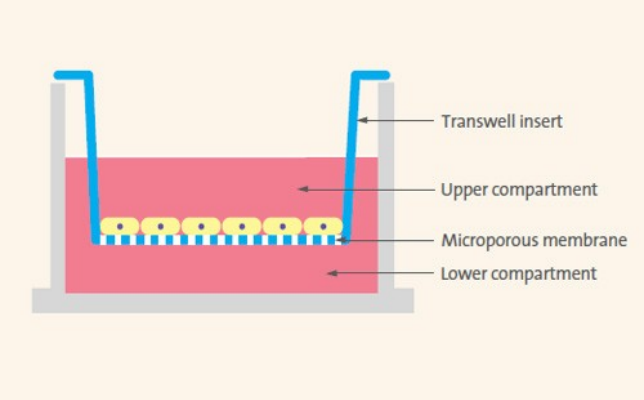

Figure 6.2: **Schematic illustration of the transwells assay.** (From www.corning.com)

of fetal bovine serum. The collected cells are mixed with 10^4 beads of 10 μm of diameter then counted using a FACS cell sorter. Adding beads at a known concentration allows to measure the volume counted at the FACS which is necessary to calculate the initial cellular concentration. After counting the upper and bottom chambers, the percentage of transmigration is calculated as the ratio between the number of cells in the bottom chamber and the sum of the cells in the upper and the bottom chamber. Comparing this percentage of transmigration in different conditions allows to conclude on the transmigration ability of cells.
However, transwells assays exhibit many limitations. Indeed, establishing a reproducible protocol is time consuming. Moreover, the stability of the gradient is not easy to determine as media of the upper and bottom wells are in contact which leads to the diffusion of chemokines and then the disturbance of the gradient. Above all, the main disadvantage of transwells assay is that cell migration cannot be uncorrelated from cell transmigration. For instance, impaired cell polarization or decrease in cell velocity will result in a decrease in the percentage of cells that reach the bottom plate. Thus transwells do not allow to strictly study cell transmigration independently to cell migration.

6.2.2 The microfabrication based setup: microchannels with constrictions

Microchannels have the great advantage compared to transwells assay to allow dynamic visualization of cellular transmigration. Indeed, the glass bottom dish on which the chamber is fixed, constitute the fourth wall of the microchannel which allows high temporal and spatial resolution live cell imaging.
Microfabrication for biological application has been introduced two decades ago with the use of lithography in the fabrication of DNA arrays [Whitesides 2001]. However, lithography is expensive, allows only a limited control over surface properties and has low applicability to proteins and cells. It is thus an inaccessible method for daily usage in cell biology. The development of soft lithography which allows a rapid, low cost an well controlled patterning of the composition, topography and properties of surfaces lead to the explosion of its application in biology [Whitesides 2001]. 'The key

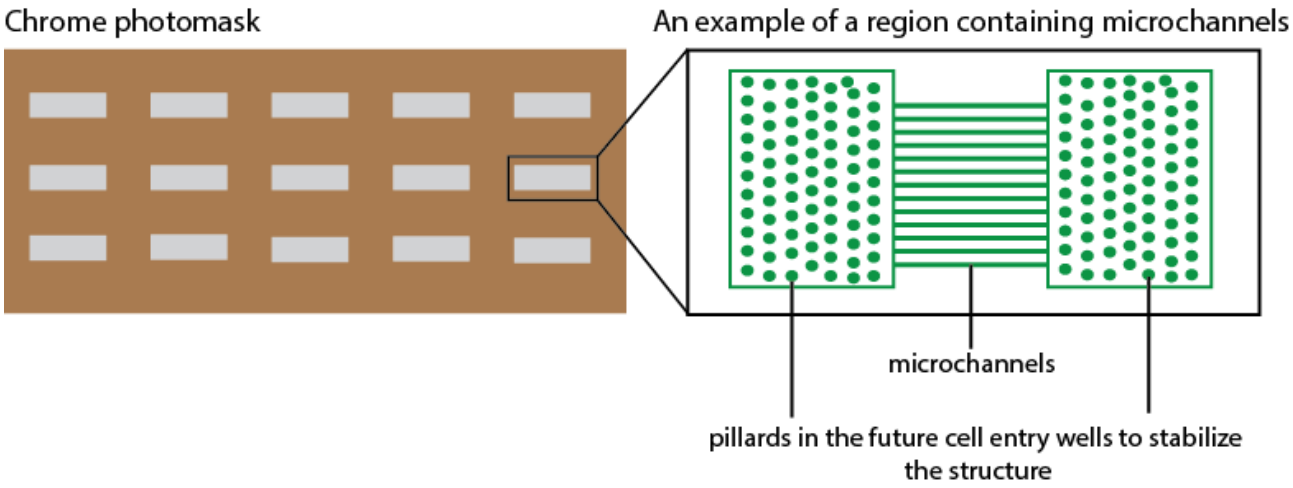

Figure 6.3: Illustration of a chrome photomask
Illustration of a chrome photomask

element of soft lithography is an elastomeric stamp with patterns as relief structures on its surface' [Qin 2010]. Soft lithography techniques including microcontact printing, replica molding, microtransfer molding, micromolding in capilary and solvent-assisted micromolding are essentially based on printing, molding and embossing with an elastomeric stamp. The wide availability and low cost of this elastomeric stamp is key for the accessibility of soft lithography.
For microchannels fabrication, replica molding is the most extensively used techniques. The 4 majors steps which leads to microchannels fabrication will be described in the following section.

6.2.2.1 From soft photolithography to PDMS chambers

The generation of microchannels starts with the designing of a mask. The mask is first drawn using a computer-aided design (CAD) software such as Adobe Freehand, illustrator and Cle Win which are well suited for quick design of patterns with feature sizes down to 1 μm [Qin 2010]. The drawn mask is then printed using high resolution printing services. For mask containing high resolution structures, such as lines separated by a μm, chrome photomasks are required. Many companies including Toppan photomask and Microtronis Photomasks can provide such photomasks.
For a brief description, the mask is a 2D quartz substrate on which a layer of chrome is deposited followed by a layer of electron sensitive resin. The resin in the zones corresponding to the design is stabilized by an electron beam. Then the rest is removed using a chemical developer. The chrome underneath the destroyed resin is also destroyed using another chemical such as 3144 Puranal. The rest of the resin is removed by exposing a second time the mask to an electron beam. Thus note that the printed photomask is in 2D, it is just a succession of rectangles which will give channels and circles which give rise to pillards (Figure 6.3). Once the photomask containing the previously designed

structures is obtained, a classical photolitography protocol will allow to produce the master mold. The master mold consists of a silicon wafer on which a structure of the mask will be patterned in 3D. As I did not have access to a clean room, I performed all my photolitography under a chemical hood where the temperature fluctuations and the micrometric particles in the air were the main parameters impairing an accurate reproduction of the mask. Nevertheless, I was able to setup a reproducible protocol for patterning structures as small as $1\mu m$ of lateral resolution. However the Z resolution was much less controlled. This protocol will be detailed in the annexes, I will here just give a brief description of the protocol. Photolithography is based on the opaque properties of the chrome. For instance, a silicon wafer on which a negative Epoxy-based photoresist was deposited will be put in tight contact with the mask. The UV light will go through the quartz but not the chrome thus weakening the regions which did not contain chrome. The weakened resin will be removed from the wafer using a chemical developer. We then obtain a master mold which consists in a wafer on which the channels are patterned in relief. Note that the height of the channels depends on the thickness of the resin deposit thus on the velocity of spin coating as well as the temperature of the resin which is set by the room temperature. The exposure time under the UV lamp defines the precision at which the width of the designed structures will be reproduced. Thus those three parameters must be optimized when patterning a new structure. Once the master mold obtained, starts the soft photolitography during which an elastomer will be poured on the wafer to reproduce its negative structures (holes become pillards). Once the elastomer polymerizes, it will be detached from the wafer then placed on another polymer for replica molding. This second polymer after polymerization around the elastomer will reproduce with a high fidelity the master mold (see figure 6.4). The soft lithography step allows the production of a high number of identical structures. Indeed, an elastomer can be poured 10 times on a wafer allowing the production of a replica mold containing 10 times more structures than the master mold. This obtained replica mold will be used in a daily basis allowing to prserve the master mold. One major element in soft lithography is the elastomer. For most of the microfluidic devices in biology, poly(dimethyl siloxane) (PDMS) is the most extensively used elastomer. This preferential use of PDMS in biolocial microfluidic devices is explained by the mechanical as well as chemical properties of this elastomer. For instance, its high shear and young moduli (respectively 0.25 MPa and O.5 MPa) allow it to conform to a surface and achieve atomic-level contact, a property which is more than useful in forming and sealing microfluidic systems. PDMS has also proven to be not toxic, medium and gas permeable, optically transparent down to 300 nm. Moreover, PDMS is intrinsically hydrophobic but can be rendered hydrophylic upon exposition to an air/oxygen plasma (the water contact angle then goes from 110° to 10°). PDMS can then adhere and seal either reversibly or irreversibly (after oxidation) to many different types of substrates particularly glass which I used during my PhD. (Adapted from [Qin 2010]). PDMS chambers sealed on glass bottom dish are ready to receive cells for migration/transmigration. However, in order to relate cell migration behavior to the level of confinement, the exact dimensions of the chambers should be measured. This can be

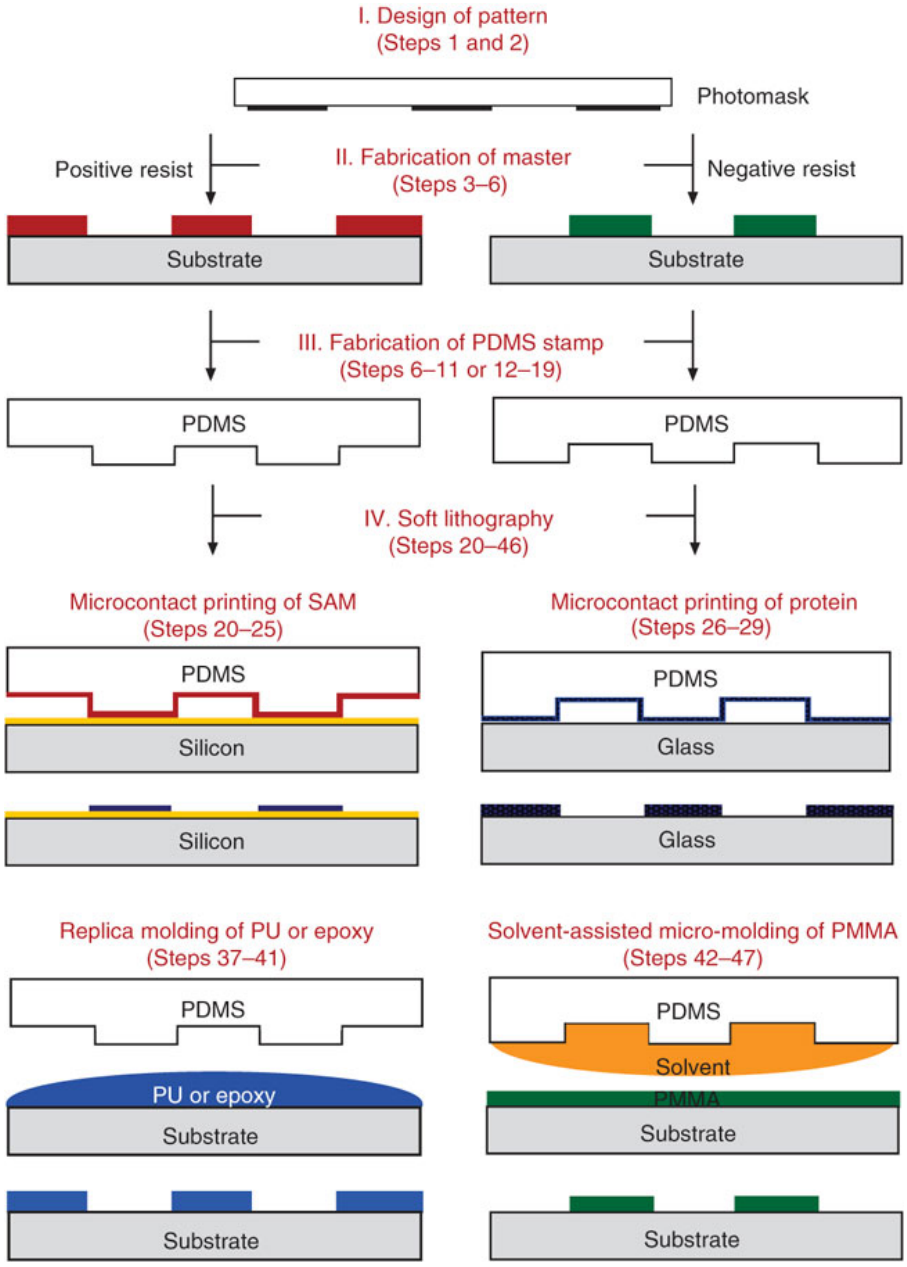

Figure 6.4: "**Shematic illustration of the four major steps involved in soft lithography and three major soft lithographic techniques**." From [Qin 2010]

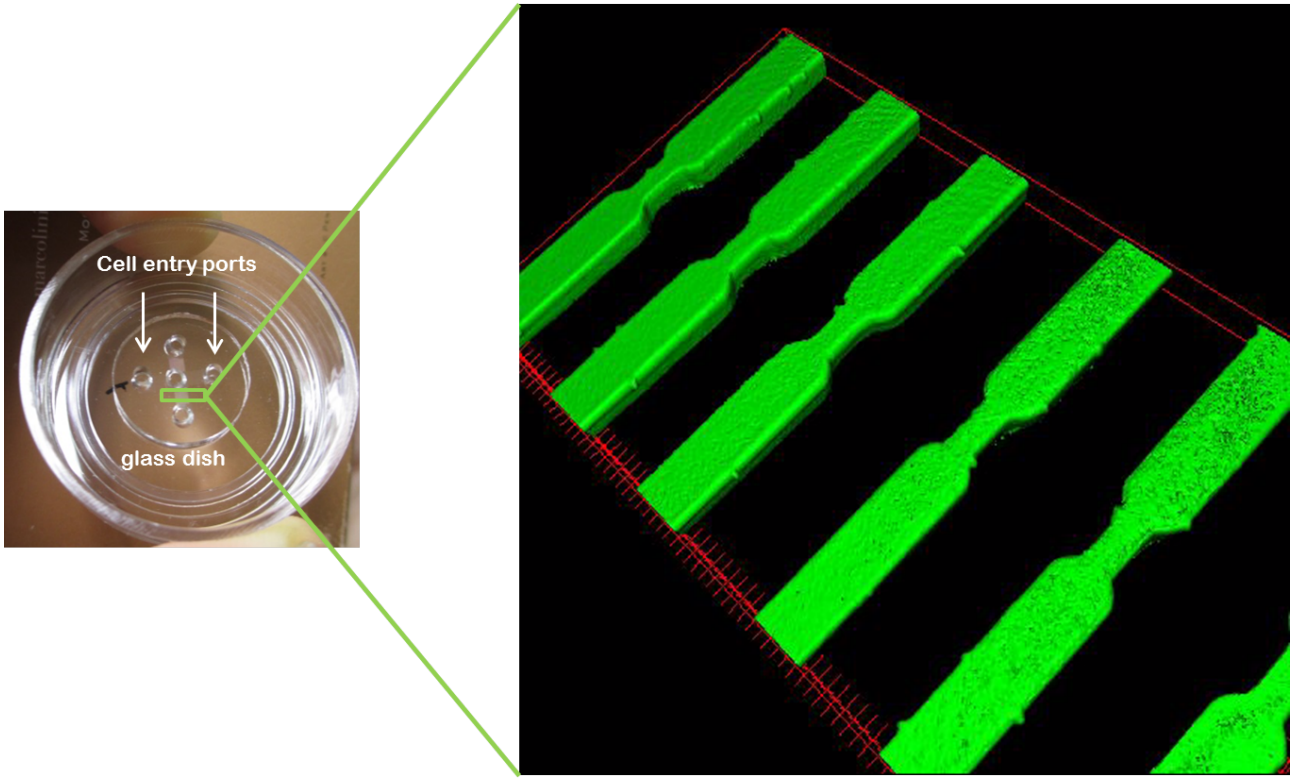

Figure 6.5: **Image illustrating my final setup**. The PDMS irreversibly seals the glass bottom dish making a 3D structures which represents the microchannels. In this picture, microchannels contains constrictions mimicking a transmigration assay.

done using optical profilometer or spinning disc imaging allowing the 3D reconstruction of the sealed chambers.

6.2.2.2 3D visualization of the channels geometry

As said earlier, the height of microchannels is set by the thickness of the resin deposit on the silicon wafer. Even though this height is supposed to be predicted by the type of resin (SU8 2005 and 2050 for respectively 5 μm and 50 μm thick deposit), the room temperature fluctuations can prevent the right achievement of this thickness. For example, in summer, I tend to obtain 3-4 μm high channels with an SU8 resin... As the height of the channels is an important parameter for the problematic I was interested in, I was then measuring the height of the master mold after photolitography. I used two methods for measuring this height: optical profilometer and confocal imaging based methods.

6.2.2.2.1 Optical profilometer Optical profilometers are interferometry based microscopes which are used to provide a 3D reconstruction of a substrate. Interferometry is widely used to measure surface irregularities. Indeed, by sending a coherent wave on the substratum and calculating the resulting interference fringes, an interferometer can detect the existence of relief as well as a variation of refractive index on a surface. For instance, on a master mold, a light beam which arrives at the bottom of the mold will have a different light path than another light beam arriving at the top of the mold. This difference of light path will result in an interference pattern which period can be used to calculate the distance between the top and the bottom of the wafer. In case of optical interferometers, optical waves will be used. The interference fringes between a light beam that interacted with the studied surface and a second one that is reflected by a mirror positioned at a known distance allows calculating the height of the spots on the surface of interest. Indeed, the mirror being considered as a flat surface, any variation of the light path is due to height variation accross the surface of interest. This allows a reconstruction of a virtual image of the master mold (see Fig 7.5a).
Using constrictions, I faced a limitation of our optical interferometer. Indeed, I could not obtain a precise measurement of the constrictions height. Constrictions were measured to be thinner than channels. Interestingly, the constriction height was a function of the constriction width. Indeed, 5 μm wide constrictions could be measured to be as height as the channels while 2 μm could not be resolved by the optical profilometer even though the theoretical lateral resolution of this instrument can go down to a submicron.
Facing this limitation, I then used another method, based on confocal imaging to measure the height of the channels.

6.2.2.2.2 Confocal imaging based channels measurement Confocal imaging allows the accurate measurement of channels height. Indeed, the high axial and lateral resolution (compared to the height of the channels) provided by confocal microscopy allows an accurate 3D reconstruction of

channels which can be then used to calculate the channel height. Here, I used spinning disc confocal microscope as I was trained on this microscope but any confocal microscope (such as the laser scanning one) could have been used. PDMS chambers were stuck on glass bottom petri dishes preactivated with an air plasma for 1 minute. After 5 minutes of vacuum followed by 2 minutes of air plasma treatment, channels were filled with mcherry-fluorescent PEG which is left to adsorb on channel walls for an hour. The mcherry-PEG was develloped in our lab by Yanjun Liu and can be visualized using a 561 nm laser. Microchannels were then rinsed by filling one of the inlet (cell entry pores see figure 6.5) with PBS and aspirating through the opposite inlet using a vacuum pump for 1 minutes. This rinsing step was repeated 3 times allowing the removal of the excess of fluorescent PEG from the channel. A Z-stack acquisition of on the entire channel section was performed using a spinning disc confocal microscope with a z-step of 0.3 μm. The so obtained z-stack video can be used to obtain a 3D reconstruction of the channels after image processing (see figure 6.5). I then wrote a small imageJ macro to automatically measure the height of the channel as function of the position in the channel. In brief, this macro makes a profile of the channel as function of the position from the Z-stack acquisition. For each position which will be a stack of the profile movie, a line is drawn at the center of the image and zones out of this line are erased (pixel intensity will be put at zero). The y-coordinates of the pixels with maximal intensity across this line are recorded. Their difference gives the height of the channel at a given position (see figure 6.6). I decided to use the center of the profile image as the channel and then the constriction has been centered.

6.3 Live cell imaging of cells migrating through constrictions

Live cell imaging allows to capture the details occuring during dynamic processes such as cell migration. Cells passage through constrictions being a rather fast process (around 10 minutes for a 15μm long and 2μm wide constriction), I extensively used live cell imaging to visualize this process. Depending on the experiment, I used low resolution epifluorescence microscopy or high resolution confocal microscopy. The low resolution video microscopy allows high statistics while the high resolution helps visualizing the details of cellular organelles. In the following, I will describe the main steps allowing the visualization of cellular transmigration using microchannels with constrictions.

6.3.1 Channels preparation

For PDMS chip preparation, a (1:10) ratio by weight of uncured silicon rubber and curing agent are mix thoroughly. The obtained mix is poured on the replica mold containing our channels of interest and will be let to polymerize overnight at room temperature. Only the right volume to obtain a thin (5 mm) PDMS chamber will be used. The air bubbles present in the mix will be gone before polymerization starts. Not that those air bubbles are usually proposed to be removed using a vacuum bell.

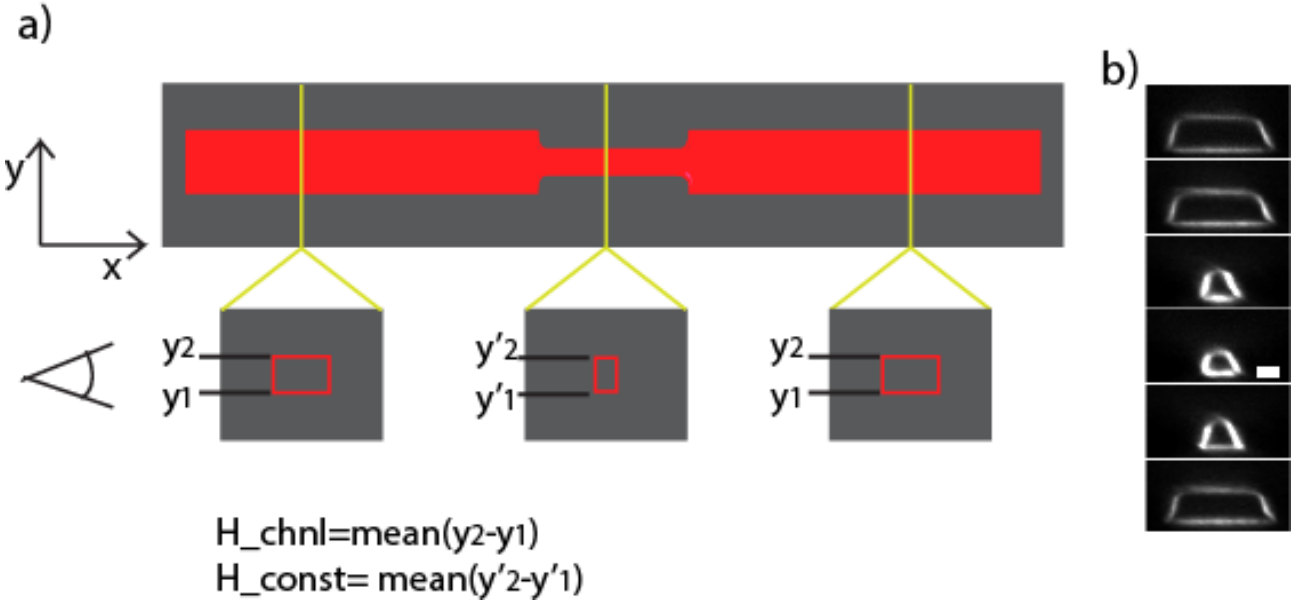

Figure 6.6: **Schematic representation of the determination of microchannels height.** a) The profile image of the channel is obtained after a z-stack acquisition along the channel section. The distance between the two maxima intensities at the center of the image gives the channel height. b) Montage of a real channel 7 μm wide coated with fluorescent surface protein. The constriction at the center of the channel was expected to be 2 μm wide. The channel height of this representative image is 4.8 μm while the constriction height is 3.6 μm

This has to be done if the PDMS chip is needed in the next 3 hours.
Once the PDMS polymerizes, a region containing microchannels is cut with a surgical blade, 2.5 *mm* diameter holes are drilled at pillards region to make the cell entry pores (see figure 6.5). A region of 2 to 3 pillards layer (Corresponding to 100-300 μm) must be left between the cell entry pores and the channels to ensure single cell entry in the channels. The PDMS chip is first cleaned by sticking and peeling an adhesive tape on it. This pre-cleaning step is followed by a deep cleaning step during which the PDMS chip is immersed in a 96% ethanol solution then sonicated for 30s. This steps allows to explode all elements present at the surface of the PDMS. A drying step using an air gun equipped with a filter will follow to remove the ethanol from the PDMS. The PDMS chip (surface containing channels toward the top) and its cleaned future glass substrate (glass bottom petri dish) are then placed on a clean support (which is usually a thick glass slide as plastic can be distorted by the plasma) and treated with air plasma at the highest power for 1 minute at 300 mTorr. Because our plasma cleaner is not equipped with a barometer, I was checking the color of the plasma and adjusting the air influx to get a bright purple. Right after plasma treatment, the surface of the PDMS containing our channels is stuck to the glass bottom petri dish. One can see when the PDMS binds to the glass substrate by observing a wave of "transparency" at the PDMS/glass interface.
The so obtained PDMS device is put back to the vacuum for 5 minutes prior to a second 2 minutes plasma treatment. The cell entry pores are filled with $5\mu l$ of a desired solution. This solution can be fibronectin (at 50 $\mu g/mL$) in PBS, fluorescent PEG or normal medium for dendritic cells and preconditioned medium for neutrophils. Note that the first step of vacuum is super important when working with constrictions as it is necessary to fill the channels. Proteins in the solution are left to adsorb for an hour at room temperature. The chambers is then covered by PBS in case of fibronecting and PEG coating or medium when coated with medium and left overnight at 4°C. In case of fibronection or PEG coating, the excess of solution is then removed the day after by filling one of the inlet with PBS and aspirating the opposite inlet with a vacuum pump. This step is repeated once with PBS and 2 more times with medium. After the last rinsing step with medium, one inlet over two is left empty to insure a proper entry of medium in the channel. The rest of the glass bottom dish is left with medium to allow lateral diffusion of medium towards the PDMS chip. The PDMS device is then left in an incubator at 37° and 5% CO_2 for at least an hour prior to adding cells. When performing a chemical treatment based experiments, medium is supplemented with the chemical at the right concentration and will be used after the first rinsing step with medium. The chamber will then be incubated with the chemical allowing its homogeneouss concentration along the chip.

6.3.2 Putting cells in channels

Cells must be well treated when performing this experiment. Thus, prewarmed PBS-EDTA(5 mM) will be used. Never use trypsin which is much stronger and will delay cells entry in channels. Den-

dritic cells at day 10 or 11 are stained with Hoechst at 200 ng/mL for 30 minutes at 37° and 5% CO_2 to label the DNA. Cells are treated while being still adherent at a concentration of 10^6 cells/ml. Hoechst can be either added to the present medium covering cells (supernatant) or be premixed with a warm medium that will be used to replace the supernatant. After Hoechst treatment, cells are detached with prewarmed PBS-EDTA(5 mM). Cell supernatant containing floating cells are thrown away and replaced by EDTA. After a 5 minutes incubation at 37° and 5% CO_2, cells are flushed using either a 1 mL cone or a 10 mL pipette. 20 μl of the obtained cells will be used for counting using a malassez counting chamber while the rest will be centrifuged at 1300 rpm for 5 minutes at room temperature. During the centrifugation, the cell entry pores of the PDMS devices are cleared of medium using a vaccum pump. The cell pellet is resuspended at 20.10^6 cells/ml and 5 μL will be deposited on each cells entry pore. Note than when working with chemicals, cells must be resuspended in medium containing the chemical at the right concentration. Cells are left to sediment and adhere to the substrate for 1 hour and a half prior to covering the PDMS chip with the right medium. After 1 hour and a half, cells should be already reaching the entry of the channels after having migrated through pillards. Note that covering the PDMS chip with medium is crucial to maintain cells alive overnight in chambers. Indeed, even though microscopes are humid area, evaporation still occurs. After covering the PDMS chip with the right medium, the device is left to incubate at 37° and 5% CO_2 for at least 2 hours before starting any timelapse acquisition. This lag time is crucial to have migrating cells in channels. When it is too short, I observed that cell tend to not enter the channel and to not cross constrictions. This lag time is much shorter for HL-60 derived neutrophils. Those cells enter the channels and migrate 30 minutes after being deposited! This rapid migration is due to the presence of preconditioned medium (medium in which HL60 cells have already grown) in the channels. For instance, when channels are coated with a regular medium, HL-60 derived neutrophils behave like dendritic cells and need 4 hours to migrate in the channels.

6.3.3 Video microscopy of cells crawling through constrictions

Once cells have been in the PDMS device for at least 4 hours, the video microscopy can start. Live cell imaging imposes that the microscope must have a temperature as well as a CO_2 and humidity controller. I performed all my experiments in conditions where the cells are 37°C, 5% CO_2 and a 60% of humidity. Performing a low resolution movie is rather simple. The glass bottom of the petri dish must be cleaned with a kimwipe prior to placing on an epifluorescent microscope holder for 35 mm dishes. Then a multidimentional acquisition (multi position, multi wavelength, timelapse movie) will be performed. A 10x, phase contrast, low numerical aperture (0.3) objective will be used when performing simple experiments where the main readout will be the velocity of migration and the kinetic of passage through constrictions. Two to four positions will be chosen for each condition (a condition being the constriction size or the drug concentration). Positions at the straight channels

region are very important as they constitute internal control for cell ability to migrate independently to nuclear deformation. Each position will contain 25 to 30 channels dependent on the binning of the image, thus allowing to rapidly obtain high statistics. After 15 to 20 hours of a timelapse movie with a temporal resolution of 2 minutes between images, many cells will have simultaneously enter the channel. With such temporal resolution, maximum 45 positions can be aquired on classic nikon video-microscopes running with metamorph. The kinetic of migration and transmigration will be analyzed using an semi-automatized imageJ macro that I developed.
When interested in the dynamic and organization of the cytoskeleton I performed either epifluorescent microscopy or spinning disc confocal microscopy. Epifluorescent microscopes, by integrating the signal nearly all along the cell thickness allows quantitative measurement of cytoskeletal local concentration. While confocal imaging allowing a high spatial resolution visualization of structures of interest requires much more sophisticated image processing for quantitative measurement. A 20X, phase contrast, high numerical aperture (0.75) objective, mounted on an epifluorescent microscope was used to quantify the dynamic of skeletal proteins such as actin or myosin II. Dentritic cells from mice expressing LifeAct-GFP (an actin binding protein) were used to visualize actin dynamics. Note that lifeAct has not been proven to have a higher binding affinity to F-actin but when put in a cell, it binds preferentially to F-actin. It is thus considered as an F-actin reporter. For myosin II visualization, dendritic cells from mice expressing MyosinIIA-GFP were used. The higher magnification of the 20X objective compared to the 10X, results in a smaller field of view which has to be compensated by acquiring more positions for good statistics. However, the temporal resolution was always kept constant at 2 minutes between two consecutive images as I was studying fast moving cells. Thus the number of conditions had to be reduced. The dynamic localization of actin filaments have been analyzed using an imageJ macro I developed.

6.4 Immunostaining in microchannels

When working with mouse dendritic cells, the first limitation that is encountered is the one concerning proteins expression. As said earlier, I could not set up a transfection protocol which would allow me to visualize proteins of interest. I then switched to the alternative immunostaining approach.
Immunostaining is a well known biochemistry approach which allows proteins localization on a fixed and permeabilized sample. It is based on the recognition and specific binding of an antibody to a given pattern on a protein. Because cells are fixed, it thus does not allow studying the dynamic localization or recruitment of proteins. Nevertheless, this was the best alternative I could have access to.
The first challenge I faced when performing immunostaining in microchannels devices was diffusion. Indeed, at the micronscale, diffusion is rather slow which can be a big limitation for antibodies. For instance, cells in channels can be fixed and permeabilized as proven by phalloidin staining but antibodies staining showed a diffuse pattern even after overnight incubation with a primary/secondary

antibody. An alternative to this diffusion limitation is the channels removal. With Pablo Vargas, a postdoctoral fellow in Ana-Maria Lennon's lab, I optimized an immunostaining protocol during which the PDMS chamber is detached from the glass coverslip after fixation.
As said earlier, an irreversible binding of the PDMS chip on a glass coverslip occurs upon treatment of both surfaces with air plasma. Interestingly, when only the glass coverslip is plasma activated and the PDMS clean enough a tight but reversible adsorption can occur. Cells that enter such channels are as well confined as in regularly stuck channels. The PDMS device preparation is done as described above with slight modifications. At first, **the PDMS chamber is not plasma activated** prior binding to the glass coverslip. Before channels coating, a 2 to 3 minutes plasma treatment is necessary to fill the channels with liquid. When performing immunostaining experiments, channels are coated with medium which viscosity allows it to penetrate much faster in channels than PBS would do.
Cells are put in channels as previously described and let to migrate overnight instead of 2 hours after adding medium. This allows to maximize the number of cells in channels particularly at the constrictions. To start immunostaining, the medium around the PDMS chamber is removed and replaced by PBS supplemented with 4% paraformaldehyde (PFA). A particular focus is made on putting drops of fixing solution on the cell entry pores to: at first remove the floating cells and second maximize the entry of the fixing solution in the channels. All the fixation protocol is performed at room temperature. Cells are then fixed for 30 minutes at room temperature then rinsed 3x5minutes with PBS alone. After the last washing, the PDMS chip is carefully and slowly lift up by putting a surgical blade between the PDMS and the glass coverslip. **Keeping the glass coverslip immobile with tweezers the PDMS chip is slowly lift up**. Note that the direction of PDMS detachment should be the same than the channels one to not lose or bend cells. Note also that the number of cells which stay bound to the glass coverslip can be increased by increasing the fixation time. For instance, after 5-10 minutes fixation, most of the cells are detached with the PDMS while they all stay on the glass coverslip after 1 hour fixation. However, a long fixation time does not suit to some antibodies such as the laminA/C one (N18 from Santa cruz) which has been optimized for methanol fixation. Thus this fixation protocol has been optimized for laminA/C antibody and must be optimized for each new antibody. After PDMS removal, a regular immunostaining protocol can be performed. Cells are thus permeabilized with PBS supplemented with 0.5% triton for 5 minutes to insure the permeabilization of the nuclear envelope. A rinsing step with PBS will be performed before blocking cells with PBS supplemented with 5% Bovine Serum Albumin (BSA) for 1 hour. Cells will then be stained with a primary antibody for our protein of interest then by a secondary antibody which will recognize the epitope of the primary antibody. Antibodies are diluted at the right concentration in PBS-BSA 1% and are incubated with cells for an hour. A rinsing step between the primary and the secondary antibody staining is necessary to avoid non specific binding of the secondary antibody. During the secondary antibody staining, F-actin and DNA staining will be performed using respectively phalloidine and Dapi. Cells are then rinsed with PBS-BSA 1% then with PBS alone before being mounted on a

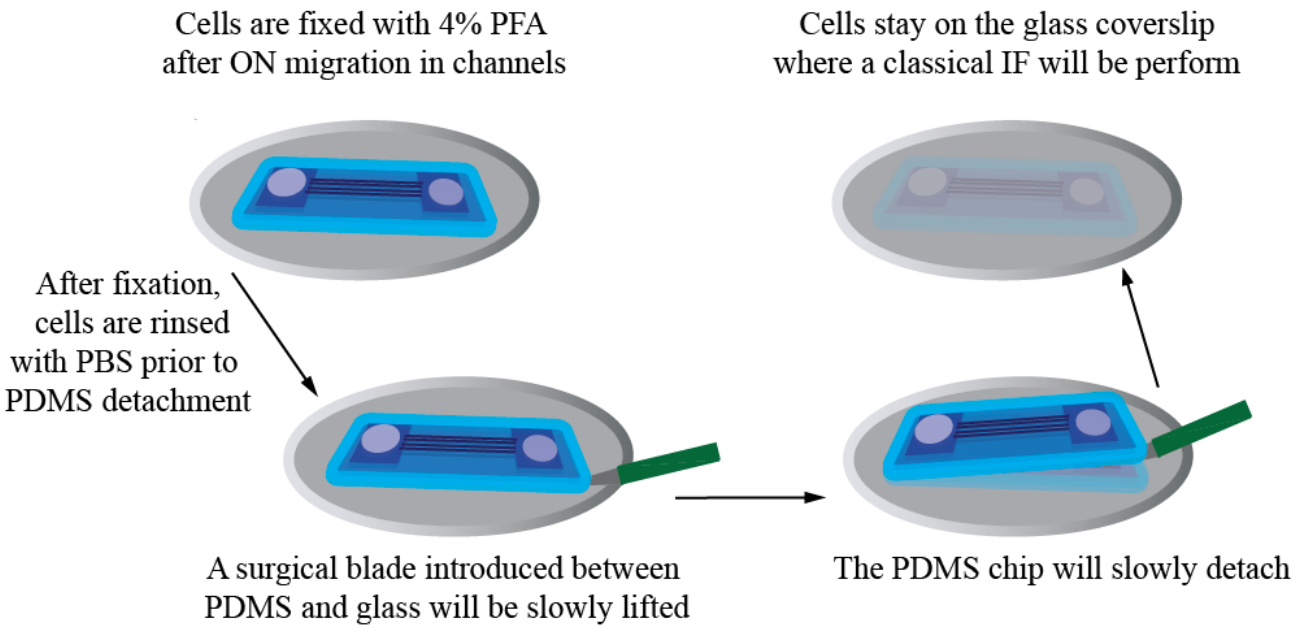

Figure 6.7: **Illustration of PDMS detachment during immunofluorescence**

glass slide. The preparation is left overnight at room temperature to allow the polymerization of the mounting media. Prior to cell observation on microscopes, the surface of the coverslip which will be in contact with the objective should be cleaned carefully using a cotton bud dipped in a 70% ethanol solution. The figure 6.8 illustrates the result of such immunostaining protocol. On this image, the cell is bent due to the flow induced by the rinsing steps.

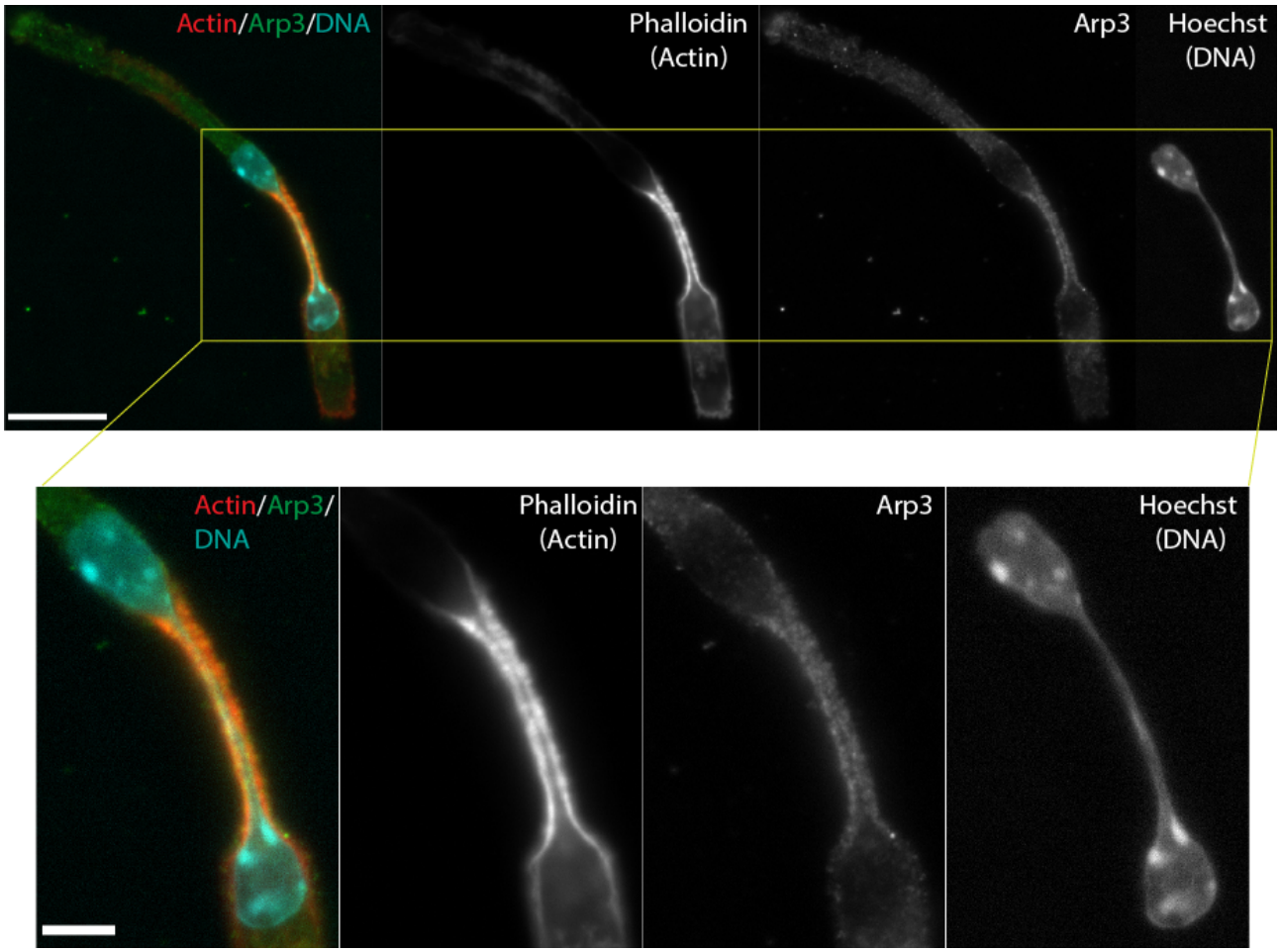

Figure 6.8: **Illustration of protein staining by immunofluorescence in microchannels.** An immature dendritic cell in a 15 μm long and 2 μm wide constriction is stained for the actin cytoskeleton, DNA and Arp3. From Left to right: overlay of the red (F-actin), green (Arp3) and cyan (DNA) channels; single channels. A zoom of the constriction region allows to observe the details of colocalization. Scale bars: 15 μm for the full image; 5 μm for the zoomed image

RESULTS

Chapter 7

Results

Contents

The results obtained during this PHD are presented here in form of a manuscript in preparation for a submission. They represent the work done for understanding the mechanisms of nuclear squeezing during immune cells, particularly dendritic cells, migration under confinement.

7.1 An Arp2/3 based nuclear squeezing allows dendritic cells to passage through micrometric constrictions

7.1.1 Summary

Cell migration is a complex process required for many physiological events including embryogenesis, wound healing and immune response. This process can also be hijack by cancer cells leading to metastatis formation. Cells migrating *in vivo* often have to encounter complex 3D environments which physico-chemical properties can tightly regulate cell forward movement. In the last years, confinement has emerged as an interesting physical property of the extracellular environment which can control cell migration. For instance, cancer cells have been shown to slow down in collagen gels of increasing density. Those cells have developed a specific ability to degrade the extracellular matrix and thus release the geometrical confinement imposed by such environments [Wolf 2013]. However, other highly migratory cells such as immune cells do not rely on matrix degradation for their migration under confinement. In contrary, confinement, to a certain extend, has proven to improve immune cells migratory efficiency. This thus raises the question of how a cell generates enough

forces to migrate under confinement. Indeed, for a forward movement to occur in confining spaces the cell must be able to deform itself or the extracellular space. Immune cells migrate throughout various tissues with a large range of mechanical properties, cellular deformability might thus be the limiting factor for cell migration in such environments. As said in the introduction (3.1), the main contributors to cell mechanical properties are the cytoskeleton, the plasma membrane and the nucleus. The cytoskeleton being a dynamic structure with a high turnover rate of filaments and the plasma membrane a compliant structure, the nucleus is then the cellular organelle which might limit cell deformation during migration.

In order to study the role of the nucleus in cell migration under confinement, we designed a microfabrication based setup consisting of microchannels in the middle of which constrictions of various sizes are placed. This configuration offers a good approximation to the *in vivo* event of a cell crossing in between 2 other cells in tissues or in the endothelial barrier of the lymph or blood vessels. We decided to focus our study on dendritic cells which *in vivo* migration is required for the onset of the adaptive immune response. Using our constrictions based setup, we first showed that dendritic cells forward movement is abrogated when constrictions are smaller than 2.2 μm^2 and strongly slowed down in constrictions cross section between 4.5 and 12 μm^2. Observing the nucleus allowed us to see that movement abrogation or slow down correlates with nuclear entry in constrictions. Moreover, between 4.5 and 12 μm^2 more than 50% of the passage time is due to nuclear passage through constrictions. Those results thus showed that nuclear deformation imposes a physical limitation to dendritic cells migration in highly confining spaces. We thus wonder how cells overcome this limit. One hypothesis was that cells would produce forces on the nucleus to allows its deformation. In order to identify such mechanism of nuclear squeezing, we performed a small scale screening on the acto-myosin and microtubules cytoskeleton which has been reported to be the force generators involved in nuclear positioning and overall in cell migration. We found that actin polymerization, particularly Arp2/3 based actin nucleation, is required for nuclear deformation in narrow constrictions. In contrary, myosin II as well as microtubules were not required for nuclear deformation in immature dendritic cells. Recording cell velocity in channels without constrictions, we found that Arp2/3 was not required for cell migration while myosin II inhibition induces cell slow down. This showed that dendritic cells possess a specific mechanism for nuclear squeezing independent of their migration mechanism.

To further understand this Arp2/3 based nuclear squeezing, we recorded actin dynamic in dendritic cells migrating through constrictions. We found that cells assemble a dense actin network around their nuclei when this organelle crosses constrictions. Interestingly, this actin overshoot starts right after nuclear entry in the constriction and stops after nuclear exit. In addition, this actin meshwork assembles only in constrictions in which nuclear passage induces cell slowing down (between 4.5 and 12 μm^2). Moreover, this actin meshwork was found to co-localize with Arp3 but not myosin II and to be independent of myosin II activity suggesting that the formation of this actin meshwork

might be involved in nuclear squeezing through narrow constrictions. Observing the nuclear lamin A/C network we found that this network ruptures in constrictions at sites of actin increase suggesting that the actin meshwork applies compressive forces on the nucleus.
We then hypothesize that the nuclear membrane-cell membrane shear stress increase induced by nuclear entry in constrictions leads to Arp2/3 local activation and thus actin polymerization. This resulting dense dendritic actin network will, by compressing the nucleus lead to lamin A/C rupture which will then release the nuclear surface tension thus facilitate cell passage through constrictions. This hypothesis first implies that softer nuclei which should not increase the nuclear membrane-cell membrane shear stress to the same extend than regular nuclei should not promote actin assembly in constrictions. Recording actin dynamics in lamin A/C depleted dendritic cells and HL-60 derived neutrophils allowed us to show that cells with softer nuclei do not assemble the actin meshwork. They, in addition, do not require Arp2/3 for their passage through narrow pores.

This work allowed us to propose that cells such as dendritic cells which daily function requires high motility in strongly confined spaces as well as high survival rate, will nucleated a dendritic actin meshwork around their nuclei to break the lamin A/C then facilitates nuclear passage through narrow pores. We believe that this transient nuclear softening allows such cells to overcome the physical limit to 3D migration imposed by nuclear deformability and at the same time conserve a stiff enough nucleus which can then resist to high extracellular forces that could otherwise induce DNA damages leading to cell death.

7.2 Manuscript in preparation for submission

(Perinuclear) Arp2/3 driven actin polymerization enables strong nuclear deformation during immune cells migration

Authors:

Hawa-Racine Thiam[1], Matthew Raab[1], Carolina Large-Crespo[3], (...), Ana-Maria Lennon-Dumenil[2], Pablo Vargas[2], Matthieu Piel[1*]

Affiliations:

[1]Institut Curie, CNRS UMR 144, 26 rue d'Ulm, 75005, Paris, FRANCE
[2]U 653, Inserm/Institut Curie, 26 rue d'Ulm 75248 Paris Cedex 05 France
[3]Division of Immunology, Transplantation and Infectious Diseases, San Raffaele Scientifc Institute, 20132 Milan, Italy
[*]Correspondence to: matthieu.piel@curie.fr

Abstract:

Cell migration has two opposite faces: necessary for physiological processes such as immune response, it can also lead to the organism death by allowing metastatic cells to invade new organs. *In vivo*, migration occurs in complex environments which often impose a high cellular deformability, a property limited by the cell nucleus. Here we show that immune cells such as dendritic cells possess a specific mechanism to pass through micrometric constrictions while preserving long term cell viability. This mechanism is based on a rapid Arp2/3 dependent actin nucleation around the nucleus which transiently ruptures the nuclear lamina, while, in these cells, Arp2/3 is not required for cell locomotion in the absence of constrictions. The requirement for Arp2/3 to pass through constrictions can be relieved when Lamin A/C expression is suppressed, but this also leads to a shorter lifespan when cells deform their nucleus while migrating. We thus propose that a specific actin based nuclear deformation mechanism allows immune cells to combine a high deformation and invasion capacity and a long term survival, two properties essential for their function.

One Sentence Summary:

Arp2/3 mediated actin nucleation around the nucleus leads to nuclear lamina rupture, allowing high invasion capacity and long lifespan of LaminA/C expressing immune cells.

7.2.1 Main text

The acto-myosin machinery required for cell locomotion has been described in great details both molecularly and physically in the past decade [Danuser 2013]. It is mostly based on two mechanisms: actin treadmilling and acto-myosin contraction [Ridley 2003]. The net rearward movement of actin filaments (in the referential frame of the cell), fuelled by cell scale organization of polymerization/depolymerization of the filaments ([Hu 2007], [Keren 2008]) and by the action of myosin motors [Burnette 2011], is transferred to the migration substratum via specific adhesion proteins (e.g. integrin receptors, [Chan 2008]), leading to forward cell locomotion ([Bangasser 2013], [Danuser 2013]). This well-defined physico-chemical set of processes, initially mostly described based on *in vitro* systems of cultured cells moving on flat glass surfaces, seems to be universally used by migrating cells. Nevertheless, recent studies performed in more complex environments proposed alternative scenarios and additional requirement for cell locomotion. The confining nature of micro-channels, gels or tissues can relieve the need for specific integrin based adhesion in immune and cancer cells ([Malawista 1997], [Lämmermann 2008], [Tozluoğlu 2013]), momentum transfer being then ensured thanks to non-specific friction ([Hawkins 2009], [Renkawitz 2009]) or geometrical entanglement [Tozluoğlu 2013]. The complexity of 3D gels also requires cells to restrict the number of their protrusions, to avoid engaging simultaneously in multiple paths and getting blocked by the gel fibers. This constrain makes polarity proteins such as Cdc42 essential for locomotion, while on 2D substrates it is only required for directionality [Lämmermann 2009].

In addition, the porous nature of gels and tissues puts a strong requirement on cell deformability/compliance [Lautenschläger 2009]. Due to the dynamic nature of the actin and microtubule cytoskeleton, and thanks to the high compliance of the plasma membrane and of the majority of membranous internal organelles, most cytoplasmic elements do not limit cell deformation through the micrometric pores found in tissues [Wolf 2009], at least at the timescale of cell locomotion. Cytoplasmic intermediate filaments can limit cell deformation ([Janmey 1991],[Wang 2000], [Seltmann 2013]). However, the involvement of vimentin, the only intermediate filament expressed in migrating cells (i.e. fibroblast and leukocytes) [Chernoivanenko 2013], in cell migration was rather related to cell polarity ([Eckes 2000], [Dupin 2011]), regulation of adhesions [Nieminen 2006] and transport of proteins involved in cell migration [Chernoivanenko 2013]. Several studies showed that in most cases, the element which limits cell deformation through narrow pores is the cell nucleus ([Wolf 2013],[Harada 2014]). Indeed, the cell nucleus possess a specific set of intermediate filaments encoded by Lamin A/C and B genes, which form a rigid shell underneath the inner nuclear membrane. To overcome this limitation, some migrating cells express a low level of Lamin genes products while others secrete proteases to enlarge pores in the extra-cellular matrix. Matrix degradation is important, but not essential, for migration of metastatic cells and does not seem to be involved in immune cell

migration ([Pflicke 2009], [Wolf 2013]), probably to preserve tissue integrity. On the other hand, while the degree of Lamin A/C expression was shown to correlate with the capacity of cells to pass through small pores in a protease independent manner ([Wolf 2013], [Rowat 2013], [Harada 2014]), low levels of Lamin A/C also correlates with lower cell viability during migration through pores [Harada 2014]. This is particularly relevant for immune cells. Indeed, some immune cells do not express Lamin A/C, such as neutrophils, and have a short lifespan (they die at the site of infection), but others, such as dendritic cells, which patrol peripheral tissues and present antigens to T cells in lymph nodes, need to combine a high migration capacity and a long term survival, a combination which might also be essential for the high metastatic capacity of some cancer cells [Harada 2014].

We indeed found that, consistent with a requirement for a long lifespan, dendritic cells express higher levels of Lamin A/C proteins compared to neutrophils or some metastatic cells (Fig 1a). This raises the question of the existence of a mechanism allowing Lamin A/C expressing cells to deform their nucleus through small pores. Myosin II action on actin filaments was proposed to play such a role, generating a pressure at the cell back pushing the nucleus forward. Nevertheless, Myosin II is required for cell locomotion per se, especially in confining environments ([Wyckoff 2006], [Wolf 2013]) and also for cell polarity, which is essential to migrate inside gels, making it difficult to clearly identify a specific role in nuclear deformation in such systems.

To ask how Lamin A/C expressing cells could deform their nucleus, we chose to study the migration of mice bone-marrow derived dendritic cells through microfabricated constrictions of well-defined sizes (Fig 1b, c, Fig S1a, b and S2a, b). Dendritic cells migrated spontaneously in such channels, and constrictions in the micron range induced a strong nuclear deformation in passing cells (Fig 1d, S1c-e and S2c). Timelpase recording of migrating cells identified four phases for cell transmigration: i) cell front entry in the constriction, which did not induce any slowdown, ii) nuclear engagement and deformation, which corresponded to the longest part of the process and led to a strong slowdown (Fig 1g-i), iii) nuclear exit, and iv) cell exit. While varying the length of the constriction (Fig S2) did not show a significant effect on the characteristics of cell passage, there was a clear effect of the section area, as reported before in gels [Wolf 2013]: at 2.2 μm^2 (1x2.2 μmxμm, see Fig S1b), the cell front could pass but only a small fraction of the nucleus could engage in the constriction (Fig S1c), leading to a very low rate of cell passage (Fig 1f, not significantly different from zero). Surprisingly, slightly increasing the constriction section area to 4.5 μm^2 (1.5x3 μmxμm, see Fig S1b) allowed a majority of cells to pass (Fig 1f, S1d and S2d). The passage rate reached a maximum above 12 μm^2 (3x4 μmxμm). Quantification of the passage rate (Fig 1f, S2d), passage time (Fig 1h, S2e) and cell velocity (Fig 1i) showed that for intermediary sizes of 4.5 and 7 μm^2, while a majority of cells could eventually pass the constriction, nuclear passage induced a significant delay. Importantly, for all sizes, non-passing cells engaged in the constriction spent at least as much

time in the constriction as passing cells (Fig S1f, S2f), showing that non passage was not due to an early change of direction of the cell induced by the constriction. In conclusion, these results show that immature bone-marrow derived dendritic cells, despite expression of Lamin A/C, can pass constriction down to about 4 μm^2 in section area and that, below 12 μm^2, the nucleus is limiting their passage.

We next performed a screen using 7 μm^2 constrictions (2x3.5 μmxμm where more than 60% of cells pass constrictions but are still slowed down by their nuclei) to identify cytoskeletal elements essential for nuclear passage. Removing microtubules rather increased cell passage (Fig 2a) and reduced passage time (Fig 2b), probably due to indirect activation of Myosin II ([Krendel 2002] and Fig S8), which increases cell speed inside channels (Our unpublished data). Inhibition of formins reduced cell speed (Fig 2c) but had no impact on the rate of passage (Fig 2a). Surprisingly, Myosin II inhibition or depletion of Myosin IIA (the only isoform expressed in dendritic cells, Immunological Genome project http://www.immgen.org), which had, as expected, a strong effect on cell shape (Our unpublished data), cell speed (Fig 2c) and thus passage time (Fig 2b), had no effect on the rate of passage of immature dendritic cells (Fig 2a and Fig S3), but completely prevented passage of mature dendritic cells in the presence of chemokine (Fig S4), suggesting an effect of chemokine signaling on the acto-myosin system in these cells ([Riol-Blanco 2005], [Sánchez-Sánchez 2006]) . This shows that Myosin II, while it plays a role to increase cell speed, is not generally required for nuclear deformation through small constrictions.
High doses of Latrunculin A, which depolymerize actin filaments, completely stopped cell migration (Our unpublished data), ruling out an osmotically driven migration mechanism ([Stroka 2014]). At low enough doses, Latrunculin A did not slow down cell movement (Fig 2c), but specifically prevented nuclear passage through constrictions (Fig 2a) and strongly reduced the speed of passage for the few passing cells (Fig 2b). A similar result was obtained when Arp2/3, or the hematopoietic specific Wave subunit Hem1, were inhibited or depleted (Fig 2a-c), and when the experiments were performed on mature dendritic cells in the presence of chemokines (Fig S4). The reduction in passage rate through constrictions was not due to an increase in changes in direction, as treated/depleted cells spent at least the same amount of time in constrictions as control/WT cells did (Fig 2d), and initiated nuclear entry inside constriction to the same extent as non-passing control/WT cells (Fig 2e). Overall, this screen revealed that Wave/Arp2/3 based actin nucleation is needed in dendritic cells specifically for nuclear passage through small constrictions (in addition to its role in micropynocitosis), and that this nuclear squeezing mechanism is uncoupled from the mechanism required for cell locomotion per se.

This result prompted us to look in more details at the localization of actin filaments in cells passing through constrictions. Dendritic cells derived from a LifeAct-GFP transgenic mice [Schachtner 2012]

showed a very strong enrichment of actin filaments around the nucleus inside constrictions (Fig 3a). The presence of filamentous actin around the nucleus in constrictions was confirmed with phalloidin staining of fixed cells (Fig S7a) and was quantified in live cells (Fig 3b,c), showing that it was temporally restricted to the time when the nucleus was deformed in the constriction and spatially limited to the constriction (Fig 3b,c). This enrichment of actin was specific to small constrictions (Fig 3d-f and Fig S5) of sizes which induced slowdown of the nucleus (Fig 1f,h,i) and which required Arp2/3 for passage (Fig 2a, SX). It was distinct from the permanent enrichment of actin at the cell back and the transient enrichments observed at the cell front (respectively yellow and pink arrow heads in Fig 3d). This suggests that a specific set of actin filaments is assembled around the nucleus when it is strongly confined.

To test if these actin filaments could be involved in the Arp2/3 dependent nuclear passage mechanism, we immunostained Arp3 in fixed cells inside constrictions (see supplementary methods). This revealed a clear enrichment of the Arp2/3 complex around the nucleus, co-localized with the enrichment in actin filaments stained by phalloidin (Fig S7a). We also found that, while more than 90% of passing control cells displayed an actin accumulation around the nucleus versus less than 30% in non-passing cells which engaged their nucleus in the constriction, the fraction of passing cells with an actin accumulation after CK666 treatment dropped down to the level observed in non-passing cells (Fig S7b-d). These results suggest that the actin accumulation observed around the nucleus in constriction depends upon Arp2/3 and that the small fraction of cells that pass in the absence of Arp2/3 possess an alternative mechanism that does not involve actin accumulation around the nucleus.

To further assess the role of Myosin II in nuclear passage, we imaged dendritic cells derived from a Myosin IIA-GFP transgenic mice (see supplementary methods). Consistent with a requirement for Myosin II for cell speed and not for nuclear passage, Myosin IIA-GFP was found exclusively at the cell back when cells were passing constrictions and did not show any enrichment inside the constriction where actin enrichment was observed (Fig S6a). Inhibition of Myosin II with Blebbistatin did not prevent actin accumulation around the nucleus in constrictions (Fig S6b). Interestingly, when microtubules were depolymerized with nocodazole, Myosin II A was found to strongly accumulate at the cell back (Fig S8c,d), consistent with the increase in cell speed and the reduction of passage time through constrictions. In these cells, actin was also found to accumulate at the cell back and was not observed to accumulate around the nucleus anymore (Fig S8b), potentially due to the well-known antagonistic effect of RhoA activation on Rac1 activity ([Sander 1999], [Burridge 2004]). Microtubule depolymerization is known to activate RhoA [Krendel 2002], while Rac1 is required for Wave/Arp2/3 based actin nucleation [Eden 2002]. This also means that activation of Myosin II contractility at the cell back might compensate the loss of Arp2/3 based actin nucleation around the nucleus. Consistent with this hypothesis, inhibition of Myosin II in Hem1KO cells further reduced

the passage rate through constrictions, while it had no effect on WT cells (Our unpublished data). These results suggest the existence of two complementary mechanisms for nuclear passage through constrictions in dendritic cells: Arp2/3 nucleated actin filaments would exert a direct pressing force on the nucleus, while acto-myosin contractility at the cell back would increase hydrostatic pressure, pushing the nucleus from behind.

This allows us to draw the following picture: in dendritic cells, Myosin II at the cell back is required for fast cell migration, but Arp2/3 actin nucleation around the nucleus is sufficient for passage through constrictions; conversely, if Myosin II induces enough contractility, Arp2/3 actin nucleation around the nucleus might become dispensable, explaining the fast passage of nocodazole treated cell across constrictions without actin around the nucleus, and the existence of a fraction of cells still passing constrictions in the absence of Arp2/3 activity and doing so without accumulating actin filaments around the nucleus.

To further understand how actin nucleation around the nucleus might help nuclear deformation, we stained Lamin A/C in fixed cells inside constrictions. We observed that in $X\%$ of the cells, the perinuclear Lamin A/C staining was interrupted or fragmented when the nucleus was fully engaged in the constriction, while such fragmentation was observed in only $Y\%$ of the cells outside constrictions (Fig 4a, Our unpublished data). The fragmented region often corresponded to the accumulation of actin filaments. This suggested that this accumulation of filaments might exert a pressure inducing the rupture or the disassembly of the Lamin A/C network [Swift 2013]. To test this hypothesis, we depleted Lamin A/C in dendritic cells and inhibited Arp2/3. In control cells, inhibition of Arp2/3 strongly reduced passage through small constrictions, but it had no effect on the rate of passage of Lamin A/C depleted cells (Fig 4f). Interestingly, depletion of Lamin A/C did not affect the passage time of passing cells (Fig 4g), suggesting that the nucleus of control cells that pass the constriction do not exert more resistance than Lamin A/C depleted nuclei, consistent with a transient disassembly/rupture of Lamin A/C network in passing cells. The passage time of Lamin A/C depleted cells was significantly reduced only for the smallest constrictions (Fig 4d), and the rate of passage in control cells was almost unaffected for all size except for the 2.2 μm^2 constriction which control cells could not pass and through which a significant fraction of Lamin A/C depleted cells could pass (Fig 4c). These results show that Arp2/3 dependent actin nucleation around the nucleus is necessary only in Lamin A/C expressing cells and suggest that its function might be to facilitate transient disassembly of the Lamin A/C network.

When imaging Lifeact-GFP expressing cells depleted for Lamin A/C, we found that actin filaments accumulation around the passing nuclei was strongly reduced (Fig 4h), down to the level found in Arp2/3 inhibited cells (Fig S7b). Performing a similar set of experiments on HL60

derived neutrophils, which do not express Lamin A/C, showed that they could pass through 2.2 μm^2 constrictions (Fig S9b), that they did not need Arp2/3 to pass small constrictions (Fig 4d, e), but that passage through the smallest constrictions (2.2 μm^2) strongly depended on Myosin II. Finally, no actin accumulation was observed around the nucleus of HL60 derived neutrophils even in the smallest constrictions (Fig 4a, h), actin being rather enriched at the cell back (Fig 4a). Overall these results confirm that Arp2/3 dependent actin nucleation around the nucleus is required only for the deformation of nuclei which possess a Lamin A/C network, while Myosin II activity is important to push nuclei through the smallest constrictions, even in the absence of Lamin A/C. They also suggest that perinuclear actin filaments accumulation also depends on the presence of a Lamin A/C intranuclear shell.

Our results allowed us to identify a new mechanism required for the migration of Lamin A/C expressing cells through small constrictions. This mechanism involves the nucleation of an Arp2/3 dependent actin network around the nucleus, which would transiently rupture the Lamin A/C nuclear shell, making the nucleus more deformable.

The requirement for a branched actin network (nucleated by Arp2/3 rather than formins) might be linked to the capacity of such networks to exert a strong pressure, due to an increase in the density of branches when growing under a load or in confinement ([van Oudenaarden 1999], [Risca 2012]; [Kawska 2012]). Building upon this hypothesis, it is possible to propose that the accumulation of actin around the nucleus could be simply induced by the high load produced by the stiff nuclear Lamin A/C mesh when it is confined in the constriction. This would be consistent with the absence of actin accumulation around soft nuclei in cells that do not express Lamin A/C. It could also be that the Lamin A/C network, in association with the trans-nuclear membrane LINC complex, recruits actin nucleation promoting factors which might be activated upon nuclear deformation.

Importantly, we could observe such actin accumulation around strongly deformed nuclei also in dendritic cells migrating in dense collagen gels (Fig S10a) and in mice ear explants (Our unpublished data), as well as in macrophages migrating in live fish (Fig 10 b). Such accumulation could be observed when the nucleus showed a significant deformation (arrowheads in Fig S10 b)

Why would some immune cells, whose function requires a high migration capacity, keep expressing Lamin A/C, since it impairs nuclear deformation? Recent results on metastatic cells suggest that Lamin A/C expression is required for their long term survival and thus invasive capacity [Harada 2014]. We thus tested the survival of dendritic cells depleted or not for Lamin A/C when migrating inside channels with or without constrictions. Strikingly, Lamin A/C depleted cells showed an increased rate of death, but only in channels with constrictions (Our unpublished data), suggesting

that Lamin A/C is necessary for survival only when cells experience strong nuclear deformation associated with migration through constrictions.

In conclusion, we propose that some immune cells and potentially also certain metastatic cells, possess a specific mechanism, based on Wave/Arp2/3 actin nucleation around the nucleus, which allows them to strongly deform their nucleus despite the presence of a stiff Lamin A/C intranuclear shell. This would allow them to combine a high migration/invasion capacity and a long term survival, which is required for immune cells, such as dendritic cells, to achieve their functions from peripheral tissue sampling to antigen presentation in lymph nodes, and for metastatic cells to colonize tissues.

Figure 7.1 *(facing page)*: Fig 1 : The nucleus imposes a physical limitation to dendritic cells migration through micrometric pores. a) Western blot showing expression level of Lamin A/C in various cell types; Myosin II heavy chain (MyoIIHC) and G-actin are shown as loading controls. Ms for mouse; iDCs for immature dendritic cells; mDCs for mature dendritic cells. b) Schematic representation of the experimental setup used to study cell transmigration. c) Top: Representative image of a field of channels with periodic constrictions (distance betwenn constrictions = 100 nm). Bottom: Zoom on a single constriction. Scale Bar 30 μm. d) Representative image of an immature BMDC squeezing in a constriction coated with PLL-PEG (grey levels). Constriction dimensions : Length (L) = 15 μm; cross section = 7 μm^2 (2 x 3.5 μmxμm). Cell staining: Iaβ-GFP for the membrane (red), Hoechst for DNA (green). Scale bar 15 μm. Middle : views of the channel cross section. Scale bar 4 μm. Bottom: Perspective view (45°) of a 3D iso-surface reconstruction from a sequential 3D stack of 17 images with 0.3 μm z-step (60X, binning 1). Scale bar 15 μm. e) Representative image of the steps of an iDC migrating through a constriction (overlay phase contrast and DNA (green)). i) cell entry, ii) nuclear entry, iii) nuclear exit, iiii) cell exit. Scale bar 30 μm. f) Quantification of cell percentage of passage through 20 μm long constrictions. n = 50 cells for each condition. g) Cell (blue) and nuclear (green) front instantaneous velocity as function of the nuclear front position. Constriction dimensions : Length (L) = 20 μm; cross section = 4.5 μm^2 (1.5x3 μmxμm). h) Cell (blue) and nuclear (green) passage time in 20μm long constrictions. n > 20 cells for each condition. f) and h) Unless when indicated by a line, statistical test done against 5x5 μmxμm constrictions . i) Cell and nuclear front velocities in constriction normalized by the cell center of mass velocity before the constriction as a function of the constriction dimensions. C.F. for Cell Front and N.F. for Nuclear Front. Error bars represent the standard error on the mean. $***$, $**$ and $*$ for Pvalue respectively < 0.0001, < 0.001, and < 0.01. ns for non significant. Statistical test: Fisher Test for f), Mann-Whitney Test for g) and i).

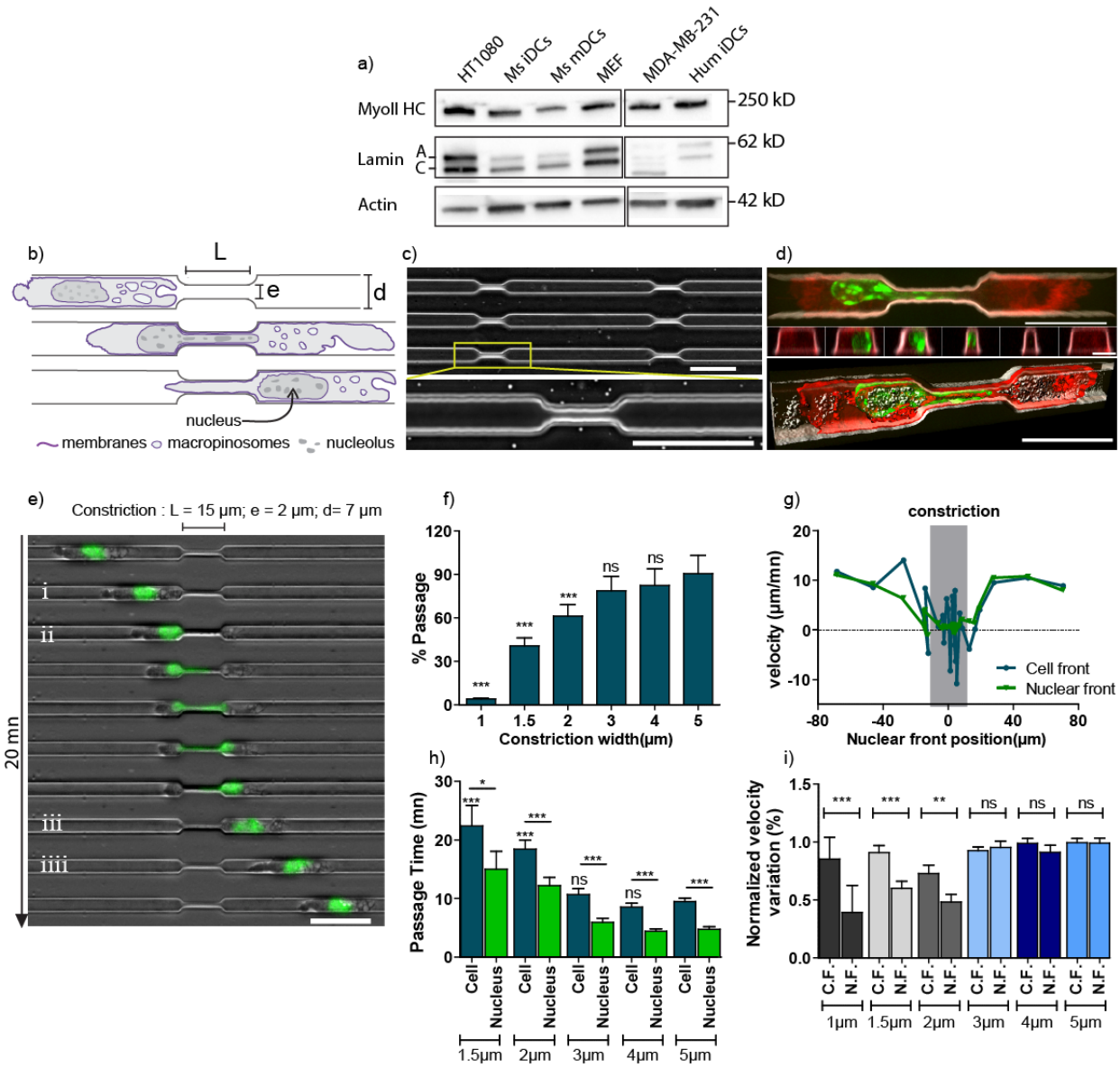

Figure 7.2 *(facing page)*: **Fig 2 : Arp2/3 based actin polymerization is required for dendritic cells passage through constrictions.** a) Normalized cell percentage of passage, b) Normalized passage time in 7 μm^2 constrictions. Red line drawn at 1. Each condition is normalized and/or compared to its control. n > 50 cells for each conditions except for Delk32-Hmz (n=18) Delk32-Htz (n=29). Hmz for homozygote, Htz for heterozygote. Frmns for formins, MT for microtubules. Data represent means of at least 2 independent experiments. c) Mean instantaneous cell velocity in straight 35 μm^2 (7 x 5 $\mu m x \mu m$) channels without constrictions. n > 200 cells for each conditions. d) Percentage of nuclear entry in non passing cells. e) Time spent in constrictions by non passing cells, red line drawn at 1, n> 35 cells per condition. In a) c) and d) error bars represent the standard error on the mean. In b) and e) box extends from the 25^{th} to 75^{th} percentiles, whiskers: Min to Max. $***$, $**$ and $*$ for Pvalue respectively < 0.0001, < 0.001, and < 0.01. ns for non significant. Statistical test: Fisher Test for a) and d), Mann-Whitney Test for b) and e).

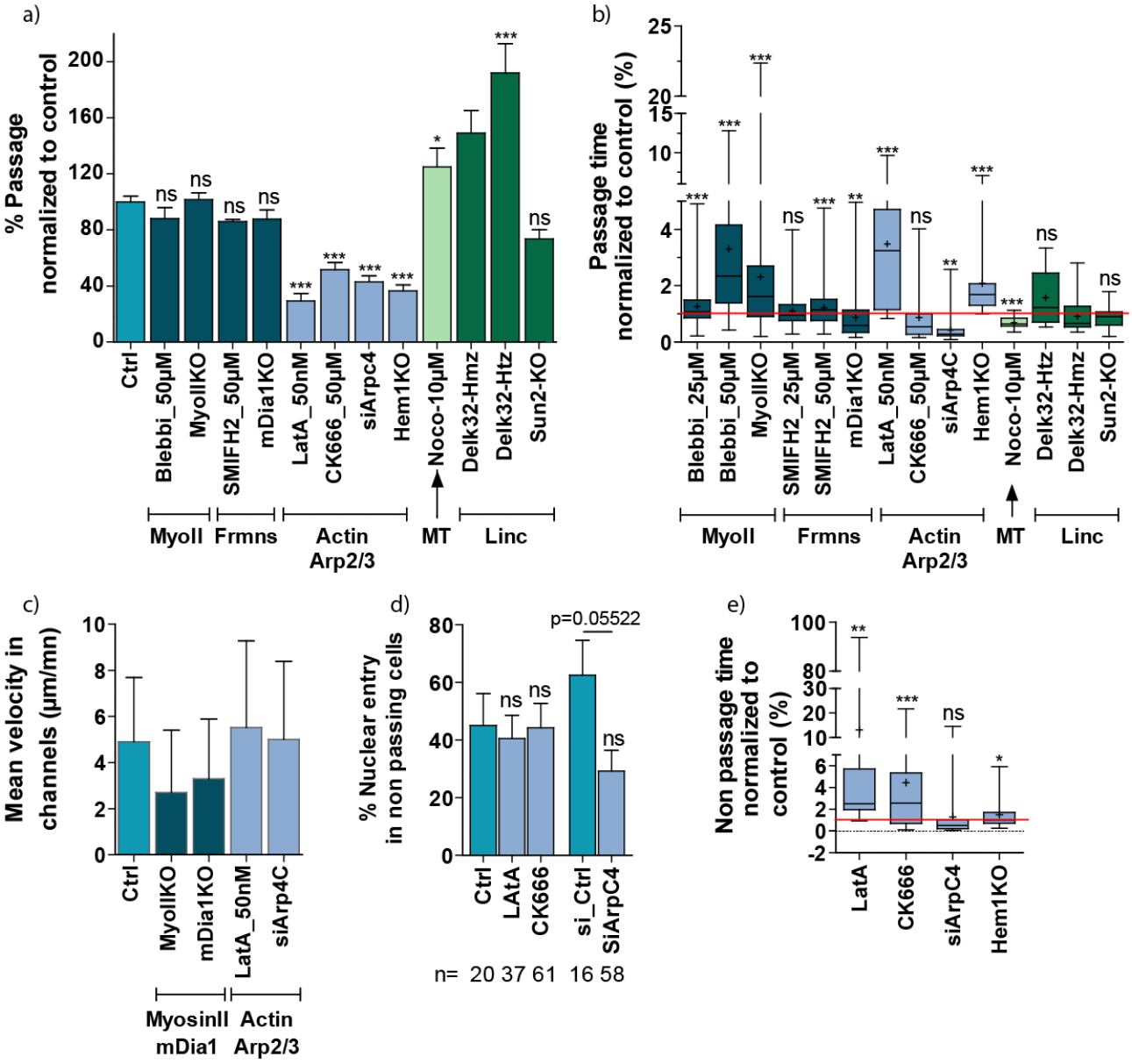
a)
% Passage normalized to control
Ctrl
Blebbi_50µM
MyoIIKO
SMIFH2_50µM
mDia1KO
LatA_50nM
CK666_50µM
siArpc4
Hem1KO
Noco-10µM
Delk32-Hmz
Delk32-Htz
Sun2-KO
MyoII
Frmns
Actin Arp2/3
MT
Linc
b)
Passage time normalized to control (%)
Blebbi_25µM
Blebbi_50µM
MyoIIKO
SMIFH2_25µM
SMIFH2_50µM
mDia1KO
LatA_50nM
CK666_50µM
siArp4C
Hem1KO
Noco-10µM
Delk32-Htz
Delk32-Hmz
Sun2-KO
MyoII
Frmns
Actin Arp2/3
MT
Linc
c)
Mean velocity in channels (µm/mn)
Ctrl
MyoIIKO
mDia1KO
LatA_50nM
siArp4C
MyosinII
mDia1
Actin Arp2/3
d)
% Nuclear entry in non passing cells
p=0.05522
Ctrl
LAtA
CK666
si_Ctrl
SiArpC4
n= 20 37 61 16 58
e)
Non passage time normalized to control (%)
LatA
CK666
siArpC4
Hem1KO

Figure 7.3 *(facing page)*: **Fig 3 : Dendritic cells assemble a dense actin network around their nucleus during nuclear deformation in constrictions.** a) Montage of an iDCs migrating through a 7 μm^2 constriction. Yellow and pink arrows for actin accumulation respectively at the cell rear and front. Scale bar overlay : 30 μm, Actin and DNA : 15 μm. b) Mean actin intensity in constriction normalized to the mean actin intensity in the whole cell as function of the nuclear passage time in constrictions. c) Green : Mean actin intensity around the nucleus normalized to the mean actin intensity in the whole cell as function of the nuclear center of mass position. Red: Nuclear circularity as function of the position of the nuclear center of mass. Dark green (red) for the mean and light green (red) for the standard error on the mean. d) Representative image of iDCs before and in 1.5 x 3 μmxμm and 5 x 5 μmxμm constrictions. Scale bar 15 μm. e) Ratio of the normalized mean actin intensity in constriction and before constrictions as function of the constriction width. Each dot represent a cell. lines represent the mean and bars standard deviation. Comparison done against the 5 x 5 μmxμm constrictions. $***$, for Pvalue < 0.0001. ns for non significant. f) Mean actin intensity around the nucleus normalized to the mean actin intensity in the whole cell as function of the nuclear center of mass position for 1.5 x 3 μmxμm and 5 x 5 μmxμm constrictions. w for constriction width

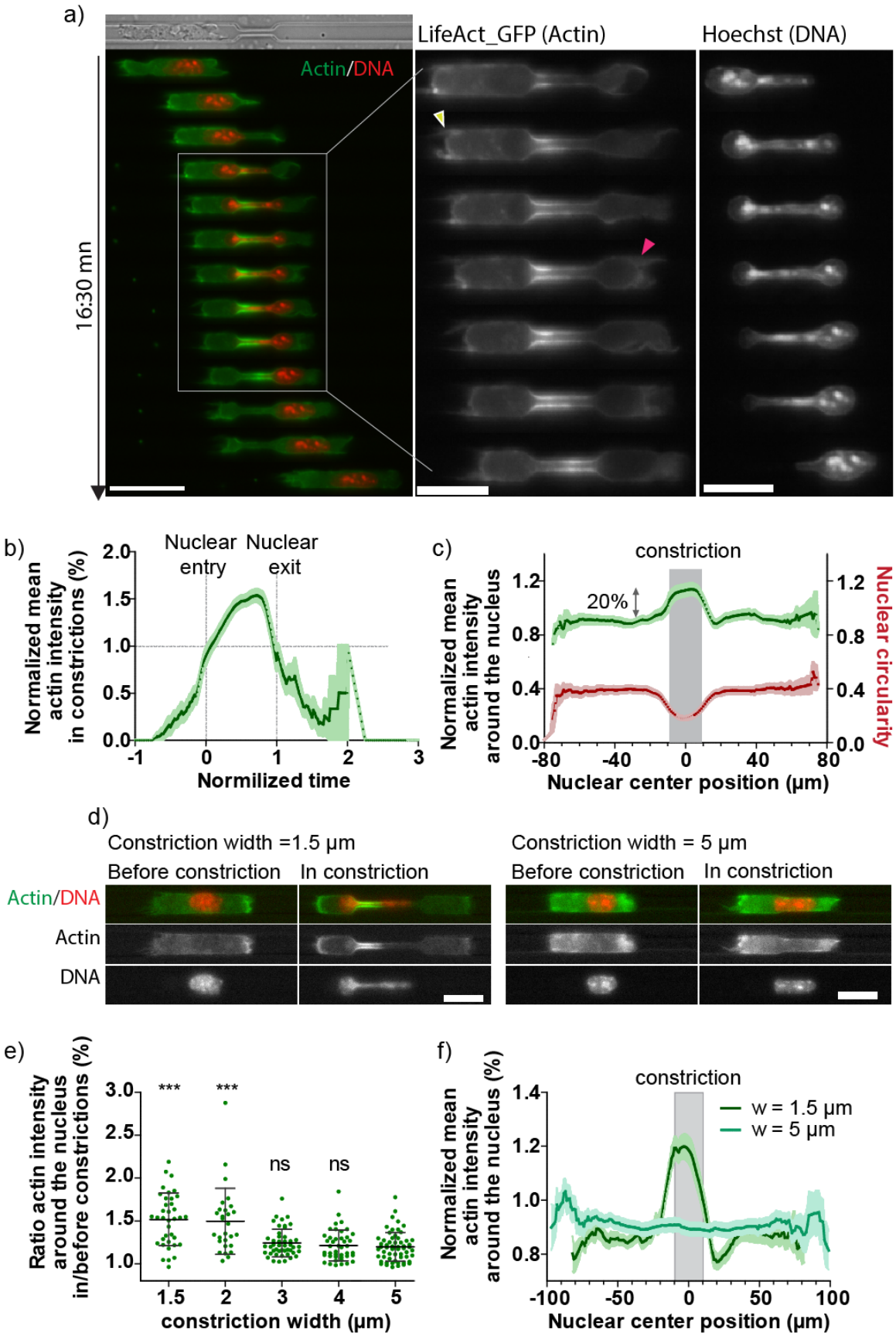
a)
Actin/DNA
LifeAct_GFP (Actin)
Hoechst (DNA)
16:30 mn
b)
Nuclear entry
Nuclear exit
Normalized mean actin intensity in constrictions (%)
Normilized time
c)
constriction
20%
Normalized mean actin intensity around the nucleus
Nuclear circularity
Nuclear center position (µm)
d)
Constriction width =1.5 µm
Before constriction
In constriction
Constriction width = 5 µm
Before constriction
In constriction
Actin/DNA
Actin
DNA
e)
Ratio actin intensity around the nucleus in/before constrictions (%)
***
***
ns
ns
constriction width (µm)
f)
constriction
w = 1.5 µm
w = 5 µm
Normalized mean actin intensity around the nucleus (%)
Nuclear center position (µm)

Figure 7.4 *(facing page)*: **Fig 4 : The Arp2/3 nucleated actin meshwork facilitates nuclear squeezing through constrictions by breaking the lamin A/C network.** a) Maximum intensity of a 3D stack of 21 images with 0.3 μm z-step (100X, binning 1). Localization of F-actin, Lamin A/C and DNA in iDC migrating through a 7 μm^2 constriction with immunostaining. Right : zoom in the constriction. Saturation of the intensity to clearly visualize the DNA and lamin A/C staining in the constriction. b), e), i) Quantification of Lamin A/C depletion after siRNA. Myosin II HC is taken as loading control. c) Percentage of passage of control and Lamin A/C depleted iDCs in 5 μm long constrictions. Percentage of passage is significantly different from zero for Lamin A/C depleted cells (Pvalue = 0.02046) but not for control cells (Pvalue=0.3134). n > 50 cells for each condition. Unless when indicated with lines, comparison is done against the rate of passage in 5 x 5 μmxμm constrictions. d) Cell (blue) and nuclear (green) passage time for control and Lamin A/C depleted iDCs as function of constrictions dimensions in 5 μm long constrictions. n > 35 cells for each condition. f) and g) Respectively percentage of passage and passage time as function of Lamin A/C depletion and Arp2/3 inhibition with CK666 in 7 μm^2 constrictions. h) Percentage of passing cells with actin assembly as function of the Lamin A/C depletion and Arp2/3 inhibition in 7 μm^2 constrictions. j) and k) Respectively percentage of passage and passage time as function of Lamin A/C depletion and Myosin II inhibition with blebbistatin in 7 μm^2 constrictions. Quantification in f), g), h), j) and k) were performed in 7 μm^2 constrictions and unless when indicated with a line, comparisons were done against the control siRNA. n > 30, 13, 50, 25 for each condition of respectively f), g) and h), j), k). c), d), f), h) and j) error bars indicate the standard error on the mean. g) and k) box extends from the 25^{th} to 75^{th} percentiles, whiskers: Min to Max. $***$, $**$ and $*$ for Pvalue respectively < 0.0001, < 0.001, and < 0.01. ns for non significant. Statistical test: Fisher Test for c), f), h) and j), Mann-Whitney Test for d), g) and k). Ctrl for siControl.

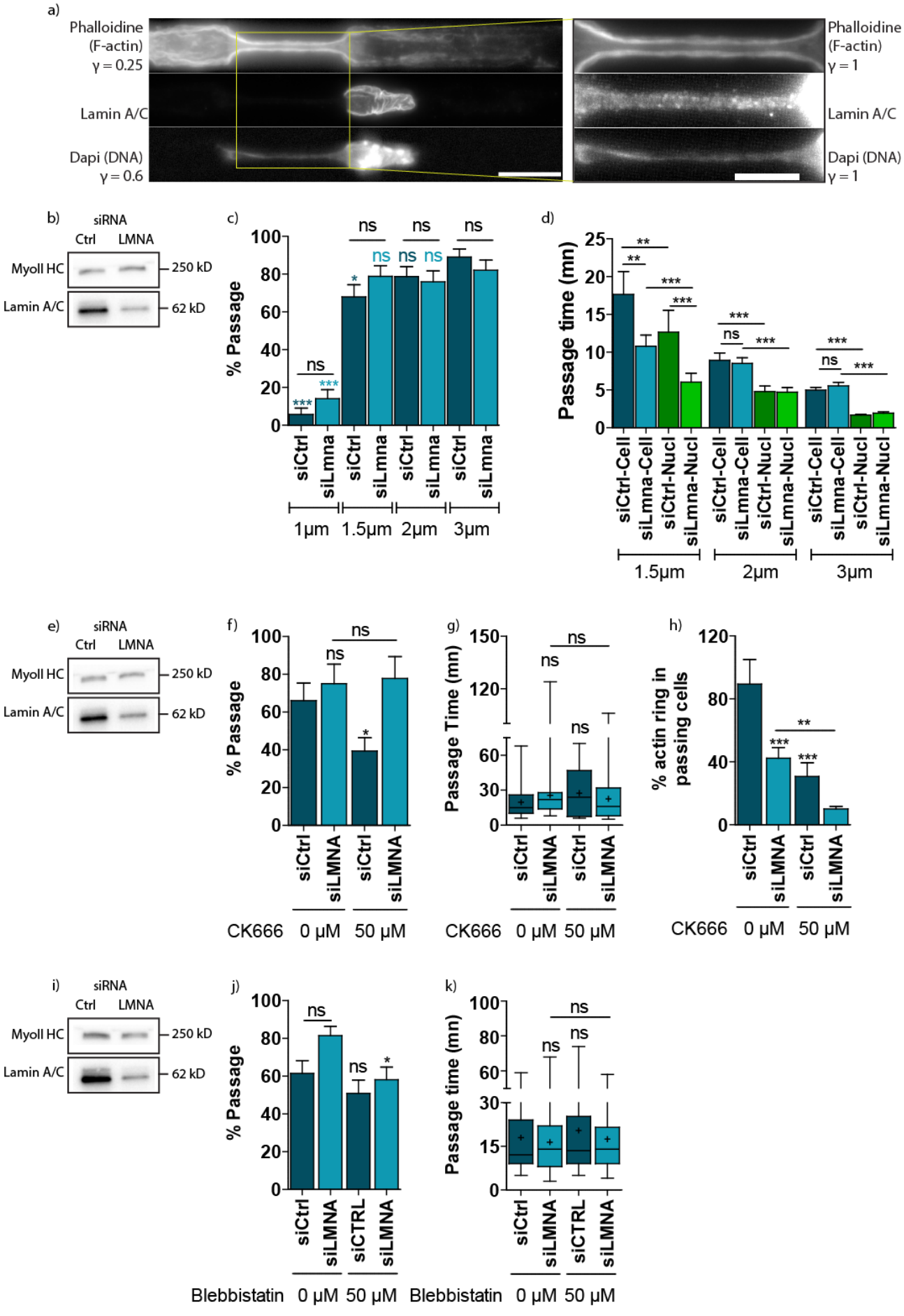
a)
Phalloidine (F-actin) γ = 0.25
Lamin A/C
Dapi (DNA) γ = 0.6
Phalloidine (F-actin) γ = 1
Lamin A/C
Dapi (DNA) γ = 1
b)
siRNA
Ctrl
LMNA
Myoll HC
Lamin A/C
250 kD
62 kD
c)
% Passage
siCtrl
siLmna
1µm 1.5µm 2µm 3µm
d)
Passage time (mn)
siCtrl-Cell
siLmna-Cell
siCtrl-Nucl
siLmna-Nucl
1.5µm 2µm 3µm
e)
siRNA
Ctrl
LMNA
Myoll HC
Lamin A/C
250 kD
62 kD
f)
% Passage
siCtrl
siLMNA
CK666 0 µM 50 µM
g)
Passage Time (mn)
CK666 0 µM 50 µM
h)
% actin ring in passing cells
CK666 0 µM 50 µM
i)
siRNA
Ctrl
LMNA
Myoll HC
Lamin A/C
250 kD
62 kD
j)
% Passage
siCtrl
siLMNA
siCTRL
Blebbistatin 0 µM 50 µM
k)
Passage time (mn)
Blebbistatin 0 µM 50 µM

Figure 7.5 *(facing page)*: **Fig S1 : Details of dendritic cells migration through 20 μm long constrictions.** a) Image from an optical profilometer of a region of a master mold containing channels with constrictions. The depletion of height in constrictions can be observed. b) Confocal imaging based channels and constrictions height determination. While the channels height is constant, the constriction height increases with the constriction width. Quantification done on 20 channels and constrictions. Line represent the mean height and the error bar the standard deviation. Chnl for channels, Const for constriction. 7 μm represents channels without constrictions. Constriction length = 20 μm c) Montage of an iDC trying to migrate through a 1 μm wide (2.2 μm^2 of cross section) constriction. Zoom on the constriction to visualize nuclear protrusion in the constriction. d) and e) Montage of an iDC migrating through a respectively 1.5 μm, 5 μm wide (4.5 μm^2, 25 μm^2 of cross section) constriction. Right: Zoom on the constriction to visualize nuclear deformation during passage through constriction. While the nucleus deforms a lot in the 4.5 μm^2, only a small nuclear deformation is observed in the 25 μm^2 constriction. Scale bar 30 μm for phase contrast and DNA overlays, 15 μm for zoom of the DNA in constrictions. L for constriction length and e for constriction width. f) Quantification of the time spent by non passing cells in constrictions function of the constriction width (thus cross section). Each dot represent a cell. The mean non passing time (> 14 minutes) is much higher than zero, meaning that cells which do not pass constrictions do not turn back because of a lack of persistence.

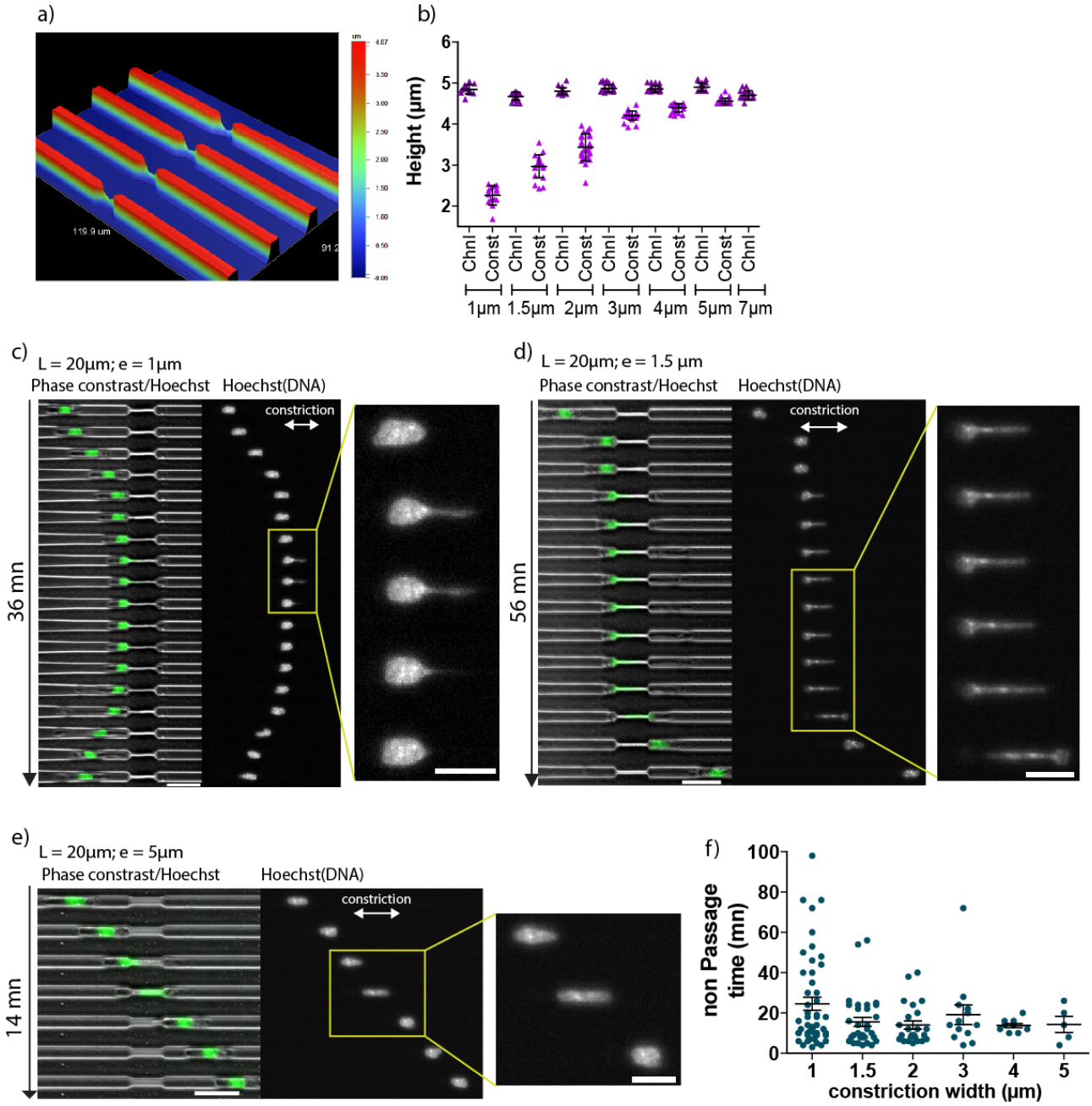
a)
b)
Height (µm)
Chnl
Const
1µm 1.5µm 2µm 3µm 4µm 5µm 7µm
c)
L = 20µm; e = 1µm
Phase constrast/Hoechst
Hoechst(DNA)
constriction
36 mn
d)
L = 20µm; e = 1.5 µm
56 mn
e)
L = 20µm; e = 5µm
14 mn
f)
non Passage time (mn)
constriction width (µm)

Figure 7.6 *(facing page)*: **Fig S2 : The physical limit imposed by the nucleus is independent of pore length. Characterization of the 5 μm long constrictions.** a) Top: phase contrast image of a channel with a 5 μm long and 2 μm wide constriction. Middle and Bottom: 3D reconstruction from a 3D stack of 21 images with 0.3 μm z-step (100X, binning 1) Iaβ-GFP (red) iDC in a 5 μm long and 1.5 μm wide constriction coated with PLL-PEG (white). The DNA in green is stained with Hoechst. Middle: Different views of the 3D reconstruction. On the left, view of the cross section. Bottom: Perspective view of the 3D reconstruction with a 45° angle. Scale bar Top: 30 μm, Middle and Bottom: 10 μm. b) Confocal imaging based channels and constrictions height determination. Each dot represents a channel or a constriction. Line represents the mean height, and the error bar the standard deviation. Chnl for channels, Const for constriction. 7 μm represents channels without constrictions. c) Montage of an iDCs crossing a 5 μm long, 2 μm wide and 4 μm high constriction. i), ii), iii), iii) respectively indicate cell entry, nuclear entry, nuclear exit, cell exit. Scale bar 30 μm height. d) Cell percentage of passage as function of the constriction width (thus cross section). n > 50 for each condition. e) Cell (blue) and nuclear (green) passage time. Comparison done against 5x5 μmxμm constrictions. $***$, $**$ and $*$ for Pvalue respectively < 0.0001, < 0.001, and < 0.01. ns for non significant. Statistical test: Fisher Test for d), Mann-Whitney Test for e). f) Cell non passage time which measures the time spent in constriction by non passing cells. Each dot represents a cell. This parameter being higher than zero indicates that cells exit from the constriction is not due to a lack of persistence.

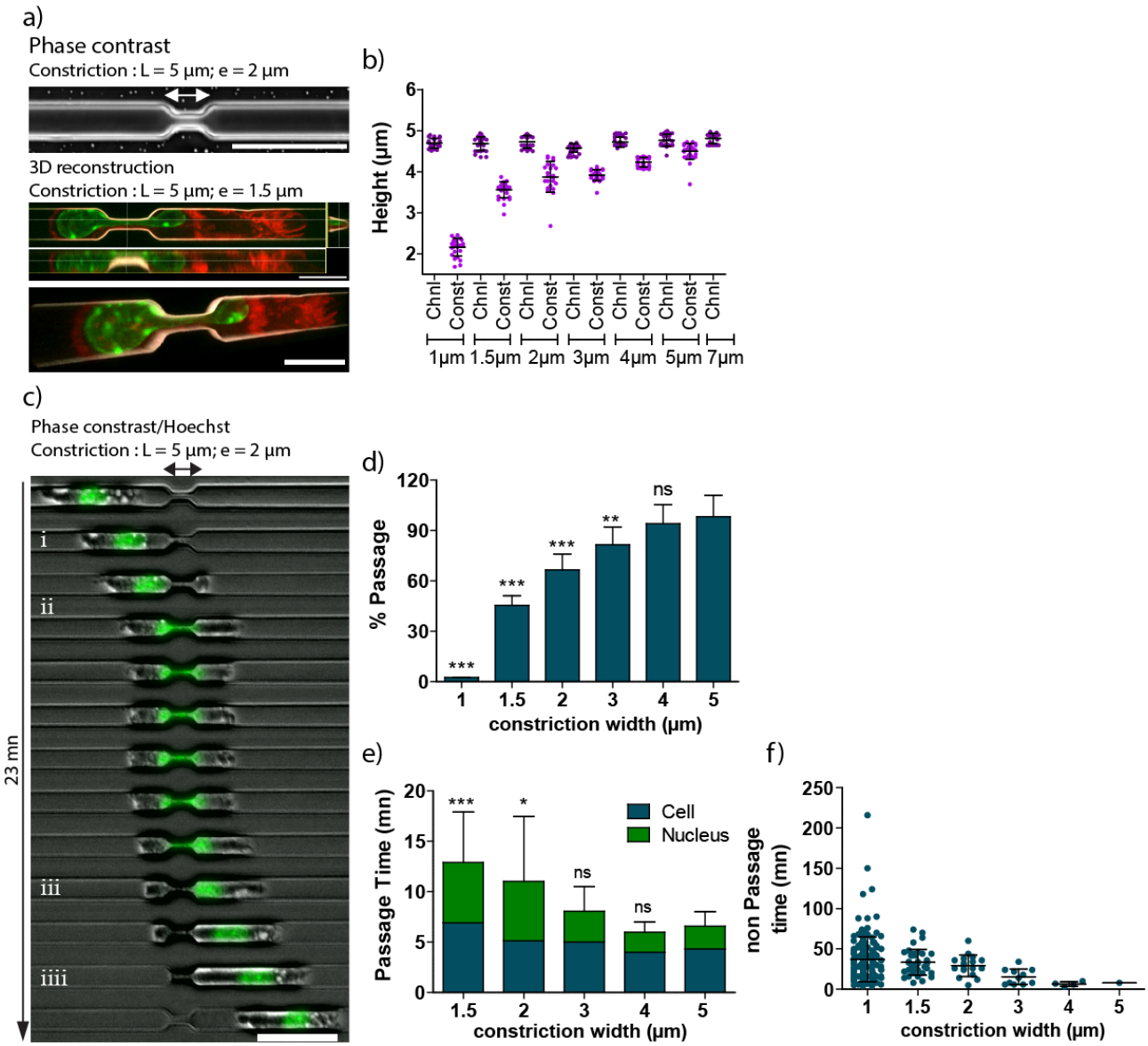
a)
Phase contrast
Constriction : L = 5 µm; e = 2 µm
3D reconstruction
Constriction : L = 5 µm; e = 1.5 µm
b)
Height (µm)
Chnl
Const
1µm 1.5µm 2µm 3µm 4µm 5µm 7µm
c)
Phase constrast/Hoechst
Constriction : L = 5 µm; e = 2 µm
23 mn
i
ii
iii
iiii
d)
% Passage
constriction width (µm)
e)
Passage Time (mn)
Cell
Nucleus
constriction width (µm)
f)
non Passage time (mn)
constriction width (µm)

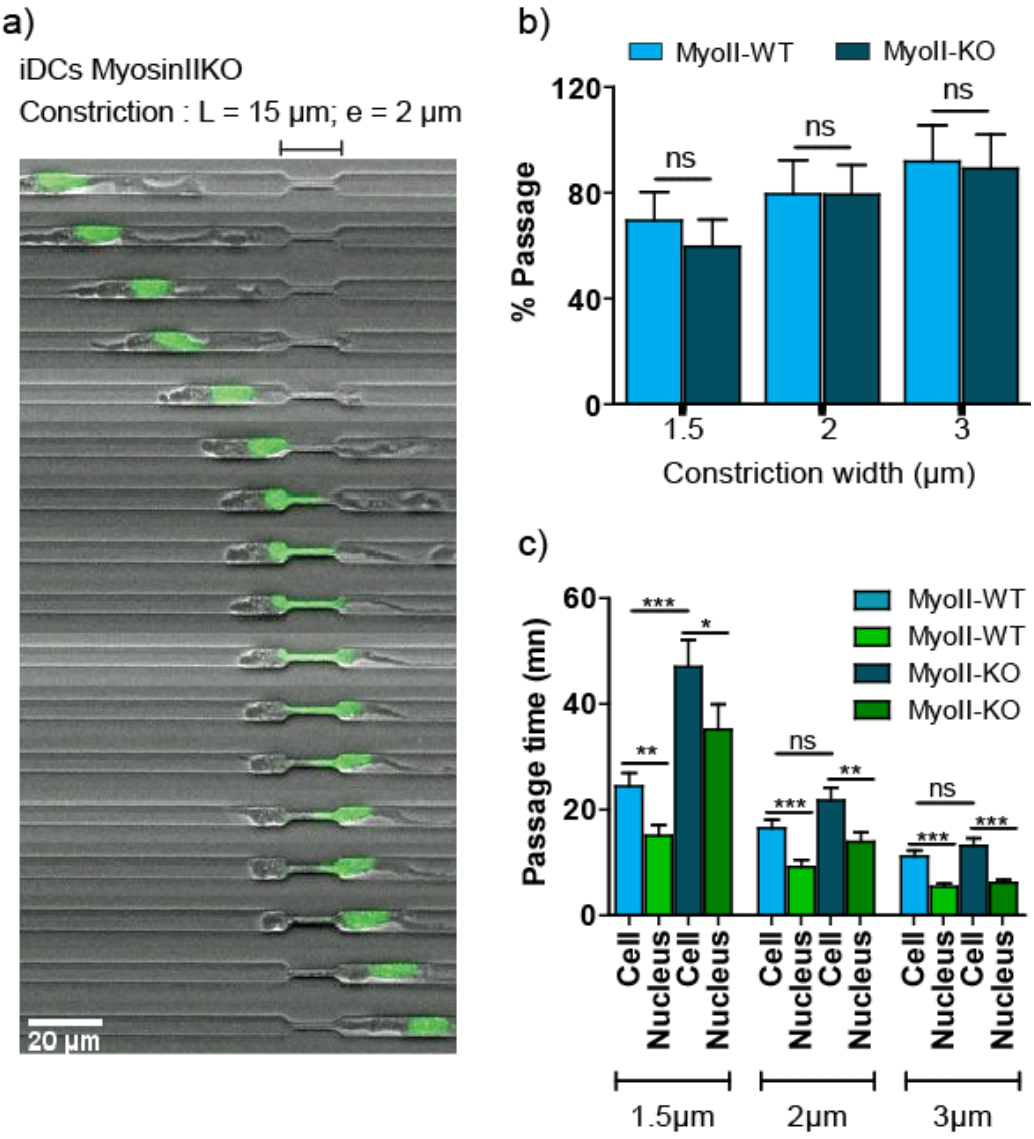

Figure 7.7: **Fig S3 : Nuclear squeezing is independent of myosin II activity even in smaller constrictions.** a) Montage of a Myosin II A conditional knock out dendritic cell migrating through a 15 μm long, 2 μm wide and 3.5 μm high constriction. We can observe the long cell front as well as cell back which are the hallmark of Myosin II inhibited dendritic cells. b) Percentage of passage as function of the constriction width. Non significant difference can be measured in all constrictions between wild type and Myosin II A KO immature dendritic cells. n > 50 for each condition. c) Cell (blue) and nuclear (green) passage time as function of the constriction width and Myosin II A depletion. We can observe a significant increase in the cell as well as the nuclear passage time upon Myosin II depletion in 1.5 μm wide constrictions. $***$, $**$ and $*$ for Pvalue respectively < 0.0001, < 0.001, and < 0.01. ns for non significant. Statistical test: Fisher Test for b), Mann-Whitney Test for c).

Figure 7.8 *(facing page)*: **Fig S4 : Mature dendritic cells nuclear squeezing requires both myosin II and Arp2/3.** a) Quantification CD86 (a co-stimulatory protein) expression in immature (blue) and mature (red) dendritic cells. Light blue (red) and dark blue (red) for cells respectively not stained and stained with with CD86 antibody. The ordinate represents the number of cells and the absciss the signal of CD 86. The light (red and blue) curves represent the background signal. We can observe an higher CB86 signal in mature dendritic cells compared to the immature ones. b) Normalized percentage of passage. Error bars represent the standard error on the mean. n > 50 for each condition excepted for (Myosin II WT + CK666; LPS (+); CCL21 200 ng/ml) where n=36 and (Myosin II KO; LPS (+); CCL21 200 ng/mL) where n=8. Samples in the WT group are normalized and compared to the control immature (WT; LPS (-)). Samples of the second group (MyoII KO) and third group (WT + CK666) are normalized and compared to corresponding samples in the first group (for example (MyoIIKO , LPS (+); CCL21 50 ng/mL (+)) is normalized and compared to (WT , LPS (+); CCL21 50 ng/mL (+)) and (WT+CK666 , LPS (+); CCL21 200 ng/mL (+)) is normalized and compared to (WT, LPS (+); CCL21 200 ng/mL (+))). c) Passage time. Box extends from the 25^{th} to 75^{th} percentiles, whiskers: Min to Max. n > 18 for each condition excepted for (Myosin II KO; LPS (+); CCL21 200 ng/mL) where n=1. CK666 was used a 50 μm. LPS for Lipopolysaccharide. CCL21 is a chemokine recognized by the chemokine receptor CCR7. Note that the passage time is not normalized. Comparison made in the same way than for b). $***$, $**$ and $*$ for Pvalue respectively $<$ 0.0001, $<$ 0.001, and $<$ 0.01. ns for non significant. Statistical test: Fisher Test for b), Mann-Whitney Test for c).

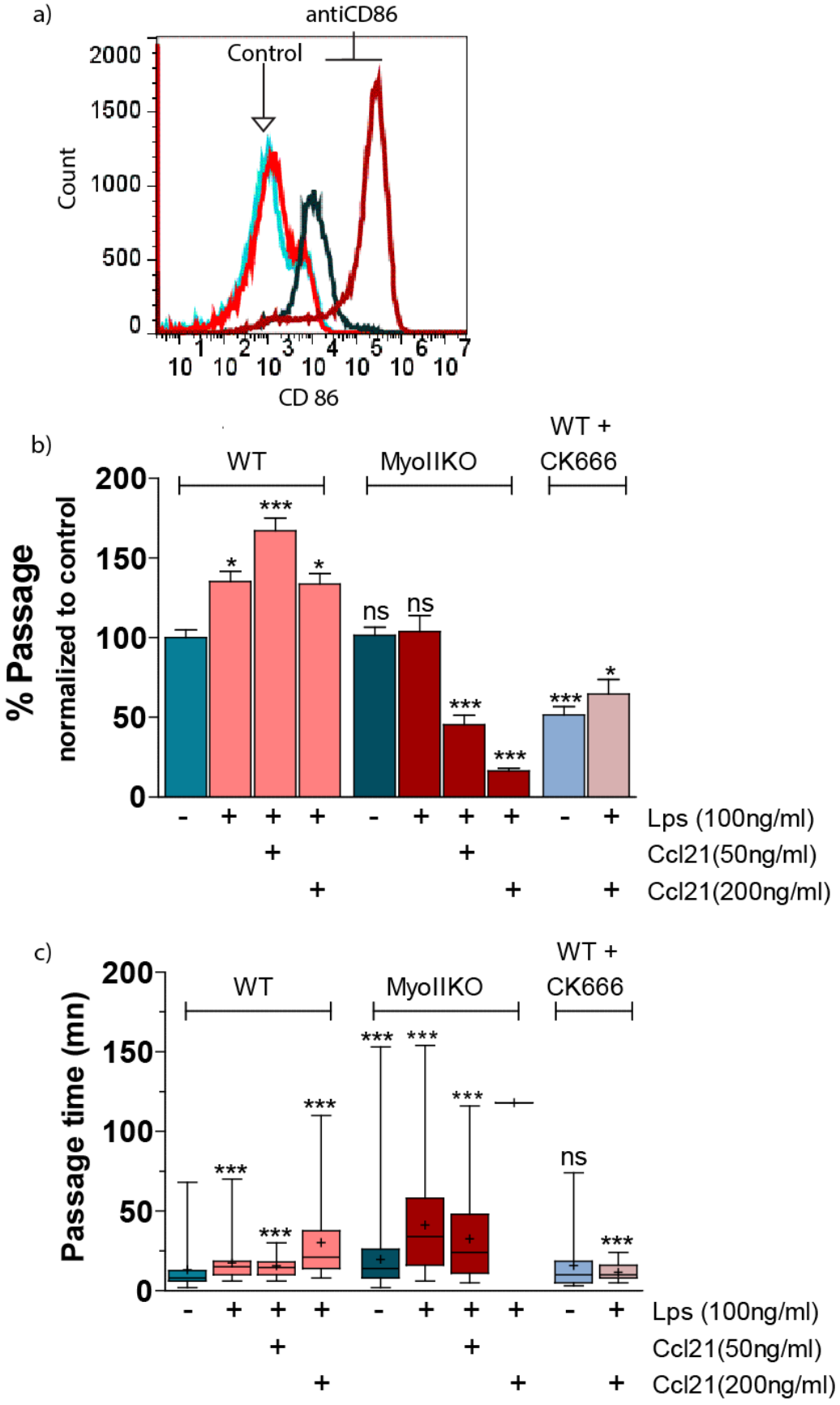
a)
antiCD86
Control
Count
CD 86
b)
WT
MyoIIKO
WT + CK666
% Passage
normalized to control
Lps (100ng/ml)
Ccl21(50ng/ml)
Ccl21(200ng/ml)
c)
Passage time (mn)
ns

Figure 7.9 *(facing page)*: **Fig S5 : Actin increases around the nucleus only above a given nuclear deformation.** a), b), c) Left- Mean actin intensity in constrictions normalized to the mean actin intensity in the whole cell as function of nuclear passage in constrictions. 0 represents nuclear entry in the constriction and 1 nuclear exit from the constriction. Right- Green curve : mean actin intensity around the nucleus normalized to the mean actin intensity in the whole cell. Red curve: nuclear circularity. Curves are plotted as function of the position of the nuclear center relatively to the constriction center. 0 indicates the center of the constriction, grey bars represent the constriction. Dark green/red : mean; light/red : standard error on the mean. a) Constrictions dimensions : Length = 20 μm; width = 1.5 μm; height = 3 μm. We can observe a 50% actin overshoot in constrictions during nuclear passage and a 30% increase of the actin concentration around the nucleus when it gets deform in the constriction (decrease in nuclear circularity). b) Constrictions dimensions : Length = 20 μm; width = 3 μm; height = 4 μm. The actin overshoot in constrictions during nuclear passage drop down to 20% and only 10% of actin increase is observed around the nucleus. c) Constrictions dimensions : Length = 20 μm; width = 5 μm; height = 5 μm. Only a faint actin overshoot is observed in constrictions during nuclear passage and no actin increase is observed around the nucleus during its deformation in constrictions.

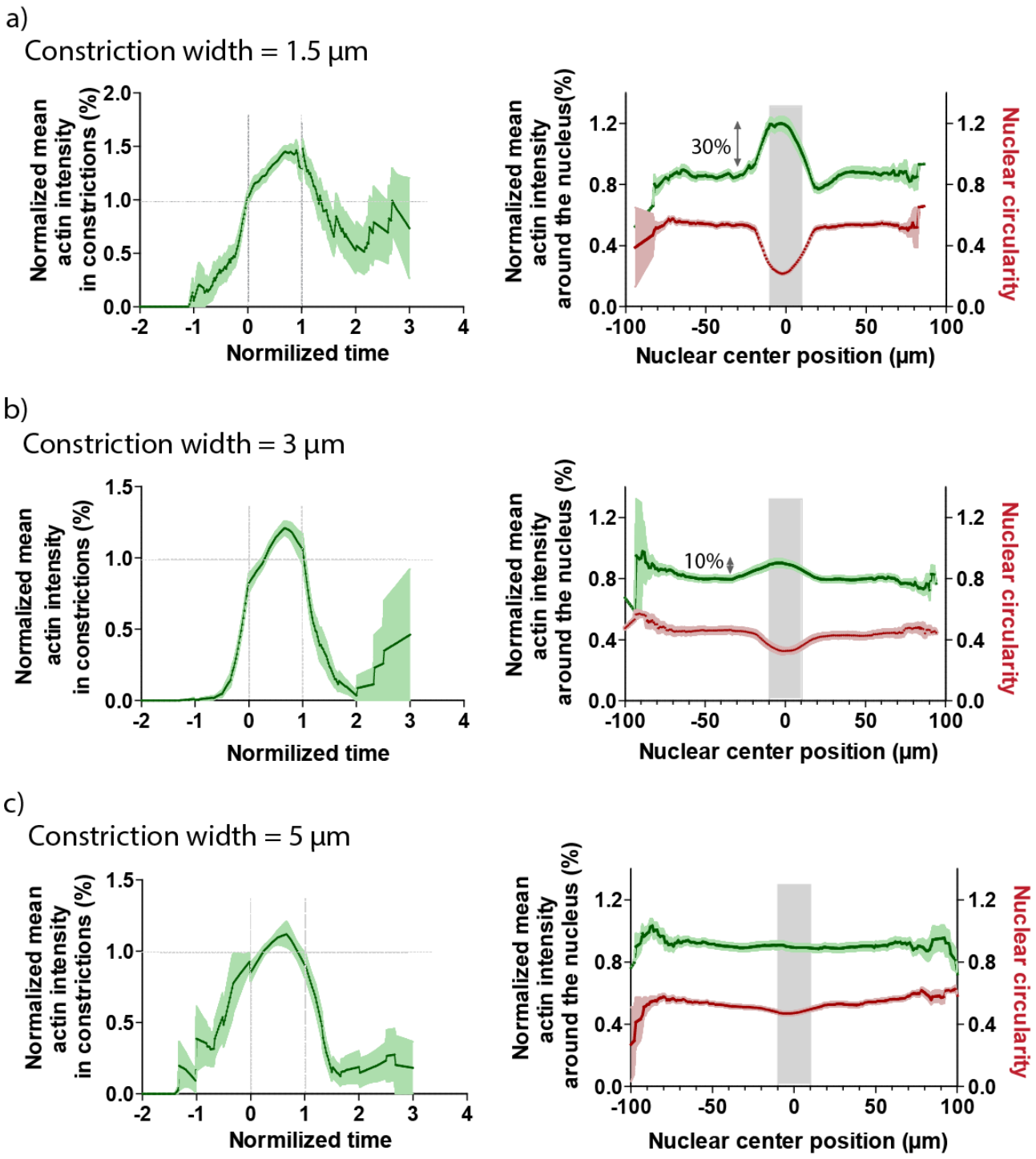
a)
Constriction width = 1.5 µm
Normalized mean actin intensity in constrictions (%)
Normilized time
Normalized mean actin intensity around the nucleus(%)
30%
Nuclear center position (µm)
Nuclear circularity
b)
Constriction width = 3 µm
Normalized mean actin intensity in constrictions (%)
Normilized time
Normalized mean actin intensity around the nucleus (%)
10%
Nuclear center position (µm)
Nuclear circularity
c)
Constriction width = 5 µm
Normalized mean actin intensity in constrictions (%)
Normilized time
Normalized mean actin intensity around the nucleus (%)
Nuclear center position (µm)
Nuclear circularity

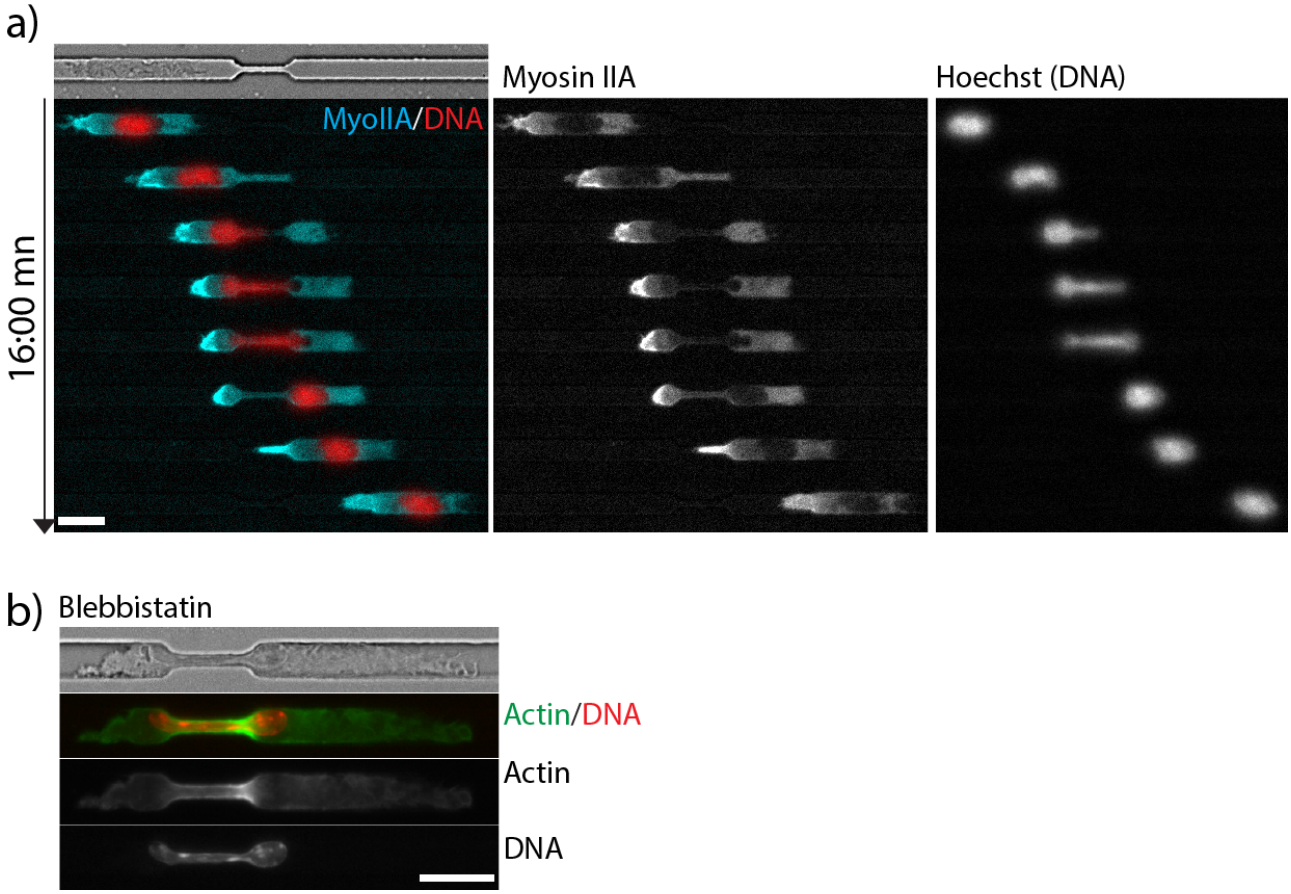

Figure 7.10: **Fig S6 : The actin meshwork formed around the nucleus is myosin II independent.** a) Myosin IIA-GFP immature dendrititc cell migrating through a 15 μm long, 2 μm wide and 3.5 μm high constriction. The transmittd light allows to visualize the position of the constriction. We can observe a high Myosin IIA accumulation at the cell back but no recruitment in the constriction upon nuclear deformation. b) Representative image of a LifeAct-GFP expressing iDC treated with 50 μM of blebbistatin in a 15 μm long, 2 μm wide and 3.5 μm high constriction. We can observe the long cell front characteristic of blebbistatin treated and Myosin IIA KO iDCs. The formation of actin meshwork can still be observed around the nucleus in the constriction. Scale bar 15 μm.

Figure 7.11 *(facing page)*: **Fig S7 : The actin meshwork formed around the nucleus is nucleated by Arp2/3.** a) Visualization of the Arp2/3 complex in constrictions with immunostaining. We can observe in representative cell 1 and 2 the colocalization of Arp3 and F-actin stained with phalloidin around the nucleus in constrictions. Control secondary antibody shows that the observed Arp2/3 localization is not an artifact induced by non specific binding of the secondary antibody. We can still observe the actin increase around the nucleus in the constriction in this cell indicating that the Arp3 signal seen in representative cell 1 and 2 is not due to a leak of the phalloidin channel in the Arp3 channel. Bottom: Zoom at the constriction or a better visualization of the Arp3/F-actin colocalization around the nucleus. Scale bar top : 15 μm; bottom : 5 μm. b) Percentage of cells which form the actin meshwork around their nuclei in constrictions as function of Arp2/3 inhibition (CK666 at 50 μm) and cell passage (y for yes and n for no). Error bars represent the standard error on the mean. $***$ for Pvalue < 0.0001. ns for non significant. c) Montage illustrating the behavior of Arp2/3 inhibited, lifeAct-GFP expressing iDCs passing a constriction. No actin increase is observed around the nucleus during its deformation through the constriction. d) Montage illustrating the behavior of Arp2/3 inhibited lifeAct-GFP expressing iDCs which fail passing a constriction. We can observe a transient and faint actin increase in the constriction correlating with nuclear entry in the constriction. Constrictions dimensions : Length = 15 μm; width = 2 μm; height = 3.5 μm. Scale bar c) and d) entire field: 30 μm; Zoom: 15 μm.

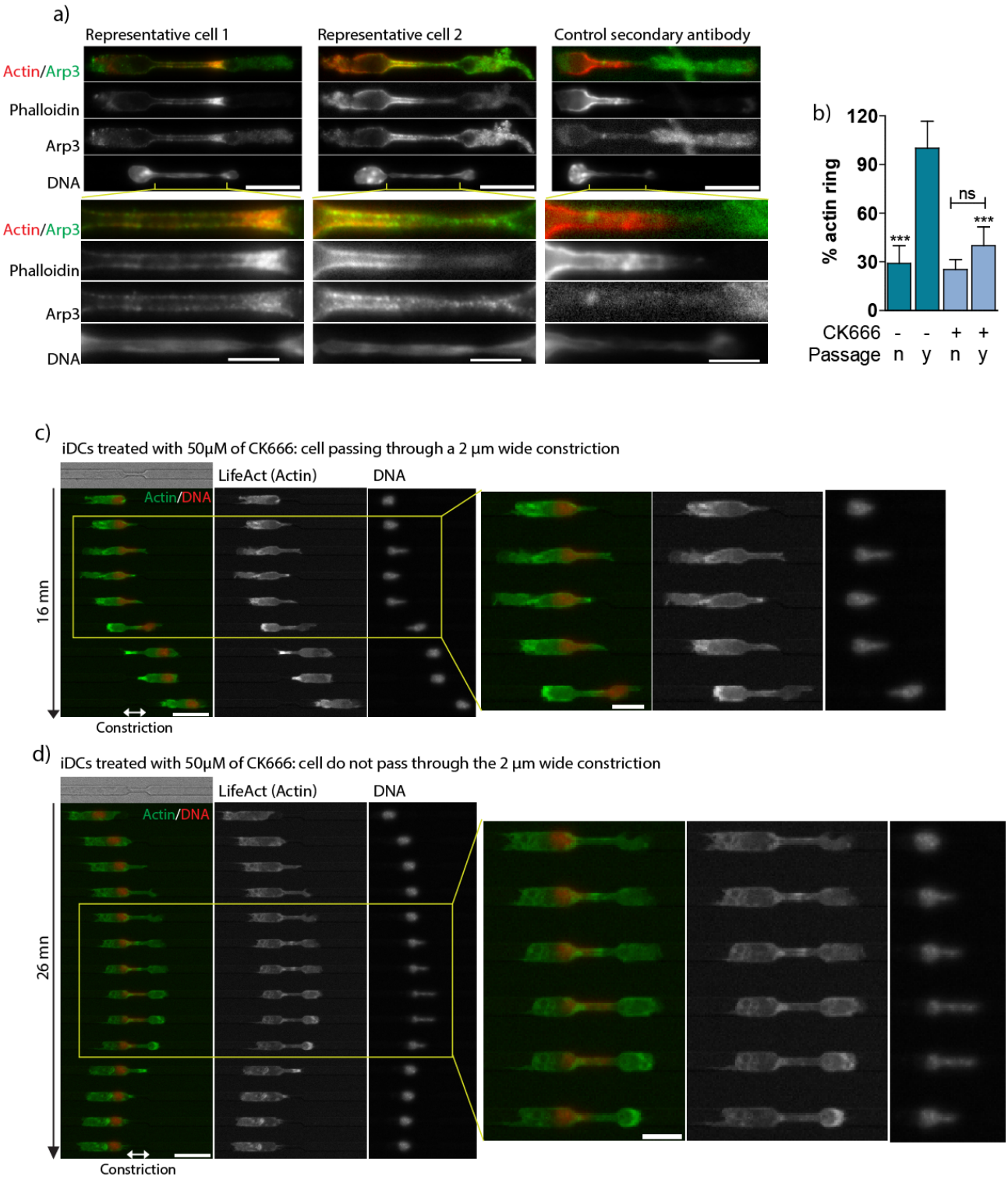
a)
Representative cell 1
Representative cell 2
Control secondary antibody
Actin/Arp3
Phalloidin
Arp3
DNA
b)
% actin ring
120
90
60
30
0
ns
***
***
CK666 - - + +
Passage n y n y
c)
iDCs treated with 50µM of CK666: cell passing through a 2 µm wide constriction
LifeAct (Actin)
DNA
Actin/DNA
16 mn
Constriction
d)
iDCs treated with 50µM of CK666: cell do not pass through the 2 µm wide constriction
LifeAct (Actin)
DNA
Actin/DNA
26 mn
Constriction

Figure 7.12 *(facing page)*: **Fig S8 : Microtubule depolymerization inhibits the actin meshwork formation and increases cell contractility.** a) Visualization of microtubule in constrictions with immunostaining. Left: Control iDC in a 5 μm long constriction showing microtubule bundles formation co-localizing with the actin meshwork around the nucleus. Right: Nocodazole treated iDC (0.5 μM) in a 15 μm long constriction. No more microtubule bundles is observed in the constriction. Some microtubule at the cell back have resisted to nocodazole treatment. A faint actin meshwork can be seen in the constriction. Most of the F-actin is localized at the cell rear. b) Montage representing a LifeAct-GFP expressing iDC treated with 10 μM of nocodazole to insure total microtubule depolymerization (not shown here). No more actin meshwork is observed around the nucleus during its deformation in the constriction. Most of the actin is localized at the cell rear. c) Montage representing a Myosin IIA-GFP expressing iDC treated with 10 μM of nocodazole. We can observe a preferential myosin II localization at the cell rear. d) Quantification of the myosin IIA-GFP ratio between the cell back and the whole cell in control as well as nocodazole treated iDC. We observe a far more myosin II localization at the cell back in nocodazole treated cell than in control iDCs. b) and c) suggest an increase in cell contractility upon microtubule depolymerization. n = 20 cells. $***$ for Pvalue $<$ 0.0001. Constrictions dimensions : Length = 15 μm or 5 μm (a)-Left); width = 2 μm; height = 3.5 μm. Scale bar a) 10 μm; b) and c) 15 μm.

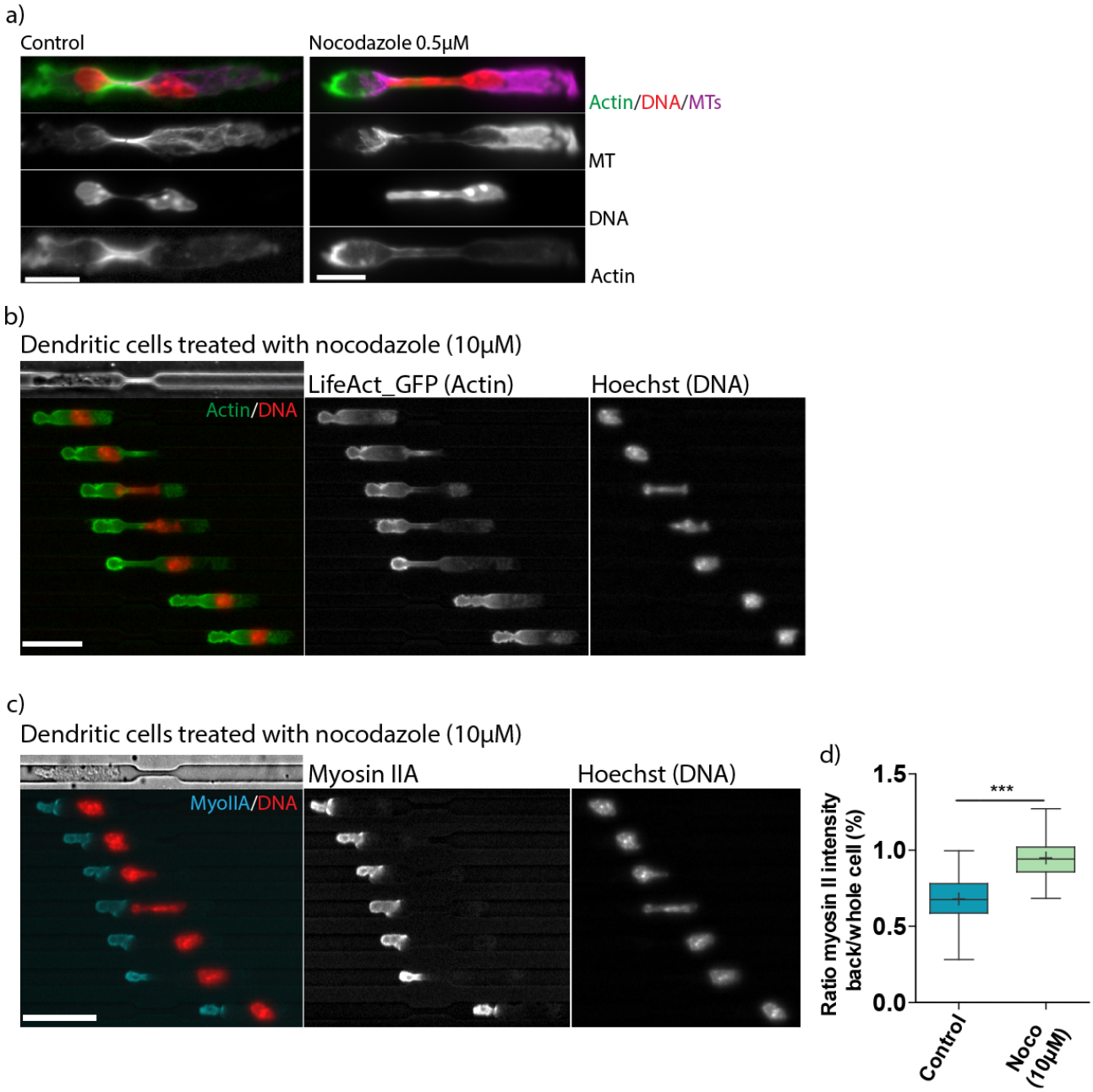
a)
Control
Nocodazole 0.5µM
Actin/DNA/MTs
MT
DNA
Actin
b)
Dendritic cells treated with nocodazole (10µM)
Actin/DNA
LifeAct_GFP (Actin)
Hoechst (DNA)
c)
Dendritic cells treated with nocodazole (10µM)
MyoIIA/DNA
Myosin IIA
Hoechst (DNA)
d)
Ratio myosin II intensity back/whole cell (%)
1.5
1.0
0.5
0.0
***
Control
Noco (10µM)

Figure 7.13 *(facing page)*: **Fig S9 : Neutrophils passage through 2.2 μm^2 constrictions requires Myosin II activity.** a) Montage illustrating HL60 derived neutrophils migration through a 20 μm long, 1 μm wide and 2.2 μm high constriction. The plasma membrane (blue) is stained with Lyn-emerald, the F-actin cytoskeleton (green) with Utrophin-mCherry and DNA with hoechst (red). We can observe a faint actin increase in the constriction during nuclear passage. Most of the actin is located at the cell back. Zoom on the nucleus (right) illustrates nuclear deformation in the 2.2 μm^2 constriction. Scale bar 30 μm and 15 μm for the zoomed image. b) Control HL60 derived neutrophils percentage of passage as function of the constrictions dimensions. We can observe that more than 60% of control cells cross the 2.2 μm^2 constrictions. c) Control HL60 derived neutrophils passage time as function of the constrictions dimensions. Most of the passage time is dedicated to nuclear passage in 1 x 2.2 μmxμm constrictions. In 2 x 3.5 μmxμm constrictions, the low passage time make difficult to discriminate between nuclear passage and cell passage. d) and e) Respectively cell percentage of passage and cell passage time as function of myosin II (Y27632 used at 10 μM inhibits ROCK which is a myosin II kinase) or Arp2/3 (CK666 used at 50 μM) inhibition. f) and g) Respectively cell percentage of passage and cell passage time as function of constrictions dimension in myosin II inhibited HL60 derived neutrophils. We can observe that myosin II inhibition does not affect HL60 derived neutrophils passage through constrictions larger than 2.2 μm^2. h) Mean actin intensity in constriction normalized by the mean actin intensity in the whole cell. No actin overshoot is observed in constrictions. b), c), f) and g) Unless when indicated with a line, comparison done against the 2 x 3.5 μmxμm constrictions. d) e) Comparison done against Ctrl for control. Except for a), quantification done with Actin-GFP expressing HL60 derived neutrophils in 5 μm long constrictions. $***$, $*$ for Pvalue respectively < 0.0001, < 0.01. ns for non significant.

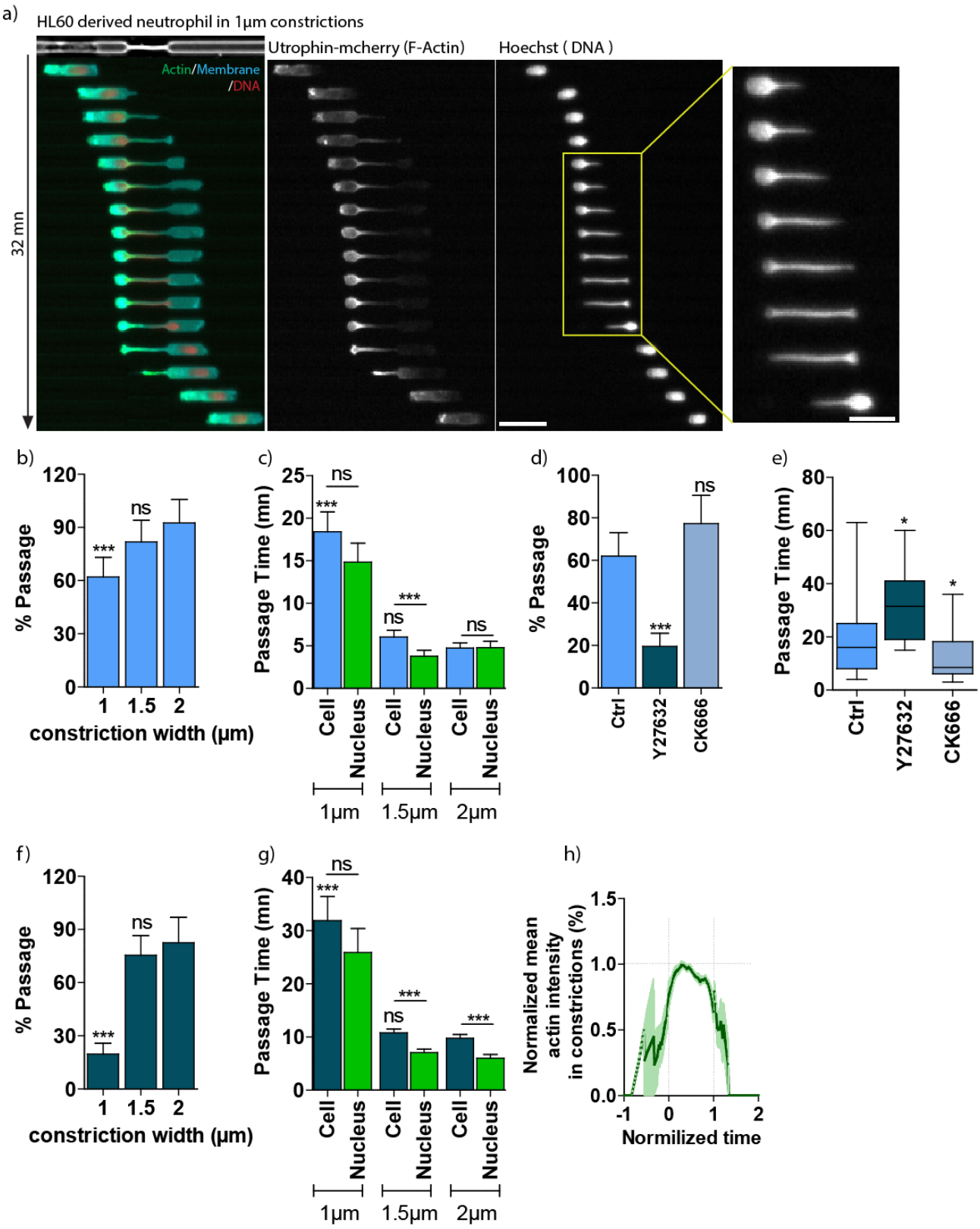
a)
HL60 derived neutrophil in 1µm constrictions
Utrophin-mcherry (F-Actin)
Hoechst (DNA)
Actin/Membrane
/DNA
32 mn
b)
% Passage
constriction width (µm)
c)
Passage Time (mn)
Cell
Nucleus
1µm
1.5µm
2µm
d)
% Passage
Ctrl
Y27632
CK666
e)
Passage Time (mn)
f)
% Passage
constriction width (µm)
g)
Passage Time (mn)
h)
Normalized mean actin intensity in constrictions (%)
Normilized time

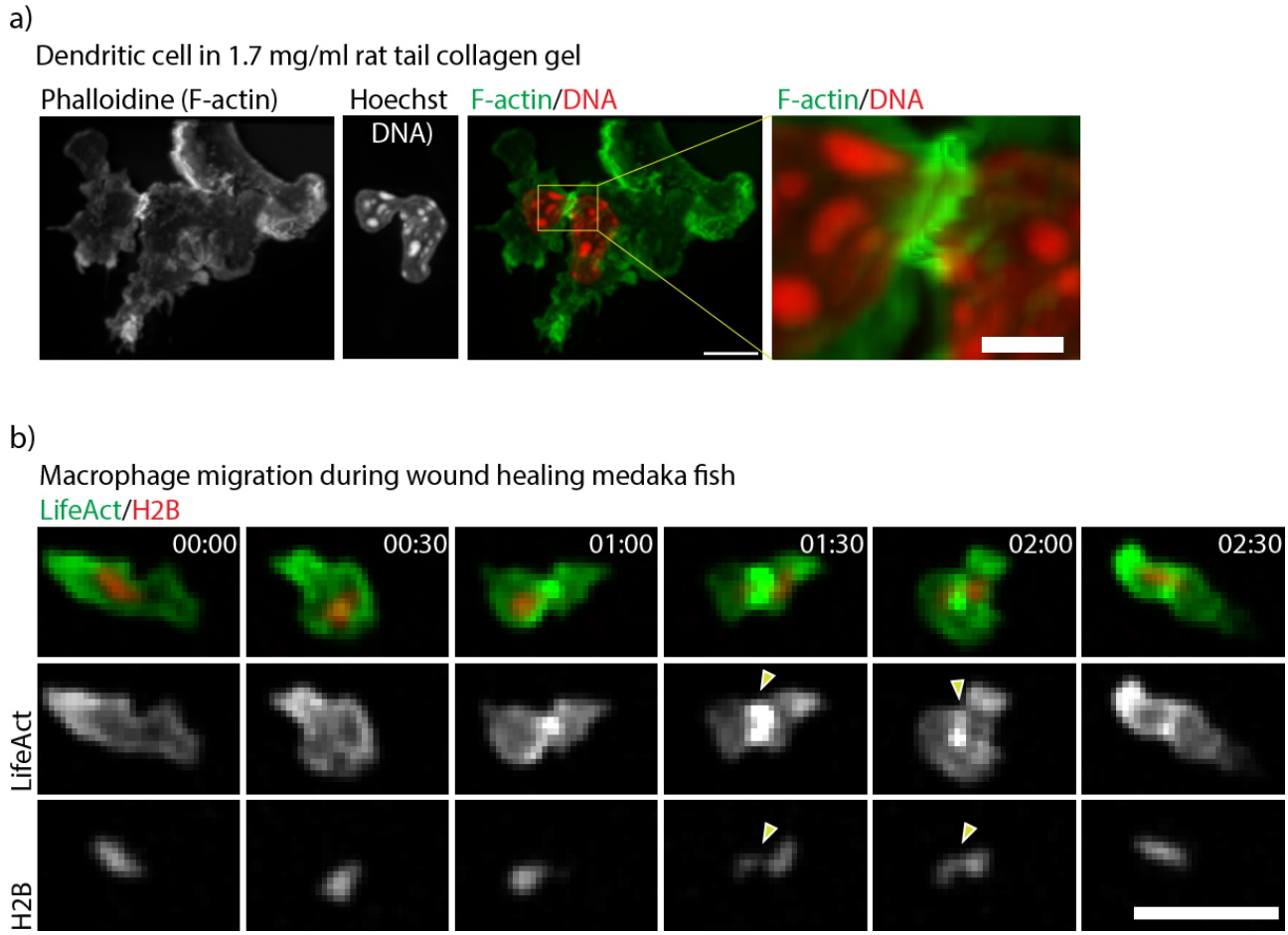

Figure 7.14: **Fig S10 : Dendritic cells in collagen gels as well as makada fish macrophages migrating *in vivo* assemble an actin meshwork around deformed nuclei.** a) Maximum intensity of a 3D stack of 24 images with 0.6 μm z-step (60X, binning 1). Illustration of actin meshwork assembly around the deformed nucleus of a LifeAct-GFP expressing iDC migrating in 2 mg/mL rat tail collagen. Zoom on the region of nuclear deformation shows the local actin assembly. Scale bar 10 μm; Zoom 3 μm. b) Montage illustrating actin meshwork assembly in makada fish macrophage migrating during *in vivo* wound healing. We can observe actin meshwork localization in regions of nuclear deformation. Time frames indicated in minutes:second. Yellow arrows indicate actin assembly and nuclear deformation. Scale bar Zoom 30 μm

7.2.2 Remarks

One of the first points that a reader can rise after consulting the above proposed manuscript is the presence of many "*Our unpublished data*", terms that I used for coming experiments and analysis which will be inserted to the actual manuscript before submission. In here, I will resume those experiments and analysis.

7.2.2.1 Analysis to perform

Some straight forward analysis still need to be performed before being incorporated in the manuscript. For instance, a better quantification of the nuclear squeezing phenotype in Arp2/3 inhibited cells will done. I will thus measure the length of nuclear protrusion in $7\mu m^2$ constrictions in control as well as Arp2/3 depleted cells. This measurement will be perform in cells which did not pass the constriction to determine the threshold of nuclear deformation above which Arp2/3 is required.
In order to better describe the observed nuclear lamina rupture, we need to quantify the percentage of nuclei with disassembled lamin A/C in constrictions and compare it to nuclei in straight channels (respectively called X% and Y% in the manuscript). This will allow us to provide a more quantitative description of the nuclear lamin A/C rupture in constrictions.
We also need to discriminate between lamin A/C rupture and lamina rupture. To do so, we will stain nuclei in constrictions with lamin A/C and Lamin B1 and quantify the distribution of both proteins in constrictions.

Another important quantification to perform is the number of dead cells in constrictions compared to straight channels for lamin A/C depleted as well as wild type cells. Even though, a decrease in cells survival rate can be observed in movies of lamin A/C depleted dendritic cells which have crosses constrictions, performing this quantification can strengthen the model we propose in this research article.

7.2.2.2 Experiments planed before submission

Two majors questions need to be answered before submission:

1. What is the effect of Myosin II inhibition in lamin A/C depleted dendritic cells. We therefore plan to inhibit myosin II activity using blebbistatin in lamin A/C depleted dendritic cells. If our hypothesis (lamin A/C null cell will require myosin II to inject their nuclei in constrictions), we expect lamin A/C depleted dendritic cells to reduce their rate as well as time of passage as already seen in HL60 derived neutrophils. This experiment was already performed once (Fig 4j,k) indicating that lamin A/C depleted cells have a lower rate of passage when myosin II is

inhibited. However, we suspect a lower effect of blebbistatin during this experiment as control cells did not exhibit the usual increase in time of passage upon myosin II inhibition.

2. Can Myosin II overactivated dendritic cells bypass the Arp2/3 based nuclear squeezing mechanism. The aim of this second question is to provide more clear evidences of the ability of myosin II overactivated dendritic cells to bypass the Arp2/3 based nuclear squeezing mechanism during their migration through 4-12 μm^2 constrictions. Indeed, we have already shown that nocodazole treated cells, which have previously been reported to have an overactivated level of myosin II, do not assemble actin around their nuclei in constrictions. We want to further assess if Arp2/3 is required in this configuration by measuring the ability of nocodazole treated Arp2/3 KD dendritic cells to passage though narrow constrictions. We will also inhibit myosin II in nocodazole treated cells then asses the existence of an actin assembly around the nucleus. This experiment will allow us to discriminate between a microtubule based actin assembly or a more general RhoA/Rac1 antagonistic effect. We will also inhibit both Arp2/3 and myosin II expecting to completely stop cells from crossing narrow constrictions. Calyculin A, a phosphatase inhibitor that increases the level of phosphorylated Myosin II regulatory Light Chain (MLC) [Gupton 2006] will also be used to have a more direct activation of myosin II.

We expect that answering those two questions will allow us to propose a more general mechanism of nuclear squeezing based on the balance between myosin II and Arp2/3. Cells with higher myosin II activity and/or softer nuclei will use a myosin II based nuclear squeezing probably due to a competition between branched and bundled actin network generation while cells with relatively stiff nuclei and/or a lower level of myosin II activity will use the Arp2/3 based nuclear squeezing mechanism.

7.2.2.3 More general remarks

The first critic one can have toward this work is that no direct proof of the role of the observed actin assembly in nuclear squeezing has been given. We indeed showed that Arp2/3 is required for nuclear squeezing and that nuclear deformation, lamin A/C disassembly and Arp2/3 local increase co-localized with the actin assembly. However, we did not show that punctually removing the actin assembly stops nuclear deformation through constrictions. We also did not show that the actin assembly apply forces on the nucleus.

Two main approaches are envisaged to tackle this problem.
The first on is based on a punctual disassembly of the actin network through local inhibition of Arp2/3 or actin polymerization. Microfluidic chambers have been designed to allow rapid fluid exchange in microchannels. Using those chambers we can inject a chemical at the cell front and measure the cell reaction to this perturbation. The aim will be to inhibit Arp2/3 at the front of cells which have engaged their nuclei in constrictions and have already assembled an actin meshwork around this organelle. If

the observed actin increase around the nucleus is really based on Arp2/3, we should observe the disassembly of this network. A subsequent nuclear turn back would be a direct proof of the requirement of the Arp2/3 generated actin meshwork around the nucleus for nuclear passage through narrow pores. The second approach we envisaged for understanding the role of the actin assembly around the nucleus is to measure the forces produced by this network. To do so, we envisaged to fill channels with deformable oil droplets and follow their deformation when a cell squeezes its nucleus in between two of those objects. Indeed, knowing the mechanical properties of those droplets, one can determine the field of forces from the deformation field. We then though that if actin still assemble around the nucleus when it passes in between two oil droplets, we can measure the local force exerted by the actin meshwork on the droplet and then obtain the force exerted on the nucleus.

The second critic toward this work is about its *in vivo* relevance. Indeed, we did not show that the proposed mechanism exist *in vivo*. Even though the observation of the actin increase around the nucleus in dendritic cells migrating in dense collagen gels as well as in ear explant and also in microphages migrating in makada fish suggest that this mechanism might be used more physiological conditions, direct proof would be great.

The main approach which has been envisaged is to inject Arp2/3 depleted dendritic cells in mouse foot pad and record their arrival to the lymph node. If this mechanism occurs *in vivo*, we expect to have a defect in dendritic cells arrival to the lymph node due to an impaired nuclear squeezing during cell migration. We could further measure a defect in T-cell activation in lymph nodes but this might be more difficult to asses due to the requirement of Arp2/3 in antigen uptake.

DISCUSSION

Chapter 8

Discussion

Contents

In this last part of this manuscript, I would like to discuss the model we propose for cell migration through narrow pores. I will start this discussion by summarizing the results obtained during my PhD. Those results will be discussed in order to explain the emergence of the proposed mechanism. When necessary, preliminary results will be used to orient the discussion. In the last part of this section, I will place our findings in a broader context and discuss the contributions of this work in the general understanding of cell migration under confinement.

8.1 An Arp2/3 based nuclear squeezing mechanism allows immature dendritic cells to pass through narrow gaps

The central finding of this PhD is that dendritic cells nuclear squeezing during migration under confinement relies on an Arp2/3 nucleated actin network. We propose a mechanism of nuclear passage through narrow pores based on this actin meshwork which by transiently breaking the lamina network lower nuclear surface tension and thus facilitates cell passage through constrictions. We further propose that this mechanism might allow cells such as dendritic cells to combine efficient migration for environment sampling with high survival rates.

To study cell migration through highly confining spaces, we designed a macrofabrication based setup which consists of microchannels with constrictions of known dimensions are placed. This setup allowed us to study the kinetics of nuclear deformation during cell migration.

We first showed that dendritic cells migration through narrow constrictions (smaller than 3x4 μm^2) is limited by nuclear deformation. Immature dendritic cells overcome this limit by nucleating a Hem1(Wave2)-Arp2/3 based actin meshwork around the nucleus above a given deformation of this organelle. This actin network formed around the nucleus does not contain myosin II and does not depend on the activity of this motor which is required for proper cellular migration. Interestingly, mature dendritic cells combine this Arp2/3 based mechanism to a myosin II based contraction to squeeze their nuclei through narrow constrictions.

We also showed that the Arp2/3 nucleated actin network assembled in immature dendritic cells co-localized with sites of lamin A/C breakage/disassembly in constrictions. Moreover, lamin A/C depleted dendritic cells as well as HL-60 derived neutrophils do not accumulate actin around their nuclei in narrow constrictions and their nuclear squeezing mechanism does not rely on Arp2/3 but on myosin II based contraction. Interestingly, this actin accumulation around the nucleus can be observed in macrophages migrating *in vivo*.

Taken together and placed in a context of the antagonistic role of nuclear stiffness in cell migration [Harada 2014], our results made us propose a model of nuclear squeezing in cells such as immature dendritic cells and macrophages which need to migrate fast and efficiently while surviving long

enough to accomplish their function. Dendritic cells lamin A/C expression level is higher than the one of the short living but highly motile neutrophils but much lower that the one of long lived and slowly migrating fibroblast. We then propose that cells which have similar lamin A/C expresssion level combined to similar motility will use the Arp2/3 based actin network formed around the nucleus to transiently break the lamin A/C thus lowering nuclear surface tension. This transient nuclear softening will allow the nucleus to passage through the narrow pores. The subsequent lamin A/C repolymarization at the exit of constrictions allows cells to survive to the next constriction.
We proposed that this mechanism allows both efficient migration through highly confining spaces while preserving cell survival.

Those findings have very important implications. At first, they show that nuclear squeezing is a process which can be uncorrelated from cell migration. It thus imply that specific machineries will be required to deform the nucleus during migration. Second, the local and transient actin increase around the nucleus suggest that the cell is able to sense local variation of nuclear shape. It further suggest that local mechanotransduction processes associated or not to the nucleus are involved in cell migration under confinement. This finding rises the question of what triggers the actin ring formation. Is it a geometrical effect? Which type of network is formed? Is this actin increase specific to the nucelus? Third, the requirement of Arp2/3 for the formation of this actin meshwork reveals the existence of a nucleus/confinement associated Arp2/3 activation. This raises the question of which NPF activates Arp2/3. Fourth, the observed lamin A/C breakage/disassembly implies either that forces are locally exerted on the nucleus or proteins involved in the lamina disassembly are mechanosensitive. Are those forces generated by the observed actin meshwork? If so, how could this actin meshwork generate enough forces? what are the effect of such forces on the cells' and nuclear fate? Fifth, the dependance of mature dendritic cells nuclear squeezing on myosin II implies that maturation induces drastic changes in dendritic cells cytoskeleton and/or nuclear mechanics. This raises the question of what trigger such a switch. In the following, I will discussed these five points.

8.2 The nucleus as a limiting factor for dendritic cells migration

The first finding of this work is that nuclear deformation imposes a physical limitation to dendritic cells migration. Using our constrictions based set up, we could identify 12 μm^2 as the constriction cross section below which the nucleus slows down dendritic cells migration. If this idea of the nucleus limiting cell migration emerged years ago, it is only recently that it has been proven in cancer cells and in lamin null cells such as polymorphonuclear neutrophils [Wolf 2013]. Our study is in our knowledge the first one showing this process in dendritic cells. Moreover, the setup used in this work allows to study nuclear squeezing independently of other parametes affecting cell migration. In the following, I will discuss the choice of the setup before discussing in more details this physical limitation imposed

by the nucleus.

8.2.1 A microchannel based set up

Until now, all studies on nuclear deformation during cell migration were performed in collagen gels or transwells. If those setups allow to obtain a global mechanism of cell migration in complex 3D environments, it does not permit to dissect the steps leading to forward movement in such environments. For a forward movement to occur, the cell must first polarize, a protrusion stabilize and the cell body translocate. In collagen gels as well as in transwells, those 3 steps cannot be uncorrelated. Indeed, the readout obtained with such system is a result of global cell migration (cell polarization and translocation). As nuclear deformation occurs during cell body translocation, specifically studying this process required a new set up.
The originality of the microchannel based setup reside in its ability to uncorrelate cell polarization from forward movement. Indeed, once the cell enters a channel, it defines a front-back polarity which will be kept for a given time (persistence time). Because turning or branching is abrogated in channels the persistence time is maximized and cells will encounter a first constriction before reaching their persistence time. To illustrate this, let's consider an immature dendritic cell in a 7x7 μm^2 straight channel in which the cell, not the nucleus is confined. The mean measured frequency of changing direction of those cells is 0.045 per minute meaning that such cell will change direction once every 22 minutes. If we consider the mean cell velocity which is 5 μm per minute, it gives a mean persistence length of 110 μm. The first constriction in the channel being placed at 100 μm, cells changing direction in constrictions must not be due to an intrinsic lack of persistence. For instance when measuring the non passing time which measures the time spent in a constriction by a non passing cell, we found that this parameter increased with a decreasing constriction width. This result, combined with the increase in the frequency of changing direction (Fig 8.1) observed in smaller constriction strongly suggests that cell non passage in constriction is due to the inability of the cell to deform itself through the constriction. Interestingly, we found that the change in direction occured when the nucleus reached the constriction which make us propose that the nuclear deformation is the limiting factor to cell migration through narrow pores. By comparing cell behavior in channels with and without constrictions, we can sort out specific mechanisms occurring during nuclear deformation.

8.2.2 The nucleus limits migration below 12 μm^2 constrictions

We showed here that dendritic cells forward movement is abrogated in 1 μm wide constrictions, is slowed down in 1.5 and 2 μm wide constrictions and reached its maximum in 3 μm wide constrictions (Figure 1 and S1 in results). We could observe that movement abrogation and slow down is due to the nucleus as those events correlate with the arrival of the nucleus at the constriction.

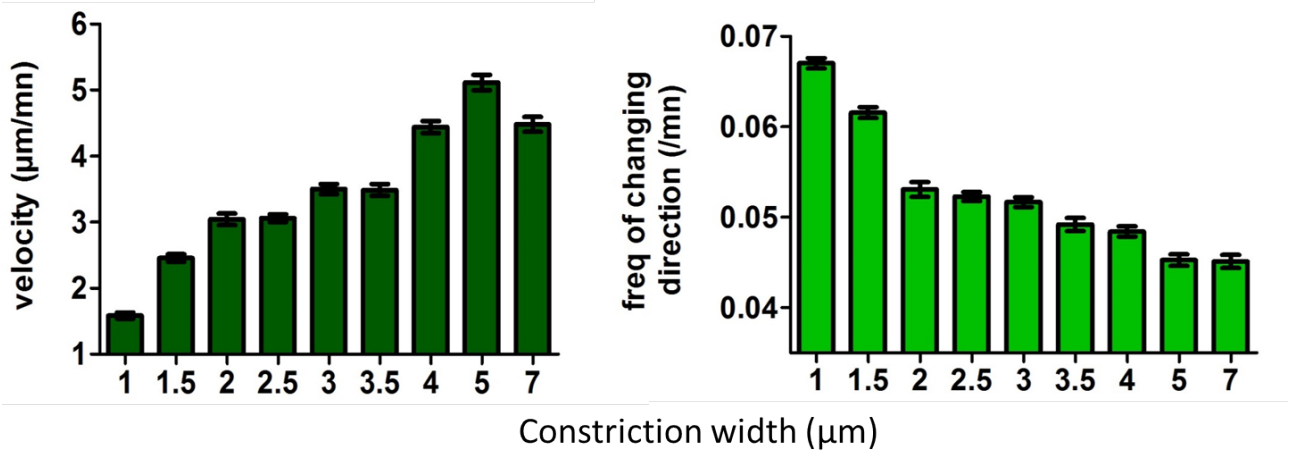

Figure 8.1: Impact of constrictions in cell migration. Cells migrate though 7x5 μm^2 channels containing 5 constrictions . Left: mean cell velocity. Right: frequency of changing directions.

A recent report has proposed that movement abrogation in dense collagen gels occurs when the mean gel's pore cross section is around 10% of the nuclear cross section [Wolf 2013]. For dendritic cells, arrest occurs at constrictions cross section of 1x2.2 μm^2 which according to the 10% 'rule', gives a mean nuclear diameter of 22 μm^2. Such theoretical nuclear diameter is much smaller than the estimated 75 μm^2 in dendritic cells suggesting that this 10% 'rule' might not be applied to dendritic cells (our unpublished data. Estimation done from the shape of the nucleus in a $5x5\mu m^2$ and 20 μm long constriction (see figure 7.5) which allows us to approximate the nuclear volume by a 5 μm sphere given a cross section of $\pi * 5^2 = 75\mu m^2$). Two hypotheses can be proposed to explain this arrest at 10%. The first one already advanced by Wolf *et al.* put forward that this limit is set by the nuclear shape (mononucleated versus polylobulated) [Wolf 2013]. The second hypothesis we considered is based on nuclear mechanical properties. A signaling based hypothesis would be a curvature sensing mechanism which would prevent nuclear deformation above a given limit. Such mechanism would prevent cells from destroying their nuclei during migration. The main argument for the first hypothesis is that even if neutrophils and T-blast cells are both depleted of lamin A/C, neutrophils which have polylobulated nuclei migrate through denser collagen gels than T-blast cells [Wolf 2013]. However, a recent study from Lammerding's lab have shown that neutrophils passage through small pores is controlled not by its polylobulated nucleus but by its nuclear stiffness [Rowat 2013]. Moreover, Wolf *et al.* did not discuss the possibility that T-blast cells might be less contractile than neutrophils. As the proposed mechanism of nuclear squeezing, in that paper, was based on myosin II contraction, higher contractility could explain the ability of neutrophils to migrate through denser collagen gels. A relative difference of nucleoplasm mechanical property was also not discussed in this paper.
The second hypothesis which we privileged could also explain why decreasing lamin A/C increases cells migration efficiency in 3D environments ([Harada 2014], our data).

However, even if lamin A/C KD dendritic cells are more able to pass 1x2.2 μm^2 constrictions, their rate of passage in such constrictions stays very low compared to HL60 derived neutrophils. We envisaged that this differentce might be due to a difference in nucleoplasm mechanical properties or in global cell ability to generate forces. Two types of experiments could be carried out to descriminate between a nuclear mechanics or cell mechanics based arrest. For instance, we can imagine an experiment where the chromatin would be decondensed using Trichostatin A (TSA) ([Pagliara 2014]) in lamin A/C KD dendritic cells and cell rate of passage through 1x2.2 μm^2 constrictions could be measured. This would allow us to asses the role of nucleaoplasm mechanics in cell passage through 1x2.2 μm^2 constrictions. On the other hand, we could increase cell contractility using for example nocodazole or calyculin A then asses lamin A/C KD ability to squeeze through 1x2.2 μm^2 constrictions.

We also defined a range of constrictions sizes where the nucleus slows dendritic cells migration. Indeed, in constriction cross sections of 1.5x3 and 2x3.5 μm^2, more than 50% of the passage time is due to nuclear passage through constrictions. Such pore sizes have been observed in vivo. For instance, mouse connective tissues such as the one in the back dermis and mammary gland contain pore sizes ranging from below 1 to 20 μm of diameter [Wolf 2009]. Conclusions drawn with our constrictions might thus be extended to in vivo systems. However, the high rigidity of the PDMS (MPa) might limit the extension to *in vivo* environments which have been reported to be much softer [Engler 2006], depending on the local crosslinking of the matrix.

8.3 Mechanisms of perinuclear actin meshwork formation

One of the first striking finding of this work is the formation of this actin meshwork around dendritic cells nuclei during migration through constrictions. Interestingly, this actin assembly is observed only above a given nuclear deformation. What induces this actin increase is one of the most important question that I tried to answer all along this PhD. To date, four hypothesis were envisaged: a retrograde flow induced actin accumulation, an adhesion induced F-actin increase, a microtubules induced F-actin recruitment and a local Arp2/3 based actin nucleation. Those hypotheses will be discussed in the following sections.

8.3.1 A retrograde flow based actin increase

We hypothesized that the actin increase around the nucleus might be due to the retrograde flow generated at the cell front. Actin filaments, polymerized at the cell front would arrive at the nucleus which would act as a clog in the constriction thus limiting further actin flow toward the cell rear. Actin filaments, would then accumulate around the nucleus as long as the nucleus is in the constriction and would disappear when the nucleus exit the constriction. A dense actin network polymerized at the

front of neutrophils migrating in 5x5μmxμm channels has been shown to undergo retrograde flow [Wilson 2013]. Even though such actin retrograde flow has been shown to vanish at the nucleus, we can still imagine that the nuclear confinement can allow the retrograde flow to survive longer. In order to asses the role of actin retrograde flow in the actin meshwork formation, direct measurement of this flow are needed. We could for example perform photoactivation experiments on a region at the cell front and follow this region over time. We would expect the bleached region to accumulate at the constriction. If our hypothesis is true, changing the velocity of the actin retrograde flow should change the intensity of this actin increase. For instance, faster retrograde flow would lead to higher actin accumulation while slower retrograde flow should inhibit the actin ring formation.
However, some of our results do not support this hypothesis. For instance, myosin II inhibition, which has been shown to slow down actin retrograde flow [Burnette 2011] does not affect the actin meshwork formation. Moreover, microtubule depolymerization with nocodazole which has been shown to over-activate myosin II [Krendel 2002] thus increase the retrograde flow inhibit actin meshwork formation. Even though we cannot exclude other motors based actin retrograde flow, this hypothesis does not seems to be the most consistent with our actual data.

8.3.2 Adhesion based actin formation

The second hypothesis we explored to explain the actin ring formation is an adhesion based F-actin recruitment. We indeed hypothesized that focal complexes at the constriction could strengthen under force then recruit actin filaments. Such mechanism would be reminiscent of the F-actin recruitment upon clutch engagement in mesenchemally migrating cells [Chan 2008].
Our hypothesis being based on the existence of focal complexes at the constriction, we tested it by inhibiting focal adhesion formation in constrictions using PLL-PEG. Actin ring was still observed in cells migrating in PLL-PEG coated constrictions suggesting that focal complexes are not required for the actin ring formation.
However, we cannot exclude that the PLL-PEG coating was not effective in constrictions. For instance, no retrograde flow measurement was performed to verify the previously reported increase in actin retrograde flow upon adhesion inhibition in dendritic cells [Renkawitz 2009]. Nevertheless, unpublished data from Emmanuel Terriac showed that focal adhesions do not form inside channels. For instance, vinculin stained dendritic cells plated on glass coverslip show nice focal complexes while the signal of the staining is rather diffuse inside channels. This result suggests that dendritic cells do not form adhesion complexes in channels or in constrictions and therefore, weaken the hypothesis of an adhesion based perinuclear actin meshwork formation.
To further test this hypothesis, we could coat our microchannels with Pluronic F-127 which efficiency in inhibiting focal adhesion formation has already been proven [Bergert 2012]. Performing immunostaining of some focal adhesion proteins such as talin and paxillin would allow us to asses the existence

of focal adhesion in constrictions. A more direct approach would be to inhibit Talin in dendritic cells ans assess cell ability to assemble the perinuclear actin network.

8.3.3 Microtubules based F-actin recruitment

We also hypothesized that the actin accumulation in constrictions might be due to microtubules dynamics.

Microtubule form bundles in constrictions as revealed by immunostaining (See 7.12a) and those filaments have been shown to regulate the actin cytoskeleton ([Preciado López 2014], [Waterman-Storer 1999a]). For instance, microtubule growth has been proposed to activate the small GTPase Rac1 [Waterman-Storer 1999b]. Moreover, the actin elongator formin which is also proposed to be an actin nucleator has been shown to promote the alignment of the microtubule and actin cytoskeleton [Ishizaki 2001]. We though that the dynamics of the perinuclear microtubule network in constrictions could promote actin polymerization/rearrangement around the nucleus. This would be done through either local Rac 1 activation or a formins mediated actin network alignment to the microtubule bundles in constrictions.

Our main argument supporting this hypothesis is that nocodazole treated cells do not assemble an actin meshwork around the nucleus (see 7.12a, b) suggesting that microtubule are involved in actin ring formation. However, microtubule depolymerization has been shown to activate myosin II contractility [Krendel 2002]. We thus can not exclude that the observed disappearance of the actin ring is due to actin recruitment at the cell rear which would then prevents the perinuclear actin meshwork formation. Formins inhibitions with the general formins FH2 domain inhibitor (SMIFH2) does not inhibit the actin meshwork assembly (Our data) suggesting that the actin network formation is independent of a formin based F-actin alignment with the microtubule network.

To test this hypothesis, we envisaged to remove the perinuclear microtubule network and assess the formation of the perinuclear actin meshwork in constrictions. Remodlin, a recently designed chemical has been proposed to detach microtubules from the nucleus [Larrieu 2014]. Using this drug could allow us to specifically study the relationship between the presence of a perinuclear microtubule network and the actin ring assembly. Some of our preliminary results suggest than dendritic cells still assemble the perinuclear actin meshwork in constrictions when treated with remodlin. Further experiments are required to asses the depolymerization of the perinuclear microtubule network upon remodlin treatment in dendritic cells.

A more direct experiment to asses the role of microtubule in the actin meshwork formation would be to silence the Rho-GEF, GEF-H1 in dendritic cells thus prevent RhoA activation upon microtubule depolymerization and asses the actin meshwork formation. Indeed, if the observed dis-appearance of the actin meshwork observed in nocodazole treated cells is due to Rac1 inhibition induced by GEF-H1 mediated RhoA activation ([Sander 1999], [Krendel 2002]), depleting this RhoA-GEF would rescue

the perinuclear actin meshwork formation upon nocodazole treatment.

8.3.4 Arp2/3 based nucleation

The last hypothesis we tested to explain the formation of this perinuclear actin meshwork in constrictions is a local polymerization mechanism. We indeed hypothesized that local activation of actin nucleators such as Arp2/3 could promote actin polymerization around the nucleus. Our main argument supporting this hypothesis is that Arp2/3 inhibition or knock down abrogates the perinuclear actin meshwork formation. Moreover, we observed an Arp2/3 increase at the site of the actin accumulation around the nucleus in constrictions.
This hypothesis involves a local recruitment and activation of Arp2/3 at the constriction during nuclear passage. Two possibilities have been envisaged to explain the local Arp2/3 activation: Arp2/3 recruitment from the nucleus and confinement driven Arp2/3 activation by nucleation promoting factors (NPFs).

8.3.4.1 Arp2/3 recruitment at the nucleus

The first hypothesis we envisaged is a local recruitment of Arp2/3 at/on the nucleus. Our main argument supporting this hypothesis is that all components of the Arp2/3 complex have been reported to exist in the nucleus [Gieni 2009]. Moreover, Arp2/3 can be activated inside the nucleus. It has indeed be shown that viruses such as the Baculovirus Autographa Californica Multiple Nucleopolyhedrovirus promote Arp2/3 accumulation in the nucleus then its activation via a viral homologue of WASP [Goley 2006]. This nuclear Arp2/3 based actin polymerization was proposed to be necessary for viral proliferation [Goley 2006]. N-WASP, an Arp2/3 activator has also been reported in the nucleus [Gieni 2009]. Moreover, the small GTPase Rac1 possess a Nuclear Localization Signal (NLS) and its GTP exchange factor SmgGDS is a nucleocytoplasmic shuttling protein. Rac1 which can activate N-WASP as well as the Wave complex can thus shuttle through the nucleus [Gieni 2009]. We can therefore imagine a model where upon nuclear deformation, Rac1 would shuttle inside the nucleus leading to Arp2/3 activation then actin polymarization. If this model is true, the actin ring must form inside the nucleus as it has already been proposed during Starfish Oocytes nuclear envelope breakdown prior cell division [Mori 2014]. However, immunostaining of the nuclear pore complex shows that the actin ring forms out of the nuclear envelope (Data from Matthew Raab). Thus, the Arp2/3 accumulation which co-localizes with the actin ring would also be expected to be localized out of the nucleus. Proper immunostaining experiments would be necessary to determine the relative position of the nuclear membrane and the Arp2/3 complex during nuclear squeezing.
We can also imagine a model where upon nuclear deformation, Rac1 or even Arp2/3 would exit from the nucleus leading to a local actin polymerization. If Rac1 is small enough (<26 kDa) to shuttle through the nuclear pores by diffusion [Gieni 2009], Arp2/3 exit from the nucleus might

require nuclear envelope breakage. In mouse dendritic cells, we observed lamin A/C breakage but not nuclear envelope rupture. However, data from Matthew Raab indicate that the nuclear envelope of Hela cells as well as human dendritic cells rupture during there passage through constrictions suggesting that mouse dendritic cells might also rupture their nuclear envelope when squeezing through narrow pores. A way to test this hypothesis would be to express fluorescent NLS in dendritic cells and follow the dynamic of this protein during nuclear squeezing. If our hypothesis is true, we will observe a fluorescence leakage in the cytosol. However, knowing the difficulties we had in expressing proteins in dendritic cells, the best option might be to perform immunostaining of the nuclear envelope and see if some rupture points are observed.

8.3.4.2 NPFs confinement induced Arp2/3 activation

The second hypothesis we envisaged for explaining a local Arp2/3 recruitment at the constriction during nuclear passage is purely based on mechanics. We indeed though that local increase of the shear stress between the nuclear membrane and the plasma membrane could induce Arp2/3 recruitment after NPFs activation. This hypothesis implies that any object large and stiff enough to be confined in a constriction would induce the actin ring formation. Our main argument supporting this hypothesis is that actin accumulates around oil droplets internalized by dendritic cells (preliminary results, see figure 8.2). In addition, lamin KD dendritic cells which have softer nuclei do not form the actin ring. Moreover, unpublished data from Dyche Mullins' and Dan Fletcher's Labs show that confining the Wave complex with micropatterns combined to an AFM tip induces a local increase of the actin gel branching density as filaments elongation is impair by the confinement. This increase in branching density leads to the formation of a dense actin network and to Arp2/3 concentration. This *in vitro* study can be reported to our *in cellulo* system where nuclear passage by confining NPFs such as the wave complex would induce the perinuclear actin network densification. This is supported by the fact that the wave complex seems to be required for nuclear squeezing through constrictions. To further test our hypothesis more experiments would be required to localize the Wave complex in constrictions. We will also need to show that the Wave complex is involve in the actin ring formation. For this purpose, we could record the actin dynamics in constrictions in Wave depleted dendritic cells. We could for example deplete Hem1, the hematopoietic lineage specific Wave complex component then asses the actin accumulation around the nucleus in cosntrictions. More oil droplets experiments are also required to confirm that droplets deformation induces local actin accumulation in constrictions. We will also need to show that Arp2/3 inhibition impairs droplets passage through constrictions.

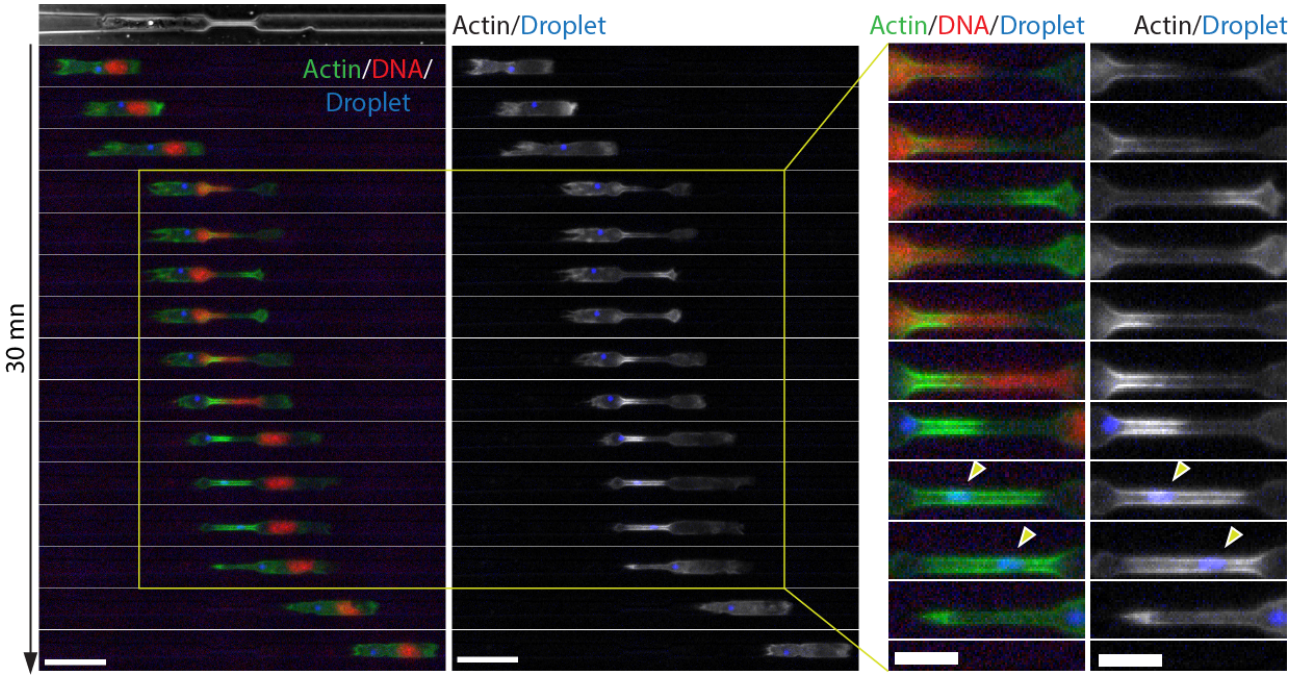

Figure 8.2: Oil droplet passage through a constriction. Montage of an immature dendritic cell passage through a constriction. The cell has internalized an oil droplet (in blue) which is used to mimic the nucleus. We can observe the expected actin increase during nuclear passage. Interestingly, the actin remains in the constriction after nuclear exit. Zooming in the constriction (Left) allows to observe an actin increase around the droplet as indicated by the white arrow on the images. Scale bar 30 μm and 10 μm for the zoomed images

8.3.5 Conclusion

In conclusion, our data put forward the hypothesis of a local Arp2/3 activation based actin formation. We propose that the local shear increase induced by nuclear confinement promotes Arp2/3 activation either through microtubules based Rac1 activation or geometrical confinement induced Wave complex activation. Even though many more evidences are required to prove this hypothesis, our data seem to exclude the possibility of a nuclear specific actin meshwork formation but rather put forward a general mechanical pathway used by cells to deform rigid objects through narrow pores.

8.4 Role of the actin accumulation in nuclear passage through constrictions

In this section, I would like to discuss how the actin ring could mediate nuclear passage though narrow pores. If we have provided some evidences about the mechanism of actin ring formation, many experiments are still required to understand the role of the actin ring in nuclear squeezing. However, based on our results, we envisaged some hypotheses which could explain the perinuclear actin meshwork based nuclear squeezing.

8.4.1 Breaking the Lamina network to allow nuclear passage through narrow pores

Our first hypothesis is that the actin ring applies compressive forces on the nucleus which, by releasing the nuclear surface tension through lamina breakage, allows cells to pass through constrictions. Our main arguments supporting this hypothesis is the requirement for Arp2/3 for the perinuclear actin meshwork formation and cell passage through constrictions as well as the observed lamina disassembly in constrictions at sites of actin increase.

As said in the section 3.1.1.2 of the introduction, stress-stiffening is an intrinsic property of crosslinked actin networks. Having such property implies that a crosslinked actin network, subjected to a mechanical load can generates opposing forces as big as the applied forces. Emerging evidences suggest that confined actin networks, under compression can generate opposing forces even higher than the applied one ([Greene 2009], unpublished data from Dyche Mullins' Lab). For instance, Greene *et al.* have shown that an actin network made of short, unconnected filaments confined between mica plates can generate repulsive forces higher than the initial compressive forces [Greene 2009]. They proposed a model in which under compression, actin filaments will bend storing enthalpic energy which when released after decompression leads to higher repulsive forces.

We expect the actin network constituting the actin ring to be a dense crosslinked actin network as it is nucleated by Arp2/3. One can thus argue that the higher repulsive forces observed by Greene *et al.*

will not be seen in the perinuclear actin network which response to mechanical load might be dominated by the entropic elasticity (discussed in 3.1.1.2). Interestingly, unpublished data from Dyche Mullins' lab suggest that a Wave2-Arp2/3 nucleated actin network confined by an AFM tip, can exert repulsive forces higher than the initially applied force.
Thus the perinuclear actin network could generate compressive forces. The lamin A/C network is viewed as an elastic solid which has been reported to stretch and even peel off under shear stress ([Rowat 2005], [Pajerowski 2007], [Swift 2013]). We can thus imagine that the compressive force generated by the actin ring applied on the nucleus could lead to the breakage of the lamin A/C network. Once the lamin A/C network is broken, the nucleoplasm which has been proposed to set the rheological properties of the nucleus [Pajerowski 2007] would flow in the constriction.
Several experiments can be carried out to further test this hypothesis. The first one would be an immunostaining experiment to see if dendritic cells still show a broken lamin A/C network during nuclear squeezing after microtubules depolymerisation (which inhibit the actin accumulation around the nucleus). We could, in addition, perform super resolution microscopy or electron microscopy to first asses the type of network constituting the perinuclear actin accumulation and second, show the broken state of the lamin A/C in constrictions. Moreover, performing live imaging of the A-type lamin and the actin network would allow us to determine the dynamic of the lamina disassembly during actin assembly in constrictions. A more direct experiment would be to use optogenetic to locally activate actin polymerization around the nucleus in cells such as Hela cell which do not pass small (2 μm wide) constrictions and see if it induces lamina breakage and cell passage through constriction.

8.4.2 Phosphorilation based nuclear passage through constrictions

The second hypothesis we envisaged to explain the actin ring based nuclear squeezing is a phosphorilation based lamin A/C disassembly. Lamin A/C contains 61 known phosphorilation sites which are targeted by various kinases including mitotic cyclin-dependent kinase CDK1, the protein kinase C family (PKC) [Simon 2013] and the serine/threonine kinase Akt/PKB [Bertacchini 2013]. Phosphorilation based lamin A/C disassembly has been well studied during mitosis and recent evidences showed the importance of phosphorilation in lamin A/C regulation during interphase [Kochin 2014]. For instance, the S^{22} residue whose phosphorilation by CDK1 is crucial for laminA/C disassembly during mitosis [Heald 1990], can also be phosphorilated in interphase cells leading to an accumulation of lamin A/C in the nucleoplasm compared to the lamina region [Kochin 2014].
We thus though that the actin accumulation could, either by retrograde transport or local increase of compression on the nucleus, drive the recruitment of kinases such as PKC which through phosphorilation of the laminA/C network would lead to its disassembly.
Tension dependent lamin A/C phosphorilation has already been proposed by Swift *et al.*. However, in their recent publication [Swift 2013], Swift *et al.* showed a decrease of the lamin A/C phosphori-

lation at the S^{390} residue when cells are subjected to increasing tension. Moreover, phosphorilation at the S^{390} residue has recently been proposed to promote lamin A/C recruitment at the lamina network [Kochin 2014]. In addition, lamin A/C recruitment at sites of force application on isolated nuclei has recently been reported [Guilluy 2014]. Those results, thus suggest that tension would rather drive lamin A/C recruitment at the nuclear lamina. However, we cannot exclude that the lamin A/C recruitment at sites of force application might be a second step [Le Berre 2012]. We can indeed imagine that tension can first trigger phosphorilation of other residues such as the S^{22} leading to the disassembly of the lamin A/C network. A second phosphorilation cycle would trigger lamin A/C recruitment back to the lamina region. To test this hypothesis, the phosphorilation state of lamin A/C must be determined. We can, for example, stain for the phosporilation state of the S^{22} and the S^{390} in cells crossing constriction. If our hypothesis is true, we would expect a high S^{22} phosphorilation in constrictions, co-localizing with the actin ring. High laminA/C phosphorilation at the S^{390} residue would be expected at the exit of the constriction where the lamin A/C network is already reformed. Another sets of experiments to asses the role of lamin A/C phosphorilation in nuclear squeezing would be to inhibit some kinases such as the PKC and asses cell passage through constrictions. However, lots of controls would be required to asses the specificity of those kinases inhibition.

8.4.3 How are forces transmitted to the nucleus

The two hypothesis discussed above imply that forces are transmitted from the perinuclear actin meshwork to the nucleus. It is then interesting to discuss how could this actin meshwork transmit forces to the nucleus.

Forces can be transmitted to the nucleus in two ways: either through a direct/adhesion-like interaction or an indirect/adhesion-independant (for example pushing) interaction. It is now believed that direct cytoskeleton-nucleus force transmission is mediated by the LINC complex (see 4.4.2). For instance, the two main actin structures which have been proposed to be involve in nuclear mechanotransduction (Actin Cap and TAN lines) require the LINC complex.

However, in confining spaces, adhesion-like force transmission might not be required. For instance, the actin accumulation being continuously in contact with the nucleus, adhesion-independant interaction would be sufficient for force transmission. In line with this reasoning, the LINC complex disruption through Sun2 knock out does not affect cell passage through narrow pores. Moreover, dendritic cells which have internalized droplets assemble actin ring around it and are able to squeeze the droplet through narrow constrictions. However, further experiments are necessary to confirm this adhesion-independent and friction-based forces transmission hypothesis. Indeed, emerging evidences suggest that Sun 1 and Sun 2 might be redundant [Guilluy 2014]. Moreover, we cannot exclude the possibility of Sun 1 upregulation upon Sun 2 downregulation. Even though the droplet passage through pores seems to exclude a linc complex based force transmission, one direct experiment to

asses the role of the LINC complex in nuclear squeezing would be to knock down Sun 1 in Sun 2 KO dendritic cells and assess their ability to squeeze through constrictions. We could also express the dominant negative KASH domain which prevents Sun-Nesprins interaction [Luxton 2010] and asses cell ability to pass through narrow constrictions. We then propose a model of force transmission to the nucleus reminiscent of the cell-substrate force transmission mechanism during dendritic cells migration in microchannels [Hawkins 2009]. We advance that the actin network, polymerized at the interface between the nuclear and the cell membrane will stiffen because of the confinement leading to compressive forces which will be applied to the nucleus via non specific interaction (pushing forces). To further test this hypothesis a detailed description of the network forming the perinuclear actin meshwork in constrictions as well as its interaction with the nucleus and the plasma membrane is requires.

8.4.4 Conclusion on the role of the perinuclear actin meshwork in constrictions

I proposed that the perinuclear actin meshwork mediates nuclear squeezing during dendritic cells migration by locally pressing on the nucleus, eventually softening it. This transient nuclear softening can be due either to mechanically rupture of the lamin A/C or to lamin A/C phosphorylation. Further experiments are required to confirm this hypothesis. For instance, we cannot exclude the involvement of other motor proteins such as the type I Myosins or Myosin 18a which could generate higher forces on the nucleus.

8.5 Role of myosin II in nuclear squeezing

One of the most intriguing observation I made during my PhD was the apparent difference between immature and mature dendrictic cells in their nuclear squeezing mechanism. Indeed, while immature dendritic cells nuclear squeezing requires only Arp2/3 but not myosin II, mature dendritic cells nuclear squeezing requires on both myosin II and Arp2/3. Even though much more experiments are requires to understand this difference, some results, obtained during this PhD already allow us to advance some hypotheses which could explain the myosin II and Arp2/3 based nuclear squeezing in mature dendritic cells.

The first hypothesis we put forward is mainly based on mechanics. We indeed proposed that upon maturation, dendritic cells nucleus softening could lead to the requirement for myosin II to generate contractile forces for pushing the nucleus through narrow constrictions. Our main argument supporting this hypothesis is that lamin A/C depleted immature dendritic cells (in 7 μm^2 constrictions, see Fig 7.4) as well as HL-60 derived neutrophils (in 2.2 μm^2 constrictions, see Fig 7.13) seem to require myosin II for their passage through constrictions. However, Lamin A/C depleted dendritic

cells as well as HL60 derived neutrophils, contrary to mature dendritic cells, do not require Arp2/3 for nuclear squeezing and do not exhibit an actin overshoot around their nuclei during passage through small pores. Even though further experiments are needed to compare the dynamic of actin increase in immature versus mature dendritic cells, we can already wonder if mature dendritic cells do not exhibit softer nuclei than the immature ones. A key experiment to asses the validity of our hypothesis is to perform immunostaining of the lamin A/C network in immature and mature dendritic cells and quantify the relative thickness of this network. If our hypothesis is true, we would measure a thinner lamin A/C network in mature dendritic cells which can then justify the still observed actin overshoot but at the same time the requirement of myosin II as the actin meshwork will not be enough to mediate nuclear passage through constrictions.

The second hypothesis we advanced to explain the difference between immature and mature dendritic cells is based on an inhibition of Arp2/3 upon maturation. Some preliminary data from Pablo Vargas suggest that Arpin (a newly discovered Arp2/3 inbhibitor [Dang 2013]) is induced at early stages of dendritic cells activation with a maximum of expression 4 hours after activation. Moreover, scanning electron microscopy carried out on mature and immature dendritic cells plated on micropatterns allowed Pablo to propose that immature dendritic cells tend to form more sheet-lamelipod like protrusions than mature dendritic cells which form more aligned actin networks. Taken together, those data put forward that Arp2/3 is more active in immature than in mature dendritic cells. We can then imagine that mature dendritic cells generate more bundled actin filaments which are more prompt to be used by myosin II to generate contraction leading to an overall higher cellular contractility compared to immature dendritic cells. This argumentation thus imply that cells with high enough contractility will switch to a myosin II based nuclear squeezing. Interestingly, nocodazole treated dendritic cells which exhibit higher contractility do not form the actin ring. They thus provide the right platform for testing this hypothesis of a (RhoA-Rac1) contractility-Arp2/3 inhibition for nuclear squeezing. Preliminary data indicate that nocodazole treatment of Myosin IIA KO cells does not completely impair cell passage through constriction. We speculate that in this condition, the actin ring should re-assemble around the nucleus. Further experiments, involving the measurement of actin dynamic in dendritic cells treated with nocodazole as well as Myosin II inhibitor, will be required to move forward.

In conclusion, the observed requirement for myosin II in mature dendritic cell nuclear squeezing is an intriguing/interesting and exiting observation which drives many question. We here exposed two hypothesis to explain this observation. The first one, based on mechanics, proposed a nuclear softening of mature dendritic cells while the second one, based on signaling proposed an Arp2/3 downregulation after dendritic cells maturation to explain the sudden myosin II requirement for nuclear squeezing. It is more likely that a mixture of mechanics and signaling will explain this

phenomenon. For instance, we cannot exclude that the observed disappearance of the actin ring in nocodazole treated cells is due to lamin A/C disassembly. We can then imagine that maturation induce both lamin A/C disassembly and increase in contractility to drive faster migration. It is interesting to keep in mind that lamin A/C up-regulation observed during mesenchymal stem cells differentiation correlates with increased cellular contractility [Swift 2013]. It is also interesting to point out that cells with softer nuclei (Lamin A/C KD and HL-60 derived neutrophils in 2.2 μm^2 constrictions) require myosin II to squeeze through constrictions while immature dendritic cells which are expected to have stiffer nuclei rely on Arp2/3.

8.6 Squeezing the nucleus through a small pore

8.6.1 Our model of nuclear squeezing during cell migration

In this section, I would like to propose a general model of nuclear squeezing through narrow pores. A scheme of this model is presented in figure 8.3.

The first assumption of our model is that a cell in a microchannel has a given front-back polarity and a given persistence which allows it to spontaneously enter the constriction. As said earlier, the persistence length of dendritic cells in 7x5 μm^2 channels is 110 μm. We can then assume that for such distance, the cell will keep moving forward unless if a force opposite to its direction of migration is applied. In the following, I will refer to this property as "homeostasis inertia". In channels, the cell is characterized by an energy state E_{chnl} which drives cell forward movement and is powered by the front-back pressure gradient in microchannels [Hawkins 2009]. This pressure gradient can be fueled by the acto-myosin contraction, membrane tension or as it has recently been proposed, osmotic pressure [Stroka 2014]. We have measured an increase in the frequency of changing direction when the width of the constriction is decreased (see figure 8.1). We then assume that the constriction is imposing an energy barrier E_{const} to the migrating cell. We think that E_{const} will be set by the constriction deformability as well as the cell deformability. The constriction being made of PDMS, a rigid elastomer, its deformability is nearly zero. In the first approach, we can assume that a cell is able to cross a constriction if it can provide a force leading to an energy E_{cell} higher than E_{const}. This can be achieved by increasing the front-back pressure gradient. Here we propose an alternative mechanism in which the cell will lower the energy barrier by changing its deformability. This can be achieved by breaking the lamina network.

We then advance that in cells such as dendritic cells, two types of forces are required to squeeze through constrictions. The first one F_1, oriented in the direction of locomotion is powered by a front-back pressure gradient which can be fueled by various sources including acto-myosin contraction, cortex-plasma membrane adhesion and osmotic pressure. F_1 allows to maintain the cell thus the nucleus inside the constriction. Indeed, without this force, the geometry of the actin network around the

nucleus, reminiscent of the actin comet tail geometry (see paragraph 3.1.1.2.4.3 of the introduction) , would rather induce nuclear expulsion from the constriction. Note that this type of force, has already been proposed during 3D migration [Wolf 2013]. We propose here that in cells such as dendritic cells which express Lamin A/C and still need to migrate fast, a second type of force F_2 is required. F_2, perpendicular to the direction of migration is applied on the nucleus leading to the lamina network disassembly thus releasing the nuclear surface tension. We further proposed that this force is powered by actin polymerization driven by the shear stress induced by nuclear confinement. Once the lamina network is broken, the nucleoplasm which is considered as a viscous material will flow inside the constriction unless if the constriction diameter is below 10% of the nuclear diameter (see section 8.2). As already proposed by Le Berre *et al.* a new lamin A/C network will repolymerize once the DNA will recontact the inner nuclear membrane [Le Berre 2012]. Once the nucleus has passed the constriction, the previously described pressure gradient will drive rear retraction. We propose that this transient nuclear softening through lamin A/C disassembly will allow cells such as dendritic cells to squeeze their nuclei in highly confining spaces without inducing many damages to their nuclei.

8.6.2 Limits of this model

The above proposed model is the one which for us, fits the best to our results as well as the actual literature. However, alternative models could be proposed. For instance, one can observe that the decrease in the percentage of passage in Arp2/3 inhibited cells does not exceed 50%. This raises the question of which mechanism is used by those 50% of cells. We could argue that Arp2/3 inhibition might not be total. However, more realistic explanations would be based on alternative mechanisms. One hypothesis we envisaged is that those cells have an intrinsically higher contractility which is then used for their nuclear squeezing as it has already been seen in nocodazole treated cells. We can also

Figure 8.3 *(facing page)*: **Proposed model for nuclear squeezing through narrow pores.1)** Cell in channel at the energy state $E_{cell} = E_{chnnl}$. Black arrows illustrate the direction of the internal pressure gradient. Green arrow represent the direction of the actin retrograde flow. **2)** Cell entering a constriction. E_{chnnl} allows first nuclear protrusion which confinement induces a local increase of the shear stress between the plasma membrane and the nuclear membrane.**2-i)**) The high shear stress leads to the confinement of Arp2/3 activators such as Wave 2 thus to local Arp2/3 activation. **2-ii)**) The positive feedback loop between confinement and Wave2 activation generates the dense actin meshwork. **2-iii)**) The confined dendritic network produce compressive forces (purple arrows) applied on the nucleus. The nuclear membrane reacts as a fluid and flow while the viscoelastic lamina network rupture. The green and black arrows indicate the velocity profile of the fluid crossing this constrictions region. **3)** Lamin A/C rupture releases the nuclear surface tension allowing the nucleoplasm which is a viscous liquid at this scale to flow in the constriction. The lamina network will repolymerize at the constriction exit.**4)** The internal pressure gradient drives back retraction. **5)** The cell exit the constriction and goes back to its initial state.

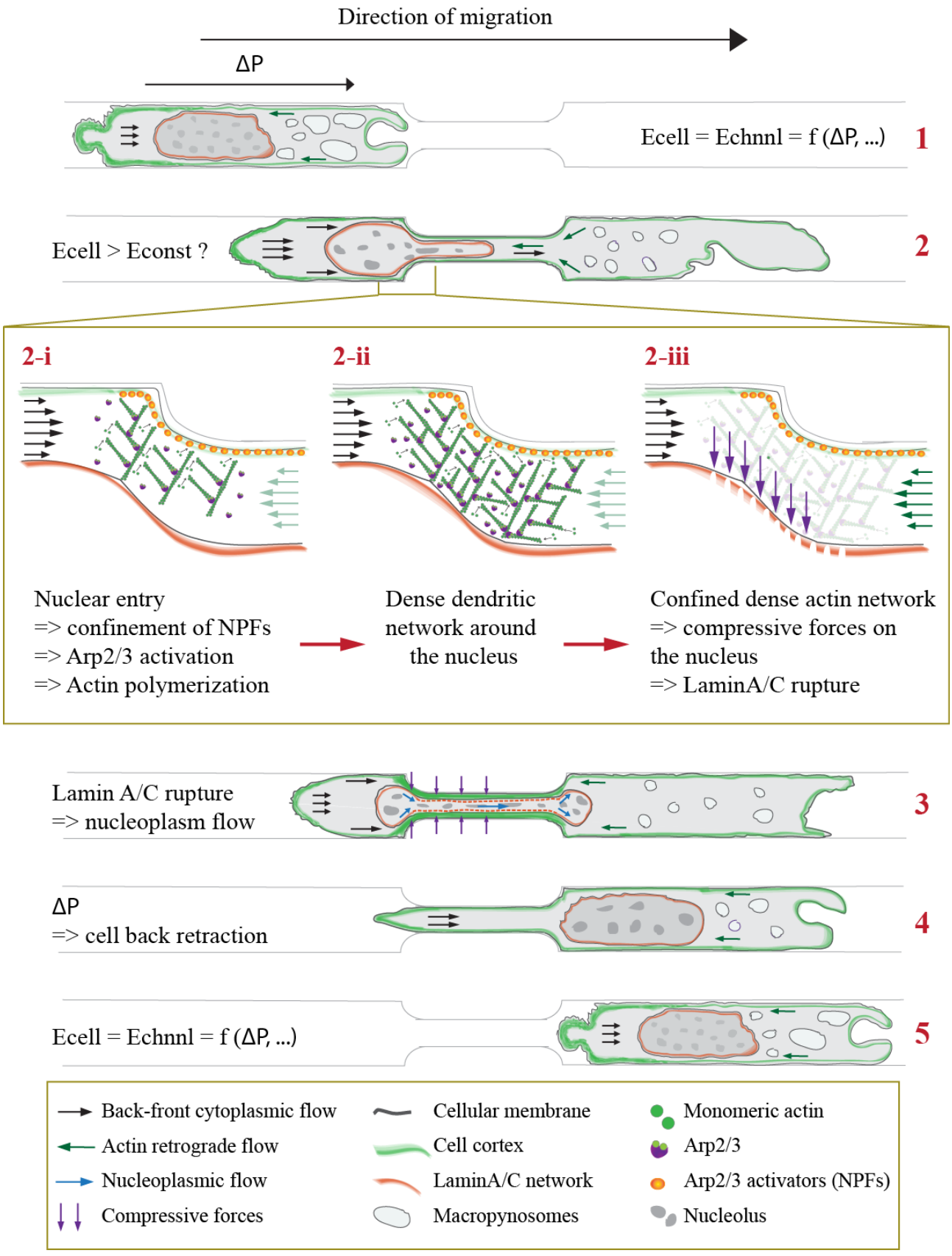
Direction of migration
ΔP
Ecell = Echnnl = f (ΔP, ...)
1
Ecell > Econst ?
2
2-i
2-ii
2-iii
Nuclear entry
=> confinement of NPFs
=> Arp2/3 activation
=> Actin polymerization
Dense dendritic network around the nucleus
Confined dense actin network
=> compressive forces on the nucleus
=> LaminA/C rupture
Lamin A/C rupture
=> nucleoplasm flow
3
ΔP
=> cell back retraction
4
Ecell = Echnnl = f (ΔP, ...)
5
Back-front cytoplasmic flow
Actin retrograde flow
Nucleoplasmic flow
Compressive forces
Cellular membrane
Cell cortex
LaminA/C network
Macropynosomes
Monomeric actin
Arp2/3
Arp2/3 activators (NPFs)
Nucleolus

think that those cells have a lower expression of Lamin A/C and would thus use only Myosin II to squeeze through pores. Our main argument supporting this hypothesis is that cells which cross constrictions when Arp2/3 is inhibited do not form the actin ring. To further test this hypothesis, we plan to inhibit both Arp2/3 and myosin II and quantify the passage through narrow pores. If this hypothesis is true, we expect to completely inhibit cell passage through constrictions.
The second hypothesis we envisaged is an actin polymerization independent nuclear squeezing. We could indeed imagine that the recently described osmotic engine model [Stroka 2014] could be used to apply high pressure on the nucleus from the back leading to its passage. It is for instance interesting to observe that the nucleus clogging the constriction, front-back diffusion might be further decreased leading to an even higher front-back osmotic pressure than the one which is measured in channels. However, one limitation of this pressure mechanism might be that it does not produce any local deformation which might be require to engage the nucleus in the constriction. Nevertheless, quantifying nuclear shape during in Arp2/3 inhibited cells might give a hint for the osmotic engine hypothesis. We would indeed expect, if the hypothesis is true, to measure a variation of the nuclear deformation field at the interface between the channel and the constriction.

8.7 Perspectives

8.7.1 An intriguing Arp2/3 based nuclear squeezing

An important role of the nucleus in cell migration has been proposed more than a decade ago with the discovery of the mechanosensitive property of the nucleus [Maniotis 1997]. However, direct proof of such hypothesis arose only during the last 2 years. Indeed, in 2013, Wolf *et al* proposed that the nuclear shape limits 3D cell migration in cancer cells as well as Lamin A/C null immune cells [Wolf 2013], and Harada *et al* advanced that nuclear lamina stiffness limits cancer cells 3D migration [Harada 2014]. With my PhD work, we also propose that the nucleus limits immune cells, particularly dendritic cells, migration under confinement.
Those works rose the question of the existence of a specific mechanism required for nuclear deformation during 3D migration. Until now, all evidences were pointing toward a myosin II based nuclear squeezing ([Lämmermann 2008], [Wolf 2013]). The originality of my PhD work resides in the discovery and description of a new Arp2/3 based actin network assembled around the nucleus during nuclear passage through narrow pores. The requirement of this actin accumulation around the nucleus for the passage of lamin A/C expressing cells but not lamin A/C null cells together with the proposed role of lamin A/C stiffness in cell survival during 3D migration allowed us to propose a new mechanism of nuclear deformation during migration under confinement. We then proposed that cells whose nuclei are stiffer than the neutrophils ones (higher lamin A/C expression level) but still softer than the fibroblast ones (lower lamin A/C expression level) will use the Arp2/3 based

nuclear squeezing to locally decrease the energy barrier set by the narrow pore. We further advanced that this mechanism will allow cells such as dendritic cells to combine efficient migration to high cell survival. As introduced in section 2.3, dendritic cells are antigen presenting cells which bridge the gap between the innate and the adaptive immune response. At steady state, they patrol the body looking for antigen which once found will lead to their activation followed by their migration towards the afferent lymph node. Their function thus require high cell locomotion under confinement as well as long term survival. Indeed, contrary to neutrophils which die at sites of infection, dendritic cells need to survive after antigen internalization and processing to activate T-cells.
We here proposed that Arp2/3 based nuclear squeezing will allow them to combine efficient antigen sampling and presentation. Macrophages are another cell type which might use the same mechanism. They are reported as long lived cells which reside and migrate in dense tissue for antigen detection. In line with this hypothesis, we have observed an actin accumulation around the nucleus of macrophages migrating *in vivo*.
In summary, this PhD work allowed us to propose a new and unexpected mechanism for nuclear squeezing during 3D migration. This mechanism based on Arp2/3 might be used *in vivo* by cells such as dendritic cells and macrophages whose function relies on efficient migration in highly confining spaces as well as long term survival for an adequate immune response.

I mainly discussed the contribution of the Lamin A/C network in cell passage though narrow pores. However, recent reports proposed a role for lamin B in nuclear mechanical properties ([Harada 2014],[Ferrera 2014]). It would thus be interesting to address the question of the role of B type lamins in cell migration under confinement. Emerin are also emerging as proteins which regulation can affect nuclear mechanics through their regulation of the Lamin A/C network. Addressing the role of emerin in cell passage through narrow pores might also help us to move forward.
As introduced in the section 4.1, the nucleoplasm also contribute to the nuclear mechanical properties it might thus play a role in nuclear squeezing through narrow pores. More experiments involving nucleoplasm mechanical properties might be required to go further. We could for instance, ask the question of the role of the reported actin network inside the nucleus ([Gieni 2009], [Belin 2013]) in nuclear passage through constriction. This actin network might indeed regulate the nucleoplasm mechanical properties.
If the constrictions based setup we chose for our study allowed us to uncorrelate nuclear squeezing from cell migration and then carefully study the first process, it also posses many limitations. Among them, the rigidity of the channels walls might limit *in vivo* extension of the proposed mechanism. On can indeed argue that tissues are much softer than 1MPa. However, the important parameter which is the higher extracellular environment rigidity compared to the cell one is more likely to be conserved *in vivo*.

8.7.2 Cell survival during migration: role of the LINC complex

One of the most interesting actual challenge in 3D cell migration is understanding how cells survive while migrating under such level of confinement. Indeed the high stresses imposed by the extracellular space mechanical properties might induce defects in the cell and more importantly in the nucleus. For instance, those stresses can induce DNA damages leading to cellular apoptosis. Emerging evidences suggest that the lamin A/C network might play a screen effect on the nucleus thus protecting the DNA from external forces (Our work, [Harada 2014]). Another interesting and again unexpected observation I made during my PhD was related to the role of the LINC complex in cell survival during migration under confinement. Indeed, I observed that Sun2 KO dendritic cells which pass narrow constrictions as efficiently as WT cells, survive less after crossing those constrictions. Interestingly, this increase of cell death seems to be specific to constriction passage as Sun 2 KO survive like Sun 2 WT cells in channels without constrictions. This observation gave rise to a whole new project which is now conducted by Matthew Raab, a post doctoral fellow in our lab. Matthew interestingly showed that this increase in cell death was related to an increase in DNA damage in Sun2 KO dendritic cells which have crossed narrow constrictions. This suggests that not only the Lamin A/C network but also the LINC complex might play a protective role in the nucleus. Thus, toward the end of my PhD, the question of the cell/nuclear fate after migration under confinement, emerged as an interesting direction to continue this study.

8.7.3 Importance of nuclear squeezing for *in vivo* cell migration

Our work, combined with the one of Wolf *et al* and Harada *et al*, highlights the importance of nuclear squeezing during cell migration. For instance, a stiff nucleus will limit cell migration while a too compliant nucleus will limit cell survival during migration. Tuning the nuclear mechanical property might allow migrating cells to control their migration efficiency in 3D environments.

In vivo environments are characterized by their high complexity [Friedl 2011]. In tissues such as the connective tissue of the mouse back dermis, dense collagen fibers with pore sections which can be smaller than a micrometer [Wolf 2009] impose a high level of confinement to migrating cells. Cancer cells overcome this physical limitation by degrading the matrix thus enlarging the pore sizes [Wolf 2013]. However, immune cells such as dendritic cells, macrophages and neutrophils which main role is to protect the organism might limit their matrix degradation activity. They thus need to be able to adapt their shape to the extracellular space. This process requires a high cellular deformability.

Cell deformability is defined by cell's mechanical properties which is set by the cytoskeleton, the plasma membrane and the nucleus (introduced in section 3). The high dynamic of the cytoskeleton and the high compliance of the plasma membrane position the nucleus as the cellular component which sets cellular deformability during the fast process of cell migration under confinement. This

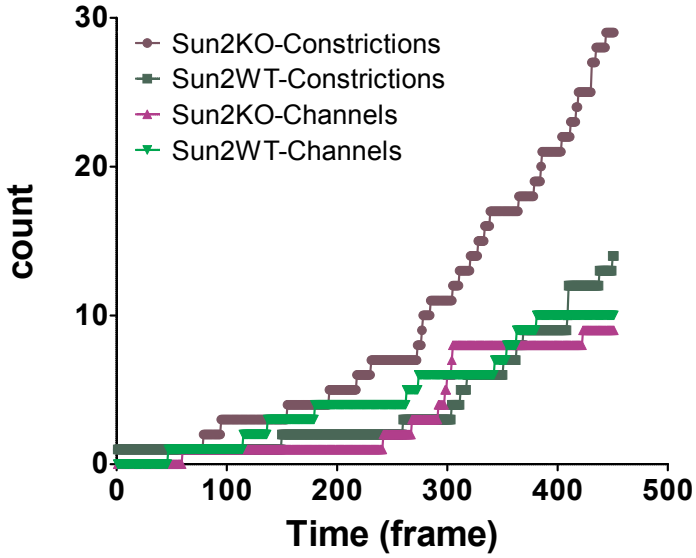

Figure 8.4: Sun 2KO cells survive less in constrictions than the WT littermates. Graph of the cumulative number of dead cells over time. Time is in frame and a snap shot was taken every 2 minutes. Cells were left to migrate in microchannels for 15 hours (451 time points). The number of dead cells was counted in straight channels as well as in channels with constrictions. This number of dead cells was much higher in Sun 2KO dendritic cells which have migrated through constrictions (dark purple) than in WT cells (green curves) or sun 2KO cells in straight channels (light purple).

justifies the requirement for specific mechanisms for nuclear deformation during cell migration. Migration is usually used *in vivo* by cells to achieve other functions. For instance, it allows immune cells to sample the organism for fast response to invasion and metastasic cells to invade new organs thus allowing cancer propagation. However such tasks are complete only if cells survive their migration. Cell must thus be able to combine efficient migration to high survival rate. Interestingly, the A-type lamins proteins which set the nuclear mechanical properties are converging as the proteins which orchestrate efficient cell migration and high survival rates in 3D environments. The interesting observations I made during this PhD concerning the role of the Sun proteins in cell survival during migration under confinement point toward a general role of nuclear deformation in controlling both cell migration and cell survival in 3D environments.

Chapter 9

Conclusion

In conclusion, important contributions to the understanding of cell migration under confinement were made by this work. For instance, our work combined to the works of Wolf *et al* and Harada *et al*, provided new insights in the role of the nucleus during 3D cell migration. The originally of our work resides in the description of a new mechanism used by Lamin A/C expressing immune cells to overcome the energy barrier set by nuclear deformation. In the context of the physics of cell migration, we propose that migrating cells can overcome the energy barrier set by the extracellular environment by transiently increasing their deformability through Lamin A/C disassembly. This new model can be inscribed in the general idea of plascitity in cell migration where migrating cell will adapt their physical and biochemical properties to the extracellular environment in order to preserve their migratory function. In the context of cell biology of cell migration under confinement, our work revealed a new role of the actin nucleator Arp2/3. We, indeed, propose Arp2/3 to be involved in local forces production inside the cell to allow rigid objects deformation during 3D migration. Our work also revealed a new role of the Sun 2 protein of the LINC complex in cell survival during migration under highly confined spaces. This interdisciplinary work thus provides new insights on how do cells combine efficient migration and high survival rate to perform their effector functions in 3D environments. It will thus be extremely interesting to extend this work to the *in vivo* context where efficient combination of cell migration and survival is required for a proper immune response but also for metastasis formation.

Bibliography

[Abu Shah 2013] Enas Abu Shah and Kinneret Keren. *Mechanical forces and feedbacks in cell motility*. Current Opinion in Cell Biology, vol. 25, no. 5, pages 550–557, October 2013. (Cited on page 26.)

[Achard 2010] Vérane Achard, Jean-Louis Martiel, Alphée Michelot, Christophe Guérin, Anne-Cécile Reymann, Laurent Blanchoin and Rajaa Boujemaa-Paterski. *A "Primer"-Based Mechanism Underlies Branched Actin Filament Network Formation and Motility*. Current Biology, vol. 20, no. 5, pages 423–428, March 2010. (Cited on page 34.)

[Aguilar-Cuenca 2014] Rocío Aguilar-Cuenca, Alba Juanes-García and Miguel Vicente-Manzanares. *Myosin II in mechanotransduction: master and commander of cell migration, morphogenesis, and cancer*. Cellular and Molecular Life Sciences, vol. 71, no. 3, pages 479–492, February 2014. (Cited on pages 38 and 39.)

[Aimes 1995] Ronald T. Aimes and James P. Quigley. *Matrix Metalloproteinase-2 Is an Interstitial Collagenase INHIBITOR-FREE ENZYME CATALYZES THE CLEAVAGE OF COLLAGEN FIBRILS AND SOLUBLE NATIVE TYPE I COLLAGEN GENERATING THE SPECIFIC $\frac{3}{4}$- AND $\frac{1}{4}$-LENGTH FRAGMENTS*. Journal of Biological Chemistry, vol. 270, no. 11, pages 5872–5876, March 1995. (Cited on page 64.)

[Akin 2008] Orkun Akin and R. Dyche Mullins. *Capping Protein Increases the Rate of Actin-Based Motility by Promoting Filament Nucleation by the Arp2/3 Complex*. Cell, vol. 133, no. 5, pages 841–851, May 2008. (Cited on pages 34 and 40.)

[Akira 2006] Shizuo Akira, Satoshi Uematsu and Osamu Takeuchi. *Pathogen Recognition and Innate Immunity*. Cell, vol. 124, no. 4, pages 783–801, February 2006. (Cited on page 16.)

[Alberts 2007] Bruce Alberts, Alexander Johnson, Julian Lewis, Martin Raff, Keith Roberts and Peter Walter. Molecular biology of the cell. Garland Science, New York, 5 edition édition, November 2007. (Cited on pages 15, 16, 17 and 22.)

[Alvarez 2008] David Alvarez, Elisabeth H. Vollmann and Ulrich H. von Andrian. *Mechanisms and Consequences of Dendritic Cell Migration*. Immunity, vol. 29, no. 3, pages 325–342, September 2008. (Cited on page 24.)

[Ananthakrishnan 2007] Revathi Ananthakrishnan. *The Forces Behind Cell Movement*. International Journal of Biological Sciences, pages 303–317, 2007. (Cited on page 61.)

[Azioune 2010] Ammar Azioune, Nicolas Carpi, Qingzong Tseng, Manuel Théry and Matthieu Piel. *Chapter 8 - Protein Micropatterns: A Direct Printing Protocol Using Deep UVs*. In Lynne Cassimeris and Phong Tran, editeur, Methods in Cell Biology, volume Volume 97 of *Microtubules: in vivo*, pages 133–146. Academic Press, 2010. (Cited on page 49.)

[Ballermann 1998] B J Ballermann, A Dardik, E Eng and A Liu. *Shear stress and the endothelium*. Kidney international. Supplement, vol. 67, pages S100–108, September 1998. (Cited on page 48.)

[Balzer 2012] Eric M. Balzer, Ziqiu Tong, Colin D. Paul, Wei-Chien Hung, Kimberly M. Stroka, Amanda E. Boggs, Stuart S. Martin and Konstantinos Konstantopoulos. *Physical confinement alters tumor cell adhesion and migration phenotypes*. The FASEB Journal, vol. 26, no. 10, pages 4045–4056, January 2012. (Cited on page 72.)

[Bangasser 2013] Benjamin L. Bangasser, Steven S. Rosenfeld and David J. Odde. *Determinants of maximal force transmission in a motor-clutch model of cell traction in a compliant microenvironment*. Biophysical Journal, vol. 105, no. 3, pages 581–592, August 2013. (Cited on pages 61, 62 and 127.)

[Baum 2005] Buzz Baum and Patricia Kunda. *Actin Nucleation: Spire — Actin Nucleator in a Class of Its Own*. Current Biology, vol. 15, no. 8, pages R305–R308, April 2005. (Cited on page 28.)

[Belin 2013] Brittany J. Belin, Beth A. Cimini, Elizabeth H. Blackburn and R. Dyche Mullins. *Visualization of actin filaments and monomers in somatic cell nuclei*. Molecular biology of the cell, vol. 24, no. 7, pages 982–994, 2013. (Cited on pages 78 and 183.)

[Bergert 2012] Martin Bergert, Stanley D Chandradoss, Ravi A Desai and Ewa Paluch. *Cell mechanics control rapid transitions between blebs and lamellipodia during migration*. Proceedings of the National Academy of Sciences of the United States of America, vol. 109, no. 36, pages 14434–14439, September 2012. (Cited on pages 69 and 169.)

[Berro 2007] Julien Berro, Alphée Michelot, Laurent Blanchoin, David R. Kovar and Jean-Louis Martiel. *Attachment Conditions Control Actin Filament Buckling and the Production of Forces*. Biophysical Journal, vol. 92, no. 7, pages 2546–2558, April 2007. (Cited on page 28.)

[Bertacchini 2013] Jessika Bertacchini, Francesca Beretti, Vittoria Cenni, Marianna Guida, Federica Gibellini, Laura Mediani, Oriano Marin, Nadir M. Maraldi, Anto de Pol, Giovanna Lattanzi, Lucio Cocco and Sandra Marmiroli. *The protein kinase Akt/PKB regulates both prelamin A degradation and Lmna gene expression*. The FASEB Journal, vol. 27, no. 6, pages 2145–2155, January 2013. (Cited on page 175.)

[Bione 1994] S Bione, E Maestrini, S Rivella, M Mancini, S Regis, G Romeo and D Toniolo. *Identification of a novel X-linked gene responsible for Emery-Dreifuss muscular dystrophy*. Nature genetics, vol. 8, no. 4, pages 323–327, December 1994. (Cited on page 86.)

[Birnie 1988] G. D. Birnie. *The HL60 cell line: a model system for studying human myeloid cell differentiation.* The British Journal of Cancer. Supplement, vol. 9, page 41, December 1988. (Cited on pages 103 and 104.)

[Blanchoin 2014] Laurent Blanchoin, Rajaa Boujemaa-Paterski, Cécile Sykes and Julie Plastino. *Actin Dynamics, Architecture, and Mechanics in Cell Motility*. Physiological Reviews, vol. 94, no. 1, pages 235–263, January 2014. (Cited on pages 27, 29, 32, 34 and 38.)

[Blaser 2006] Heiko Blaser, Michal Reichman-Fried, Irinka Castanon, Karin Dumstrei, Florence L Marlow, Koichi Kawakami, Lilianna Solnica-Krezel, Carl-Philipp Heisenberg and Erez Raz. *Migration of zebrafish primordial germ cells: a role for myosin contraction and cytoplasmic flow*. Developmental cell, vol. 11, no. 5, pages 613–627, November 2006. (Cited on page 65.)

[Bohnet 2006] Sophie Bohnet, Revathi Ananthakrishnan, Alex Mogilner, Jean-Jacques Meister and Alexander B. Verkhovsky. *Weak Force Stalls Protrusion at the Leading Edge of the Lamellipodium*. Biophysical Journal, vol. 90, no. 5, pages 1810–1820, March 2006. (Cited on page 39.)

[Bonne 1999] G Bonne, M R Di Barletta, S Varnous, H M Bécane, E H Hammouda, L Merlini, F Muntoni, C R Greenberg, F Gary, J A Urtizberea, D Duboc, M Fardeau, D Toniolo and K Schwartz. *Mutations in the gene encoding lamin A/C cause autosomal dominant Emery-Dreifuss muscular dystrophy*. Nature genetics, vol. 21, no. 3, pages 285–288, March 1999. (Cited on page 86.)

[Borrego-Pinto 2012] Joana Borrego-Pinto, Thibaud Jegou, Daniel S. Osorio, Frederic Auradé, Mátyás Gorjánácz, Birgit Koch, Iain W. Mattaj and Edgar R. Gomes. *Samp1 is a component of TAN lines and is required for nuclear movement*. Journal of Cell Science, vol. 125, no. 5, pages 1099–1105, January 2012. (Cited on page 90.)

[Brangwynne 2006] Clifford P Brangwynne, Frederick C MacKintosh, Sanjay Kumar, Nicholas A Geisse, Jennifer Talbot, L Mahadevan, Kevin K Parker, Donald E Ingber and David A Weitz. *Microtubules can bear enhanced compressive loads in living cells because of lateral reinforcement*. The Journal of cell biology, vol. 173, no. 5, pages 733–741, June 2006. (Cited on page 44.)

[Breitsprecher 2013] Dennis Breitsprecher and Bruce L. Goode. *Formins at a glance*. Journal of Cell Science, vol. 126, no. 1, pages 1–7, January 2013. (Cited on pages 31, 32 and 42.)

[Buehler 2013] Markus J. Buehler. *Mechanical Players—The Role of Intermediate Filaments in Cell Mechanics and Organization*. Biophysical Journal, vol. 105, no. 8, pages 1733–1734, October 2013. (Cited on page 44.)

[Burnette 2011] Dylan T Burnette, Suliana Manley, Prabuddha Sengupta, Rachid Sougrat, Michael W Davidson, Bechara Kachar and Jennifer Lippincott-Schwartz. *A role for actin arcs in the leading-edge advance of migrating cells*. Nature cell biology, vol. 13, no. 4, pages 371–381, April 2011. (Cited on pages 56, 57, 127 and 169.)

[Burridge 2004] Keith Burridge and Krister Wennerberg. *Rho and Rac Take Center Stage*. Cell, vol. 116, no. 2, pages 167–179, January 2004. (Cited on page 130.)

[Burridge 2013] Keith Burridge and Erika S. Wittchen. *The tension mounts: Stress fibers as force-generating mechanotransducers*. The Journal of Cell Biology, vol. 200, no. 1, pages 9–19, July 2013. (Cited on page 58.)

[Caille 2002] Nathalie Caille, Olivier Thoumine, Yanik Tardy and Jean-Jacques Meister. *Contribution of the nucleus to the mechanical properties of endothelial cells*. Journal of biomechanics, vol. 35, no. 2, pages 177–187, 2002. (Cited on page 47.)

[Carisey 2013] Alex Carisey, Ricky Tsang, Alexandra M. Greiner, Nadja Nijenhuis, Nikki Heath, Alicja Nazgiewicz, Ralf Kemkemer, Brian Derby, Joachim Spatz and Christoph Ballestrem. *Vinculin Regulates the Recruitment and Release of Core Focal Adhesion Proteins in a Force-Dependent Manner*. Current Biology, vol. 23, no. 4, pages 271–281, February 2013. (Cited on page 58.)

[Cartwright 2014] Sarah Cartwright and Iakowos Karakesisoglou. *Nesprins in health and disease*. Seminars in Cell & Developmental Biology, vol. 29, pages 169–179, May 2014. (Cited on page 84.)

[Chambliss 2013] Allison B. Chambliss, Shyam B. Khatau, Nicholas Erdenberger, D. Kyle Robinson, Didier Hodzic, Gregory D. Longmore and Denis Wirtz. *The LINC-anchored actin cap connects the extracellular milieu to the nucleus for ultrafast mechanotransduction*. Scientific Reports, vol. 3, January 2013. (Cited on page 93.)

[Chan 2008] Clarence E. Chan and David J. Odde. *Traction dynamics of filopodia on compliant substrates*. Science, vol. 322, no. 5908, pages 1687–1691, December 2008. (Cited on pages 61, 127 and 169.)

[Charras 2005] Guillaume T. Charras, Justin C. Yarrow, Mike A. Horton, L. Mahadevan and T. J. Mitchison. *Non-equilibration of hydrostatic pressure in blebbing cells*. Nature, vol. 435, no. 7040, pages 365–369, May 2005. (Cited on page 45.)

[Charras 2008] Guillaume Charras and Ewa Paluch. *Blebs lead the way: how to migrate without lamellipodia*. Nature Reviews Molecular Cell Biology, vol. 9, no. 9, pages 730–736, September 2008. (Cited on pages 46, 65, 66 and 67.)

[Chaudhuri 2007] Ovijit Chaudhuri, Sapun H. Parekh and Daniel A. Fletcher. *Reversible stress softening of actin networks*. Nature, vol. 445, no. 7125, pages 295–298, January 2007. (Cited on pages 36, 37 and 40.)

[Chen 2010] Zhucheng Chen, Dominika Borek, Shae B Padrick, Timothy S Gomez, Zoltan Metlagel, Ayman M Ismail, Junko Umetani, Daniel D Billadeau, Zbyszek Otwinowski and Michael K Rosen. *Structure and control of the actin regulatory WAVE complex*. Nature, vol. 468, no. 7323, pages 533–538, November 2010. (Cited on page 31.)

[Chernoivanenko 2013] I. S. Chernoivanenko, An A. Minin and A. A. Minin. *[Role of vimentin in cell migration]*. Ontogenez, vol. 44, no. 3, pages 186–202, June 2013. (Cited on page 127.)

[Chesarone 2009] Melissa A Chesarone and Bruce L Goode. *Actin nucleation and elongation factors: mechanisms and interplay*. Current Opinion in Cell Biology, vol. 21, no. 1, pages 28–37, February 2009. (Cited on pages 28, 30 and 31.)

[Chesarone 2010] Melissa A. Chesarone, Amy Grace DuPage and Bruce L. Goode. *Unleashing formins to remodel the actin and microtubule cytoskeletons*. Nature Reviews Molecular Cell Biology, vol. 11, no. 1, pages 62–74, January 2010. (Cited on pages 31, 32 and 42.)

[Cojoc 2007] Dan Cojoc, Francesco Difato, Enrico Ferrari, Rajesh B. Shahapure, Jummi Laishram, Massimo Righi, Enzo M. Di Fabrizio and Vincent Torre. *Properties of the Force Exerted by Filopodia and Lamellipodia and the Involvement of Cytoskeletal Components*. PLoS ONE, vol. 2, no. 10, page e1072, October 2007. (Cited on page 39.)

[Cukierman 2001] Edna Cukierman, Roumen Pankov, Daron R. Stevens and Kenneth M. Yamada. *Taking Cell-Matrix Adhesions to the Third Dimension*. Science, vol. 294, no. 5547, pages 1708–1712, November 2001. (Cited on page 64.)

[Dang 2013] Irene Dang, Roman Gorelik, Carla Sousa-Blin, Emmanuel Derivery, Christophe Guérin, Joern Linkner, Maria Nemethova, Julien G. Dumortier, Florence A. Giger, Tamara A. Chipysheva, Valeria D. Ermilova, Sophie Vacher, Valérie Campanacci, Isaline Herrada, Anne-Gaelle Planson, Susan Fetics, Véronique Henriot, Violaine David, Ksenia Oguievetskaia, Goran Lakisic, Fabienne Pierre, Anika Steffen, Adeline Boyreau, Nadine Peyriéras, Klemens Rottner, Sophie Zinn-Justin, Jacqueline Cherfils, Ivan Bièche, Antonina Y. Alexandrova, Nicolas B. David, J. Victor Small, Jan Faix, Laurent Blanchoin and Alexis Gautreau. *Inhibitory signalling to the Arp2/3 complex steers cell migration*. Nature, vol. 503, no. 7475, pages 281–284, November 2013. (Cited on page 178.)

[Danuser 2013] Gaudenz Danuser, Jun Allard and Alex Mogilner. *Mathematical modeling of eukaryotic cell migration: insights beyond experiments*. Annual Review of Cell and Developmental Biology, vol. 29, no. 1, pages 501–528, 2013. (Cited on page 127.)

[del Rio 2009] Armando del Rio, Raul Perez-Jimenez, Ruchuan Liu, Pere Roca-Cusachs, Julio M Fernandez and Michael P Sheetz. *Stretching single talin rod molecules activates vinculin binding*. Science (New York, N.Y.), vol. 323, no. 5914, pages 638–641, January 2009. (Cited on page 58.)

[DINGLE 2007] HUGH DINGLE and V. ALISTAIR DRAKE. *What Is Migration?* BioScience, vol. 57, no. 2, pages 113–121, February 2007. (Cited on pages 3 and 4.)

[Diz-Muñoz 2013] Alba Diz-Muñoz, Daniel A. Fletcher and Orion D. Weiner. *Use the force: membrane tension as an organizer of cell shape and motility*. Trends in Cell Biology, vol. 23, no. 2, pages 47–53, February 2013. (Cited on page 47.)

[Dupin 2011] Isabelle Dupin and Sandrine Etienne-Manneville. *Nuclear positioning: Mechanisms and functions*. The International Journal of Biochemistry & Cell Biology, vol. 43, no. 12, pages 1698–1707, December 2011. (Cited on pages 89, 92 and 127.)

[Eckes 2000] B. Eckes, E. Colucci-Guyon, H. Smola, S. Nodder, C. Babinet, T. Krieg and P. Martin. *Impaired wound healing in embryonic and adult mice lacking vimentin*. Journal of Cell Science, vol. 113, no. 13, pages 2455–2462, January 2000. (Cited on page 127.)

[Eden 2002] Sharon Eden, Rajat Rohatgi, Alexandre V. Podtelejnikov, Matthias Mann and Marc W. Kirschner. *Mechanism of regulation of WAVE1-induced actin nucleation by Rac1 and Nck*. Nature, vol. 418, no. 6899, pages 790–793, August 2002. (Cited on page 130.)

[Engler 2006] Adam J. Engler, Shamik Sen, H. Lee Sweeney and Dennis E. Discher. *Matrix Elasticity Directs Stem Cell Lineage Specification*. Cell, vol. 126, no. 4, pages 677–689, August 2006. (Cited on pages 49 and 168.)

[Esue 2006] Osigwe Esue, Ashley A Carson, Yiider Tseng and Denis Wirtz. *A direct interaction between actin and vimentin filaments mediated by the tail domain of vimentin*. The Journal of biological chemistry, vol. 281, no. 41, pages 30393–30399, October 2006. (Cited on page 44.)

[Faure-André 2008] Gabrielle Faure-André, Pablo Vargas, Maria-Isabel Yuseff, Mélina Heuzé, Jheimmy Diaz, Danielle Lankar, Veronica Steri, Jeremy Manry, Stéphanie Hugues, Fulvia Vascotto, Jérôme Boulanger, Graça Raposo, Maria-Rosa Bono, Mario Rosemblatt, Matthieu

Piel and Ana-Maria Lennon-Duménil. *Regulation of dendritic cell migration by CD74, the MHC Class II-Associated invariant chain*. Science, vol. 322, no. 5908, pages 1705–1710, December 2008. (Cited on pages 102 and 103.)

[Ferrera 2014] Denise Ferrera, Claudio Canale, Roberto Marotta, Nadia Mazzaro, Marta Gritti, Michele Mazzanti, Sabina Capellari, Pietro Cortelli and Laura Gasparini. *Lamin B1 overexpression increases nuclear rigidity in autosomal dominant leukodystrophy fibroblasts*. The FASEB Journal, pages fj.13–247635, May 2014. (Cited on pages 81 and 183.)

[Flynn 2013] Kevin C Flynn. *The cytoskeleton and neurite initiation*. Bioarchitecture, vol. 3, no. 4, August 2013. (Cited on page 4.)

[Franke 1978] W. W. Franke, E. Schmid, M. Osborn and K. Weber. *Different intermediate-sized filaments distinguished by immunofluorescence microscopy*. Proceedings of the National Academy of Sciences, vol. 75, no. 10, pages 5034–5038, January 1978. (Cited on page 44.)

[Friedl 2009a] Peter Friedl and Darren Gilmour. *Collective cell migration in morphogenesis, regeneration and cancer*. Nature Reviews Molecular Cell Biology, vol. 10, no. 7, pages 445–457, July 2009. (Cited on page 8.)

[Friedl 2009b] Peter Friedl and Katarina Wolf. *Proteolytic interstitial cell migration: a five-step process*. Cancer and Metastasis Reviews, vol. 28, no. 1-2, pages 129–135, June 2009. (Cited on pages 62 and 64.)

[Friedl 2010] Peter Friedl and Katarina Wolf. *Plasticity of cell migration: a multiscale tuning model*. The Journal of Cell Biology, vol. 188, no. 1, pages 11–19, November 2010. (Cited on pages 9, 52, 62, 64, 69, 70 and 102.)

[Friedl 2011] Peter Friedl and Stephanie Alexander. *Cancer Invasion and the Microenvironment: Plasticity and Reciprocity*. Cell, vol. 147, no. 5, pages 992–1009, November 2011. (Cited on pages 9, 11 and 184.)

[Gardel 2008] Margaret L. Gardel, Karen E. Kasza, Clifford P. Brangwynne, Jiayu Liu and David A. Weitz. *Chapter 19 Mechanical Response of Cytoskeletal Networks*. In III Dr. John J. Correia and Dr. H. William Detrich, editeur, Methods in Cell Biology, volume Volume 89 of *Biophysical Tools for Biologists, Volume Two: In Vivo Techniques*, pages 487–519. Academic Press, 2008. (Cited on pages 27, 28, 34, 35, 38 and 42.)

[Geissmann 2010] Frederic Geissmann, Markus G. Manz, Steffen Jung, Michael H. Sieweke, Miriam Merad and Klaus Ley. *Development of Monocytes, Macrophages, and Dendritic Cells*. Science, vol. 327, no. 5966, pages 656–661, May 2010. (Cited on pages 20 and 24.)

[Giannone 2009] Grégory Giannone, René-Marc Mège and Olivier Thoumine. *Multi-level molecular clutches in motile cell processes*. Trends in Cell Biology, vol. 19, no. 9, pages 475–486, September 2009. (Cited on pages 61 and 62.)

[Gieni 2009] Randall S. Gieni and Michael J. Hendzel. *Actin dynamics and functions in the interphase nucleus: moving toward an understanding of nuclear polymeric actinThis paper is one of a selection of papers published in this Special Issue, entitled 29th Annual International*

Asilomar Chromatin and Chromosomes Conference, and has undergone the Journal's usual peer review process. Biochemistry and Cell Biology, vol. 87, no. 1, pages 283–306, February 2009. (Cited on pages 171 and 183.)

[Gittes 1993] Frederick Gittes, Brian Mickey, Jilda Nettleton and Jonathon Howard. *Flexural rigidity of microtubules and actin filaments measured from thermal fluctuations in shape.* The Journal of cell biology, vol. 120, no. 4, pages 923–934, 1993. (Cited on page 28.)

[Goldberg 2008] Martin W. Goldberg, Irm Huttenlauch, Christopher J. Hutchison and Reimer Stick. *Filaments made from A- and B-type lamins differ in structure and organization*. Journal of Cell Science, vol. 121, no. 2, pages 215–225, January 2008. (Cited on page 80.)

[Goley 2006] Erin D. Goley and Matthew D. Welch. *The ARP2/3 complex: an actin nucleator comes of age*. Nature Reviews Molecular Cell Biology, vol. 7, no. 10, pages 713–726, October 2006. (Cited on pages 30 and 171.)

[Gomes 2005] Edgar R. Gomes, Shantanu Jani and Gregg G. Gundersen. *Nuclear Movement Regulated by Cdc42, MRCK, Myosin, and Actin Flow Establishes MTOC Polarization in Migrating Cells*. Cell, vol. 121, no. 3, pages 451–463, May 2005. (Cited on pages 90, 92 and 97.)

[Grange 2002] John M. Grange, John L. Stanford and Cynthia A. Stanford. *Campbell De Morgan's 'Observations on cancer', and their relevance today*. Journal of the Royal Society of Medicine, vol. 95, no. 6, pages 296–299, 2002. (Cited on page 8.)

[Grebecki 2001] A Grebecki, L Grebecka and A Wasik. *Minipodia and rosette contacts are adhesive organelles present in free-living amoebae*. Cell biology international, vol. 25, no. 12, pages 1279–1283, 2001. (Cited on page 66.)

[Greene 2009] George W. Greene, Travers H. Anderson, Hongbo Zeng, Bruno Zappone and Jacob N. Israelachvili. *Force amplification response of actin filaments under confined compression*. Proceedings of the National Academy of Sciences, vol. 106, no. 2, pages 445–449, 2009. (Cited on page 174.)

[Gucht 2005] Jasper van der Gucht, Ewa Paluch, Julie Plastino and Cécile Sykes. *Stress release drives symmetry breaking for actin-based movement*. Proceedings of the National Academy of Sciences, vol. 102, no. 22, pages 7847–7852, May 2005. (Cited on page 40.)

[Guilak 2000] Farshid Guilak, John R. Tedrow and Rainer Burgkart. *Viscoelastic Properties of the Cell Nucleus*. Biochemical and Biophysical Research Communications, vol. 269, no. 3, pages 781–786, March 2000. (Cited on page 78.)

[Guilluy 2014] Christophe Guilluy, Lukas D. Osborne, Laurianne Van Landeghem, Lisa Sharek, Richard Superfine, Rafael Garcia-Mata and Keith Burridge. *Isolated nuclei adapt to force and reveal a mechanotransduction pathway in the nucleus*. Nature Cell Biology, vol. 16, no. 4, pages 376–381, April 2014. (Cited on pages 81, 94 and 176.)

[Gundersen 2013] Gregg G. Gundersen and Howard J. Worman. *Nuclear Positioning*. Cell, vol. 152, no. 6, pages 1376–1389, March 2013. (Cited on pages 84, 88, 89 and 90.)

[Guo 2010] S. Guo and L. A. DiPietro. *Factors Affecting Wound Healing*. Journal of Dental Research, vol. 89, no. 3, pages 219–229, March 2010. (Cited on page 7.)

[Guo 2013] Ming Guo, Allen J. Ehrlicher, Saleemulla Mahammad, Hilary Fabich, Mikkel H. Jensen, Jeffrey R. Moore, Jeffrey J. Fredberg, Robert D. Goldman and David A. Weitz. *The Role of Vimentin Intermediate Filaments in Cortical and Cytoplasmic Mechanics*. Biophysical Journal, vol. 105, no. 7, pages 1562–1568, October 2013. (Cited on page 44.)

[Gupton 2006] Stephanie L Gupton and Clare M Waterman-Storer. *Spatiotemporal feedback between actomyosin and focal-adhesion systems optimizes rapid cell migration*. Cell, vol. 125, no. 7, pages 1361–1374, June 2006. (Cited on pages 58 and 159.)

[Harada 2014] Takamasa Harada, Joe Swift, Jerome Irianto, Jae-Won Shin, Kyle R. Spinler, Avathamsa Athirasala, Rocky Diegmiller, P. C. Dave P. Dingal, Irena L. Ivanovska and Dennis E. Discher. *Nuclear lamin stiffness is a barrier to 3D migration, but softness can limit survival*. The Journal of Cell Biology, vol. 204, no. 5, pages 669–682, March 2014. (Cited on pages V, 80, 87, 96, 127, 128, 132, 164, 167, 182, 183, 184 and 231.)

[Hawkins 2009] R. Hawkins, M. Piel, G. Faure-Andre, A. Lennon-Dumenil, J. Joanny, J. Prost and R. Voituriez. *Pushing off the Walls: A Mechanism of Cell Motility in Confinement*. Physical Review Letters, vol. 102, no. 5, February 2009. (Cited on pages 46, 66, 67, 72, 73, 127, 177 and 179.)

[Hawkins 2010] Taviare Hawkins, Matthew Mirigian, M. Selcuk Yasar and Jennifer L. Ross. *Mechanics of microtubules*. Journal of Biomechanics, vol. 43, no. 1, pages 23–30, January 2010. (Cited on pages 41 and 42.)

[Hawkins 2011] Rhoda J. Hawkins, Renaud Poincloux, Olivier Bénichou, Matthieu Piel, Philippe Chavrier and Raphaël Voituriez. *Spontaneous Contractility-Mediated Cortical Flow Generates Cell Migration in Three-Dimensional Environments*. Biophysical Journal, vol. 101, no. 5, pages 1041–1045, September 2011. (Cited on page 66.)

[Heald 1990] Rebecca Heald and Frank McKeon. *Mutations of phosphorylation sites in lamin A that prevent nuclear lamina disassembly in mitosis*. Cell, vol. 61, no. 4, pages 579–589, May 1990. (Cited on page 175.)

[Herrmann 2007] Harald Herrmann, Harald Bär, Laurent Kreplak, Sergei V. Strelkov and Ueli Aebi. *Intermediate filaments: from cell architecture to nanomechanics*. Nature Reviews Molecular Cell Biology, vol. 8, no. 7, pages 562–573, July 2007. (Cited on page 44.)

[Heuzé 2011] Mélina L. Heuzé, Olivier Collin, Emmanuel Terriac, Ana-Maria Lennon-Duménil and Matthieu Piel. *Cell migration in confinement: a micro-channel-based assay*. Methods in Molecular Biology (Clifton, N.J.), vol. 769, pages 415–434, 2011. (Cited on pages V and 231.)

[Hirata 2014] Hiroaki Hirata, Hitoshi Tatsumi, Chwee Teck Lim and Masahiro Sokabe. *Force-dependent vinculin binding to talin in live cells: a crucial step in anchoring the actin cytoskeleton to focal adhesions*. American journal of physiology. Cell physiology, vol. 306, no. 6, pages C607–620, March 2014. (Cited on page 58.)

[Ho 2012] Chin Yee Ho and Jan Lammerding. *Lamins at a glance*. Journal of Cell Science, vol. 125, no. 9, pages 2087–2093, January 2012. (Cited on pages 80, 86, 87 and 88.)

[Hoffman 2011] Brenton D. Hoffman, Carsten Grashoff and Martin A. Schwartz. *Dynamic molecular processes mediate cellular mechanotransduction*. Nature, vol. 475, no. 7356, pages 316–323, July 2011. (Cited on page 81.)

[Houk 2012] Andrew R Houk, Alexandra Jilkine, Cecile O Mejean, Rostislav Boltyanskiy, Eric R Dufresne, Sigurd B Angenent, Steven J Altschuler, Lani F Wu and Orion D Weiner. *Membrane tension maintains cell polarity by confining signals to the leading edge during neutrophil migration*. Cell, vol. 148, no. 1-2, pages 175–188, January 2012. (Cited on page 47.)

[Hu 2007] Ke Hu, Lin Ji, Kathryn T. Applegate, Gaudenz Danuser and Clare M. Waterman-Storer. *Differential Transmission of Actin Motion Within Focal Adhesions*. Science, vol. 315, no. 5808, pages 111–115, May 2007. (Cited on page 127.)

[Hutson 2007] Mary R. Hutson and Margaret L. Kirby. *Model systems for the study of heart development and disease: Cardiac neural crest and conotruncal malformations*. Seminars in Cell & Developmental Biology, vol. 18, no. 1, pages 101–110, February 2007. (Cited on pages 5 and 6.)

[Inaba 1992] K. Inaba, M. Inaba, N. Romani, H. Aya, M. Deguchi, S. Ikehara, S. Muramatsu and R. M. Steinman. *Generation of large numbers of dendritic cells from mouse bone marrow cultures supplemented with granulocyte/macrophage colony-stimulating factor.* The Journal of Experimental Medicine, vol. 176, no. 6, pages 1693–1702, January 1992. (Cited on page 102.)

[Irimia 2007] Daniel Irimia, Guillaume Charras, Nitin Agrawal, Timothy Mitchison and Mehmet Toner. *Polar stimulation and constrained cell migration in microfluidic channels*. Lab on a chip, vol. 7, no. 12, pages 1783–1790, December 2007. (Cited on pages 69 and 70.)

[Isermann 2013] Philipp Isermann and Jan Lammerding. *Nuclear Mechanics and Mechanotransduction in Health and Disease*. Current Biology, vol. 23, no. 24, pages R1113–R1121, December 2013. (Cited on pages 50, 52, 77, 83 and 93.)

[Ishizaki 2001] Toshimasa Ishizaki, Yosuke Morishima, Muneo Okamoto, Tomoyuki Furuyashiki, Takayuki Kato and Shuh Narumiya. *Coordination of microtubules and the actin cytoskeleton by the Rho effector mDia1*. Nature Cell Biology, vol. 3, no. 1, pages 8–14, January 2001. (Cited on pages 42 and 170.)

[Jaalouk 2009] Diana E. Jaalouk and Jan Lammerding. *Mechanotransduction gone awry*. Nature Reviews Molecular Cell Biology, vol. 10, no. 1, pages 63–73, January 2009. (Cited on page 52.)

[Jahed 2014] Zeinab Jahed, Hengameh Shams, Mehrdad Mehrbod and Mohammad R. K. Mofrad. *Chapter Five - Mechanotransduction Pathways Linking the Extracellular Matrix to the Nucleus*. In Kwang W. Jeon, editeur, International Review of Cell and Molecular Biology, volume Volume 310, pages 171–220. Academic Press, 2014. (Cited on pages 58 and 59.)

[Janmey 1991] P. A. Janmey, U. Euteneuer, P. Traub and M. Schliwa. *Viscoelastic properties of vimentin compared with other filamentous biopolymer networks.* The Journal of Cell Biology, vol. 113, no. 1, pages 155–160, January 1991. (Cited on pages 42 and 127.)

[Kageyama 1977] Tetsuo Kageyama. *Motility and Locomotion of Embryonic Cells of the Medaka, Oryzias Latipes, During Early Development*. Development, Growth & Differentiation, vol. 19, no. 2, pages 103–110, January 1977. (Cited on page 67.)

[Kawska 2012] Agnieszka Kawska, Kévin Carvalho, John Manzi, Rajaa Boujemaa-Paterski, Laurent Blanchoin, Jean-Louis Martiel and Cécile Sykes. *How actin network dynamics control the onset of actin-based motility*. Proceedings of the National Academy of Sciences of the United States of America, vol. 109, no. 36, pages 14440–14445, September 2012. (Cited on page 132.)

[Keren 2008] Kinneret Keren, Zachary Pincus, Greg M. Allen, Erin L. Barnhart, Gerard Marriott, Alex Mogilner and Julie A. Theriot. *Mechanism of shape determination in motile cells*. Nature, vol. 453, no. 7194, pages 475–480, May 2008. (Cited on page 127.)

[Keren 2011] Kinneret Keren. *Cell motility: the integrating role of the plasma membrane*. European Biophysics Journal, vol. 40, no. 9, pages 1013–1027, September 2011. (Cited on page 46.)

[Khatau 2009] Shyam B. Khatau, Christopher M. Hale, P. J. Stewart-Hutchinson, Meet S. Patel, Colin L. Stewart, Peter C. Searson, Didier Hodzic and Denis Wirtz. *A perinuclear actin cap regulates nuclear shape*. Proceedings of the National Academy of Sciences, vol. 106, no. 45, pages 19017–19022, October 2009. (Cited on page 93.)

[Kim 2012] Dong-Hwee Kim, Shyam B. Khatau, Yunfeng Feng, Sam Walcott, Sean X. Sun, Gregory D. Longmore and Denis Wirtz. *Actin cap associated focal adhesions and their distinct role in cellular mechanosensing*. Scientific Reports, vol. 2, August 2012. (Cited on pages 93 and 95.)

[Kochin 2014] Vitaly Kochin, Takeshi Shimi, Elin Torvaldson, Stephen A. Adam, Anne Goldman, Chan-Gi Pack, Johanna Melo-Cardenas, Susumu Y. Imanishi, Robert D. Goldman and John E. Eriksson. *Interphase phosphorylation of lamin A*. Journal of Cell Science, vol. 127, no. 12, pages 2683–2696, June 2014. (Cited on pages 175 and 176.)

[Kojima 1994] H Kojima, A Ishijima and T Yanagida. *Direct measurement of stiffness of single actin filaments with and without tropomyosin by in vitro nanomanipulation*. Proceedings of the National Academy of Sciences of the United States of America, vol. 91, no. 26, pages 12962–12966, December 1994. (Cited on page 28.)

[Kozlov 2007] Michael M. Kozlov and Alex Mogilner. *Model of Polarization and Bistability of Cell Fragments*. Biophysical Journal, vol. 93, no. 11, pages 3811–3819, December 2007. (Cited on page 46.)

[Krendel 2002] Mira Krendel, Frank T. Zenke and Gary M. Bokoch. *Nucleotide exchange factor GEF-H1 mediates cross-talk between microtubules and the actin cytoskeleton*. Nature Cell Biology, vol. 4, no. 4, pages 294–301, April 2002. (Cited on pages 43, 129, 130, 169 and 170.)

[Kreplak 2005] L Kreplak, H Bär, J F Leterrier, H Herrmann and U Aebi. *Exploring the mechanical behavior of single intermediate filaments*. Journal of molecular biology, vol. 354, no. 3, pages 569–577, December 2005. (Cited on page 44.)

[Kreplak 2007] Laurent Kreplak and Douglas Fudge. *Biomechanical properties of intermediate filaments: from tissues to single filaments and back*. BioEssays: news and reviews in molecular, cellular and developmental biology, vol. 29, no. 1, pages 26–35, January 2007. (Cited on page 44.)

[Kurosaka 2008] Satoshi Kurosaka and Anna Kashina. *Cell biology of embryonic migration*. Birth Defects Research Part C: Embryo Today: Reviews, vol. 84, no. 2, pages 102–122, June 2008. (Cited on pages 4, 5 and 6.)

[Lammerding 2004] Jan Lammerding, P. Christian Schulze, Tomosaburo Takahashi, Serguei Kozlov, Teresa Sullivan, Roger D. Kamm, Colin L. Stewart and Richard T. Lee. *Lamin A/C deficiency causes defective nuclear mechanics and mechanotransduction*. Journal of Clinical Investigation, vol. 113, no. 3, pages 370–378, February 2004. (Cited on page 81.)

[Lammerding 2006] Jan Lammerding, Loren G Fong, Julie Y Ji, Karen Reue, Colin L Stewart, Stephen G Young and Richard T Lee. *Lamins A and C but not lamin B1 regulate nuclear mechanics*. The Journal of biological chemistry, vol. 281, no. 35, pages 25768–25780, September 2006. (Cited on page 87.)

[Lämmermann 2008] Tim Lämmermann, Bernhard L Bader, Susan J Monkley, Tim Worbs, Roland Wedlich-Söldner, Karin Hirsch, Markus Keller, Reinhold Förster, David R Critchley, Reinhard Fässler and Michael Sixt. *Rapid leukocyte migration by integrin-independent flowing and squeezing*. Nature, vol. 453, no. 7191, pages 51–55, May 2008. (Cited on pages 66, 67, 96, 97, 127 and 182.)

[Lämmermann 2009] Tim Lämmermann, Jörg Renkawitz, Xunwei Wu, Karin Hirsch, Cord Brakebusch and Michael Sixt. *Cdc42-dependent leading edge coordination is essential for interstitial dendritic cell migration*. Blood, vol. 113, no. 23, pages 5703–5710, June 2009. (Cited on page 127.)

[Larrieu 2014] Delphine Larrieu, Sébastien Britton, Mukerrem Demir, Raphaël Rodriguez and Stephen P. Jackson. *Chemical Inhibition of NAT10 Corrects Defects of Laminopathic Cells*. Science, vol. 344, no. 6183, pages 527–532, February 2014. (Cited on page 170.)

[Larsson 2005] Jonas Larsson and Stefan Karlsson. *The role of Smad signaling in hematopoiesis*. Oncogene, vol. 24, no. 37, pages 5676–5692, 2005. (Cited on page 18.)

[Lauffenburger 1996] Douglas A Lauffenburger and Alan F Horwitz. *Cell Migration: A Physically Integrated Molecular Process*. Cell, vol. 84, no. 3, pages 359–369, February 1996. (Cited on page 54.)

[Lautenschläger 2009] Franziska Lautenschläger, Stephan Paschke, Stefan Schinkinger, Arlette Bruel, Michael Beil and Jochen Guck. *The regulatory role of cell mechanics for migration of differentiating myeloid cells*. Proceedings of the National Academy of Sciences of the United States of America, vol. 106, no. 37, pages 15696–15701, September 2009. (Cited on page 127.)

[Lautenschläger 2013] Franziska Lautenschläger and Matthieu Piel. *Microfabricated devices for cell biology: all for one and one for all*. Current Opinion in Cell Biology, vol. 25, no. 1, pages 116–124, February 2013. (Cited on pages 50 and 51.)

[Le Berre 2012] Maël Le Berre, Johannes Aubertin and Matthieu Piel. *Fine control of nuclear confinement identifies a threshold deformation leading to lamina rupture and induction of specific genes*. Integrative Biology, vol. 4, no. 11, page 1406, 2012. (Cited on pages 176 and 180.)

[Le Berre 2013] M. Le Berre, Yan-Jun Liu, J. Hu, Paolo Maiuri, O. Bénichou, R. Voituriez, Y. Chen and M. Piel. *Geometric Friction Directs Cell Migration*. Physical Review Letters, vol. 111, no. 19, November 2013. (Cited on pages 88 and 96.)

[Lecuit 2011] Thomas Lecuit, Pierre-François Lenne and Edwin Munro. *Force Generation, Transmission, and Integration during Cell and Tissue Morphogenesis*. Annual Review of Cell and Developmental Biology, vol. 27, no. 1, pages 157–184, 2011. (Cited on page 39.)

[Lieber 2013] Arnon D. Lieber, Shlomit Yehudai-Resheff, Erin L. Barnhart, Julie A. Theriot and Kinneret Keren. *Membrane Tension in Rapidly Moving Cells Is Determined by Cytoskeletal Forces*. Current Biology, vol. 23, no. 15, pages 1409–1417, August 2013. (Cited on page 46.)

[Lieleg 2007] Oliver Lieleg and Andreas R. Bausch. *Cross-linker unbinding and self-similarity in bundled cytoskeletal networks*. Physical review letters, vol. 99, no. 15, page 158105, 2007. (Cited on page 38.)

[Lin 2007] Yi-Chia Lin, Gijsje H. Koenderink, Frederick C. MacKintosh and David A. Weitz. *Viscoelastic Properties of Microtubule Networks*. Macromolecules, vol. 40, no. 21, pages 7714–7720, October 2007. (Cited on page 42.)

[Lin 2011] Yi-Chia Lin, Gijsje H. Koenderink, Frederick C. MacKintosh and David A. Weitz. *Control of non-linear elasticity in F-actin networks with microtubules*. Soft Matter, vol. 7, no. 3, page 902, 2011. (Cited on pages 42 and 43.)

[Lo 2000] Chun-Min Lo, Hong-Bei Wang, Micah Dembo and Yu-li Wang. *Cell movement is guided by the rigidity of the substrate*. Biophysical journal, vol. 79, no. 1, pages 144–152, 2000. (Cited on pages 52 and 58.)

[Loisel 1999] Thomas P. Loisel, Rajaa Boujemaa, Dominique Pantaloni and Marie-France Carlier. *Reconstitution of actin-based motility of Listeria and Shigella using pure proteins*. Nature, vol. 401, no. 6753, pages 613–616, October 1999. (Cited on page 39.)

[Loitto 2009] Vesa M. Loitto, Thommie Karlsson and Karl-Eric Magnusson. *Water flux in cell motility: Expanding the mechanisms of membrane protrusion*. Cell Motility and the Cytoskeleton, vol. 66, no. 5, pages 237–247, May 2009. (Cited on page 65.)

[Luxton 2010] G. W. Gant Luxton, Edgar R. Gomes, Eric S. Folker, Erin Vintinner and Gregg G. Gundersen. *Linear Arrays of Nuclear Envelope Proteins Harness Retrograde Actin Flow for Nuclear Movement*. Science, vol. 329, no. 5994, pages 956–959, August 2010. (Cited on pages 84, 90, 92, 97 and 177.)

[Luxton 2011] GW Gant Luxton and Gregg G Gundersen. *Orientation and function of the nuclear–centrosomal axis during cell migration*. Current Opinion in Cell Biology, vol. 23, no. 5, pages 579–588, October 2011. (Cited on pages 92 and 93.)

[Machesky 1994] L M Machesky, S J Atkinson, C Ampe, J Vandekerckhove and T D Pollard. *Purification of a cortical complex containing two unconventional actins from Acanthamoeba by affinity chromatography on profilin-agarose*. The Journal of cell biology, vol. 127, no. 1, pages 107–115, October 1994. (Cited on page 30.)

[Maiuri 2012] Paolo Maiuri, Emmanuel Terriac, Perrine Paul-Gilloteaux, Timothée Vignaud, Krista McNally, James Onuffer, Kurt Thorn, Phuong A. Nguyen, Nefeli Georgoulia, Daniel Soong, Asier Jayo, Nina Beil, Jürgen Beneke, Joleen Chooi Hong Lim, Chloe Pei-Ying Sim, Yeh-Shiu Chu, Andrea Jiménez-Dalmaroni, Jean-François Joanny, Jean-Paul Thiery, Holger Erfle, Maddy Parsons, Timothy J. Mitchison, Wendell A. Lim, Ana-Maria Lennon-Duménil, Matthieu Piel and Manuel Théry. *The first World Cell Race*. Current Biology, vol. 22, no. 17, pages R673–R675, September 2012. (Cited on page 49.)

[Malawista 1997] Stephen E. Malawista and Anne de Boisfleury Chevance. *Random locomotion and chemotaxis of human blood polymorphonuclear leukocytes (PMN) in the presence of EDTA: PMN in close quarters require neither leukocyte integrins nor external divalent cations*. Proceedings of the National Academy of Sciences, vol. 94, no. 21, pages 11577–11582, October 1997. (Cited on page 127.)

[Malawista 2000] S E Malawista, A de Boisfleury Chevance and L A Boxer. *Random locomotion and chemotaxis of human blood polymorphonuclear leukocytes from a patient with leukocyte adhesion deficiency-1: normal displacement in close quarters via chimneying*. Cell motility and the cytoskeleton, vol. 46, no. 3, pages 183–189, July 2000. (Cited on page 67.)

[Maniotis 1997] A J Maniotis, C S Chen and D E Ingber. *Demonstration of mechanical connections between integrins, cytoskeletal filaments, and nucleoplasm that stabilize nuclear structure*. Proceedings of the National Academy of Sciences of the United States of America, vol. 94, no. 3, pages 849–854, February 1997. (Cited on pages 78, 81, 89, 92 and 182.)

[Marcy 2004] Yann Marcy, Jacques Prost, Marie-France Carlier and Cécile Sykes. *Forces generated during actin-based propulsion: A direct measurement by micromanipulation*. Proceedings of the National Academy of Sciences of the United States of America, vol. 101, no. 16, pages 5992–5997, April 2004. (Cited on pages 39 and 40.)

[Margadant 2011] Felix Margadant, Li Li Chew, Xian Hu, Hanry Yu, Neil Bate, Xian Zhang and Michael Sheetz. *Mechanotransduction In Vivo by Repeated Talin Stretch-Relaxation Events Depends upon Vinculin*. PLoS Biol, vol. 9, no. 12, page e1001223, December 2011. (Cited on page 58.)

[Marín 2010] Oscar Marín, Manuel Valiente, Xuecai Ge and Li-Huei Tsai. *Guiding Neuronal Cell Migrations*. Cold Spring Harbor Perspectives in Biology, vol. 2, no. 2, page a001834, January 2010. (Cited on pages 90 and 91.)

[Mayor 2007] Satyajit Mayor and Richard E Pagano. *Pathways of clathrin-independent endocytosis*. Nature reviews. Molecular cell biology, vol. 8, no. 8, pages 603–612, August 2007. (Cited on page 23.)

[Méndez-López 2012] Iván Méndez-López and Howard J Worman. *Inner nuclear membrane proteins: impact on human disease*. Chromosoma, vol. 121, no. 2, pages 153–167, April 2012. (Cited on page 86.)

[Merad 2013] Miriam Merad, Priyanka Sathe, Julie Helft, Jennifer Miller and Arthur Mortha. *The Dendritic Cell Lineage: Ontogeny and Function of Dendritic Cells and Their Subsets in the Steady State and the Inflamed Setting*. Annual Review of Immunology, vol. 31, no. 1, pages 563–604, 2013. (Cited on page 20.)

[Millius 2010] Arthur Millius and Orion D. Weiner. *Manipulation of neutrophil-like HL-60 cells for the study of directed cell migration*. Methods in Molecular Biology (Clifton, N.J.), vol. 591, pages 147–158, 2010. (Cited on pages 104 and 105.)

[Mitchison 1984] T Mitchison and M Kirschner. *Dynamic instability of microtubule growth*. Nature, vol. 312, no. 5991, pages 237–242, November 1984. (Cited on page 40.)

[Moeendarbary 2013] Emad Moeendarbary, Léo Valon, Marco Fritzsche, Andrew R. Harris, Dale A. Moulding, Adrian J. Thrasher, Eleanor Stride, L. Mahadevan and Guillaume T. Charras. *The cytoplasm of living cells behaves as a poroelastic material*. Nature Materials, vol. 12, no. 3, pages 253–261, January 2013. (Cited on page 46.)

[Morgan 2011] Joshua T Morgan, Emily R Pfeiffer, Twanda L Thirkill, Priyadarsini Kumar, Gordon Peng, Heidi N Fridolfsson, Gordon C Douglas, Daniel A Starr and Abdul I Barakat. *Nesprin-3 regulates endothelial cell morphology, perinuclear cytoskeletal architecture, and flow-induced polarization*. Molecular biology of the cell, vol. 22, no. 22, pages 4324–4334, November 2011. (Cited on page 93.)

[Mori 2014] Masashi Mori, Kálmán Somogyi, Hiroshi Kondo, Nilah Monnier, Henning J. Falk, Pedro Machado, Mark Bathe, François Nédélec and Péter Lénárt. *An Arp2/3 nucleated F-actin shell fragments nuclear membranes at nuclear envelope breakdown in starfish oocytes*. Current Biology, vol. 24, no. 12, pages 1421–1428, June 2014. (Cited on page 171.)

[Moseley 2004] James B Moseley, Isabelle Sagot, Amity L Manning, Yingwu Xu, Michael J Eck, David Pellman and Bruce L Goode. *A conserved mechanism for Bni1- and mDia1-induced actin assembly and dual regulation of Bni1 by Bud6 and profilin*. Molecular biology of the cell, vol. 15, no. 2, pages 896–907, February 2004. (Cited on page 31.)

[Mücke 2004] N Mücke, L Kreplak, R Kirmse, T Wedig, H Herrmann, U Aebi and J Langowski. *Assessing the flexibility of intermediate filaments by atomic force microscopy*. Journal of molecular biology, vol. 335, no. 5, pages 1241–1250, January 2004. (Cited on page 44.)

[Mullins 1998] R. Dyche Mullins, John A. Heuser and Thomas D. Pollard. *The interaction of Arp2/3 complex with actin: Nucleation, high affinity pointed end capping, and formation of branching networks of filaments*. Proceedings of the National Academy of Sciences, vol. 95, no. 11, pages 6181–6186, May 1998. (Cited on page 30.)

[Nakaya 2013] Yukiko Nakaya and Guojun Sheng. *EMT in developmental morphogenesis*. Cancer Letters, vol. 341, no. 1, pages 9–15, November 2013. (Cited on page 8.)

[Ng 2008] Lai Guan Ng, Alice Hsu, Michael A Mandell, Ben Roediger, Christoph Hoeller, Paulus Mrass, Amaya Iparraguirre, Lois L Cavanagh, James A Triccas, Stephen M Beverley, Phillip Scott and Wolfgang Weninger. *Migratory dermal dendritic cells act as rapid sensors of protozoan parasites*. PLoS pathogens, vol. 4, no. 11, page e1000222, November 2008. (Cited on page 20.)

[Nguyen 2009] Don X. Nguyen, Paula D. Bos and Joan Massagué. *Metastasis: from dissemination to organ-specific colonization*. Nature Reviews Cancer, vol. 9, no. 4, pages 274–284, April 2009. (Cited on page 8.)

[Nieminen 2006] Mikko Nieminen, Tiina Henttinen, Marika Merinen, Fumiko Marttila–Ichihara, John E. Eriksson and Sirpa Jalkanen. *Vimentin function in lymphocyte adhesion and transcellular migration*. Nature Cell Biology, vol. 8, no. 2, pages 156–162, February 2006. (Cited on page 127.)

[Nilius 2012] Bernd Nilius and Eric Honoré. *Sensing pressure with ion channels*. Trends in Neurosciences, vol. 35, no. 8, pages 477–486, August 2012. (Cited on pages 52 and 55.)

[Pagliara 2014] Stefano Pagliara, Kristian Franze, Crystal R. McClain, George W. Wylde, Cynthia L. Fisher, Robin J. M. Franklin, Alexandre J. Kabla, Ulrich F. Keyser and Kevin J. Chalut. *Auxetic nuclei in embryonic stem cells exiting pluripotency*. Nature Materials, vol. 13, no. 6, pages 638–644, June 2014. (Cited on pages 79 and 168.)

[Pajerowski 2007] J David Pajerowski, Kris Noel Dahl, Franklin L Zhong, Paul J Sammak and Dennis E Discher. *Physical plasticity of the nucleus in stem cell differentiation*. Proceedings of the National Academy of Sciences of the United States of America, vol. 104, no. 40, pages 15619–15624, October 2007. (Cited on pages 79 and 175.)

[Paluch 2005] Ewa Paluch, Matthieu Piel, Jacques Prost, Michel Bornens and Cécile Sykes. *Cortical actomyosin breakage triggers shape oscillations in cells and cell fragments*. Biophysical journal, vol. 89, no. 1, pages 724–733, July 2005. (Cited on page 65.)

[Paluch 2013] Ewa K Paluch and Erez Raz. *The role and regulation of blebs in cell migration*. Current Opinion in Cell Biology, vol. 25, no. 5, pages 582–590, October 2013. (Cited on pages 65 and 66.)

[Papadopoulos 2008] M C Papadopoulos, S Saadoun and A S Verkman. *Aquaporins and cell migration*. Pflügers Archiv: European journal of physiology, vol. 456, no. 4, pages 693–700, July 2008. (Cited on page 72.)

[Petrie 2012] Ryan J. Petrie, Núria Gavara, Richard S. Chadwick and Kenneth M. Yamada. *Nonpolarized signaling reveals two distinct modes of 3D cell migration*. The Journal of Cell Biology, vol. 197, no. 3, pages 439–455, April 2012. (Cited on page 69.)

[Pflicke 2009] Holger Pflicke and Michael Sixt. *Preformed portals facilitate dendritic cell entry into afferent lymphatic vessels*. The Journal of Experimental Medicine, vol. 206, no. 13, pages 2925–2935, December 2009. (Cited on page 128.)

[Plotkin 2005] Stanley A. Plotkin. *Vaccines: past, present and future*. Nature Medicine, vol. 11, pages S5–S11, April 2005. (Cited on page 14.)

[Plotnikov 2013] Sergey V Plotnikov and Clare M Waterman. *Guiding cell migration by tugging*. Current Opinion in Cell Biology, vol. 25, no. 5, pages 619–626, October 2013. (Cited on pages 58 and 60.)

[Poincloux 2011] Renaud Poincloux, Olivier Collin, Floria Lizárraga, Maryse Romao, Marcel Debray, Matthieu Piel and Philippe Chavrier. *Contractility of the cell rear drives invasion of breast tumor cells in 3D Matrigel*. Proceedings of the National Academy of Sciences, vol. 108, no. 5, pages 1943–1948, January 2011. (Cited on page 66.)

[Pollard 2000] Thomas D. Pollard, Laurent Blanchoin and R. Dyche Mullins. *Molecular Mechanisms Controlling Actin Filament Dynamics in Nonmuscle Cells*. Annual Review of Biophysics and Biomolecular Structure, vol. 29, no. 1, pages 545–576, 2000. (Cited on page 28.)

[Pollard 2009] Thomas D. Pollard and John A. Cooper. *Actin, a Central Player in Cell Shape and Movement*. Science, vol. 326, no. 5957, pages 1208–1212, November 2009. (Cited on page 27.)

[Prass 2006] Marcus Prass, Ken Jacobson, Alex Mogilner and Manfred Radmacher. *Direct measurement of the lamellipodial protrusive force in a migrating cell*. The Journal of cell biology, vol. 174, no. 6, pages 767–772, September 2006. (Cited on page 39.)

[Preciado López 2014] Magdalena Preciado López, Florian Huber, Ilya Grigoriev, Michel O Steinmetz, Anna Akhmanova, Marileen Dogterom and Gijsje H Koenderink. *In vitro reconstitution of dynamic microtubules interacting with actin filament networks*. Methods in enzymology, vol. 540, pages 301–320, 2014. (Cited on pages 42, 43 and 170.)

[Pruyne 2002] David Pruyne, Marie Evangelista, Changsong Yang, Erfei Bi, Sally Zigmond, Anthony Bretscher and Charles Boone. *Role of Formins in Actin Assembly: Nucleation and Barbed-End Association*. Science, vol. 297, no. 5581, pages 612–615, July 2002. (Cited on page 31.)

[Pujol 2012] Thomas Pujol, Olivia du Roure, Marc Fermigier and Julien Heuvingh. *Impact of branching on the elasticity of actin networks*. Proceedings of the National Academy of Sciences, vol. 109, no. 26, pages 10364–10369, June 2012. (Cited on pages 35 and 36.)

[Qin 2010] Dong Qin, Younan Xia and George M. Whitesides. *Soft lithography for micro- and nanoscale patterning*. Nature Protocols, vol. 5, no. 3, pages 491–502, March 2010. (Cited on pages 107, 108 and 109.)

[Reis e Sousa 2004] Caetano Reis e Sousa. *Activation of dendritic cells: translating innate into adaptive immunity*. Current Opinion in Immunology, vol. 16, no. 1, pages 21–25, February 2004. (Cited on page 22.)

[Renkawitz 2009] Jörg Renkawitz, Kathrin Schumann, Michele Weber, Tim Lämmermann, Holger Pflicke, Matthieu Piel, Julien Polleux, Joachim P Spatz and Michael Sixt. *Adaptive force transmission in amoeboid cell migration*. Nature cell biology, vol. 11, no. 12, pages 1438–1443, December 2009. (Cited on pages 67, 69, 127 and 169.)

[Renkawitz 2010] Jörg Renkawitz and Michael Sixt. *Mechanisms of force generation and force transmission during interstitial leukocyte migration*. EMBO reports, vol. 11, no. 10, pages 744–750, October 2010. (Cited on pages 65 and 66.)

[Retief 1998] F P Retief and L Cilliers. *The epidemic of Athens, 430-426 BC*. South African medical journal = Suid-Afrikaanse tydskrif vir geneeskunde, vol. 88, no. 1, pages 50–53, January 1998. (Cited on page 14.)

[Reymann 2010] Anne-Cécile Reymann, Jean-Louis Martiel, Théo Cambier, Laurent Blanchoin, Rajaa Boujemaa-Paterski and Manuel Théry. *Nucleation geometry governs ordered actin networks structures*. Nature Materials, vol. 9, no. 10, pages 827–832, October 2010. (Cited on page 34.)

[Ridley 2003] Anne J. Ridley, Martin A. Schwartz, Keith Burridge, Richard A. Firtel, Mark H. Ginsberg, Gary Borisy, J. Thomas Parsons and Alan Rick Horwitz. *Cell migration: integrating signals from front to back*. Science, vol. 302, no. 5651, pages 1704–1709, May 2003. (Cited on pages 54, 56 and 127.)

[Riol-Blanco 2005] Lorena Riol-Blanco, Noelia Sánchez-Sánchez, Ana Torres, Alberto Tejedor, Shuh Narumiya, Angel L. Corbí, Paloma Sánchez-Mateos and José Luis Rodríguez-Fernández. *The Chemokine Receptor CCR7 Activates in Dendritic Cells Two Signaling Modules That Independently Regulate Chemotaxis and Migratory Speed*. The Journal of Immunology, vol. 174, no. 7, pages 4070–4080, January 2005. (Cited on page 129.)

[Risca 2012] Viviana I. Risca, Evan B. Wang, Ovijit Chaudhuri, Jia Jun Chia, Phillip L. Geissler and Daniel A. Fletcher. *Actin filament curvature biases branching direction*. Proceedings of the National Academy of Sciences, vol. 109, no. 8, pages 2913–2918, February 2012. (Cited on page 132.)

[Rossy 2007] Jérémie Rossy, Marc C Gutjahr, Nelsy Blaser, Dominique Schlicht and Verena Niggli. *Ezrin/moesin in motile Walker 256 carcinosarcoma cells: signal-dependent relocalization and role in migration*. Experimental cell research, vol. 313, no. 6, pages 1106–1120, April 2007. (Cited on page 65.)

[Rotty 2013] Jeremy D. Rotty, Congying Wu and James E. Bear. *New insights into the regulation and cellular functions of the ARP2/3 complex*. Nature Reviews Molecular Cell Biology, vol. 14, no. 1, pages 7–12, 2013. (Cited on pages 30 and 31.)

[Rowat 2005] A. C. Rowat, L. J. Foster, M. M. Nielsen, M. Weiss and J. H. Ipsen. *Characterization of the elastic properties of the nuclear envelope*. Journal of The Royal Society Interface, vol. 2, no. 2, pages 63–69, March 2005. (Cited on pages 77, 80, 94 and 175.)

[Rowat 2006] A C Rowat, J Lammerding and J H Ipsen. *Mechanical properties of the cell nucleus and the effect of emerin deficiency*. Biophysical journal, vol. 91, no. 12, pages 4649–4664, December 2006. (Cited on pages 77 and 79.)

[Rowat 2008] Amy C. Rowat, Jan Lammerding, Harald Herrmann and Ueli Aebi. *Towards an integrated understanding of the structure and mechanics of the cell nucleus*. BioEssays, vol. 30, no. 3, pages 226–236, March 2008. (Cited on page 80.)

[Rowat 2013] Amy C. Rowat, Diana E. Jaalouk, Monika Zwerger, W. Lloyd Ung, Irwin A. Eydelnant, Don E. Olins, Ada L. Olins, Harald Herrmann, David A. Weitz and Jan Lammerding. *Nuclear envelope composition determines the ability of Neutrophil-type cells to passage*

through micron-scale constrictions. Journal of Biological Chemistry, vol. 288, no. 12, pages 8610–8618, March 2013. (Cited on pages 96, 104, 128 and 167.)

[Rs 1993] Kirsner Rs and Eaglstein Wh. *The wound healing process.* Dermatologic clinics, vol. 11, no. 4, pages 629–640, October 1993. (Cited on page 7.)

[Sachs 2010] Frederick Sachs. *Stretch-Activated Ion Channels: What Are They?* Physiology, vol. 25, no. 1, pages 50–56, February 2010. (Cited on page 52.)

[Sagot 2002] Isabelle Sagot, Avital A. Rodal, James Moseley, Bruce L. Goode and David Pellman. *An actin nucleation mechanism mediated by Bni1 and Profilin*. Nature Cell Biology, vol. 4, no. 8, pages 626–631, August 2002. (Cited on page 31.)

[Sánchez-Sánchez 2006] Noelia Sánchez-Sánchez, Lorena Riol-Blanco and José Luis Rodríguez-Fernández. *The Multiple Personalities of the Chemokine Receptor CCR7 in Dendritic Cells*. The Journal of Immunology, vol. 176, no. 9, pages 5153–5159, January 2006. (Cited on page 129.)

[Sander 1999] Eva E. Sander, Jean P. ten Klooster, Sanne van Delft, Rob A. van der Kammen and John G. Collard. *Rac Downregulates Rho Activity Reciprocal Balance between Both Gtpases Determines Cellular Morphology and Migratory Behavior*. The Journal of Cell Biology, vol. 147, no. 5, pages 1009–1022, November 1999. (Cited on pages 130 and 170.)

[Sanz-Moreno 2008] Victoria Sanz-Moreno, Gilles Gadea, Jessica Ahn, Hugh Paterson, Pierfrancesco Marra, Sophie Pinner, Erik Sahai and Christopher J Marshall. *Rac activation and inactivation control plasticity of tumor cell movement*. Cell, vol. 135, no. 3, pages 510–523, October 2008. (Cited on page 64.)

[Schachtner 2012] Hannah Schachtner, Ang Li, David Stevenson, Simon D. J. Calaminus, Steven G. Thomas, Steve P. Watson, Michael Sixt, Roland Wedlich-Soldner, Douglas Strathdee and Laura M. Machesky. *Tissue inducible Lifeact expression allows visualization of actin dynamics in vivo and ex vivo*. European Journal of Cell Biology, vol. 91, no. 11–12, pages 923–929, November 2012. (Cited on page 129.)

[Schreiber 2013] Katherine H. Schreiber and Brian K. Kennedy. *When Lamins Go Bad: Nuclear Structure and Disease*. Cell, vol. 152, no. 6, pages 1365–1375, March 2013. (Cited on page 86.)

[Schuermann 2014] Annika Schuermann, Christian S M Helker and Wiebke Herzog. *Angiogenesis in zebrafish*. Seminars in cell & developmental biology, May 2014. (Cited on page 4.)

[Schwab 2012] Albrecht Schwab, Anke Fabian, Peter J. Hanley and Christian Stock. *Role of Ion Channels and Transporters in Cell Migration*. Physiological Reviews, vol. 92, no. 4, pages 1865–1913, October 2012. (Cited on pages 53, 54, 72, 74 and 75.)

[Seltmann 2013] Kristin Seltmann, Anatol W. Fritsch, Josef A. Käs and Thomas M. Magin. *Keratins significantly contribute to cell stiffness and impact invasive behavior*. Proceedings of the National Academy of Sciences of the United States of America, vol. 110, no. 46, pages 18507–18512, November 2013. (Cited on page 127.)

[Sheetz 1996] M P Sheetz and J Dai. *Modulation of membrane dynamics and cell motility by membrane tension*. Trends in cell biology, vol. 6, no. 3, pages 85–89, March 1996. (Cited on page 46.)

[Shimi 2008] Takeshi Shimi, Katrin Pfleghaar, Shin-ichiro Kojima, Chan-Gi Pack, Irina Solovei, Anne E. Goldman, Stephen A. Adam, Dale K. Shumaker, Masataka Kinjo, Thomas Cremer and Robert D. Goldman. *The A- and B-type nuclear lamin networks: microdomains involved in chromatin organization and transcription*. Genes & Development, vol. 22, no. 24, pages 3409–3421, December 2008. (Cited on page 80.)

[Shortman 2002] Ken Shortman and Yong-Jun Liu. *Mouse and human dendritic cell subtypes*. Nature Reviews Immunology, vol. 2, no. 3, pages 151–161, March 2002. (Cited on page 21.)

[Simon 2013] Dan N. Simon and Katherine L. Wilson. *Partners and post-translational modifications of nuclear lamins*. Chromosoma, vol. 122, no. 1-2, pages 13–31, March 2013. (Cited on page 175.)

[Sosa 2012] Brian A. Sosa, Andrea Rothballer, Ulrike Kutay and Thomas U. Schwartz. *LINC Complexes Form by Binding of Three KASH Peptides to Domain Interfaces of Trimeric SUN Proteins*. Cell, vol. 149, no. 5, pages 1035–1047, May 2012. (Cited on page 84.)

[Sosa 2013] Brian A Sosa, Ulrike Kutay and Thomas U Schwartz. *Structural insights into LINC complexes*. Current Opinion in Structural Biology, vol. 23, no. 2, pages 285–291, April 2013. (Cited on pages 82, 84 and 85.)

[Sroka 2002] J Sroka, M von Gunten, G A Dunn and H U Keller. *Phenotype modulation in non-adherent and adherent sublines of Walker carcinosarcoma cells: the role of cell-substratum contacts and microtubules in controlling cell shape, locomotion and cytoskeletal structure*. The international journal of biochemistry & cell biology, vol. 34, no. 7, pages 882–899, July 2002. (Cited on page 66.)

[Starodubtseva 2011] Maria N. Starodubtseva. *Mechanical properties of cells and ageing*. Ageing Research Reviews, vol. 10, no. 1, pages 16–25, January 2011. (Cited on pages 26, 45 and 46.)

[Starr 2010] Daniel A. Starr and Heidi N. Fridolfsson. *Interactions Between Nuclei and the Cytoskeleton Are Mediated by SUN-KASH Nuclear-Envelope Bridges*. Annual Review of Cell and Developmental Biology, vol. 26, no. 1, pages 421–444, 2010. (Cited on pages 82 and 84.)

[Steinman 1974] Ralph M. Steinman, Dinah S. Lustig and Zanvil A. Cohn. *Identification of a Novel Cell Type in Peripheral Lymphoid Organs of Mice Iii. Functional Properties in Vivo*. The Journal of Experimental Medicine, vol. 139, no. 6, pages 1431–1445, January 1974. (Cited on page 20.)

[Storm 2005] Cornelis Storm, Jennifer J Pastore, F C MacKintosh, T C Lubensky and Paul A Janmey. *Nonlinear elasticity in biological gels*. Nature, vol. 435, no. 7039, pages 191–194, May 2005. (Cited on pages 35 and 44.)

[Stricker 2010] Jonathan Stricker, Tobias Falzone and Margaret L. Gardel. *Mechanics of the F-actin cytoskeleton*. Journal of Biomechanics, vol. 43, no. 1, pages 9–14, January 2010. (Cited on pages 35, 38, 39 and 43.)

[Stroka 2014] Kimberly M. Stroka, Hongyuan Jiang, Shih-Hsun Chen, Ziqiu Tong, Denis Wirtz, Sean X. Sun and Konstantinos Konstantopoulos. *Water permeation drives tumor cell migration in confined microenvironments*. Cell, vol. 157, no. 3, pages 611–623, April 2014. (Cited on pages 72, 129, 179 and 182.)

[Svitkina 2003] Tatyana M Svitkina, Elena A Bulanova, Oleg Y Chaga, Danijela M Vignjevic, Shinichiro Kojima, Jury M Vasiliev and Gary G Borisy. *Mechanism of filopodia initiation by reorganization of a dendritic network*. The Journal of cell biology, vol. 160, no. 3, pages 409–421, February 2003. (Cited on page 34.)

[Swift 2013] Joe Swift, Irena L Ivanovska, Amnon Buxboim, Takamasa Harada, P C Dave P Dingal, Joel Pinter, J David Pajerowski, Kyle R Spinler, Jae-Won Shin, Manorama Tewari, Florian Rehfeldt, David W Speicher and Dennis E Discher. *Nuclear lamin-A scales with tissue stiffness and enhances matrix-directed differentiation*. Science (New York, N.Y.), vol. 341, no. 6149, page 1240104, August 2013. (Cited on pages 80, 94, 131, 175 and 179.)

[Tozluoğlu 2013] Melda Tozluoğlu, Alexander L. Tournier, Robert P. Jenkins, Steven Hooper, Paul A. Bates and Erik Sahai. *Matrix geometry determines optimal cancer cell migration strategy and modulates response to interventions*. Nature Cell Biology, vol. 15, no. 7, pages 751–762, July 2013. (Cited on pages 66 and 127.)

[Trainor 2005] Paul A. Trainor. *Specification of neural crest cell formation and migration in mouse embryos*. Seminars in Cell & Developmental Biology, vol. 16, no. 6, pages 683–693, December 2005. (Cited on page 5.)

[Tseng 2004] Yiider Tseng, Jerry S. H. Lee, Thomas P. Kole, Ingjye Jiang and Denis Wirtz. *Micro-organization and visco-elasticity of the interphase nucleus revealed by particle nanotracking*. Journal of Cell Science, vol. 117, no. 10, pages 2159–2167, April 2004. (Cited on page 79.)

[Tsuda 1996] Y Tsuda, H Yasutake, A Ishijima and T Yanagida. *Torsional rigidity of single actin filaments and actin-actin bond breaking force under torsion measured directly by in vitro micromanipulation*. Proceedings of the National Academy of Sciences of the United States of America, vol. 93, no. 23, pages 12937–12942, November 1996. (Cited on page 44.)

[Tucker 2004] Richard P Tucker. *Neural crest cells: a model for invasive behavior*. The International Journal of Biochemistry & Cell Biology, vol. 36, no. 2, pages 173–177, February 2004. (Cited on page 5.)

[van Oudenaarden 1999] Alexander van Oudenaarden and Julie A. Theriot. *Cooperative symmetry-breaking by actin polymerization in a model for cell motility*. Nature Cell Biology, vol. 1, no. 8, pages 493–499, December 1999. (Cited on page 132.)

[Verstraeten 2008] Valerie L. R. M. Verstraeten and Jan Lammerding. *Experimental techniques for study of chromatin mechanics in intact nuclei and living cells*. Chromosome Research, vol. 16, no. 3, pages 499–510, May 2008. (Cited on pages 78 and 87.)

[Vicente-Manzanares 2005] Miguel Vicente-Manzanares, Donna J. Webb and A. Rick Horwitz. *Cell migration at a glance*. Journal of Cell Science, vol. 118, no. 21, pages 4917–4919, January 2005. (Cited on page 4.)

[Wang 2000] Ning Wang and Dimitrije Stamenović. *Contribution of intermediate filaments to cell stiffness, stiffening, and growth*. American Journal of Physiology - Cell Physiology, vol. 279, no. 1, pages C188–C194, July 2000. (Cited on pages 44 and 127.)

[Wang 2009] Ning Wang, Jessica D. Tytell and Donald E. Ingber. *Mechanotransduction at a distance: mechanically coupling the extracellular matrix with the nucleus*. Nature Reviews Molecular Cell Biology, vol. 10, no. 1, pages 75–82, January 2009. (Cited on pages 92, 93 and 94.)

[Waterman-Storer 1999a] Clare M Waterman-Storer and ED Salmon. *Positive feedback interactions between microtubule and actin dynamics during cell motility*. Current Opinion in Cell Biology, vol. 11, no. 1, pages 61–67, February 1999. (Cited on page 170.)

[Waterman-Storer 1999b] Clare M. Waterman-Storer, Rebecca A. Worthylake, Betty P. Liu, Keith Burridge and E. D. Salmon. *Microtubule growth activates Rac1 to promote lamellipodial protrusion in fibroblasts*. Nature Cell Biology, vol. 1, no. 1, pages 45–50, May 1999. (Cited on page 170.)

[Webb 2002] Donna J. Webb, J. Thomas Parsons and Alan F. Horwitz. *Adhesion assembly, disassembly and turnover in migrating cells – over and over and over again*. Nature Cell Biology, vol. 4, no. 4, pages E97–E100, April 2002. (Cited on page 58.)

[Weber 2013] Michele Weber, Robert Hauschild, Jan Schwarz, Christine Moussion, Ingrid de Vries, Daniel F. Legler, Sanjiv A. Luther, Tobias Bollenbach and Michael Sixt. *Interstitial Dendritic Cell Guidance by Haptotactic Chemokine Gradients*. Science, vol. 339, no. 6117, pages 328–332, January 2013. (Cited on pages 24 and 102.)

[Welch 1998] M D Welch, J Rosenblatt, J Skoble, D A Portnoy and T J Mitchison. *Interaction of human Arp2/3 complex and the Listeria monocytogenes ActA protein in actin filament nucleation*. Science (New York, N.Y.), vol. 281, no. 5373, pages 105–108, July 1998. (Cited on page 39.)

[West 2008] Michele A. West, Alan R. Prescott, Kui Ming Chan, Zhongjun Zhou, Stefan Rose-John, Jürgen Scheller and Colin Watts. *TLR ligand-induced podosome disassembly in dendritic cells is ADAM17 dependent*. The Journal of Cell Biology, vol. 182, no. 5, pages 993–1005, September 2008. (Cited on page 103.)

[Whitesides 2001] George M. Whitesides, Emanuele Ostuni, Shuichi Takayama, Xingyu Jiang and Donald E. Ingber. *Soft Lithography in Biology and Biochemistry*. Annual Review of Biomedical Engineering, vol. 3, no. 1, pages 335–373, 2001. (Cited on page 106.)

[Wilson 2013] Kerry Wilson, Alexandre Lewalle, Marco Fritzsche, Richard Thorogate, Tom Duke and Guillaume Charras. *Mechanisms of leading edge protrusion in interstitial migration*. Nature Communications, vol. 4, December 2013. (Cited on pages 67, 70, 71, 72 and 169.)

[Wolf 2003] Katarina Wolf, Irina Mazo, Harry Leung, Katharina Engelke, Ulrich H von Andrian, Elena I Deryugina, Alex Y Strongin, Eva-B Bröcker and Peter Friedl. *Compensation mechanism in tumor cell migration: mesenchymal-amoeboid transition after blocking of pericellular proteolysis*. The Journal of cell biology, vol. 160, no. 2, pages 267–277, January 2003. (Cited on pages 62, 64, 67 and 69.)

[Wolf 2007] Katarina Wolf, Yi I. Wu, Yueying Liu, Jörg Geiger, Eric Tam, Christopher Overall, M. Sharon Stack and Peter Friedl. *Multi-step pericellular proteolysis controls the transition from individual to collective cancer cell invasion*. Nature Cell Biology, vol. 9, no. 8, pages 893–904, August 2007. (Cited on page 64.)

[Wolf 2009] Katarina Wolf, Stephanie Alexander, Vivien Schacht, Lisa M. Coussens, Ulrich H. von Andrian, Jacco van Rheenen, Elena Deryugina and Peter Friedl. *Collagen-based cell migration models in vitro and in vivo*. Seminars in Cell & Developmental Biology, vol. 20, no. 8, pages 931–941, October 2009. (Cited on pages 48, 49, 127, 168 and 184.)

[Wolf 2013] Katarina Wolf, Mariska Te Lindert, Marina Krause, Stephanie Alexander, Joost Te Riet, Amanda L Willis, Robert M Hoffman, Carl G Figdor, Stephen J Weiss and Peter Friedl. *Physical limits of cell migration: control by ECM space and nuclear deformation and tuning by proteolysis and traction force*. The Journal of cell biology, vol. 201, no. 7, pages 1069–1084, June 2013. (Cited on pages V, 64, 67, 69, 88, 96, 102, 123, 127, 128, 165, 167, 180, 182, 184 and 231.)

[Wyckoff 2006] Jeffrey B. Wyckoff, Sophie E. Pinner, Steve Gschmeissner, John S. Condeelis and Erik Sahai. *ROCK- and Myosin-dependent matrix deformation enables protease-independent tumor-cell invasion in vivo*. Current Biology, vol. 16, no. 15, pages 1515–1523, August 2006. (Cited on page 128.)

[Yang 2013] Yali Yang, Mo Bai, William S. Klug, Alex J. Levine and Megan T. Valentine. *Microrheology of highly crosslinked microtubule networks is dominated by force-induced crosslinker unbinding*. Soft Matter, vol. 9, no. 2, page 383, 2013. (Cited on page 42.)

[Zaidel-Bar 2007] Ronen Zaidel-Bar, Shalev Itzkovitz, Avi Ma'ayan, Ravi Iyengar and Benjamin Geiger. *Functional atlas of the integrin adhesome*. Nature Cell Biology, vol. 9, no. 8, pages 858–867, August 2007. (Cited on page 54.)

[Zhelev 1994] D V Zhelev, D Needham and R M Hochmuth. *Role of the membrane cortex in neutrophil deformation in small pipets*. Biophysical journal, vol. 67, no. 2, pages 696–705, August 1994. (Cited on page 46.)

[Zwerger 2011] Monika Zwerger, Chin Yee Ho and Jan Lammerding. *Nuclear Mechanics in Disease*. Annual Review of Biomedical Engineering, vol. 13, no. 1, pages 397–428, 2011. (Cited on pages 78 and 80.)

APPENDICES

Appendix A

Appendix 1 : Research article

A.1 A computational mechanics approach to assess the link between cell morphology and forces during confined migration

Authors:

Denis Aubry[1], **Hawa-Racine Thiam**[2], Matthieu Piel[2], Rachele Allena[1]

Affiliations:

[1]Laboratoire MSSMat UMR CNRS 8579, Ecole Centrale Paris, 92295 , Chatenay-Malabry, France.
[2]Institut Curie, CNRS UMR 144, 26 rue d'Ulm, 75005, Paris, FRANCE

Biomechanics and Modelling in Mechanobiology, 2014 Jun 4;

Biomech Model Mechanobiol
DOI 10.1007/s10237-014-0595-3

ORIGINAL PAPER

A computational mechanics approach to assess the link between cell morphology and forces during confined migration

D. Aubry · H. Thiam · M. Piel · R. Allena

Received: 12 December 2013 / Accepted: 12 May 2014

Abstract Confined migration plays a fundamental role during several biological phenomena such as embryogenesis, immunity and tumorogenesis. Here, we propose a two-dimensional mechanical model to simulate the migration of a HeLa cell through a micro-channel. As in our previous works, the cell is modelled as a continuum and a standard Maxwell model is used to describe the mechanical behaviour of both the cytoplasm (including active strains) and the nucleus. The cell cyclically protrudes and contracts and develops viscous forces to adhere to the substrate. The micro-channel is represented by two rigid walls, and it exerts an additional viscous force on the cell boundaries. We test four channels whose dimensions in terms of width are i) larger than the cell diameter, ii) sub-cellular, ii) sub-nuclear and iv) much smaller than the nucleus diameter. The main objective of the work is to assess the necessary conditions for the cell to enter into the channel and migrate through it. Therefore, we evaluate both the evolution of the cell morphology and the cell-channel and cell-substrate surface forces, and we show that there exists a link between the two, which is the essential parameter determining whether the cell is permeative, invasive or penetrating.

Keywords Confined cell migration · Continuum mechanics · Computational mechanics · Forces

Electronic supplementary material The online version of this article (doi:10.1007/s10237-014-0595-3) contains supplementary material, which is available to authorized users.

D. Aubry
Laboratoire MSSMat UMR CNRS 8579, Ecole Centrale Paris, 92295 Châtenay-Malabry, France

H. Thiam · M. Piel
Biologie systémique de la division et de la polarité cellulaire, Institut Curie UMR 144, 12 Rue Lhomond, 75005 Paris, France

R. Allena (✉)
Arts et Metiers ParisTech, LBM, 151 Bd de l'hôpital, 75013 Paris, France
e-mail: Rachele.allena@ensam.eu

1 Introduction

In our previous works (Allena and Aubry 2012; Allena 2013), we have presented numerical models which helped to understand the mechanisms controlling cell motility on two-dimensional (2D) flat surfaces. Nevertheless, during many biological processes such as embryogenesis, immunity and tumorogenesis, cell migration takes place in confined environments of tissues (Friedl and Wolf 2010). In these cases, cell locomotion is influenced by the presence of attractant molecules, but also by the morphology of the extracellular matrix (ECM). In fact, the surrounding tissues may vary in terms of heterogeneity, fibres density and organization. As shown both experimentally (Erler and Weaver 2009; Wolf et al. 2009; Egeblad et al. 2010; Friedl and Wolf 2010) and theoretically (Zaman et al. 2005, 2006, 2007; Scianna et al. 2013), the width of the ECM pores, the degree of ECM alignment as well as the ECM stiffness are fundamental parameters, which determine how and how much the ECM steers or inhibits the cell movement. Therefore, the cell needs to continuously adapt its shape and consequently its migratory behaviour. In tumorogenesis for instance, cancer cells develop an invasive behaviour, which allows them to enter and progressively invade healthy tissue as they are constantly exposed to biomechanical and biophysical stimuli. Such adaptation requires an internal reorganization of both the cytoskeleton and the embedded organelles, among which the nucleus is the stiffest and the most voluminous. Consequently, it has become essen-

Published online: 04 June 2014

tial to quantitatively assess the cell ability to deform as well as which mechanical forces the cell has to develop in order to move forward within a confined micro-structure.

In the last few years, several experimental studies have tried to provide such data. Systems like collagen gels or lattices are commonly used to simulate cell migration in confined connective tissues (Wolf et al. 2009). Although very simplified, such systems are highly complex and difficult to control since many physical parameters (i.e. gel density and elasticity, local constrictions) may affect the global mobility of the cell and furthermore fail to reproduce spatial tracks or obstacles (Provenzano et al. 2008; Wolf et al. 2009; Egeblad et al. 2010). More recently, it has been possible to better control, vary and tune the geometrical characteristics of the patterned micro-structure using micro-laser techniques (Ilina et al. 2011) or photolithography (Heuzé et al. 2011). In the latter work, cells migrate through straight micro-channels made of silicone rubber (i.e. polydimethylsiloxane, PDMS), whose sub-cellular dimensions vary between 2 and 10 μm in width and highly depend on cell type. Such an approach has provided interesting results for cancer cells (Irimia and Toner 2009; Ronot et al. 2000), immune cells (Irimia et al. 2007; Faure-André et al. 2008) and neurons (Taylor et al. 2005). Micro-channels may be modulated in order to investigate specific biological problems such as trans-migration ability within a well-defined geometry or the influence of the substrate stiffness by letting channel material vary. Additionally, more complex geometries can be obtained to force the cell to take turns and explore its 2D confined environment.

From a numerical point of view, many models have been proposed to simulate single cell migration on 2D flat surfaces or in three-dimensional (3D) environment (Rangarajan and Zaman 2008). Such models have used different approaches resulting in force-based dynamics models (Zaman et al. 2005, 2006), stochastic models to simulate persistent random walks (Tranquillo and Lauffenburger 1987; Tranquillo et al. 1988; Stokes et al. 1991; Stokes and Lauffenburger 1991), models reproducing the movement of cancer cell spheroids (McElwain and Ponzo 1977; McElwain 1978; McElwain et al. 1979), Monte Carlo models (Zaman et al. 2007; Scianna and Preziosi 2013; Scianna et al. 2013) or purely mechanical models (Allena and Aubry 2012; Allena 2013). Active gel layers submitted to external forces have been used to represent acto-myosin cells migrating in a free (Recho and Truskinovsky 2013; Recho et al. 2013) or confined (Hawkins et al. 2009; Hawkins and Voituriez 2010) environment. Scianna and Preziosi (Scianna and Preziosi 2013) have presented a cellular potts model (CPM), which reproduces an experimental assay very similar to those used in (Taylor et al. 2005; Irimia et al. 2007; Faure-André et al. 2008; Irimia and Toner 2009; Rolli et al. 2010; Heuzé et al. 2011). In this model, the cell is modelled as a discrete physical unit, including the cytosol and the nucleus, while channels of different widths constitute the migration chamber. The authors have investigated the invasiveness of tumour cells by evaluating their displacement and velocity as well as their deformability, which seems to be strongly linked to the deformability of the nucleus. In (Tozluoğlu et al. 2013), a hybrid agent-based finite element model is proposed to evaluate the migration strategy of the cell in different environments such as confinement. The model is able to simulate both the protrusion–contraction and the membrane blebbing modes of migration. Therefore, the authors estimate the effects of the ECM geometry on the relationship between cell velocity, contractility and adhesion, and they also find interesting effects of membrane blebbing on cell velocity and morphology. Finally, in (Giverso et al.), an energetic continuum approach is employed to investigate the necessary condition for which a cell migrate through a cylindrical channel. They consider the nucleus either as an elastic membrane surrounding a liquid droplet or as an incompressible elastic material. By taking into account and balancing different forces exerted by and on the cell during confined movement, they are able to determine the minimal size of the cylindrical structure and they observe that cell ability to migrate through it depends on both nucleus stiffness and adhesion to ECM.

1.1 Objective of the present work

In the present paper, a finite element model that reproduces the experimental set-up used in (Heuzé et al. 2011) for HeLa cells is proposed, which is based on the following hypotheses:

- the 2D geometry represents a top view of the global structure, and a plane stress hypothesis has been made;
- as in (Giverso et al.), a purely mechanical approach is used to describe the cell behaviour. However, a different mathematical method is applied. In fact, the decomposition of the deformation gradient is employed to consider both the active (i.e. protrusion and contraction) and the elastic (i.e. strains generated by the interaction with the environment) strains undergone by the cell;
- contrary to previous works (Scianna and Preziosi 2013; Scianna et al. 2013; Tozluoğlu et al. 2013), the cell is modelled as a continuum. Nonetheless, both the cytoplasm and the nucleus have been originally represented through two characteristic functions, and a standard Maxwell model has been used to describe their viscoelastic behaviour (Allena and Aubry 2012; Allena 2013; Tozluoğlu et al. 2013);
- the cell is able to cyclically protrude and contract. Such active strains are triggered respectively by the polymerization and depolymerization of the actin filaments and are synchronized with the viscous adhesion forces between the cell and the substrate (Allena and Aubry 2012; Allena 2013);

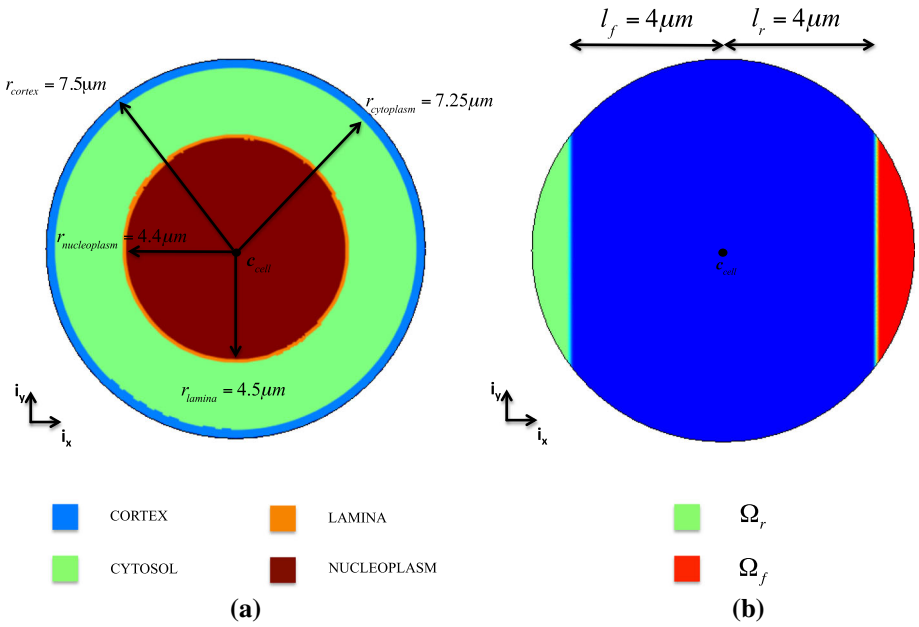

Fig. 1 Geometry of the cell (**a**) and frontal and rear adhesion surfaces (**b**)

– the micro-channel is represented by two rigid walls, which are described by two characteristic functions, and exerts an additional normal viscous force on the cell boundaries when contact condition is fulfilled.

The main objective of our work is to assess the necessary conditions for the cell to enter into the channel and migrate through it. In order to do so, we test four different channels whose dimensions in width are i) larger than the cell diameter, ii) sub-cellular, iii) sub-nuclear and iv) much smaller than the nucleus diameter. We analyse the evolution of the cell morphology by consistently comparing it with experimental observations, and we classify the cell behaviour according to the covered distance inside the channel. Additionally, we evaluate both the cell-substrate and the cell-channel surface forces during migration, and we find that there exists a link between such forces and the changes in cell shape, which may be essential in determining the invasive behaviour of the cell.

The paper is organized as follows: in Sect. 2, the geometry of the cell, the constitutive model and the mechanical approach are described. In Sect. 3, the results of the numerical simulations are presented. First, we analyse the cell behaviour (Sect. 3.1). Second, we evaluate the mechanical cell-substrate and cell-channel surface forces (Sect. 3.2), and we find the necessary conditions determining whether the cell is penetrating, invasive or permeative.

2 The model

In this section, we provide the general framework of the model. First, we describe the geometry of the cell including the cytoplasm and the nucleus. Second, we focus on the mechanics of the system. Specifically, we introduce the standard Maxwell models, which are used to reproduce the viscoelastic behaviour of the nucleus and the cytoplasm. Third, the intra-synchronization is presented. As in our previous works (Allena and Aubry 2012; Allena 2013), this represents the key ingredient of the cell movement. In fact, we show how the cyclic active strains (i.e. protrusion and contraction) are strongly coupled with the viscous forces generated by the cell to adhere to the substrate and necessary to efficiently move forward. Finally, we describe the geometry of the micro-channel and the associated viscous force exerted on the cell boundaries, which allows the cell to squeeze and pass (or not) through it.

2.1 Cell geometry

HeLa cells are human cells with a rather rounded initial shape and a diameter of about 15 µm (Ronot et al. 2000; Ngalim et al. 2013). For the numerical model, the geometry of the cell has been simplified by a circular domain Ω_{cell} of radius r_{cell} (Fig. 1a). Here, we consider two main components of the cell: the cytoplasm ($\Omega_{\text{cytoplasm}}$) and the nucleus ($\Omega_{\text{nucleus}}$) (Fig. 1a, Sect. 5.1). Additionally, the cell cyclically generates a frontal (Ω_f) and a rear (Ω_r) adhesion region in order to move forward (Allena and Aubry 2012; Allena 2013) (Fig. 1b, Sect. 5.1).

2.2 Constitutive model and mechanics of the cell

Both the nucleus and the cytoplasm are assumed to be viscoelastic materials, and their behaviour is described by two

standard Maxwell models (Larson 1998) (Sect. 5.2). On one hand, the nucleus is composed by the nuclear lamina Ω_{lamina} (the solid phase, Sects. 5.1 and 5.2), which surrounds the viscoelastic nucleoplasm $\Omega_{\text{nucleoplasm}}$ (the fluid phase, Sects. 5.1 and 5.2). On the other hand, the cytoplasm is essentially made of a solid phase represented by the cell cortex Ω_{cortex} (Sects. 5.1 and 5.3) and a fluid-like phase, the cytosol Ω_{cytosol} (Sects. 5.1 and 5.3) in which the organelles such as the actin filaments are embedded. As in our previous works (Allena and Aubry 2012; Allena 2013), we assume that the polymerization of the actin filaments inside the cytosol, which mostly occurs at the front of the cell (Schaub et al. 2007), generates the protrusive force at the leading edge, and their contraction due to binding of myosin generates the contractile stress at the rear of the cell (Mogilner 2009). Such active strains triggering the deformability of the cell are then described through a deformation tensor $\boldsymbol{F}_{\text{cytosol},a}$ (Sects. 2.3 and 5.3) in the fluid-like branch of the symbolic standard Maxwell model of the cytoplasm.

As described in (Allena and Aubry 2012; Allena 2013), the global equilibrium of the system is expressed as

$$\rho \boldsymbol{a} = \boldsymbol{Div}_{\boldsymbol{p}} \left(J \sigma \boldsymbol{F}^{-T} \right) + \boldsymbol{f}_{\text{adh}} + \boldsymbol{f}_{\text{channel}} \tag{1}$$

where ρ is the cell density, $\boldsymbol{a}$ is the acceleration, $\boldsymbol{Div}_{\boldsymbol{p}}$ is the divergence with respect to the initial position $\boldsymbol{p}$, J is the determinant of the deformation gradient $\boldsymbol{F}$ and $\boldsymbol{A}^{-T}$ denotes the inverse transpose of the matrix $\boldsymbol{A}$ (Holzapfel 2000; Taber 2004). $\boldsymbol{f}_{\text{adh}}$ and $\boldsymbol{f}_{\text{channel}}$ indicate, respectively, the viscous adhesion forces between the cell and the substrate (Sect. 2.3) and the viscous force exerted by the channel on the cell boundaries (Sect. 2.4). Here, all the body forces but the inertial effects are neglected (Gracheva and Othmer 2004; Allena and Aubry 2012; Allena 2013).

2.3 Intra-synchronization

To describe the oscillating movement of the cell, two main assumptions have been made:

1) the active strains of protrusion and contraction are only applied in the cytosol. In fact, as in our previous works (Allena and Aubry 2012; Allena 2013), we assume that the oscillatory movement of the cell is triggered by the periodic polymerization and depolymerization of the actin filaments, which are embedded in the cytosol. The former only occurs at the front of the cell, while the latter takes place from the front towards the rear of the cell. Therefore, although the nucleus does not undergo any active strain, it will interact with the surrounding cytosol apart from the protrusion phase (Friedl et al. 2011);
2) although the cell may form multiple pseudopodia (Allena 2013), here only one is generated in the direction of migration, which, to reproduce the experimental set-up where the cell is constrained into a micro-channel (Heuzé et al. 2011), corresponds to the horizontal axis $\boldsymbol{i}_x$.

Therefore, the solid active deformation tensor $\boldsymbol{F}_{\text{cytosol},a}$ reads

$$\boldsymbol{F}_{\text{cytosol},a} = \begin{cases} e_{a0} \sin\left(2\pi \frac{t}{T}\right) h_{\text{cytosol,front}} \boldsymbol{i}_x \otimes \boldsymbol{i}_x & \text{if } \sin\left(2\pi \frac{t}{T}\right) > 0 \\ \frac{e_{a0}}{2} \sin\left(2\pi \frac{t}{T}\right) h_{\text{cytosol}} \boldsymbol{i}_x \otimes \boldsymbol{i}_x & \text{if } \sin\left(2\pi \frac{t}{T}\right) < 0 \end{cases} \tag{2}$$

where e_{a0} is the amplitude of the active strain, t is time, T is the migration period, h_{cytosol} and $h_{\text{cytosol,front}}$ are two characteristic functions (Sect. 5.1) and $\otimes$ indicates the tensorial product.

As shown in (Allena and Aubry 2012), in order to be able to effectively migrate, the cell must adhere on the substrate otherwise it would only deform on place. Thus, an intra-synchronization is required which coordinates the cyclic protrusion–contraction deformations with the adhesion forces $\boldsymbol{f}_{\text{adh}}$ (Eq. 1) generated between the cell frontal and rear adhesion surfaces and the underneath substrate. As in previous works (Phillipson et al. 2006; Sakamoto et al. 2011; Allena and Aubry 2012; Allena 2013), such forces are assumed to be viscous and may be distinguished into a frontal ($\boldsymbol{f}_{\text{adh},f}$) and a rear ($\boldsymbol{f}_{\text{adh},r}$) force as follows

$$\begin{aligned} \boldsymbol{f}_{\text{adh},f}(\boldsymbol{n}_{\text{cell}}) &= -\mu_{\text{adh}} h_{\text{sync}} \left(-\frac{\partial e_a}{\partial t} \right) \boldsymbol{v} \quad \text{on}\Omega_f \\ \boldsymbol{f}_{\text{adh},r}(\boldsymbol{n}_{\text{cell}}) &= -\mu_{\text{adh}} h_{\text{sync}} \left(\frac{\partial e_a}{\partial t} \right) \boldsymbol{v} \quad \text{on}\Omega_r \end{aligned} \tag{3}$$

with $\boldsymbol{n}_{\text{cell}}$ the outward normal to the cell boundary, μ_{adh} the friction coefficient and $\boldsymbol{v}$ the velocity. The characteristic function h_{sync} is the key ingredient of the preceding equations since it couples the adhesion forces with the active strains, which results in the intra-synchronization mentioned above. Thus, we observe two main phases during the migratory movement of the cell: i) the protrusion and the adhesion at the rear edge; ii) the contraction and the adhesion at the frontal edge.

2.4 Micro-channel

Here, we want to reproduce the micro-channel-based assay presented in (Heuzé et al. 2011). Thus, the micro-channel domain Ω_{channel} is represented by two pseudo-elliptical rigid walls with no top roof (Sect. 5.4).

When the cell enters into the micro-channel, it is then submitted to a viscous force $\boldsymbol{f}_{\text{channel}}$ (Eq. 1), which can be distinguished into an upper ($\boldsymbol{f}_{\text{channel},uw_i}$) and a lower ($\boldsymbol{f}_{\text{channel},lw_i}$) force as follows

$$
\begin{aligned}
&\boldsymbol{f}_{\text{channel},uw_i}\left(\boldsymbol{n}_{uw,i}\right) \\
&\quad = -\mu_{\text{channel}} \frac{1}{\left(l_{uw,i}+1\right)^8+\alpha}\left(\frac{\partial \boldsymbol{u}}{\partial t}, \boldsymbol{n}_{uw,i}\right) n_{uw,i} \quad \text{on} \partial\Omega_{uw,i} \\
&\boldsymbol{f}_{\text{channel},lw_i}\left(\boldsymbol{n}_{lw,i}\right) \\
&\quad = -\mu_{\text{channel}} \frac{1}{\left(l_{lw,i}+1\right)^8+\alpha}\left(\frac{\partial \boldsymbol{u}}{\partial t}, \boldsymbol{n}_{lw,i}\right) \boldsymbol{n}_{lw,i} \quad \text{on} \partial\Omega_{lw,i}
\end{aligned}
\tag{4}
$$

where μ_{channel} is the viscosity of the micro-channel, $l_{uw,i}$ and $l_{lw,i}$ are two level set functions (Sect. 5.4), α is a constant and $\boldsymbol{n}_{uw,i}$ and $\boldsymbol{n}_{lw,i}$ are the outward normal to the boundaries $\partial\Omega_{uw,i}$ and $\partial\Omega_{lw,i}$ of the upper and lower wall, respectively, which are here originally calculated (Sect. 5.4) (the subscript 'i' indicates the channel number as explained in Sect. 3.1 and 5.4). Finally, (***a,b***) defines the scalar product between two vectors.

3 Results

The numerical simulations have been run using the finite element software COMSOL Multiphysics® 3.5a. As described in Sect. 2.2, the viscoelastic behaviour of the cell has been taken into account. The components of the cytoplasm and the nucleus have been implicitly described by specific characteristic functions (Sect. 5.1) in order to be able to define the parameters of the standard Maxwell models. The radius r_{cortex}, r_{cytosol}, r_{lamina} and $r_{\text{nucleoplasm}}$ of the HeLa cell have been fixed to 7.5, 7.25, 4.5 and 4.4 μm, respectively. Then, the cell cortex and the nuclear lamina have a thickness t_{cortex} and t_{lamina} of 0.25 μm (Pesen and Hoh 2005; Tinevez et al. 2009; Jiang and Sun 2013) and 0.1 μm (Righolt et al. 2010), respectively. The nominal values of the Young moduli $E_{\text{cortex},0}$ of the cell cortex and $E_{\text{cytosol},0}$ of the cytosol have been chosen equal to 100 and 10 Pa (Crick and Hughes 1950). For the nucleus, assuming that its stiffness is mostly provided by the nuclear lamina, we have set $E_{\text{lamina},0}$ and $E_{\text{nucleoplasm},0}$ to 3,000 Pa (Caille et al. 2002; Dahl et al. 2008) and 25 Pa (Vaziri et al. 2006), respectively. According to a simple spatial homogenization approach (Christensen 1991; Larson 1998), such moduli have then been recalculated according to the surface occupied by each component in the cell to obtain E_{cortex}, E_{cytosol}, E_{lamina} and $E_{\text{nucleoplasm}}$ (Table 1). Since we consider here that the cell cortex and the nuclear lamina are rather elastic, while the cytosol and the nucleoplasm are rather viscoelastic, the Poisson's ratios ν_{cortex} and ν_{lamina} have been set to 0.3, while ν_{cytosol} and $\nu_{\text{nucleoplasm}}$ to 0.4. The viscosities μ_{cytosol} and $\mu_{\text{nucleoplasm}}$ are equal to 3×10^5 Pa-s (Bausch et al. 1999; Drury and Dembo 2001). The cell density ρ has been set to 1,000 kg/m^3 (Fukui et al. 2000), and the viscous friction coefficient μ_{adh} is equal 10^8Pa-s/m. Finally, the intensity of the active strain e_{a0} and the migration period T have been chosen equal to 0.2 and 600 s, respectively, in order to obtain an average migration velocity of the order of magnitude of the one experimentally observed for HeLa cells (Ronot et al. 2000; Ngalim et al. 2013).

All the parameters of the model have been reported in Table 1.

3.1 Cell behaviour and morphology

As described in Sect. 2.4, the channel is represented by two pseudo-elliptical walls ($l_{uw,i}$ and $l_{lw,i}$), whose semi-axes a and b are 30 and 2 μm long, respectively.

For the simulations, only two-thirds of the total length of the channel are considered, which corresponds to 40 μm.

By letting the position of the upper and lower walls centres $\boldsymbol{c}_{uw,i}$ and $\boldsymbol{c}_{lw,i}$ vary, we have tested four channels with different width as follows:

- *channel 16* has a width $W_{c,1}$ of 16 μm, which is larger than the cell diameter with $\boldsymbol{c}_{uw,16}$ (42.5, 10 μm) and $\boldsymbol{c}_{lw,16}$ (42.5 μm, −10 μm);
- *channel 12* has an intermediate width $W_{c,2}$ of 12 μm, which is smaller than the cell diameter and bigger than the nucleus diameter, with $\boldsymbol{c}_{uw,12}$ (42.5, 8 μm) and $\boldsymbol{c}_{lw,12}$ (42.5, −8 μm);
- *channel 7* has a width $W_{c,3}$ of 7μm, which is slightly smaller than the nucleus diameter with $\boldsymbol{c}_{uw,7}$ (42.5, 5.5 μm) and $\boldsymbol{c}_{lw,7}$ (42.5, −5.5 μm);
- *channel 4* has a width $W_{c,4}$ of 4μm, which is much smaller than the nucleus diameter with $\boldsymbol{c}_{uw,4}$ (42.5, 4 μm) and $\boldsymbol{c}_{lw,4}$ (42, −4 μm).

For the first set of simulations, the viscous friction coefficient μ_{channel} and the constant α have been set equal to 10^{10} Pa-s/m and 0.1, respectively.

We have studied the cell behaviour for each of the previous configurations by analysing specific aspects of the confined movement, and the main results are listed in Table 2.

First, we have evaluated the efficiency of the migration in terms of covered distance. In Fig. 3, the total displacement of the frontal edge of the cell is reported for the four simulations. Then, as previously proposed by (Rolli et al. 2010; Scianna et al. 2013), we can classify the cell as permeative, invasive or penetrating. The permeative behaviour is observable for *channel 16* and *channel 12* (Fig. 2a, b) where the cell reaches the other side of the channel by covering a distance of 38 μm in 9,000 s (blue and red lines in Fig. 3, and Movie 1 and Movie 2, respectively). The invasive behaviour occurs when the cell enters into the channel, but it is not able to achieve the other side (Fig. 2c). This is the case of *channel 7* where the cell only migrates over 25 μm in 6,000 s (green line in Fig. 3 and Movie 3). Finally, the cell is penetrating (Fig. 2d)

Table 1 Main geometrical and material parameters of the model

Parameter	Description	Value (unit)	References
r_{cell}	Cell radius	7.5 μm	
r_{cortex}	Cortex radius	7.5 μm	
r_{cytosol}	Cytosol radius	7.25 μm	
r_{lamina}	Lamina radius	4.5 μm	
$r_{\text{nucleoplasm}}$	Nucleoplasm radius	4.4 μm	
t_{cortex}	Cortex thickness	0.25 μm	Pesen and Hoh (2005), Tinevez et al. (2009), Jiang and Sun (2013)
t_{lamina}	Lamina thickness	0.1 μm	Righolt et al. (2010)
l_f	Distance cell centre—boundary of frontal adhesion region	4 μm	
l_r	Distance cell centre—boundary of rear adhesion region	4 μm	
Ω_{cell}	Initial cell area	176.6 μm^2	
Ω_{cortex}	Initial cortex area	11.6 μm^2	
Ω_{cytosol}	Initial cytosol area	101.4 μm^2	
$\Omega_{\text{cytoplasm}}$	Initial cytoplasm area	113 μm^2	
Ω_{lamina}	Initial lamina area	2.8 μm^2	
$\Omega_{\text{nucleoplasm}}$	Initial nucleoplasm area	60.8 μm^2	
Ω_{nucleus}	Initial nucleus area	63.6 μm^2	
Ω_f	Initial frontal adhesion region area	31 μm^2	
Ω_r	Initial rear adhesion region area	31 μm^2	
$E_{\text{cortex},0}$	Nominal cortex Young modulus	100 Pa	
$E_{\text{cytosol},0}$	Nominal cytosol Young modulus	10 Pa	Crick and Hughes (1950)
$E_{\text{lamina},0}$	Nominal lamina Young modulus	3,000 Pa	Caille et al. (2002), Dahl et al. (2008)
$E_{\text{nucleoplasm},0}$	Nominal nucleoplasm Young modulus	25 Pa	Vaziri et al. (2006)
E_{cortex}	Equivalent cortex Young modulus	15 Pa	
E_{cytosol}	Equivalent cytosol Young modulus	8 Pa	
E_{lamina}	Equivalent lamina Young modulus	196 Pa	
$E_{\text{nucleoplasm}}$	Equivalent nucleoplasm Young modulus	23 Pa	
ν_{cortex}	Cortex Poisson ratio	0.3	
ν_{cytosol}	Cytosol Poisson ratio	0.4	
ν_{lamina}	Lamina Poisson ratio	0.3	
$\nu_{\text{nucleoplasm}}$	Nucleoplasm Poisson ratio	0.4	
μ_{cytosol}	Cytosol viscosity	3×10^5 Pa-s	Bausch et al. (1999), Drury and Dembo (2001)
$\mu_{\text{nucleoplasm}}$	Nucleoplasm viscosity	3×10^5 Pa-s	Bausch et al. (1999), Drury and Dembo (2001)
ρ	Cell density	1,000 kg/m^3	Fukui et al. (2000)
e_{a0}	Amplitude of the active strain	0.8	
T	Migration period	600 s	
μ_{adh}	Cell friction coefficient	10^8 Pa-s/m	
a	Semi-axis of the pseudo-elliptical walls	30 μm	

Table 1 continued

Parameter	Description	Value (unit)	References
b	Semi-axis of the pseudo-elliptical walls	2 μm	
x_0	x-coordinate of the pseudo-elliptical walls centre	42.5 μm	
$y_{uw0,i}$	y-coordinate of the upper pseudo-elliptical wall centre	$y_{uw0,1}$: 10 $y_{uw0,2}$: 8 $y_{uw0,3}$: 6 $y_{uw0,4}$: 4 μm	
$y_{lw0,i}$	y-coordinate of the lower pseudo-elliptical wall centre	$y_{lw0,1}$: −10 $y_{lw0,2}$: −8 $y_{lw0,3}$: −6 $y_{lw0,4}$: −4 μm	
μ_{channel}	Channel viscous friction coefficient	10^{10} Pa-s/m	
α		0.1	
$W_{c,16}$	Width of *channel 1*	16 μm	
$W_{c,12}$	Width of *channel 3*	12 μm	
$W_{c,7}$	Width of *channel 3*	8 μm	
$W_{c,4}$	Width of *channel 4*	4 μm	

Table 2 Main numerical results for the different channels

	Channel 16	Channel 12	Channel 7	Channel 4
Displacement (μm)	38	38	25	7.5
Protrusion average velocity (μm/s)	0.0055	0.0051	0.0055	0.0053
Contraction average velocity (μm/s)	0.0102	0.0122	0.0118	0.0115
t_{contact} (s)	–	1,950	1,250	1,220
$t_{\text{penetration}}$ (s)	3,900	4,600	4,610	–
T_{entry} (s)	–	2,650	3,360	–
Maximal ratio cell area/nucleus area	3.29	2.89	2.25	3.29
Minimal ratio cell area/nucleus area	2.11	1.93	1.35	2.11
t_{regime1} (s)	–	1,800	1,250	1,230
t_{regime2} (s)	–	2,450	1,350	1,250
t_{regime3} (s)	–	2,600	1,850	–

when only part of the body (or nothing) penetrates within the channel as it takes place for *channel 4* (purple line in Fig. 3 and Movie 4) where the total displacement is only equal to 7.5 μm.

In Fig. 4, the trend of the cell average velocity is represented. As a general remark, the velocity during the contraction phase is slightly higher than during the contraction phase, since the former only involves the frontal portion of the cytoplasm (see Sect. 2.3). While the average protrusion velocity remains rather constant for all the channels (roughly $5 \cdot 10^{-3}$ μm/s), the average contraction velocity varies between a minimal value of about $10^{-2}\mu$m/s for channel 16 (blue line Fig. 4) and a maximal value of $1.2 \cdot 10^{-2}$ μm/s for channel 12 (red line Fig. 4). Additionally, for *channel 7* (green line Fig. 4), we observe a peak of the velocity up to $1.3 \cdot 10^{-2}$ μm/s at the entrance of the channel, while afterwards the cell acquires again a constant velocity. Such values are of the same order of magnitude of those experimentally observed for HeLa cells (Ronot et al. 2000; Ngalim et al. 2013).

Second, for each configuration, we have quantified the entry time (T_{entry}), which has been defined by Lautenschläger et al. (Lautenschlager et al. 2009) as the time interval between the first contact of the cell with the channel walls (t_{contact}) and the complete penetration of the cell body within the channel ($t_{\text{penetration}}$). For *channel 16* and *channel 4*, such a parameter cannot be evaluated since the cell either does not enter in contact with the channel (*channel 16*) or does not migrate through it (*channel 4*). For *channel 12* and *channel 7*, we found 2,650 and 3,360 s respectively, which confirms that the smaller the channel, the more the difficult is for the cell to get in. In fact, the contact cell channel occurs earlier for *channel 7* than for *channel 12* ($t_{\text{contact}} = 1{,}250$ s versus $t_{\text{contact}} = 1{,}950$ s), while $t_{\text{penetration}}$ is almost the same

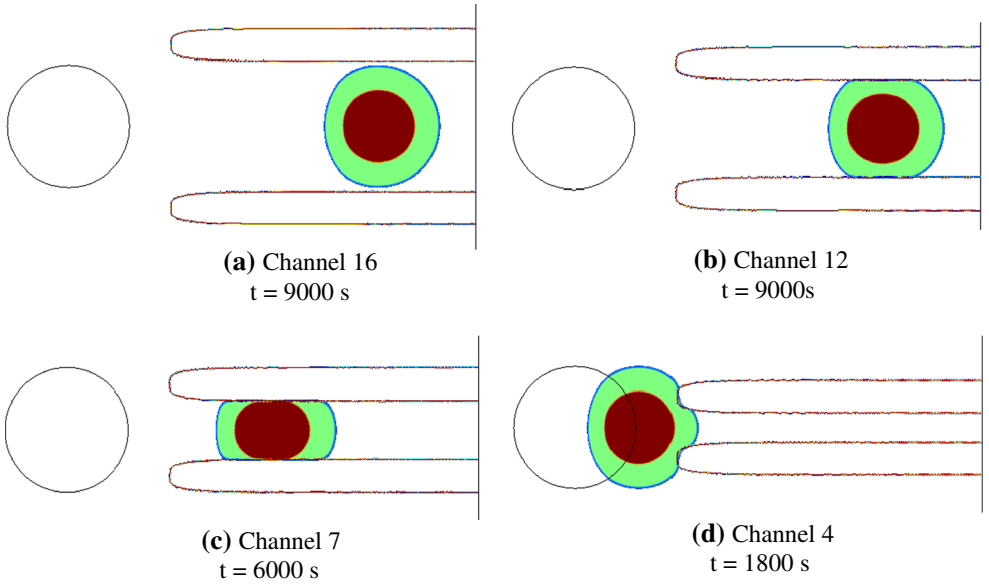

Fig. 2 Snaphots of the permeative (**a** and **b**), invasive (**c**) and penetrating (**d**) cell

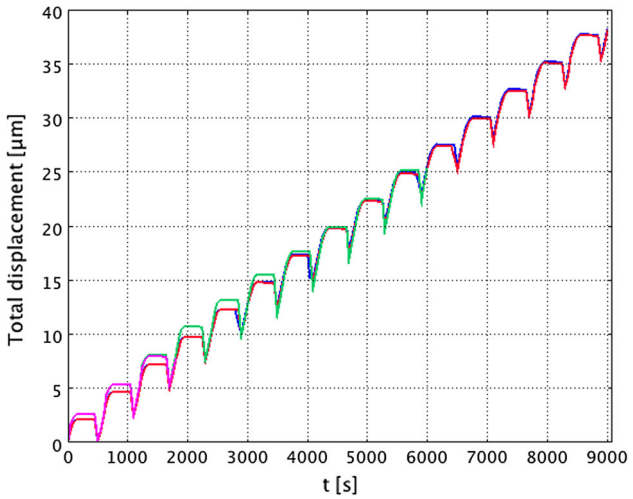

Fig. 3 Total displacement of the cell for *channel 16* (*blue line*), *channel 12* (*red line*), *channel 7* (*green line*) and *channel 4* (*purple line*)

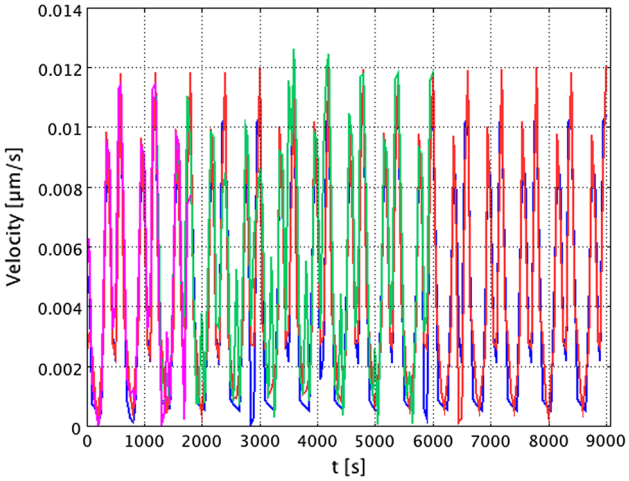

Fig. 4 Migration average velocity of the cell for *channel 16* (*blue line*), *channel 12* (*red line*), *channel 7* (*green line*) and *channel 4* (*purple line*)

for both channels ($t_{\text{penetration}} = 4{,}610\,s$ versus $t_{\text{penetration}} = 4{,}600$ s).

Third, we have evaluated the ratio between the total cell area and the nucleus area. At the initial configuration, such ratio is equal to 2.8, but it undergoes an oscillatory variation due to the protrusion–contraction movement of the cell. In the case of *channel 16* (Fig. 5, blue line), it varies between a maximal value of 3.3 during protrusion and a minimal value of 2.1 during contraction. Here, such values are the same at the end of each phase during the whole simulation since the cell overall deformation is not perturbed by the contact with channel. For *channel 12* instead, we observe a decrease of the maximal value of the ratio to 2.9 once the cell has completely entered the channel ($t_{\text{penetration}} = 4{,}600$ s, Fig. 5, red line), while the minimal value decreases to 1.9. Such drop is mainly due to a bigger shrinkage of the cell cytoplasm rather than of the nucleus due to the subcellular dimensions of the channel. However, in the case of *channel 7* (Fig. 5, green line), both cytoplasm and nucleus contribute to the progressive decrease of the ratio. In fact, the nucleus must squeeze too to move forward since the channel has sub-nuclear dimensions. Then, the maximal and minimal values of the ratio at $t_{\text{penetration}} = 4{,}610$ s decrease down to 2.25 and 1.35, respectively. For *channel 4* (Fig. 5, purple line), the ratio evolution is the same as for *channel 16* since the cell is not able to penetrate the channel and neither cytoplasm nor nucleus do not undergo large deformation.

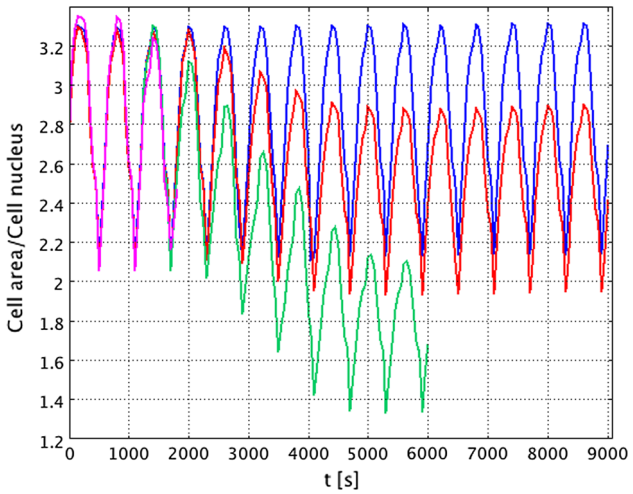

Fig. 5 Ratio between the cell area and the nucleus area for *channel 16* (*blue line*), *channel 12* (*red line*), *channel 7* (*green line*) and *channel 4* (*purple line*)

Finally, we have analysed the morphology of the cell relative to the channel, which can actually be divided into three regimes. The first regime is observed when the length L_p of the cell protrusion into the channel is smaller than half the width of the channel $W_{c,i}$ ($2L_p/W_{c,i} < 1$), and it has been indicated as t_{regime1}. The second regime occurs when $2L_p/W_{c,i} = 1$, and the protrusion is hemicircular with radius equal to $W_{c,I}$ (t_{regime2}). Finally, the third regime is obtained when $2L_p/W_{c,i} > 1$ (t_{regime3}). At this point, the first half of the protrusion is rectangular of length $W_{c,i}$ and the second half is hemicircular of radius L_c.

In the case of *channel 16*, the migration mode and the morphology of the cell do not change and are very similar to those observed for cell migrating over flat surfaces (Allena and Aubry 2012; Allena 2013). In fact, there is no contact between the cell cortex and the channel walls, and thus, the cell body is not perturbed during its movement. This is not the case for *channel 12* and *channel 7* where the cell needs to squeeze in order to enter the channel. For *channel 12* , regime 1 is observed at $t_{\text{regime1}} = 1{,}800$ s, while L_p becomes equal to $W_{c,2}/2$ at $t_{\text{regime2}} = 2{,}450$ s. Starting from $t_{\text{regime3}} = 2{,}600$ s, regime 3 is achieved and the protrusion is clearly half rectangular and half hemicircular. For *channel 7* (Fig. 6), steps occur earlier. In fact, regime 1 and regime 2 are reached at $t_{\text{regime1}} = 1{,}250$ s and $t_{\text{regime2}} = 1{,}350$ s, respectively, while regime 3 starts at $t_{\text{regime3}} = 1{,}850$ s. For *channel 4* instead, only regime 1 and 2 observed at $t_{\text{regime1}} = 1{,}230$ s and $t_{\text{regime2}} = 1{,}250$ s, respectively. The reason why regime 3 is not achieved is mainly due to the fact that, despite the cell tries to enter the channel by protruding and contracting, the force $\boldsymbol{f}_{\text{channel}}$ exerted by the channel walls on the cell boundaries is too high. This means that reaching regime 3 is a necessary, but not sufficient condition for the cell to be invasive. In fact, a second necessary condition need to be satisfied, that is, the cell-channel surface force $\boldsymbol{f}_{\text{channel}}$ at t_{regime3} must be low enough for the cell to enter.

We have also been able to experimentally observe such changes in morphology for two types of cells using a micro-channel-based essay as proposed in (Heuzé et al. 2011). Figure 7a–d shows the successive steps (top view) of bone marrow-derived dendritic cells (BDMCs) migration through a 5μm (Fig. 7a–b) and 1.5μm (Fig. 7c, d) wide micro-channel. It is possible to clearly distinguish the three regimes undergone by the whole cell body (Fig. 7b, d) and by the stained nucleus (Fig. 7a, c). Figure 7e shows instead a sagittal view of the successive steps of a HeLa cell migrating through a 20 μm wide micro-channel. We observe the deformation undergone by the stained nucleus along the z axis. In fact, in this specific case, the cell is confined in the x–y plane,

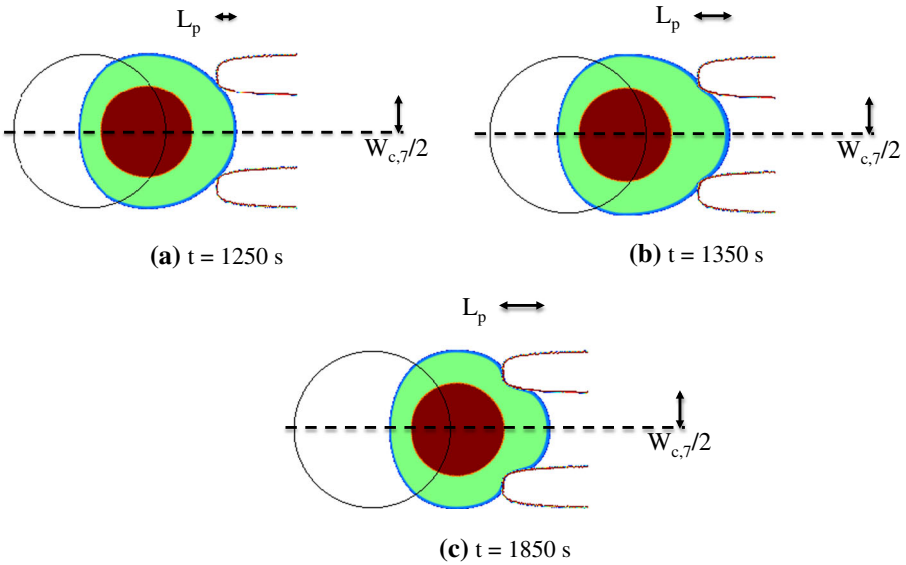

Fig. 6 The three regimes of the cell morphology during the migration through *channel 7*

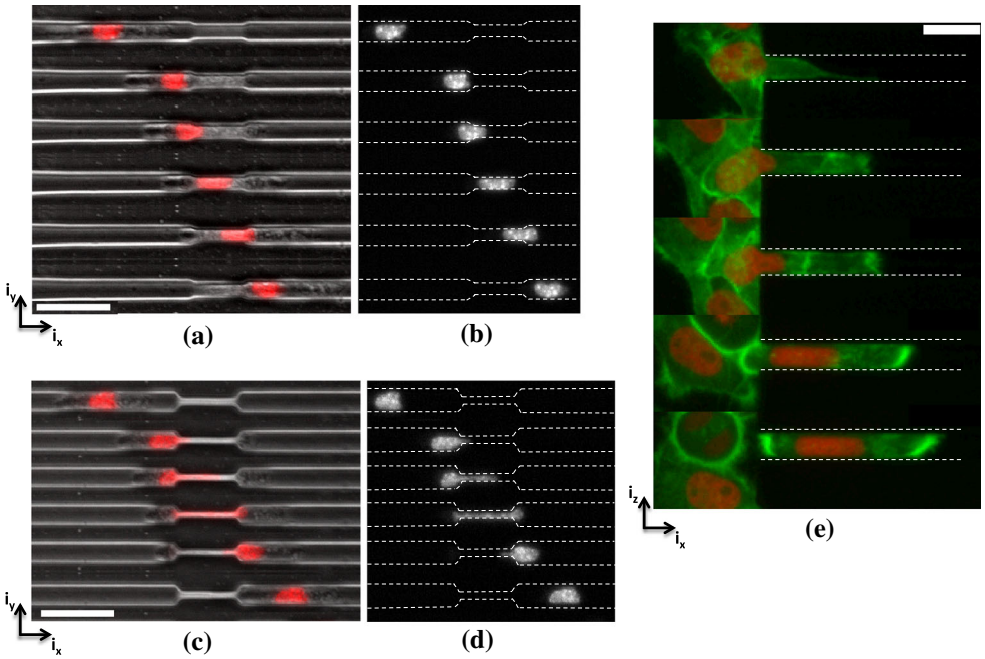

Fig. 7 (**a**:**d**) Top view of successive steps of a bone marrow-derived dendritic cell (BMDC) migration (from the *left* to the *right*) through a 5μm **a**–**b** and 1.5μm **c**–**d** wide micro-channels. Nuclear staining with Hoechst (**a** and **c**) (*scale bar*: 30μm) **e** Sagittal view of successive steps of a HeLa cell entering (from the *left* to the *right*) a 20μm wide micro-channel (HeLa Histone2B-mcherry (nucleus), MyrPalm-GFP (plasma membrane), *scale bar*: 15μm)

Table 3 Values of the mechanical forces for the different channels

	Channel 16	Channel 12	Channel 7	Channel 4
Maximal frontal cell-substrate surface force (Pa)	10	10	10	10
Maximal rear cell-substrate surface force (Pa)	4	4	4	4
Maximal cell-channel surface force at t_{contact} (Pa)	–	3.3	3.1	7.2
Maximal cell-channel surface force at $t_{\text{penetration}}$ (Pa)	–	3.3	3.9	–
Average cell-substrate surface force between t_{contact} and $t_{\text{penetration}}$ (Pa)	–	3.3	3.3	3.3
Average cell-channel surface force between t_{contact} and $t_{\text{penetration}}$ (Pa)	–	2.5	3.2	$t_{\text{contact}} - t_{\text{regime2}}$ 4.5
Absolute maximal cell-channel surface force (Pa)	–	4.2	6.2	8.6

but also in the x–z plane. Although such an aspect has not been numerically considered so far, we are currently working to improve the model in order to have a three-dimensional representation of the cell and the micro-channel and therefore being able to implement this further confinement

3.2 Mechanical forces

In this section, we try to evaluate the cell-substrate and cell-channel surface forces, in particular during the time interval between t_{contact} and $t_{\text{penetration}}$ in which t_{regime3} is included. The main values are summarized in Table 3.

Some general remarks may be pointed out:

- given the asymmetry of the active strain (Sect. 2.3) and the equation expressing the cell-substrate surface forces (Eq. 3), we found 10 and 4 Pa, respectively, at the front and rear edge of the cell. Additionally, such values do not change from one configuration;
- the cell-channel surface force increases as the channel width $W_{c,i}$ decreases (maximal absolute value of 4.25,

6.25 and 8.5 Pa for *channel 12, channel 7* and *channel 4* , respectively);

- as mentioned in Sect. 3.1, the necessary condition for the cell to be invasive is that the average cell-channel surface force at t_{regime3} must be lower than the average cell-substrate surface force at the same time point. This allows the cell to pull enough to penetrate within the channel without being obstructed by the channel. Since t_{regime3} is included in the time interval between t_{contact} and $t_{\text{penetration}}$, we have calculated the average cell-channel surface force during this period. For *channel 12* and *channel 7*, we have found an average value for the cell-channel surface force of about 2.5 Pa and 3.2, respectively, which is lower than the average cell-substrate surface force of 3.3 Pa. As a result, the cell is able to enter the channel. For *channel 4*, since the cell-channel surface force between t_{contact} and $t_{\text{penetration}}$ cannot be calculated, we have evaluated it between t_{contact} and t_{regime2} finding an average value of 4.5 Pa and a maximal value of 8.6 Pa, which is twice the cell-substrate surface force. Therefore, the cell is stuck at the entrance of the channel and shows a penetrating behaviour;
- once the cell has completely penetrated into the channel, the upper and lower central boundaries of the cell come very close or directly in contact with the nucleus, which is the stiffest component of the system. Then, a higher cell-channel surface force is necessary at this specific region to maintain the cell squeezing during the whole migration process and in order for the cell to be permeative. This is the case for *channel 12* for which the cell is able to reach the opposite end of the channel (Movie 5). However, for *channel 7*, the cell-channel surface force is slightly higher at the rear of the cell. Thus, the cell is slowed down and shows a penetrating behaviour (Movie 6).

For *channel 16*, only the cell-substrate surface force can be evaluated while the cell-channel surface force is null since no contact between the cell boundaries and the channel walls occurs.

4 Conclusions

In this paper, we have proposed a 2D mechanical model to simulate the migration of HeLa cell under confinement. The model reproduces the set-up used in a micro-channel assay as presented in (Heuzé et al. 2011). As in our previous works (Allena and Aubry 2012; Allena 2013), the cell is modelled as continuum and a standard Maxwell model is used to describe the mechanical behaviour of the cytoplasm (including active strains) and the nucleus. The cell is able to cyclically develop protrusion–contraction strains, which are synchronized with the adhesion forces between the cell and the substrate. By approaching the channel, which is represented here by two pseudo-elliptical rigid walls, the cell is submitted to an additional viscous force. We have tested four channels whose dimensions in terms of width are larger than the cell diameter (*channel 16*), sub-cellular (*channel 12*), sub-nuclear (*channel 7*) and much smaller than the nucleus diameter (*channel 4*). We have analysed the cell behaviour and classified it as permeative (*channel 16* and *channel 12*), invasive (*channel 7*) or penetrating (*channel 4*) according to the distance covered by the cell inside the channel. From a morphological point of view, we have identified three different regimes in relation to the ratio between the cell protrusion length in the channel and the width of the channel. Additionally, we have evaluated the evolution of the cell shape and the cell-substrate and cell-channel surface forces between the first contact between the cell and the channel (t_{contact}) and the complete penetration of the cell body within the channel ($t_{\text{penetration}}$).

Therefore, we have been able to define the necessary conditions in order for the cell to be invasive or permeative. In the first case, two main conditions must be satisfied: i) regime 3 (i.e. cell protrusion length in the channel larger than half the channel width) has to be achieved, and ii) simultaneously, the cell-substrate surface force must be higher than the cell-channel surface force so that the cell is able to pull on the substrate and enter into the channel. For the second behaviour to occur, a further condition must be satisfied, that is, the cell-channel surface force during the whole migration has to be maximal along the upper and lower central boundaries of the cell. Those boundaries may come very close or directly in contact with the cell nucleus, which is the stiffest component of the system. Then, a larger force is required to maintain the squeezed cell shape.

Despite the consistent results shown in the present paper, our model still presents some limitations. Firstly, the geometry is 2D, which does not allow considering a top-roofed micro-channel and the cell deformation in the third direction. Secondly, the active strains of protrusion and contraction have been defined through a sinusoidal function, which may lead to a rather stable periodic deformation of the cytoplasm and consequently of the nucleus. In order to control the effects of such a phenomenon, some stochastic active input close to cell perception may be introduced and improve the global movement. Finally, so far all the cell components have been considered as viscoelastic materials. However, the nucleus may be able to adapt its deformation to the forces exerted by the micro-channel on the cell boundaries. Therefore, a viscoplastic behaviour with restoration (Mandel 1972; Lubliner 2008) would probably be more appropriate. We are currently working on this aspect in order to be able to investigate the ability of the cell to penetrate micro-channels with significant sub-nuclear dimensions.

5 Appendix

5.1 Geometry of the cell

For any spatial point $\boldsymbol{p}$, the four components of the cell body (the cortex Ω_{cortex}, the cytosol Ω_{cytosol}, the lamina Ω_{lamina} and the nucleoplasm $\Omega_{\text{nucleoplasm}}$) are described through characteristic functions (i.e. composition of a Heaviside and a level set function (Allena 2013) as follows

$$h_{\text{cortex}}(\boldsymbol{p}) = \begin{cases} 1 & \text{if} r^2_{\text{cytoplasm}} < \|\boldsymbol{p} - \boldsymbol{c}_{\text{cell}}\| < r^2_{\text{cortex}} \\ 0 & \text{otherwise} \end{cases} \tag{5}$$

$$h_{\text{cytosol}}(\boldsymbol{p}) = \begin{cases} 1 & \text{if} r^2_{\text{lamina}} < \|\boldsymbol{p} - \boldsymbol{c}_{\text{cell}}\| < r^2_{\text{cytosol}} \\ 0 & \text{otherwise} \end{cases} \tag{6}$$

$$h_{\text{lamina}}(\boldsymbol{p}) = \begin{cases} 1 & \text{if} r^2_{\text{nucleoplasm}} < \|\boldsymbol{p} - \boldsymbol{c}_{\text{cell}}\| < r^2_{\text{lamina}} \\ 0 & \text{otherwise} \end{cases} \tag{7}$$

$$h_{\text{nucleoplasm}}(\boldsymbol{p}) = \begin{cases} 1 & \text{if } \|\boldsymbol{p} - \boldsymbol{c}_{\text{cell}}\| < r^2_{\text{nucleoplasm}} \\ 0 & \text{otherwise} \end{cases} \tag{8}$$

where $\boldsymbol{p} = \boldsymbol{x} - \boldsymbol{u}$, with $\boldsymbol{x}$ and $\boldsymbol{u}$ being, respectively, the actual position and the displacement, $\boldsymbol{c}_{\text{cell}}$ is the cell centre and r_{cortex}, r_{cytosol}, r_{lamina} and $r_{\text{nucleoplasm}}$ are the external radius of the cell cortex, the cytosol, the nuclear lamina and nucleoplasm, respectively (Fig. 1a). Therefore, the cytoplasm $\Omega_{\text{cytoplasm}}$ and the nucleus Ω_{nucleus} domains are defined by the following characteristic functions

$$\begin{aligned} h_{\text{cytoplasm}}(\boldsymbol{p}) &= h_{\text{cortex}}(\boldsymbol{p}) + h_{\text{cytosol}}(\boldsymbol{p}) \\ h_{\text{nucleus}}(\boldsymbol{p}) &= h_{\text{lamina}}(p) + h_{\text{nucleoplasm}}(\boldsymbol{p}) \end{aligned} \tag{9}$$

The frontal portion of cytosol where the polymerization of the actin filaments takes place is described as follows

$$h_{\text{cytosol,front}}(\boldsymbol{p}) = \begin{cases} h_{\text{cytosol}} & if \boldsymbol{p} > \boldsymbol{c}_{\text{cell}} \\ 0 & \text{otherwise} \end{cases} \tag{10}$$

The frontal (Ω_f) and rear (Ω_r) adhesion regions are also defined by two characteristic functions as

$$\begin{aligned} h_f(\boldsymbol{p}) &= \begin{cases} 1 & (\boldsymbol{p} - \boldsymbol{c}_{\text{cell}}, \boldsymbol{i}_x) > l_f \\ 0 & \text{otherwise} \end{cases} \\ h_r(\boldsymbol{p}) &= \begin{cases} 1 & (\boldsymbol{p} - \boldsymbol{c}_{\text{cell}}, \boldsymbol{i}_x) < -l_r \\ 0 & \text{otherwise} \end{cases} \end{aligned} \tag{11}$$

with l_f and l_r the distances of $\boldsymbol{c}_{\text{cell}}$ from the boundaries of Ω_f and Ω_r, respectively, (Fig. 1b). As soon as the cell moves, the argument $\boldsymbol{p}$ is replaced by $\boldsymbol{x}$-$\boldsymbol{u}$, with $\boldsymbol{x}$ the actual spatial position and $\boldsymbol{u}$ the displacement.

5.2 Nucleus constitutive law

As mentioned in Sect. 2.2, the nucleus is described through a viscoelastic constitutive equation based on a standard Maxwell model including a solid phase (i.e. the lamina) and a fluid phase (i.e. the nucleoplasm) (Fig. 8).

The Cauchy stress $\boldsymbol{\sigma}_{\text{nucleus}}$ and the deformation tensor $\boldsymbol{F}_{\text{nucleus}}$ in the nucleus are defined by

$$\begin{aligned} \boldsymbol{\sigma}_{\text{nucleus}} &= \boldsymbol{\sigma}_{\text{lamina}} + \boldsymbol{\sigma}_{\text{nucleoplasm}} \\ \boldsymbol{F}_{\text{nucleus}} &= \boldsymbol{D}_p\boldsymbol{u} + \boldsymbol{I} = \boldsymbol{F}_{\text{lamina}} = \boldsymbol{F}_{\text{nucleoplasm}} \end{aligned} \tag{12}$$

where $\boldsymbol{D_p u} = \sum_{m=1}^{3} \frac{\partial \boldsymbol{u}}{\partial p_m} \otimes \boldsymbol{i}_m$, with $\boldsymbol{u}$ the displacement and $\boldsymbol{I}$ the identity matrix (Holzapfel 2000; Taber 2004), and $\boldsymbol{F}_{\text{nucleoplasm}} = \boldsymbol{F}_{\text{nucleoplasm},e}\boldsymbol{F}_{\text{nucleoplasm},v}$. The solid part of the stress $\boldsymbol{\sigma}_{\text{lamina}}$ in the lamina reads

$$\boldsymbol{\sigma}_{\text{lamina}} = \frac{1}{J_{\text{lamina}}} \boldsymbol{F}_{\text{lamina}} \boldsymbol{S}_{\text{lamina}} \boldsymbol{F}^T_{\text{lamina}} \tag{13}$$

where J_{lamina} is the determinant of $\boldsymbol{F}_{\text{lamina}}$ and $\boldsymbol{S}_{\text{lamina}}$ is the second Piola–Kirchoff stress tensor, which is computed as an isotropic hyperelastic Saint Venant material as follows

$$\boldsymbol{S}_{\text{lamina}} = \lambda_{\text{lamina}} Tr\left(\boldsymbol{E}_{\text{lamina}}\right) \boldsymbol{I} + 2\mu_{\text{lamina}} \boldsymbol{E}_{\text{lamina}} \tag{14}$$

with λ_{lamina}, μ_{lamina} and $\boldsymbol{E}_{\text{lamina}}$ the Lame's coefficients and the Green-Lagrange strain tensor of the solid phase, respectively.

The fluid part of the stress $\boldsymbol{\sigma}_{\text{nucleoplasm}}$ in the nucleoplasm can be expressed as

$$\boldsymbol{\sigma}_{\text{nucleoplasm}} = 2\mu_{\text{nucleoplasm}} \boldsymbol{D}_{\text{nucleoplasm,v}} \tag{15}$$

with $\mu_{\text{nucleoplasm}}$, the viscosity of the nucleoplasm and the eulerian strain rate $\boldsymbol{D}_{\text{nucleoplasm},v}$ is computed from the strain gradient velocity as

$$\begin{aligned} 2\boldsymbol{D}_{\text{nucleoplasm},v} &= \dot{\boldsymbol{F}}_{\text{nucleoplasm},v} \boldsymbol{F}^{-1}_{\text{nucleoplasm},v} \\ &\quad + \boldsymbol{F}^{-T}_{\text{nucleoplasm},v} \dot{\boldsymbol{F}}^{T}_{\text{nucleoplasm},v} \end{aligned} \tag{16}$$

5.3 Cytoplasm constitutive law

The cytoplasm is composed by two phases: i) a solid phase represented by the cell cortex and ii) a fluid phase represented by the viscous cytosol with the embedded organelles such as the actin filaments that undergo the active strains (Fig. 8). It is assumed that the Cauchy stress $\boldsymbol{\sigma}_{\text{cytoplasm}}$ and the deformation tensor $\boldsymbol{F}_{\text{cytoplasm}}$ read

$$\begin{aligned} \boldsymbol{\sigma}_{\text{cytoplasm}} &= \boldsymbol{\sigma}_{\text{cortex}} + \boldsymbol{\sigma}_{\text{cytosol}} \\ \boldsymbol{F}_{\text{cytoplasm}} &= \boldsymbol{F}_{\text{cortex}} = \boldsymbol{F}_{\text{cytosol}} \end{aligned} \tag{17}$$

Additionally, the fluid deformation tensor $\boldsymbol{F}_{\text{cytosol}}$ is multiplicatively decomposed as follows

$$\boldsymbol{F}_{\text{cytosol}} = \boldsymbol{F}_{\text{cytosol},v} \boldsymbol{F}_{\text{cytosol},e} \boldsymbol{F}_{\text{cytosol},a} \tag{18}$$

where e and v stand for elastic and viscous, respectively.

The solid stress $\boldsymbol{\sigma}_{\text{cortex}}$ in the organelles can be written as

$$\boldsymbol{\sigma}_{\text{cortex}} = \frac{1}{J_{\text{cortex}}} \boldsymbol{F}_{\text{cortex}} \boldsymbol{S}_{\text{cortex}} \boldsymbol{F}^T_{\text{cortex}} \tag{19}$$

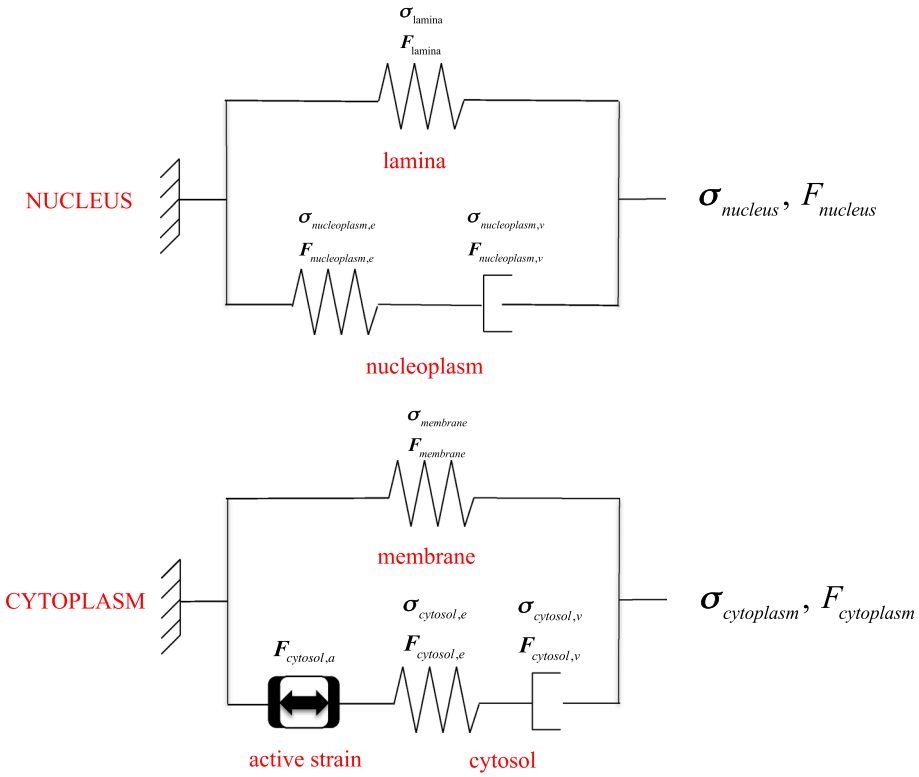

Fig. 8 Symbolic schemas for the standard Maxwell models used to describe the nucleus (*top*) and the cytoplasm (*bottom*) behaviours

with J_{cortex} the determinant of $\boldsymbol{F}_{\text{cortex}}$ and $\boldsymbol{S}_{\text{cortex}}$ the second Piola–Kirchoff stress tensor, which, similarly to the nucleus (Sect. 5.2), is defined as an isotropic hyperplastic Saint Venant material as follows

$$S_{\text{cortex}} = \lambda_{\text{cortex}} Tr\left(\boldsymbol{E}_{\text{cortex}}\right) \boldsymbol{I} + 2\boldsymbol{\mu}_{\text{cortex}} \boldsymbol{E}_{\text{cortex}} \tag{20}$$

where λ_{cortex}, μ_{cortex} and $\boldsymbol{E}_{\text{cortex}}$ the Lame's coefficients and the Green-Lagrange strain tensor of the solid phase, respectively.

Finally, the fluid stress $\boldsymbol{\sigma}_{\text{cytosol}}$ in the cytosol reads

$$\boldsymbol{\sigma}_{\text{cytosol}} = 2\mu_{\text{cytosol}} \boldsymbol{D}_{\text{cytosol},v} \tag{21}$$

with μ_{cytosol} the viscosity of the cytosol and $\boldsymbol{D}_{\text{cytosol},v}$ the eulerian strain rate expressed as follows

$$2\boldsymbol{D}_{\text{cytosol},v} = \dot{\boldsymbol{F}}_{\text{cytosol},v} \boldsymbol{F}^{-1}_{\text{cytosol},v} + \boldsymbol{F}^{-T}_{\text{cytosol},v} \dot{\boldsymbol{F}}^{T}_{\text{cytosol},v} \tag{22}$$

5.4 Micro-channel geometry

As mentioned in Sect. 2.4, the micro-channel domain Ω_{channel} is modelled as two pseudo-elliptical rigid walls: a upper one (Ω_{uw}) and a lower one (Ω_{lw}). They are described through two characteristic functions as follows

$$\begin{aligned} h_{uw,i}\left(\boldsymbol{p}\right) &= \begin{cases} 1 & \text{if} l_{uw,i} < 1 \\ 0 & \text{otherwise} \end{cases} \\ h_{lw,i}\left(\boldsymbol{p}\right) &= \begin{cases} 1 & \text{if} l_{lw,i} < 1 \\ 0 & \text{otherwise} \end{cases} \end{aligned} \tag{23}$$

where the subscript 'i' indicates the number of the channel, and $l_{uw,i}$ and l_{lw} are two level set functions expressed as

$$\begin{aligned} l_{uw,i} &= \left(\frac{x - x_0}{a}\right)^4 + \left(\frac{y - y_{uw0,i}}{b}\right)^4 \\ l_{lw,i} &= \left(\frac{x - x_0}{a}\right)^4 + \left(\frac{y + y_{lw0,i}}{b}\right)^4 \end{aligned} \tag{24}$$

with a and b are the semi-axes of the pseudo-elliptical walls with centres $\boldsymbol{c}_{uw,i}\left(x_0, y_{uw0,i}\right)$ and $\boldsymbol{c}_{lw,i}\left(x_0, y_{lw0,i}\right)$. Thus, the micro-channel is the composition of the two previous characteristic functions as follows

$$\Omega_{\text{channel}} = h_{uw,i}\left(\boldsymbol{p}\right) + h_{lw,i}\left(\boldsymbol{p}\right) \tag{25}$$

The c outward normals $\boldsymbol{n}_{uw}$ and $\boldsymbol{n}_{lw}$ to the boundary $\partial\Omega_{uw}$ and $\partial\Omega_{lw}$, respectively, given by

$$\begin{aligned} \boldsymbol{n}_{uw,i} &= h'\left(l_{uw,i}\right) \frac{\nabla l_{uw,i}}{\left\|\nabla l_{uw,i}\right\|} \\ \boldsymbol{n}_{lw,i} &= h'\left(l_{lw,i}\right) \frac{\nabla l_{lw,i}}{\left\|\nabla l_{lw,i}\right\|} \end{aligned} \tag{26}$$

where h' indicates the Dirac function.

References

Allena R (2013) Cell migration with multiple pseudopodia: temporal and spatial sensing models. Bull Math Biol 75:288–316. doi:10.1007/s11538-012-9806-1

Allena R, Aubry D (2012) "Run-and-tumble" or "look-and-run"? A mechanical model to explore the behavior of a migrating amoeboid cell. J Theor Biol 306:15–31. doi:10.1016/j.jtbi.2012.03.041

Bausch AR, Möller W, Sackmann E (1999) Measurement of local viscoelasticity and forces in living cells by magnetic tweezers. Biophys J 76:573–579

Caille N, Thoumine O, Tardy Y, Meister J-J (2002) Contribution of the nucleus to the mechanical properties of endothelial cells. J Biomech 35:177–187

Christensen RM (1991) Mechanics of composite materials. Krieger Publishing Company, NY

Crick FHC, Hughes AFW (1950) The physical properties of cytoplasm. Exp Cell Res 1:37–80. doi:10.1016/0014-4827(50)90048-6

Dahl KN, Ribeiro AJS, Lammerding J (2008) Nuclear shape, mechanics, and mechanotransduction. Circ Res 102:1307–1318. doi:10.1161/CIRCRESAHA.108.173989

Drury JL, Dembo M (2001) Aspiration of human neutrophils: effects of shear thinning and cortical dissipation. Biophys J 81:3166–3177

Egeblad M, Rasch MG, Weaver VM (2010) Dynamic interplay between the collagen scaffold and tumor evolution. Curr Opin Cell Biol 22:697–706. doi:10.1016/j.ceb.2010.08.015

Erler JT, Weaver VM (2009) Three-dimensional context regulation of metastasis. Clin Exp Metastas 26:35–49. doi:10.1007/s10585-008-9209-8

Faure-André G, Vargas P, Yuseff M-I et al (2008) Regulation of dendritic cell migration by CD74, the MHC class II-associated invariant chain. Science 322:1705–1710. doi:10.1126/science.1159894

Friedl P, Wolf K (2010) Plasticity of cell migration: a multiscale tuning model. J Cell Biol 188:11–19. doi:10.1083/jcb.200909003

Friedl P, Wolf K, Lammerding J (2011) Nuclear mechanics during cell migration. Curr Opin Cell Biol 23:55–64. doi:10.1016/j.ceb.2010.10.015

Fukui Y, Uyeda TQP, Kitayama C, Inoué S (2000) How well can an amoeba climb? PNAS 97:10020–10025. doi:10.1073/pnas.97.18.10020

Giverso C, Grillo A, Preziosi L, Influence of nucleus deformability on cell entry into cylindrical structures. Biomech Model Mechanobiol, pp 1–22. doi:10.1007/s10237-013-0510-3

Gracheva ME, Othmer HG (2004) A continuum model of motility in ameboid cells. Bull Math Biol 66:167–193. doi:10.1016/j.bulm.2003.08.007

Hawkins RJ, Piel M, Faure-Andre G et al (2009) Pushing off the walls: a mechanism of cell motility in confinement. Phys Rev Lett 102:058103. doi:10.1103/PhysRevLett.102.058103

Hawkins RJ, Voituriez R (2010) Mechanisms of cell motion in confined geometries. Math Model Nat Phenom 5:84–105. doi:10.1051/mmnp/20105104

Heuzé ML, Collin O, Terriac E et al (2011) Cell migration in confinement: a micro-channel-based assay. Methods Mol Biol 769:415–434. doi:10.1007/978-1-61779-207-6_28

Holzapfel GA (2000) Nonlinear solid mechanics: a continuum approach for engineering, 1st edn. Wiley, London

Ilina O, Bakker G-J, Vasaturo A et al (2011) Two-photon laser-generated microtracks in 3D collagen lattices: principles of MMP-dependent and -independent collective cancer cell invasion. Phys Biol 8:015010. doi:10.1088/1478-3975/8/1/015010

Irimia D, Charras G, Agrawal N et al (2007) Polar stimulation and constrained cell migration in microfluidic channels. Lab Chip 7:1783–1790. doi:10.1039/b710524j

Irimia D, Toner M (2009) Spontaneous migration of cancer cells under conditions of mechanical confinement. Integr Biol (Camb) 1:506–512. doi:10.1039/b908595e

Jiang H, Sun SX (2013) Cellular pressure and volume regulation and implications for cell mechanics. Biophys J 105:609–619. doi:10.1016/j.bpj.2013.06.021

Larson RG (1998) The structure and rheology of complex fluids. Oxford University Press, USA

Lautenschlager F, Paschke S, Schinkinger S et al (2009) The regulatory role of cell mechanics for migration of differentiating myeloid cells. Proc Natl Acad Sci 106:15696–15701. doi:10.1073/pnas.0811261106

Lubliner J (2008) Plasticity theory. Dover Publications, New York

Mandel J (1972) Plasticité classique et viscoplasticité: course held at the Department of Mechanics of Solids, September-October, 1971. Springer, Berlin

McElwain DLS (1978) A re-examination of oxygen diffusion in a spherical cell with michaelis-menten oxygen uptake kinetics. J Theor Biol 71:255–263. doi:10.1016/0022-5193(78)90270-9

McElwain DLS, Callcott R, Morris LE (1979) A model of vascular compression in solid tumours. J Theor Biol 78:405–415. doi:10.1016/0022-5193(79)90339-4

McElwain DLS, Ponzo PJ (1977) A model for the growth of a solid tumor with non-uniform oxygen consumption. Math Biosci 35:267–279. doi:10.1016/0025-5564(77)90028-1

Mogilner A (2009) Mathematics of cell motility: have we got its number? J Math Biol 58:105–134. doi:10.1007/s00285-008-0182-2

Ngalim SH, Magenau A, Zhu Y et al (2013) Creating adhesive and soluble gradients for imaging cell migration with fluorescence microscopy. J Vis Exp. doi:10.3791/50310

Pesen D, Hoh JH (2005) Micromechanical architecture of the endothelial cell cortex. Biophys J 88:670–679. doi:10.1529/biophysj.104.049965

Phillipson M, Heit B, Colarusso P et al (2006) Intraluminal crawling of neutrophils to emigration sites: a molecularly distinct process from adhesion in the recruitment cascade. J Exp Med 203:2569–2575. doi:10.1084/jem.20060925

Provenzano PP, Inman DR, Eliceiri KW et al (2008) Collagen density promotes mammary tumor initiation and progression. BMC Med 6:11. doi:10.1186/1741-7015-6-11

Rangarajan R, Zaman MH (2008) Modeling cell migration in 3D. Cell Adhes Migr 2:106–109

Recho P, Putelat T, Truskinovsky L (2013) Contraction-driven cell motility. Phys Rev Lett 111:108102. doi:10.1103/PhysRevLett.111.108102

Recho P, Truskinovsky L (2013) An asymmetry between pushing and pulling for crawling cells. arXiv:1302.4002 [cond-mat, physics:physics, q-bio]

Righolt CH, Raz V, Vermolen BJ et al (2010) Molecular image analysis: quantitative description and classification of the nuclear lamina in human mesenchymal stem cells. Int J Mol Imaging. doi:10.1155/2011/723283

Rolli CG, Seufferlein T, Kemkemer R, Spatz JP (2010) Impact of tumor cell cytoskeleton organization on invasiveness and migration: a microchannel-based approach. PLoS ONE 5:e8726. doi:10.1371/journal.pone.0008726

Ronot X, Doisy A, Tracqui P (2000) Quantitative study of dynamic behavior of cell monolayers during in vitro wound healing by optical flow analysis. Cytometry 41:19–30

Sakamoto Y, Prudhomme S, Zaman MH (2011) Viscoelastic gel-strip model for the simulation of migrating cells. Ann Biomed Eng 39:2735–2749. doi:10.1007/s10439-011-0360-z

Schaub S, Bohnet S, Laurent VM et al (2007) Comparative maps of motion and assembly of filamentous actin and myosin II in migrating cells. Mol Biol Cell 18:3723–3732. doi:10.1091/mbc.E06-09-0859

Scianna M, Preziosi L (2013) Modeling the influence of nucleus elasticity on cell invasion in fiber networks and microchannels. J Theor Biol 317:394–406. doi:10.1016/j.jtbi.2012.11.003

Scianna M, Preziosi L, Wolf K (2013) A cellular potts model simulating cell migration on and in matrix environments. Math Biosci Eng 10:235–261

Stokes CL, Lauffenburger DA (1991) Analysis of the roles of microvessel endothelial cell random motility and chemotaxis in angiogenesis. J Theor Biol 152:377–403. doi:10.1016/S0022-5193(05)80201-2

Stokes CL, Lauffenburger DA, Williams SK (1991) Migration of individual microvessel endothelial cells: stochastic model and parameter measurement. J Cell Sci 99(Pt 2):419–430

Taber LA (2004) Nonlinear theory of elasticity: applications in biomechanics. World Scientific Pub Co Inc., Singapore

Taylor AM, Blurton-Jones M, Rhee SW et al (2005) A microfluidic culture platform for CNS axonal injury, regeneration and transport. Nat Methods 2:599–605. doi:10.1038/nmeth777

Tinevez J-Y, Schulze U, Salbreux G, et al. (2009) Role of cortical tension in bleb growth. PNAS pnas.0903353106. doi:10.1073/pnas.0903353106

Tozluoğlu M, Tournier AL, Jenkins RP et al (2013) Matrix geometry determines optimal cancer cell migration strategy and modulates response to interventions. Nat Cell Biol 15:751–762. doi:10.1038/ncb2775

Tranquillo RT, Lauffenburger DA (1987) Stochastic model of leukocyte chemosensory movement. J Math Biol 25:229–262

Tranquillo RT, Lauffenburger DA, Zigmond SH (1988) A stochastic model for leukocyte random motility and chemotaxis based on receptor binding fluctuations. J Cell Biol 106:303–309

Vaziri A, Lee H, Mofrad MRK (2006) Deformation of the cell nucleus under indentation: mechanics and mechanisms. J Mater Res 21:2126–2135. doi:10.1557/jmr.2006.0262

Wolf K, Alexander S, Schacht V et al (2009) Collagen-based cell migration models in vitro and in vivo. Semin Cell Dev Biol 20:931–941. doi:10.1016/j.semcdb.2009.08.005

Zaman MH, Kamm RD, Matsudaira P, Lauffenburger DA (2005) Computational model for cell migration in three-dimensional matrices. Biophys J 89:1389–1397. doi:10.1529/biophysj.105.060723

Zaman MH, Matsudaira P, Lauffenburger DA (2007) Understanding effects of matrix protease and matrix organization on directional persistence and translational speed in three-dimensional cell migration. Ann Biomed Eng 35:91–100. doi:10.1007/s10439-006-9205-6

Zaman MH, Trapani LM, Sieminski AL et al (2006) Migration of tumor cells in 3D matrices is governed by matrix stiffness along with cell-matrix adhesion and proteolysis. Proc Natl Acad Sci USA 103:10889–10894. doi:10.1073/pnas.0604460103

Abstract:

Cell migration has two opposite faces; necessary for many physiological processes such as immune response, it can also lead to the organism death by allowing metastatic cells to invade new organs. *In vivo* migration often occurs in complex 3D environments which impose high cellular deformability. Recently, the limit of cellular deformability during 3D migration has been shown to be limited by the nucleus [Wolf 2013]. For instance, cell migration can be increased by decreasing nuclear stiffness. However, below a given nuclear stiffness 3D cell migration can be reduced as a result of impaired cell survival [Harada 2014]. Cancer cells which display slow migration and have rather stiff nuclei have been shown to overcome the physical limits of 3D migration through adhesion combined to matrix degradation or high actomyosin contraction [Wolf 2013]. Immune cells such as neutrophils which are fast moving cells with soft nuclei have been reported to die at sites of infection. Interestingly, dendritic cells function as antigen presenting cells requires high migratory ability as well as high survival. They thus constitute an interesting model for studying nuclear deformation in fast moving and long lived cells. During my PhD, I studied the mechanism by which dendritic cells deform their nuclei to achieve proper migration in highly confining space while preserving a high survival rate. I used an original micro fabricated experimental set up [Heuzé 2011] consisting of microchannels with constrictions to mimic cellular transmigration. Those channels combined with genetic manipulation and live cell imaging followed by image processing were used to assess the mechanism dendritic cells use to deform their nucleus, which we found to be specific and not required for cell motility per se. I showed that dendritic cells overcome the physical limitation imposed by nuclear deformation through small gaps by nucleating an Arp2/3 based actin network around the nucleus. Surprisingly, the formation of this actin network is independent of myosin II based contraction. This actin accumulation around the nucleus co-localized with sites of nuclear Lamin A/C breakage. Moreover, Lamin A/C depletion in dendritic cells leads to the disappearance of this actin ring and the release of the need for Arp2/3 for nuclear deformation. We thus propose a new mechanism of nuclear squeezing through narrow gaps based on an Arp2/3 nucleated actin meshwork which, by transiently breaking the Lamin A/C network, releases the nuclear surface tension and allows nuclear thus cell passage through micrometric constrictions. Lamin A/C repolymerization around the nucleus at the exit of constrictions would then restore nuclear stiffness, allowing cell survival. Interestingly, this actin accumulation around the nucleus was also observed in vivo in migrating macrophages but not in HL-60 derived neutrophils. Taken together, our data suggest that the Arp2/3 based nuclear squeezing mechanism would be a general feature of highly migratory cells which need to survive long enough to accomplish their functions.

Keywords: cell migration, confinement, Arp2/3, nucleus, lamin A/C
